RUTHENIUM (II) POLYPYRIDYL COMPLEXES AS MODELS FOR ARTIFICIAL PHOTOSYNTHESIS – SYNTHESIS AND CHARACTERISATION

by

Jonathan Scott Killeen, BSc.

A Thesis presented to Dublin City University for the degree of Doctor of Philosophy.

Supervisor Prof. J.G. Vos

School of Chemical Sciences

Dublin City University

December 2001

To my parents

I hereby certify that this material, which I now submit for assessment on the programme of study leading to award of Doctor of Philosophy by research and thesis, is entirely my own work and has not been taken from work of others, save and to extent that such work has been cited and acknowledged within the text of my work.

Signed: Scott Killeen

Scott Killeen

I.D. No. 97970719

Date 13/12/01

As an adolescent I aspired to lasting fame,

I craved factual certainty,

and I thirsted for a meaningful vision of human life

- so I became a scientist.

This is like becoming an archbishop to meet girls.

-Matt Cartmill

Professor of Biological Anthropology and Anatomy

Duke University, USA

American Scientist, **1988,** 76, 453

Acknowledgements

Wow! I can't believe I'm here. My student days are over. After four years of dreaming about it, I finally get to write my acknowledgements. Here goes…..

First and foremost, I have to thank Prof. Han Vos, the boss, the man with the money and the whip. If you hadn't agreed to take me on in the first place, I wouldn't have suffered half as much over the last couple of months, nor would I have known how good it feels to say "I'm finished!". Thanks Han! Any chance of you sending me away somewhere nice as a little reward for finally finishing and getting out of your hair?

Ich möchte mich vielmals bei Prof. Jurgen Fuhrhop in Berlin bedanken. . Das Jahr in Berlin war eine einmalige Erfahrung. Danke für Ihre Unterstützung, Ihre Geduld und Gastfreundschaft Herzlich bedanken möchte ich mich auch bei Andrea, Andreas, Arvid, Beate, Christian D., Christian M., Kerstin, Kirsten, Li, Marc, Marie, Matthias, Sara und Werner. Ich habe mich bei Euch in Berlin sehr wohl gefühlt. I'd like to express my sincere thanks to everybody in Sweden, who helped make my stay there so productive and enjoyable. Thanks to Prof. Björn Åkkermark, Dr. Licheng Sun, Dr. Leif Hammarström, Marcus, Heimo, Morten, Maria, Anh and Pierre. A huge thanks to the people in Paris, Prof. Jean-Jacques Girerd, Belèn Albela and especially Sebastien Blanchard. I'm sorry for not being able to give you any clean compounds. Thanks for being so understanding and helpful. I really appreciate it!!

I would like to thank Enterprise Ireland and the EU TMR Network "Ru-Mn Artificial Photosynthesis" for financial assistance during the course of my studies.

I also owe a huge thanks to the technicians: Mick, Damien, Maurice, Veronica, Ann, Ambrose, Vinny, John and Mary. I'd never have managed to get out of here if you hadn't helped me with NMR, mass specs, electrochemistry, demonstrating, ordering, etc, etc....

Now to my fellow postgrads (and postdocs). Firstly the HVRG past and present: Adrian (New Boy), (Auntie) Anthea, Benedicte, Christine (The original Mama), Conni, Dec ("Let's go fishing!"), Egbert, Fiona 1 (We'll always have Semisonic), Fiona 2 (You'll be lost without me), Frances, Helen (and her amazing invisible compounds!), Luke, Marco (I win!), Moss (Turn down the music), Stefano, Tia and Wesley (Bombs...hmm?). Thanks for the support along the way. Then there's the CLRG: Bronagh (Boogie!), Davnat (Pooh's biggest fan), Jennifer, Johnny, Karl, Kevin, Kieran, Siobhan and Peter. Now for the list of bucket chemists and button pushers: Ben, Carol (sing a song, Des), Cathal (6 in an hour!), Clodagh, Colm, Conor, Darren, David, Eadaoin, Edel (The Ruhland Survivor), Edna, Frank (Nice car, but change the station), Ger K.(Owner of Waterford's finest hostel), Ger McD., Jenni (The next Madonna), Joe, Johan, Lorraine, Mary, Mairead S. (and her amazing beanbag!), Mairead F., Marion, Michaela, Mick, Paddy, Ray, Rob, Richard and Sonia. Thanks to all my non-DCU chemistry department friends: Aideen, Blanaid, Dee, Emer, Gerard, Julie, Keith, Lynn, Nick, Paul, Sally, Sinead, Steve C, Steve H and Susi. It's good to be able to go out and not talk shop.

Finally, and most importantly, I want to thank my family: My brothers Adam, Stuart and Warren (and their beautiful spouses!), my baby sister Lindsey and most of all my parents. Thanks for making me possible! Without your help and patience I'd never have made it this far. But now the "eternal student" jokes can stop!

Abstract

This thesis presents a study on the synthesis and characterisation of a series of novel ruthenium (II) polypyridyl complexes, which are potentially models for artificial photosynthesis.

Chapter 1, the introduction, highlights the literature relevant to the topic. In Chapter 2, the experimental conditions of the various methods of characterisation are described. The synthesis and characterisation of a range of novel 5-phenyl-3-(2-pyridyl)-1,2,4-triazoles, their $Ru(bpy)_2$ and their $Ru(d_8\text{-}bpy)_2$ complexes are discussed in Chapter 3. Each of the new ligands bear terminal functional groups which allow larger supramolecular systems to be constructed. Complexes were characterised by spectroscopic (NMR, UV/Vis, Luminescence) and electrochemical techniques. Their properties were found to be pH dependent. In every case, the emissive excited state of the ruthenium complexes was determined to be located on the bpy ligands.

Chapter 4 is concerned with the synthesis and characterisation of the $Ru(bpy)_2$ and $Ru(d_8\text{-}bpy)_2$ complexes of novel 5-phenyl-3-(2-pyrazyl)-1,2,4-triazoles, analogous to those described in Chapter 3. The presence of the strongly π-accepting pyrazine alters the electronic properties, with respect to the pyridyl triazole complexes. Again, spectroscopic and electrochemical studies display a strong pH dependency. The location of the excited state was pH dependent, with it being bpy-based above pH 4, while below this pH, results were inconclusive.

In Chapter 5, the complexes prepared in Chapters 3 and 4 are used to prepare more complex systems. In collaboration with Prof. Åkkermark in Sweden, two tyrosine containing complexes were prepared, as models of the tyrosine Y_z, which is located between P_{680} and the manganese cluster in Photosystem II. A range of ruthenium complexes containing potential manganese chelating ligands were also prepared. Due to chromatographic problems, it was not possible to isolate them in a pure form. In collaboration with Prof. Girerd in Paris, a Ru-Tyr-Mn_2 system was prepared and characterised. The manganese atoms were found to be antiferromagnetically coupled, giving rise to similar EPR and magnetic susceptibility measurements to a known model manganese complex.

The work presented in Chapter 6 was carried out in collaboration with Prof. Fuhrhop in Berlin, where a novel bola amphiphile was prepared. It is hoped that this may be used to prepare a rigid membrane containing Ångstrom gaps, which may be closed by complexation with ruthenium. The ruthenium complexes of the interemediates were also prepared and characterised by spectroscopic and electrochemcial techniques.

Finally, Chapter 7 gives an overview of the work that is presented in this thesis and suggests further experiments, which may be carried out in future studies.

Table of Contents

Chapter 3 The Synthesis and Characterisation of Ruthenium (II) Complexes Containing Novel 3-(2'-Pyridyl)1,2,4-Triazole Ligands

Chapter 4 The Synthesis and Characterisation of Ruthenium (II) Complexes Containing Novel 3-(2'-Pyrazyl)1,2,4-Triazole Ligands

Chapter 5 Ruthenium Pyridyl Triazole and Pyrazyl Triazole Complexes as Building Blocks for Supramolecular Systems

Chapter 6 The Synthesis and Characterisation of a Novel Lipid and its Ruthenium Complex

Chapter 1

Introduction

1.1 Photosynthesis

Literally, photosynthesis means assembly by light. It is probably the second most important process in the world, with only respiration being more important. Reduced to its most basic terms, it is how plants make food and oxygen from carbon dioxide, water and sunlight (*Fig. 1.1*). All forms of life in the universe require energy to live and grow. Whereas animals cannot directly use sunlight to provide us with energy, plants and photosynthetic bacteria can. They utilise it to make the food, which they and animals need to survive. Thus all life in the universe owes its existence to the sun and the energy it supplies.

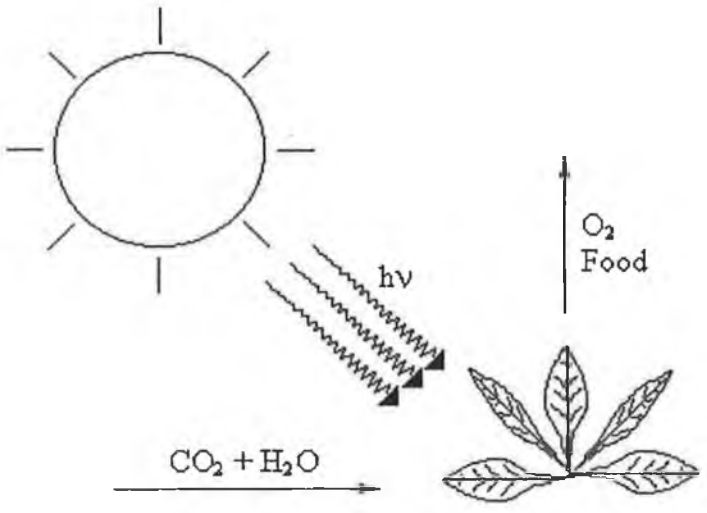

Fig. 1.1 Photosynthesis

The sun provides the Earth with a huge amount of energy. Every year, about 5.6 x 10^{24} J of heat strike the Earth's atmosphere. However, the Earth is not very efficient at using this energy. About 50% of it is reflected directly back off the atmosphere, another 40% of what filters through is reflected back by seas, oceans and deserts and

from what is left, only about 50% is usable by plants (the rest being low energy infra red radiation). Even plants only use approximately 0.2% of this usable incident radiation in photosynthesis[1]. But this is still enough to produce more than 10 times the amount of food/fuel needed by the world each year.

Apart from providing us with a source of energy (food), photosynthesis has another extremely important function. It regulates the composition of the atmosphere. During photosynthesis, carbon dioxide is removed from and oxygen is added to the atmosphere. This is achieved this very efficiently. All the CO_2 in the atmosphere is recycled every 300 years, and the O_2 each 2000 years.

Research into photosynthesis has been ongoing for the last 350 years. Starting with very simple experiments, like van Helmont who concluded that the material of a tree came from water and not from soil, experiments may now involve techniques such as x-ray measurements on mutated chloroplasts[2]. Many fundamental discoveries were made along the way. Priestly found that green plants were able to reverse the respiratory process of animals. Ingenhousz discovered that the green parts of plants evolved oxygen only when in sunlight. Pelletier and Caventou isolated chlorophyll in the early 19th century and later that century Engelman showed that oxygen was actually evolved from the chloroplasts. Nowadays the research being carried out into photosynthesis is at a much more advanced level, looking at its molecular and supramolecular aspects. Advances in instrumentation in the last 100 years have lead to such research becoming a reality.

As previously mentioned, photosynthesis occurs in green plants, algae and photosynthetic bacteria. Photosynthetic organisms can be split into two distinct classes of organisms shown in the following table[3].

Prokaryotes	**Eukaryotes**
Single cell or little complexity	Multicellular, complex intercellular interaction
Cell nucleus without membrane	Cell nucleus with membrane
Photosynthesis in vesicular membranes not in discrete compartment	Photosynthesis in vesicular membranes in discrete compartment – chloroplast
Anoxygenic forms – Sulphur bacteria Do not evolve O_2 – Evolve S	Anoxygenic forms – None
Oxygenic forms – Blue green algae Evolve O_2. Reduce gaseous N_2	Oxygenic forms – Algae, Higher Plants Evolve O_2. Do not reduce gaseous N_2

Table 1.1 Comparison of photosynthetic organisms

The mechanism by which photosynthesis occurs in prokaryotes differs significantly from the mechanism in eukaryotes. In prokaryotes, the light absorbed causes H^+ to be transported to the outside of the cell. This sets up a pH gradient and a charge on the membrane, which provide the energy for the synthesis of ATP as the protons diffuse back into the cell through an ATP synthesising enzyme. There is no electron transfer associated with this type of photosynthesis.

Photosynthesis takes place in the thylakoid membrane in the chloroplast of cells of green plants. Chloroplast can be seen as being like an envelope, which contains the thylakoid membrane. The membrane is arranged in such a manner such that there are stacks (grana lamellae) interconnected by a system of loosely arranged membranes called the stroma lamellae.

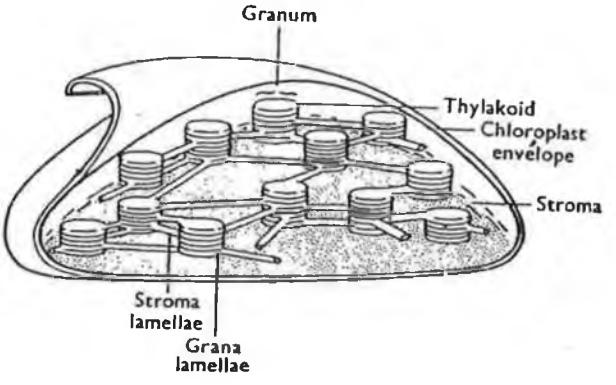

Fig. 1.2 Arrangement of thylakoid membrane within chloroplast[4]

The thylakoid membrane is of vital importance in the photosynthetic process. Photosystems (PS) I and II are both imbedded in it in optimal positions to ensure the oxygen is evolved far away from the site where NADP is reduced[5].

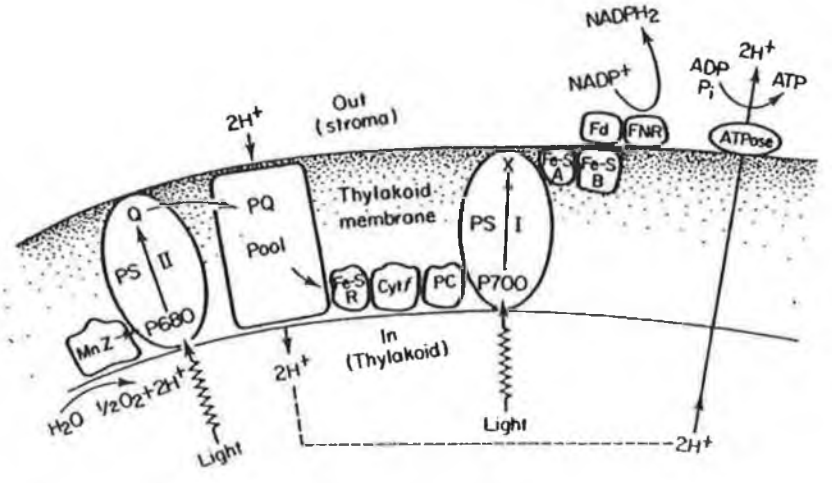

Fig. 1.3 Relative positioning of PSI and PSII in thylakoid membrane[4]

In 1984 Deisenhofer et al. reported the three dimensional of the photosynthetic reaction centre of Rps. viridis[6]. This has resulted in a much greater interest[7], and hence, understanding of the mechanism of photosynthesis in bacteriochlorophyll[8]. However, although no adequate crystal structure has yet been obtained of PSII, the use of many other analytical techniques has lead to a general understanding of its structure (See Fig. 1.4).

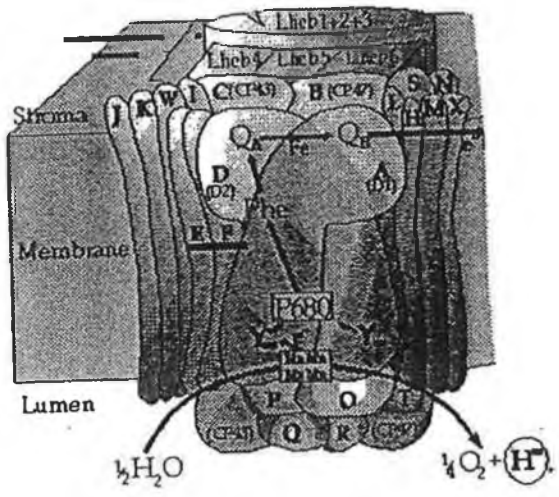

Fig. 1.4 Schematic representation of PSII[9]

Upon illumination of the chloroplast, light is absorbed by the "antenna" of chlorophylls and carotenoids. The chromophores in the antenna are capable of absorbing light of various wavelengths, thus increasing the efficiency of the system. Regardless of which species absorbs the light, the net effect is always the same. This photoexcited electron is channelled to P_{680}, to the special pair of chlorophylls. The P_{680} donates its electron to a pheophytin molecule (H_A) and on to the quinones (Q, Q_B)[5]. At this point the electron migrates via cytochrome f to P_{700} in PSI[10]. It is in PSI

that $NADP^{2+}$ gets reduced to $NADPH_2$. This, along with the ATP formed upon the transfer of electrons from the quinones to cytochrome f, is required for fixation of CO_2 when synthesising carbohydrates. Having lost an electron, the P_{680} is now capable of oxidising a tyrosine residue, called Z or Yz, which in turn receives its electron back from a cluster of manganese atoms. The manganese cluster acts as a store for positive charge. After completing the cycle four times, it has accumulated a +4 charge. By receiving four electrons from water it returns to its ground state and two molecule of water is oxidised to a molecule of O_2 and four protons. As of yet no definite structure for the manganese cluster has been determined, but it is generally thought to be a dimer of dimers. This electron transfer mechanism between the two photosystems is clearly shown in the "Z" scheme in *Fig. 1.5*.

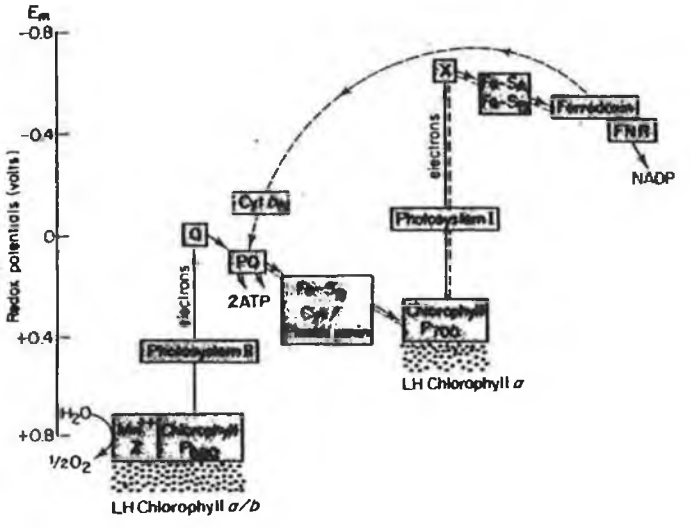

Fig. 1.5 The Z scheme of photosynthesis[4]

It must be stressed that the exact structure of PSII is not yet known. However, most of its elements have been well characterised and documented. There has been much debate on the structure of units such as the manganese cluster and the exact role of chloride or calcium[11]. Issues such as the location of the water which is ultimately

split by the system, or the amount of hydrogen bonding which is present, have produced many varying theories. Until a crystal structure of high resolution is obtained, one will not be able to say conclusively what the precise orientation and role of each component is, in relation to the overall system[12]. However, the amount of information there is available about the system at present is sufficient for preliminary artificial models to be designed.

As there are two different photosystems involved in photosynthesis, artificial photosynthetic models may be concerned with either the oxidation (PSII) or the reduction (PSI) of water. In either case, the same principles apply. A suitable photosensitiser must be coupled to a suitable electron donor or acceptor and of course, a high turnover for the reaction is required. Research is still striving for the "Holy Grail", a clean renewable storable fuel source from sunlight and water.

In the remainder of this chapter, the issues related to mimicking photosynthesis shall be discussed. Many of the artificial systems which have been prepared no longer use porphyrins as the photosensitiser[13], but metal complexes, such as $[Ru(bpy)_3]^{2+}$, whose properties may be altered by ligand substitution[14]. Some examples of these will be examined in Section 1.2. Various examples of supramolecular systems which may carry out complex functions, such as vectorial electron transfer, are presented in Section 1.3. Water oxidation catalysis shall be introduced in Section 1.4, which deals with both the oxygen evolving complex (OEC) and some synthetic attempts to bring about water oxidation. Finally, all of these aspects are combined in Section 1.5, which focuses on the study of Ru-Mn systems.

1.2 The Chemistry of Ruthenium

Ruthenium was first reported as a distinct metal in 1884 by Karl K. Klaus, an Estonian scientist, who named it after the Latin name for Russia[15]. It is one of the six platinum group metals and has many uses, ranging from the hardening of platinum alloys to its use in the formulation of eye drops. However, its most common and perhaps its most significant use is in catalysts. Although ruthenium has shown up to 10 different oxidation states, most research into ruthenium chemistry has focused on the +2 state.

In particular, the chemistry of ruthenium(II) complexes containing polypyridyl ligands such as 2,2'-bipyridine (bpy). $[Ru(bpy)_3]^{2+}$ is probably the most important of all the ruthenium complexes. Since the discovery of its luminescence in 1959[16], an extremely detailed study of its photochemical and electrochemical properties has been undertaken[17]. It presents itself as an ideal chromophore for use in supramolecular systems and as a result, large numbers of derivatives have also been prepared and characterised[18]. Ru(II) complexes are stable low spin d_6 species which can be oxidised by the removal of a metal centred electron, or reduced by the addition of an electron into a π^* orbital of a ligand. It is capable of coordination with a wide range of ligands. Nitrogen[19], oxygen[20] and phosphorous-containing ligands have all been reported as forming complexes with Ru(II).

In the case of octahedral transition metal-ligand complexes a wide variety of electronic transitions are possible as shown in *Fig. 1.6*. In the case of the complexes,

whose preparation and characterisation is presented in this work, the transitions which are principally of interest are MC (metal centred), LC (ligand centred) and MLCT (metal to ligand charge transfer). LMCT (ligand to metal charge transfer) transitions are also possible, but are not observed for any of the model complexes cited in this thesis.

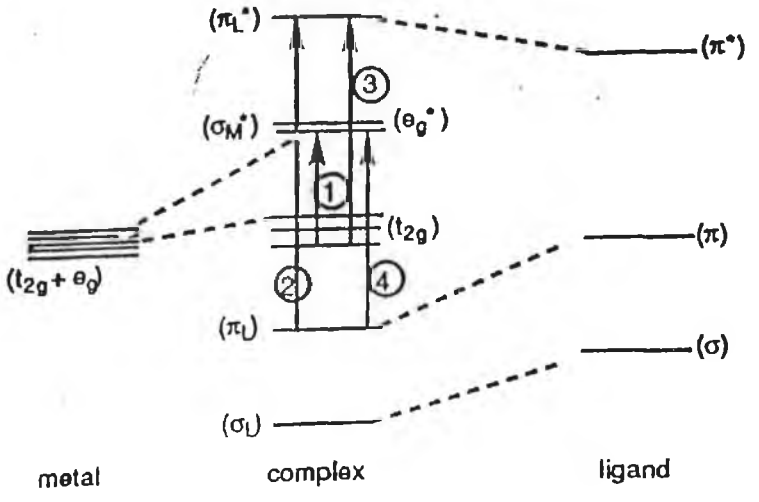

Fig. 1.6 Relative disposition of metal and ligand orbitals and possible electronic transitions in an octahedral ligand field of a transition metal complex[21]

The main feature in the UV-Vis spectrum of $[Ru(bpy)_3]^{2+}$ is the intense ($\varepsilon \sim 10^5$ $M^{-1}cm^{-1}$) MLCT absorption at 452nm, which is due to excitation of an electron to a π^* level of a ligand (LUMO) from the t_{2g} level of the ruthenium centre (HOMO). Hence this is also the lowest energy transition in the absorption spectrum. Excitation of an electron from the ground state results in population of the ^{1}MLCT level. This state is unstable and decays via inter system crossing to the triplet state[22], with an efficiency of 1. Deactivation of the triplet state can occur by any of three different processes:

i. Emission to the ground state (k_r)

ii. Radiationless decay to the ground state (k_{nr})[23]

iii. Population of the ^{3}MC state

In the diagram below, these basic photophysical transitions observed in $[Ru(bpy)_3]^{2+}$ are illustrated[21].

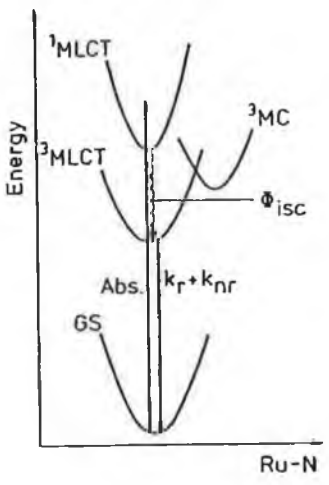

Fig. 1.7 Schematic representation of photophysical properties of $[Ru(bpy)_3]^{2+}$

The excited state lifetime of this compound is of the order of 1μs. This in itself is one of the main features which makes it such a suitable candidate for use in photomolecular devices (PMD). Despite this, it is not a perfect photosensitiser, due to the nature of the possible deactivation pathways. Population of the ^{3}MC state is in most cases undesirable. Due to the proximity of the MLCT and ^{3}MC states, thermal activation is sufficient to promote an electron from the MLCT to the ^{3}MC. This results in non-radiative decay or even photodecomposition of the complex. Photodecompostion occurs in a stepwise manner. It proceeds in the following manner. Photoexcitation of $[Ru(bpy)_3]^{2+}$ results in the population of the MLCT. Thermal activation of the excited species leads to the population of the ^{3}MC. Subsequently a Ru-N bond is broken, resulting in a five coordinate intermediate[17].

This can then react in a number of ways. A molecule of solvent or counterion may coordinate in the place of the pyridyl or the pyridyl may recombine with the ruthenium to give the bicoordinate bpy ligand once more[24]. Temperature dependency studies have shown the decreased photochemical stability at elevated temperatures. In fact, at 95°C in aqueous solution, the degree of photodecomposition is quite dramatic[25]. This has resulted in much interest into the possibility of increasing the photostability of similar compounds by changing the energy difference between the MLCT and the ^{3}MC states.

In general, the properties of a coordination complex are governed by the electronic properties of both the metal and the ligands involved. In the case of improving the properties of $[Ru(bpy)_3]^{2+}$, either the metal centre or the ligands must be substituted in order to give the desired range of properties. Should one wish to alter the metal centre, there are two other metals which one would instantly suggest, iron or osmium. These metals have the same outer shell electronic configuration (Group 8A) as ruthenium and should therefore possess similar properties. However, this is found not to be the case. $[Fe(bpy)_3]^{2+}$ does not luminesce or absorb significantly in the visible region. This is due to the low lying MC state[26]. $[Os(bpy)_3]^{2+}$ on the other hand does emit, albeit at a longer wavelength (>700nm) and with a short excited state lifetime. It is also more stable to photodissociation due to its low lying MLCT state[27]. However, synthetically it poses a different problem due to its lack of reactivity.

Should one desire to alter the ligands, which are bound to the metal centre, there is an important factor which one should note. Ligands may be classed based on two

criteria: σ-donation and π-acceptance. A σ-donor (class A ligand) donates electron density to the metal centre, resulting in a shift in reduction potentials of the complex to more negative values. Conversely, π-acceptor (class B) ligands remove electron density from the metal centre of the complex. This results in less negative reduction potentials. Examples of strong π-acceptors are 2,2'-bipyridine[28], 2,2'-bipyrazine (bpz)[29], 2,2'-biquinoline (biq)[30] and 1,10-phenanthroline (phen)[31], whereas imidazoles[32], pyrazoles[33] and triazoles[34] have all been used as strong σ-donors. Both homo- and heteroleptic Ru(II) complexes of these ligands have been prepared and characterised.

The characteristics of a ligand also affect the photochemical properties of a complex. π-Acceptor ligands result in a shift to lower energy of the absorption spectrum of the corresponding Ru complex. As a result, the complex harvests a larger portion of the solar energy[35]. Unfortunately, they also have a disadvantage associated with them. The resulting complex has a smaller ligand field splitting. Consequently, the ^{3}MC is more easily accessible and photodecomposition is a greater problem[36]. The emission yield of the complex is also diminished by this reduction in field splitting. On the other hand, σ-donor ligands increase this splitting. Accordingly, the ^{3}MC is raised in energy compared to the ^{3}MLCT. The desired effect of increased photostability is thus obtained. Unfortunately, the π^* level of the ligand is at quite a high energy, so the energy gap between it and the d-orbital of the metal is significantly increased. The net result is a blue shift in the absorption and emission spectra.

However, by combining the two systems, a π-acceptor and a σ-donor, it is possible to synthesise a system which possesses both the low energy absorption of π-acceptors and the photostability of σ-donors. Mixed ligand systems are the method by which this state is achieved. It is thought that substitution of just one of the bpy ligands in $[Ru(bpy)_3]^{2+}$ with a σ-donor ligand could give the desired result. The new ligand serves as a spectator ligand – altering the properties but not partaking in the photochemistry.

Pyridyl triazoles (ptr), (a bidentate ligand containing a triazole), have been shown to be very versatile type of ligand. The triazole contains two different coordination sites, giving rise to the possibility of coordination isomers (shown in *Fig. 1.8*). In general these isomers are easy to separate by chromatography or recrystalisation and possess differing photochemical and electrochemical properties[37]. The ruthenium may bind via the N2' or the N4' of the triazole. The N2' site is known to be a stronger σ-donor than the N4' site. This stronger σ-donation of N2' can be observed in the value of the pK_a for the protonation of the free nitrogen in the complex. N2' coordination results in a lower pK_a than for N4'[38].

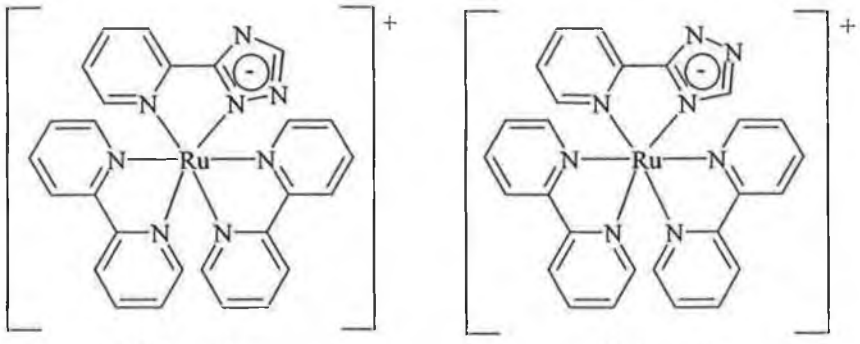

Fig. 1.8 Coordination isomers of [Ru(bpy)2ptr](PF6)

As well as the possibility of coordination isomers, the properties of pyridyl triazoles may be altered by adjusting the pH[39]. Normally, the triazole is deprotonated upon coordination to the metal centre. This may easily be protonated in acidic medium. Upon protonation, the photochemical and electrochemical properties of the complex are significantly altered. The emission intensity tends to decrease considerably upon protonation. The MLCT of the complex also shifts to lower energy at low pH. This occurs because the triazole is no longer such a good σ-donor when it does not have a negative charge[39]. The oxidation potential for the Ru(II) centre in a complex containing a negatively charged triazole is typically around 0.85V vs. SCE. However, this can be simply increased by up to 300mV by protonation (or methylation – See Appendix B) of the triazole[40]. This gives a new oxidation potential of approx. 1.2 V (vs. SCE), compared with 1.26 V (vs. SCE) for $[Ru(bpy)_3]^{2+}$. This demonstrates the loss in σ-donation of the triazole upon protonation, and how a pyridyl triazole complex may be used as a "molecular switch" in which its properties are altered by changing the pH.

A further method for improving the properties of $[Ru(bpy)_3]^{2+}$, is by the use of terpy, (2,2':6',2''-terpyridine) instead of bpy. Terpy is a tridentate ligand. In photophysics studies, it is usually desirable to know the exact distance between the electron donor and acceptor of a dyad in order to calculate accurate rates of electron transfer. However, in the case of a complex containing three bidentate ligands, the geometry is complicated. The components cannot be in a linear arrangement, which results in inaccurate rate constants being obtained. However, $[Ru(terpy)_2]^{2+}$ possesses C_2 symmetry. This symmetrical arrangement of the complex (*Fig. 1.9*), in which an

electron donor and acceptor may be placed on opposite sides of the central Ru atom at 180° to each other, lends itself to the possibility of obtaining vectorial electron transfer.

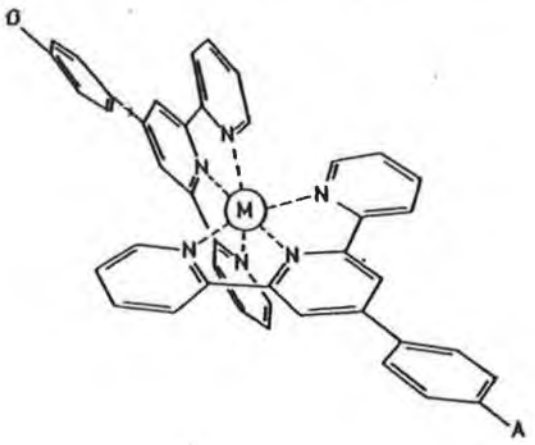

Fig. 1.9 Linear arrangement of components in a $[Ru(terpy)_2]^{2+}$ triad[41]

However, terpy has two major disadvantages when compared with bpy. The excited state lifetime of $[Ru(bpy)_3]^{2+}$ in MeCN is approximately 1μs[42], whereas the lifetime of $[Ru(terpy)_2]^{2+}$ is approximately 250ps[43]. Weak emission is observed for the terpy complex. Much of the current research into this compound is focussed on the improvement of the excited state lifetime. If it were possible to design a system with the rigidity and symmetry of $[Ru(terpy)_3]^{2+}$ with the photochemical properties of $[Ru(bpy)_3]^{2+}$, then an ideal photosensitiser for a triad could be obtained.

Work currently being carried out[44] has resulted in a terpy analogue containing of a novel ligand containing both a good π-acceptor and a good σ-donor. This tridentate ligand consists of a pyridine flanked on either side by a triazole and is shown in *Fig. 1.10*. As already mentioned, triazoles are extremely versatile ligands. Their

properties are easily altered by adjusting the pH. Substitution of one of the terpy ligands in the ruthenium complex with this "triazole terpy" has produced some very interesting results. The new complex, shown below, has a longer lifetime and dramatically increased luminescence. It appears that this compound will be much more useful in triads than both $[Ru(bpy)_3]^{2+}$ and $[Ru(terpy)_2]^{2+}$.

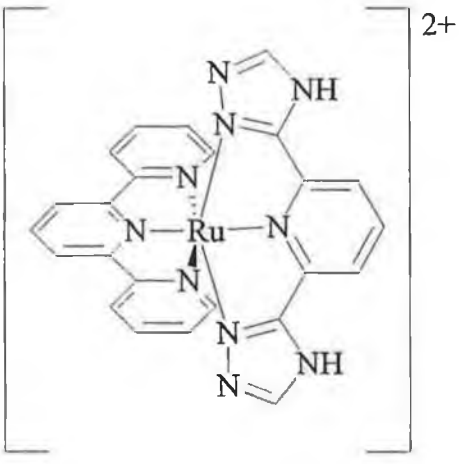

Fig. 1.10 [Ru(terpy)(triazole terpy)]$^{2+}$

Ruthenium polypyridyl complexes are extremely interesting compounds due to their photochemical and electrochemical properties. However, their basic electronic structure can also result in some significant problems with their usage. Modifications of standard systems, such as $[Ru(bpy)_3]^{2+}$ or $[Ru(terpy)_2]^{2+}$, by ligand substitution have resulted in a wide range of complexes with significantly altered characteristics. By careful choice of ligands with which to make the mixed ligand systems, it is possible to eliminate the undesired characteristics while still maintaining the important properties of the initial compound[45]. Triazoles have proven themselves to be a useful substitute in ruthenium polypyridyl complexes. The replacement of a

pyridyl ligand with a triazole should improve stability in bpy type complexes and also significantly improve the photophysical properties of terpy type complexes.

1.3 Supramolecular Chemistry

From a photochemical and electrochemical viewpoint, a supramolecular species may be defined as a complex system made of molecular components with definite individual properties. The properties of the supramolecular species are a combination of the properties of the individual constituents. The criteria for the classification of a species as a supramolecular species as distinct from a large molecule are shown in *Fig. 1.11* below.

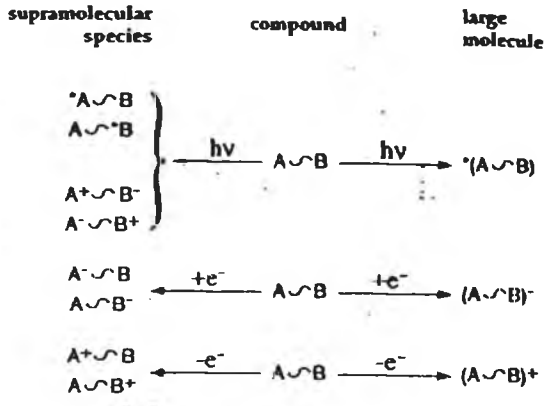

Fig. 1.11 Criteria for the classification of a species as a supramolecular species[46]

This illustrates that when a supramolecular system undergoes an electronic transition, the effect of the transition is localised on a certain part or parts of the species and not delocalised over the whole molecule as would happen with a large molecule. This fact is fundamental in supramolecular chemistry, in which systems are made to carry out complex transformations. Supramolecular systems come in many different forms. Ranging from rotaxanes[47] to metal complex dendrimers[48], their functions are many and varied[49].

Molecular devices of various types have recently been synthesised in this rapidly growing area of research. Of the many different synthetic approaches to complicated molecular structures, two frequently used methods are "self assembly" (Chapter 6) or "template synthesis"[50]. In many cases, the procedure involves the use of coordination chemistry to position the molecules in a specific orientation[51]. This is similar to many methods for asymmetric synthesis in organic chemistry. Complexation reactions with suitable metals and subsequent demetallation reactions at various stages of the synthesis are of key importance.

With clever planning, some remarkable structures have been obtained. P. N. Baxter et al[52]. have synthesised multicomponent and multicompartmental cylindrical nanoarchitectures (as in *Fig. 1.12*) by means of self-assembly. Using Ag(I) and Cu(I), they have made cylindrical compounds with a combination of linear oligobiypyridines and the circular ligand hexaazatriphenylene. The metals act as a sort of glue, holding the structure in place. This style of compound could prove to be of interest in nanotechnology due to the host guest phenomenon observed. It was noted that the cavities in the system showed a preference for the inclusion of triflate ions over PF_6^- ions was observed. This was accounted for by means of molecular modelling, which proved that the portals in the walls were slightly smaller than a PF_6^- ion. Multiple guest inclusion and compartmentalisation are characteristic features of the organisation of living organisms, ensuring that the correct chemical events take place within spatially confined, well-defined domains. Thus, these types of compounds could be thought of as biomimetic models for multicompartmental proteases, for example.

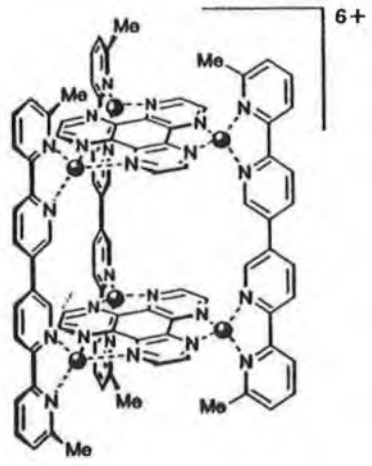

Fig. 1.12 An example of a compartmental nanoarchitecture[52]

This idea of designing supramolecular systems to carry out an operation on a nanoscale has been adopted by many researchers. A molecular level "plug/socket" system has been reported[53], employing a crown ether derivative as the socket and a wirelike compound bearing an anthracene unit as the plug (*Fig. 1.13*). The properties of the supramolecular system change depending on whether the system is "plugged in" or "unplugged". Under basic conditions, the system was deemed to be unplugged, i.e. there was no supramolecular interaction between the two components of the system. Rapid exchange between the complexed and uncomplexed forms of the two constituent parts was observed indicating no net interaction. The normal properties of both species could still be observed. However, protonation of the "plug" by lowering the pH, resulted in the "plugged in" state. Under these conditions, the system remained in the complexed form. Upon illumination, it was noted that energy transfer form the binaphthyl to the anthracenyl unit took place. This energy was then re-emitted by the anthracene moiety at a longer wavelength.

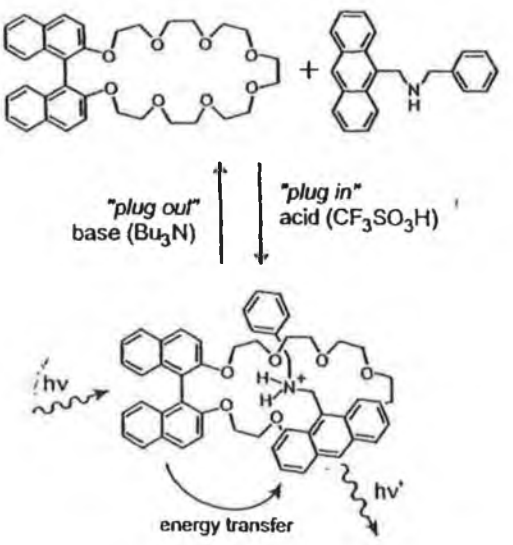

Fig. 1.13 Reversible acid/base properties of a molecular plug/socket[53]

A system such as this is an excellent model for a molecular switch, due to the significant alteration in the properties of the species, in this case the photophysical properties, upon changing of the pH. The reaction is reversible and thus presents itself as a potentially useful component for nanotechnology.

Supramolecular chemistry is of vital importance in the area of sensor research. By taking advantage of potential changes in photochemical properties, extremely sensitive sensors may be produced. Host-guest chemistry in particular plays a critical role in this area. Calixarenes, crown ethers and cyclodextrins have all been used in a variety of applications[49]. However, by covalently linking such receptors to fluorescent compounds such as $[Ru(bpy)_3]^{2+}$, a wide range of sensors may be prepared which display the selectivity of the receptor and the photochemical properties of the ruthenium complex[54]. The range of functions which the complex may serve is wide. Crown ethers linked to $[Ru(bpy)_3]^{2+}$ via amide linkages have shown selectivity towards HPO_4^- over Cl^-, in the absence of K^+, but the reverse was

found to be true when in the presence of K^+ ions[55]. The addition of a pendant terpy ligand to $[Ru(terpy)_2]^{2+}$ provides a simple sensor for zinc (II), resulting in a 10 fold increase in the luminescent lifetime upon detection[56]. Even without the use of an auxiliary receptor, complexes such as $[Ru(dpp)_3]^{2+}$ (where dpp = 1, 10-diphenyl phenanthroline) may serve as sensors in their own right. The intensity of its luminescence has been found to be quenched in the presence of oxygen. As a result, immobilisation of a small amount of such a compound in a suitable polymer results in a simple oxygen sensor[57].

Although the possibility of designing novel systems for nanotechnology is very appealing, biological systems offer an even wider range of challenges to the supramolecular chemist. One of these challenges is in the emulation of route specific electron transfer. In the case of the bacterial photosynthetic centre, there is such a problem. Electron transfer from the photoexcited porphyrin special pair to a quinone moiety takes place along the L-branch rather than the M-branch. This problem has been investigated by a number of researchers, utilising different approaches.

One of these systems utilises a relatively small compound (*Fig. 1.14*), which displays this electron transfer path selectivity[58]. It offers two almost identical pathways for electron transfer, differing by only a slight modification in the amine donor. It was noted that the positioning of the electron donor, and hence the PET route, was more important than the exact nature of the donor in determining the direction from which the electron comes.

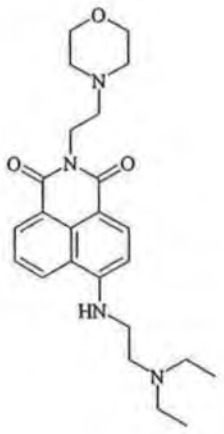

Fig. 1.14 Supramolecular system with two possible electron transfer pathways[58]

Other approaches have involved the synthesis of catenanes covalently linked to ruthenium (II) complexes[59,60]. The complexes act as photosensitisers, whilst a 4,4'-bipyridinium moiety incorporated into the cyclophane served as the electron acceptor. Again, different electron transfer routes would be possible, but electrochemical and spectroscopic means clearly indicated a preference for one route over another. It could be deduced that apparent chemical equivalence was not always true. Environmental aspects, such as the interaction between the two interlocking rings of the catenane, could be large enough to introduce a degree of electronic asymmetry into a symmetrical molecule. The importance of environmental (e.g. solvent, hydrogen bonding, 3-D structures, etc.) factors is fundamental in supramolecular chemistry.

Much work has been done on supramolecular dyad/triad and even hexad[61] systems as models for photosynthetic reaction centres. These usually consist of larger, more complex structures than some of the previous systems and examine the

supramolecular interactions on a larger scale. The types of systems studied range from porphyrins to catenanes to dendrimers, but each compound emulates one or many features found in complex natural systems. They provide an insight into the workings of the natural world and bring us a step closer to being able to produce biomimetic systems, which reproduce important natural reactions, e.g. artificial photosynthesis.

The first step in the photosynthetic system is absorption of light by the antenna system. This can contain over 200 chlorophylls, which channel the energy obtained from the incident light to a special pair of chlorophylls, from which the main process of water splitting commences. This process has been the source of inspiration for work done on the synthesis and characterisation of metal complex dendrimers[62]. The use of dendrimers requires an excellent knowledge of the physical properties of various ligands and metals. If a dendrimer system is to act as an antenna device, then the photoexcited electrons must be channelled through the molecule in an organised fashion. The figure below shows some possible routes for electron migration in a tetranuclear dendrimer.

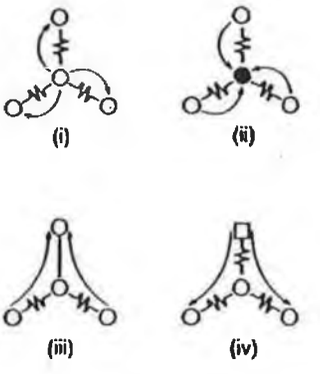

Fig. 1.15 Energy migration patterns in tetranuclear compounds[46]

The number of possible routes increases again upon creation of another coordination sphere. The synthesis of a useful dendrimer requires careful planning of the route, along which the energy transfer will take place. However, by breaking this transfer in the compound down into a series of stepwise events, an effective system can be come upon. For example, in the case of a tetranuclear dendrimer where it is hoped to channel energy to the central metal atom, the three peripheral complexes should all be the same. Also, the π^* level of the terminal ligands must be higher than that of the bridging ligands. This would make population of the bridging ligand π^* more energetically favourable and therefore channel the energy to the central metal atom. The use of ligands such as bpy, and 2,3-bis(2-pyridyl)pyrazine in conjunction with metal such as ruthenium and osmium have produced many systems exhibiting directional electron transfer[63].

The benefits reaped by directing the flow of electrons in a system is also evident in the use of dyads and triads. A dyad consists of a photosensitiser and an electron donor or acceptor, while a triad contains all three species[64]. Two types of sensitiser have been studied extensively, porphyrin systems and ruthenium polypyridyl complexes. Both examples have the advantage of being easy to functionalise, which is necessary when synthesising a dyad or triad. While porphyrins are present in many natural systems and zinc porphyrins have proven themselves to be excellent electron donors[65], ruthenium complexes can easily be tuned to possess certain photochemical properties[66].

Many electron donors have been put forward for use in dyads, e.g. phenothiazines[67,68], or manganese complexes (See Chapter 1.6). A wide variety of bridging ligands have been investigated[69,70] and the results obtained have all pointed to the exact positioning of the donor as being crucial in determining electron transfer rates. Electron acceptors for such systems are often fullerene based[71] due to their ability to be functionalised and their excellent capability to accept large amounts of electrons. By combining a compatible electron donor, sensitiser and acceptor in the one ruthenium (II) complex, one can obtain good electron transfer data, such as in the case of Ru-Anthraquinone dyads[72] or Phenothiazine-Ru-Viologen triads[73], due to the knowledge of the exact donor-sensitiser-acceptor distances. Such systems can be seen to mimic the initial events which occur in natural photosynthesis.

Almost all of the supramolecular systems mentioned in this section have been studied in solution. While this is synthetically easier to achieve, it is not an accurate picture of a biological system. In biological systems there are many more aspects which influence reactions which occur. One of the most important factors is that most of the vital components in a system such as PSII are actually held in place by a protein or a membrane. As a result, artificial photosynthetic models have also been prepared in proteins[74] and lipid membranes[75].

Surfactant ester derivatives of $[Ru(bpy)_3]^{2+}$ have been prepared and characterised. Langmuir Blodgett films of the complexes on water surface have been prepared and displayed a luminescence dependency on the counterion[76]. Possible hydrogen evolution has also been observed for monolayers at a solid/water interface upon

illumination[77]. In another approach, $[Ru(dcHb)_3]^{4-}$, where (dcHb) is 4,4'-dicarboxy 2,2'-bipyridyl, was found to bind to a preformed lipid bilayer incorporating a methyl viologen (MV) derivative. This resulted in a Ru-MV dyad[78] (shown in *Fig. 1.*16) in which the reduced acceptors formed by photoinduced electron transfer could possibly be withdrawn from the external interface of the vesicle to the interior, where their electrochemical energy might potentially be utilised in secondary reactions. This would be analogous to the transmembrane electron transfer featuring in photosynthesis.

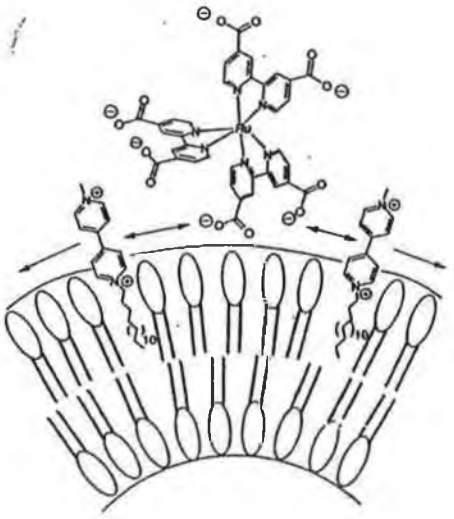

Fig. 1.16 A membrane bound Ru-MV^{2+} dyad[78]

The area of supramolecular chemistry is bringing us more and more insight into complex biological functions and into the possibilities of nanotechnology. By synthesising rather basic systems, complex electronic reactions may be observed. These, in turn, lead to more effective biomimetic models which will hopefully lead

to a fuller understanding of natural processes and possibly to successful mimicking of natural systems for our benefit.

1.4 Water Oxidation Catalysis

In photosystem II, water oxidation is carried out by a cluster of four manganese atoms. This cluster is known to be located in close proximity to a tyrosine moiety, (Yz). However, the mechanism of photosynthetic water oxidation remains, for the most part, an unresolved problem[79]. Despite the recent publication of the first x-ray diffraction model of an oxygen evolving photosystem II complex[80], the resolution was not sufficient to give a clear picture of the environment in which the manganese cluster lies. While the precise structure of the manganese cluster remains unknown, x-ray absorption and EPR results aid in the proposal of plausible structures. In particular, EXAFS studies have pointed to the presence of a di-μ-oxo Mn dimeric unit. Despite the information available on the nature of the OEC (oxygen evolving complex), no model systems have yet been prepared, which match its catalytic properties.

Water oxidation is a four electron process, and the OEC is known to cycle through five intermediate oxidation states ($S_0 - S_4$), a cycle called the Kok cycle[81] (See *Fig. 1.17* below). Each transition requires one quantum of light, except for the final transition ($S_4 - S_0$), which is the spontaneous dark oxidation of water.

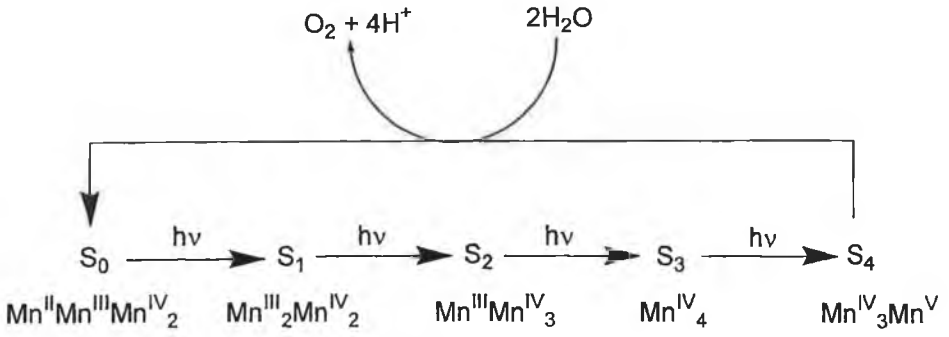

Fig.1.17 The Kok cycle

The S_0 and S_2 states may be studied using EPR spectroscopy, due to their being odd electron states. S_1 is the dark-stable state. It may be obtained from S_0 by either light or dark reactions. S_2 and S_3 are called metastable states; they are reduced spontaneously back to the S_1 state in the dark by recombination with electrons from reduced electron acceptors or by diffusible reductants in the chloroplast. S_4 is unstable and decays spontaneously back to the S_0 state. Upon decay, two molecules of water are oxidised to give one molecule of dioxygen.

Although the exact arrangement of the four manganese atoms in the manganese cluster is not yet known, many possible structures, including cubane[82] and dimer of dimer forms[83], have been proposed. Two of these in particular are widely accepted as being close to the real structure.

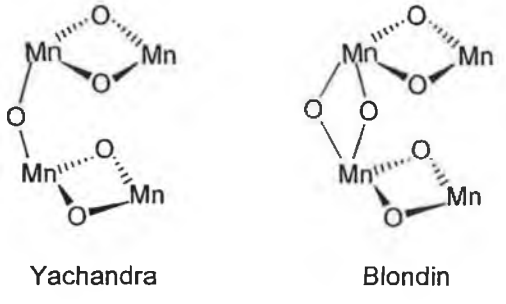

Fig. 1.18 Proposed structures of the OEC by Yachandra[2] and Blondin[84]

These two structures have helped in the development of possible mechanisms for the oxidation of water. However, there are many other factors to be considered when proposing a mechanism[85]. Calcium and chlorine are both necessary for the system to function properly. Calcium or chlorine depleted systems show no water oxidation, and even replacement of one or both of them, by strontium or bromine respectively, results in significantly lower O_2 evolution rates. Tyrosine is known to lie in close proximity to the manganese cluster and is thought to participate in hydrogen abstraction from a water molecule coordinated to a manganese centre[86]. There is also at least one histidine moiety present in the OEC. Again, its role is not totally understood, but it is assumed to have an activating effect on the Mn^{V}=O species[87], thought to be present in S_4, by being coordinated trans to the oxo group as shown in *Figs. 1.19 and 1.20.* In proposing a mechanism for the oxidation of water, all of the above-mentioned cofactors must be included and pieced together along with the various slivers of information, which may be elucidated from various spectroscopic methods of analysis. This makes the task of assigning a mechanism to the reaction an extremely challenging one.

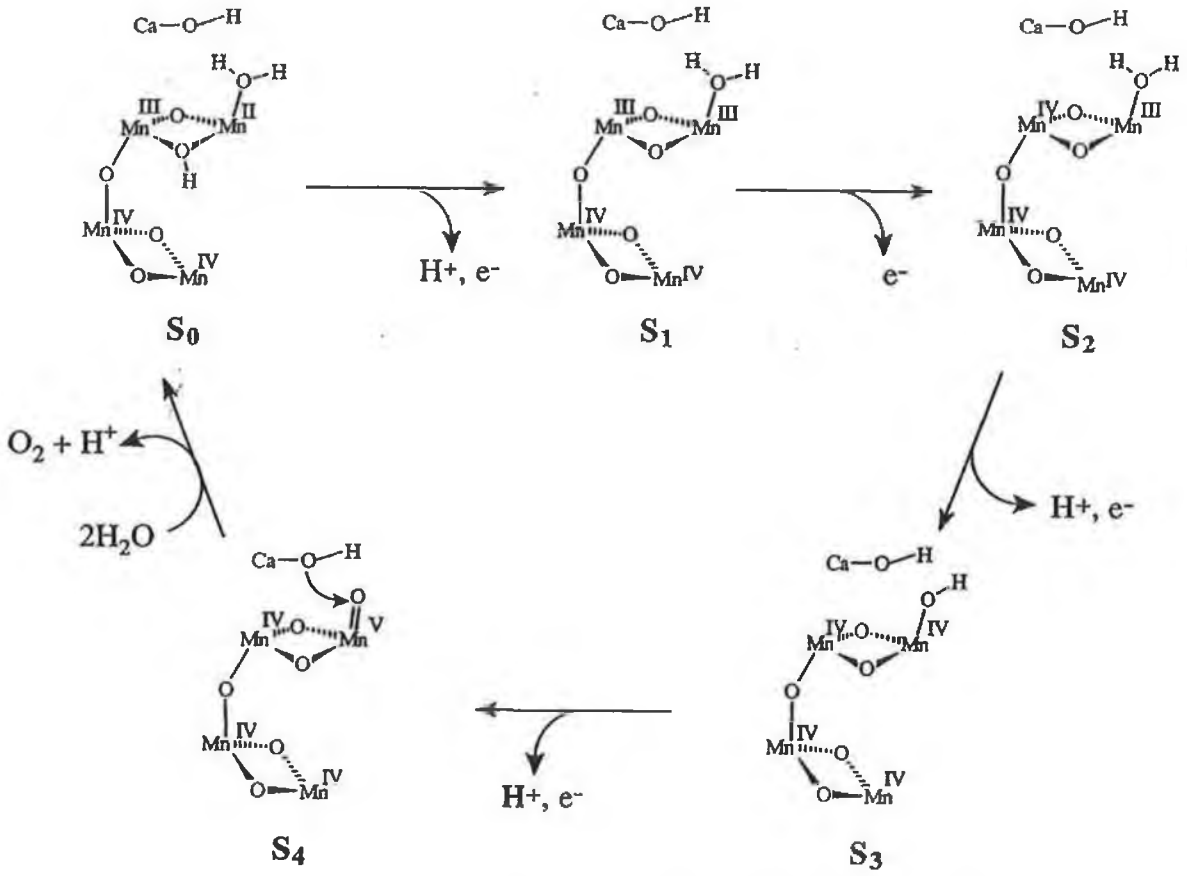

Fig. 1.19 Proposed S-state cycle of the OEC in PSII[87]

A more detailed view of the transitions from S_3 to S_4 and back to S_0, in which the chlorine, calcium, histidine and tyrosine are taken into account, is shown below.

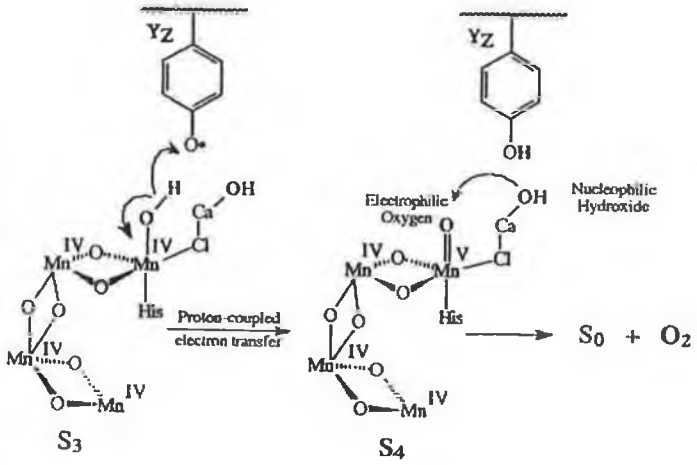

Fig. 1.20 Hypothetical O-O bond forming steps, showing the positions of Ca^{2+}, Cl^-, Yz and the Mn_4 cluster[87]

Well-defined catalysts for water oxidation are rare[88]. The thermodynamic requirements for the reaction are very demanding. However, catalysts have been prepared which do oxidise water successfully. One of these consists simply of an o-phenylene-bridged porphyrin manganese dimer[89]. This is the first example of the oxidation of water by a manganese complex via a four electron process. The exact mechanism is not known. However, due to the spatial arrangement of the porphyrins and knowledge of the coordination chemistry of manganese, a tentative mechanism may be suggested. $Mn^{III}OH$ may undergo a two electron oxidation to give the corresponding $Mn^{V}=O$. If HO^- ions coordinate to each Mn ion of the dimer inside the cavity, the resultant $Mn^{V}=O$ dimer could form a Mn^{IV}-O-O-Mn^{IV} complex, because of the proximity of the Mn ions. The peroxy bridge could be replaced by HO^- ions, and the simultaneous decomposition would give O_2 and the original Mn^{III} complex. Unfortunately this system is relatively unstable and only gives a turnover number of 9.2.

Ruthenium complexes may also serve as water oxidation catalysts. The use of ruthenium complexes as photosensitisers has been well documented. However, their use as potential water oxidation catalysts has not been studied to the same degree[90]. One ruthenium compound in particular has received a certain amount of interest. The μ-oxo dimer $[(bpy)_2(H_2O)Ru^{III}ORu^{III}(H_2O)(bpy)_2]^{4+}$ was first reported as a potential water oxidation catalyst in 1982[91]. As with most of the water catalysts studied, the turnover number is quite small – only 25 in this case, due to oxidative degradation of the catalyst[92]. (Even more dramatic degradation of the catalyst by substitution of ligands has been seen in $[(H_2O)_2(tpy)Ru^{III}ORu^{III}(tpy)(H_2O)]^{4+}$)[93]. The exact

mechanism by which oxidation of the water takes place is as yet uncertain. But it is known that sequential oxidation occurs in this "blue dimer" from $Ru^{III}ORu^{III}$ to $Ru^{V}ORu^{V}$ with loss of four electrons and four protons. The di-Ru=O species formed then evolves O_2 rapidly.

All of the above-mentioned water oxidation catalysts have been found to produce oxygen from water. However, in each case, the energy necessary for the oxidation was provided by chemical or electrochemical means, e.g. $Ru^{V}ORu^{V}$ was prepared by the addition of Ce(IV) to a solution of $Ru^{III}ORu^{III}$. None of them have been shown to produce oxygen photocatalytically. A photogenerated source of oxidant could possibly be used in order to generate these high energy species. This has been function for the incorporation of "Ru-Red" and "Pt-Black" in a Nafion membrane by using $[Ru(bpy)_3]^{2+}$ as a photosensitiser for the reaction[94].

To date, the mechanism of water oxidation in PSII is still unknown. Many model systems have been designed to try to elucidate the structure of the OEC. However, until a *satisfactory* crystal structure of PSII is obtained, the exact nature of the OEC will not be known. Assignment of mechanisms to any forms of water oxidation is extremely difficult, and even for the few synthetic water oxidation catalysts, the clarification of the mechanism is rarely satisfactory.

1.5 Ruthenium–Manganese Systems for Artificial Photosynthesis

The initial and most important step in photosynthesis is the photochemical oxidation of water in PSII. As previously stated, this is accomplished via absorption of light by the chlorophyll P_{680} followed by subsequent electron transfer from the manganese cluster, which itself oxidises the water. It was because of the presence of manganese in the natural system that many scientists now wish to incorporate manganese into artificial systems. With the correct ligands, manganese is capable of storing enough charge to oxidise water. Thus, by linking it with a suitable photosensitiser it should be capable to synthesise a system, which will be capable of mimicking the initial water splitting step of photosynthesis.

Although porphyrin systems are suitable photosensitisers and are present in very many natural systems, not only in PSII, ruthenium polypyridyl complexes are also a popular choice as photosensitiser. Ruthenium polypyridyl complexes have long been known to be potential catalysts for the photochemical oxidation of water. They are relatively stable and by careful choice of ligands, the photochemical properties can be fine-tuned and hence the catalyst can be optimised to maximum efficiency.

At the moment, almost all of the work focusing on ruthenium – manganese systems is based upon $[Ru(bpy)_3]^{2+}$ derivatives. Since its properties have already been extensively studied over the last 40 years, it presents itself as an excellent starting point for this work. However the strategy for the synthesis of such a binuclear complex is extremely important. Starting from $[Ru(bpy)_3]^{2+}$ would be problematic

due to the formation of various isomers upon modification of one bpy ligand into a bridging ligand. Therefore one must start from $[Ru(bpy)_2Cl_2]^{2+}$ and one bpy derivative. This would ensure a pure starting complex. Subsequent reactions on this complex to prepare the covalent linkage to the manganese would only involve the modified bpy. The extension of the covalent linkage must be carried out on the complex rather than the free ligand. Should one start from an asymmetric bridging ligand containing chelating sites at two or more positions, then complex mixtures of monomers, dimers and coordination isomers would be formed upon complexation with ruthenium. In general 4,4'-dimethyl bpy (dmbpy) is used as the modified bpy since it can easily be asymmetrically altered, e.g. oxidised to the mono aldehyde, before complexation. This can then undergo a series of reactions to extend the bridging ligand to incorporate manganese chelating sites.

In 1997 Sun *et al.* reported a covalently linked ruthenium tris bpy manganese system as a biomimetic model for PSII[95]. It was the first supramolecular system where a manganese complex had been used as an electron donor to a photo-oxidised photosensitiser. It was a very basic system, synthesised by the elongation of $[Ru(bpy)_2(dmbpy)]^{2+}$ to incorporate another bpy or a bispicen (N'-methyl-N,N'-bis(2-pyridylmethyl)-1,2-ethanediamine) ligand. The bpy (or bispicen) would later be complexed with manganese (shown in *Fig. 1.21*). The length of the spacer between the two bridging ligands was kept quite short, typically a methyl or ethyl group, but this was enough to investigate the importance of the distance between the two metal centres[96].

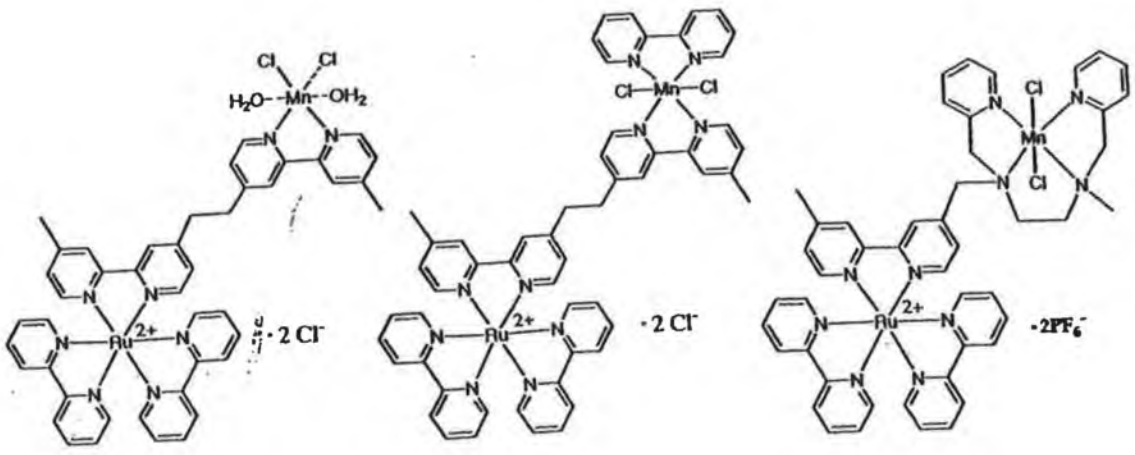

Fig. 1.21 A selection of bimetallic complexes synthesised by Sun et al.[96]

The results obtained were very promising. They did indeed find electron transfer occurred upon photoexcitation of the ruthenium. Although the bis bpy coordinated manganese system proved to be unstable in solution[97], photophysical and photochemical studies showed that for the mono bpy coordinated Mn complex shown above, the lifetime decreased from 950ns to 260ns upon coordination of the manganese. The use of methyl viologen as an external electron acceptor allowed electron transfer from the manganese to the ruthenium to be observed. It was found that the rate of production of the methyl viologen radical remained the same regardless of whether the Mn was complexed or not, while the rate of decay of the Ru(III) signal was approximately 1 order of magnitude faster. This means that the photogenerated Ru(III) in the bimetallic complex must have received an electron from a source not present in the mononuclear (only Ru) complex and which is not methyl viologen. They proposed that this source was the Mn(II), which was coordinated to the bridging ligand. They further proved this theory by showing that an external source of chemically oxidised $[Ru(bpy)_3]^{3+}$ can oxidise the bimetallic complex. Using EPR, they followed the signals from both the Ru(III) and the Mn(II)

as they decayed into the Ru(II) and Mn(III). This importantly showed that Ru(III) is capable of oxidising Mn(II) to Mn(III). Combining this fact with the evidence obtained from the electron transfer studies gives fairly conclusive proof that in this dinuclear complex electron transfer does occur between the manganese and the photogenerated Ru(III) (*Fig. 1.22*) to yield a long lived charge separated state[98].

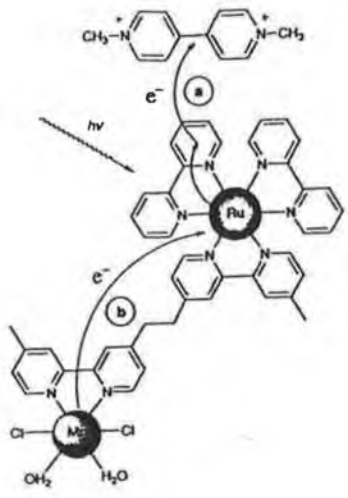

Fig. 1.22. Photoinduced electron transfer pathway[95]

The binuclear complex containing the bispicen ligand was also interesting to study. It was found to be less dissociative than the bpy complexes in solution. This showed that bispicen is a better manganese chelating ligand than bpy. However, the photoinduced electron transfer of this complex could not be studied conclusively. Firstly, it has a much shorter Ru-Mn distance (9Å vs. 13Å), resulting in extremely rapid intramolecular quenching of the Ru(III) excited state. Secondly, oxidation of the ligand and not of the manganese centre by Ru(III) was observed.

From this and other work[99] the authors concluded that by having a short Ru-Mn distance, quenching of the excited state was observed, but that a longer Ru-Mn

distance resulted in a slow electron transfer rate. To solve this problem they suggested the inclusion of an intermediate electron donor between the two metals. By including a second donor, e.g. a phenol, a stepwise electron transfer from the phenol to the ruthenium and then from the manganese to the phenol may be obtained. This would reduce the possibility of a back electron transfer from the ruthenium to the phenol and so result in a long lived charge separated state.

With this in mind, Magnuson *et al.* synthesised a ruthenium tris bpy complex with a covalently linked tyrosine[100]. Tyrosine is an excellent choice of donor to insert between the ruthenium and the manganese. It is the linkage between the manganese cluster and P_{680} in PSII, firstly donating an electron to the photochemically oxidised P_{680} and then retrieving it from the manganese cluster. Optical and EPR measurements, using the alanine derivative as a reference compound, all pointed to the fact that oxidation of the tyrosine was occurring after photochemical excitation of the ruthenium via intramolecular electron transfer from the phenol of the tyrosine to the Ru(III) (*Fig. 1.23*). The oxidation potentials of the two species involved ($[Ru(bpy)_3]^{2+}$ and tyrosine) also show that this reaction would be thermodynamically favourable.

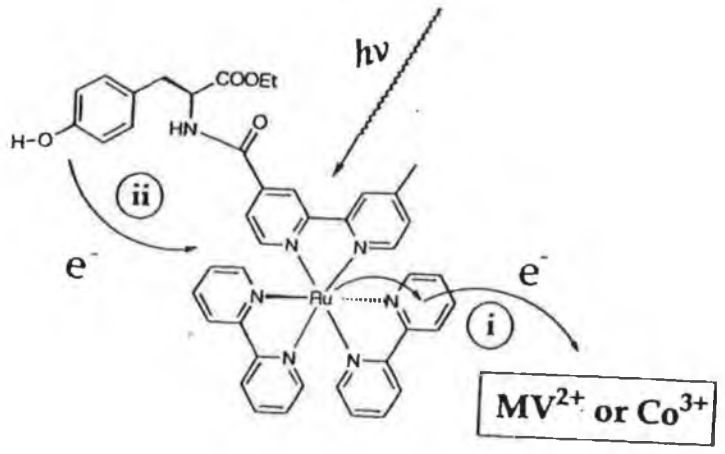

Fig. 1.23 Electron transfer reaction for covalently linked tyrosine[100]

In the case of biomimetic models of the water oxidising triad in PSII containing a ruthenium photosensitiser, tyrosine and a manganese system, research is still in its infancy. Two systems, one covalently linked[101] and the other not covalently linked[102], have been reported. For the non-covalently linked sytstem, the manganese complex is added to a solution of the Ru-TYR compound mentioned above, and intermolecular electron transfer is observed. An important fact about this triad is that it was the first reported triad to use a Mn(III) Mn(III) dimer instead of a mononuclear manganese system. This opens up new possibilities approaching the natural system where 4 electrons from 4 manganese atoms are necessary for the oxidation of water. The ligands involved are also interesting, consisting not only of Mn-amine coordination but also Mn-phenol coordination. The negative charge on the deprotonated phenol is hoped to stabilise high charges on the Mn.

Upon photoexcitation of the ruthenium, electron transfer from the manganese to the ruthenium via the tyrosine took place, resulting in a 16 line hyperfine signal being

seen in the EPR spectrum. This signal is characteristic of a Mn(III) Mn(IV) system. It was also shown that the electron transfer proceeded via the tyrosine and not directly from the manganese to the ruthenium by carrying out the same experiments using $[Ru(bpy)_3]^{2+}$, which has a much higher oxidation potential than that of tyrosine. Oxidation of the manganese dimer by this method caused an oxidation of the ligands to also be observed, a process tyrosine would not be capable of achieving. However, in the triad, virtually no oxidation of the ligands of the manganese dimer were observed, thus proving that the oxidation of the manganese was carried out by the tyrosyl radical and not by the Ru(III).

The covalently bound triad also incorporates a Mn dimer (*Fig. 1.24*), coordinated through both Mn-N and Mn-O bonds. Two sites are available on each manganese for exogenous ligands, which are normally occupied by bridging aceate ligands but may be changed in solution[103]. Initial work has shown that electron transfer from the Mn(II)-Mn(II) to the photoexcited ruthenium centre is possible to yield a Mn(II)-Mn(III) state[104]. Subsequent flashing of the ruthenium may lead to a Mn(III)-Mn(IV) state, in which the manganese has undergone a three electron transfer process[105].

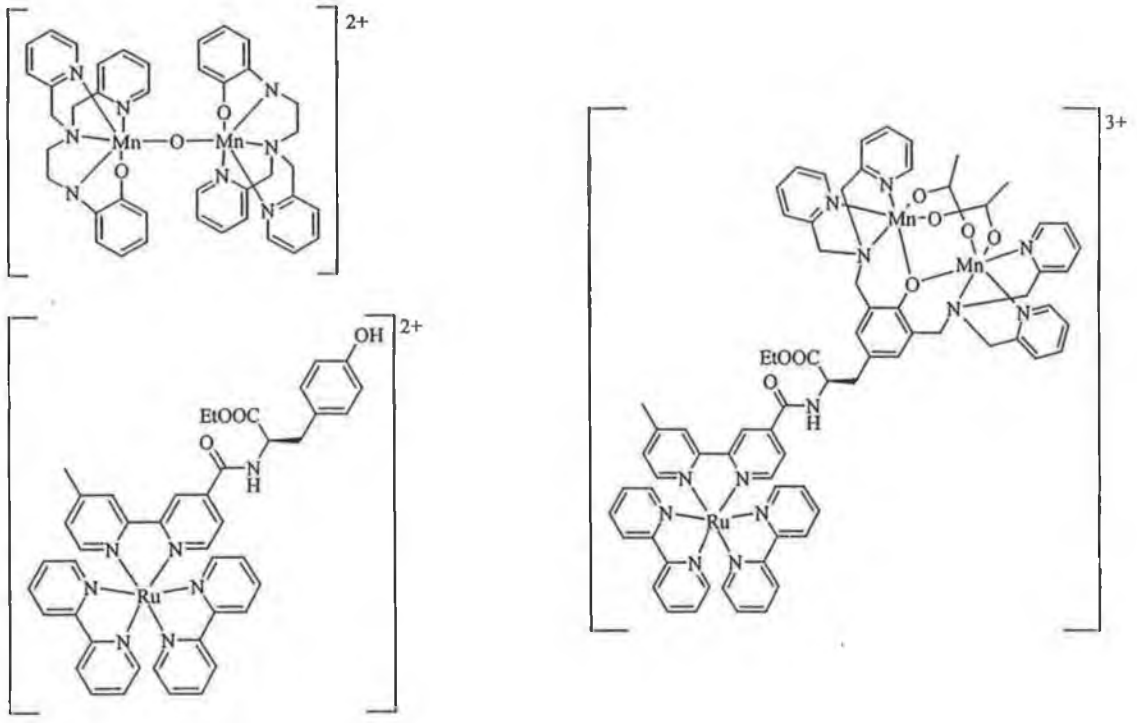

Fig. 1.24 Ruthenium-Tyrosine-Manganese Triads[101, 102]

A different approach to the synthesis of a ruthenium manganese system has been adopted by Burdinski et al.[106], which involved the synthesis and characterisation of Ru_2Mn_2, Ru_3Mn and Ru_6Mn_3 species (See *Fig. 1.25* below). One major difference between these complexes and those mentioned above is in the choice of ligand for the manganese. Monomeric and dimeric forms of 1,4,7 Triazacyclononane were covalently linked to $[Ru(bpy)_2(L)]^{2+}$, where L=modified bpy or phen. Interestingly, these complexes also utilised phenolate ligands in order to stabilise the charge on the manganese centres.

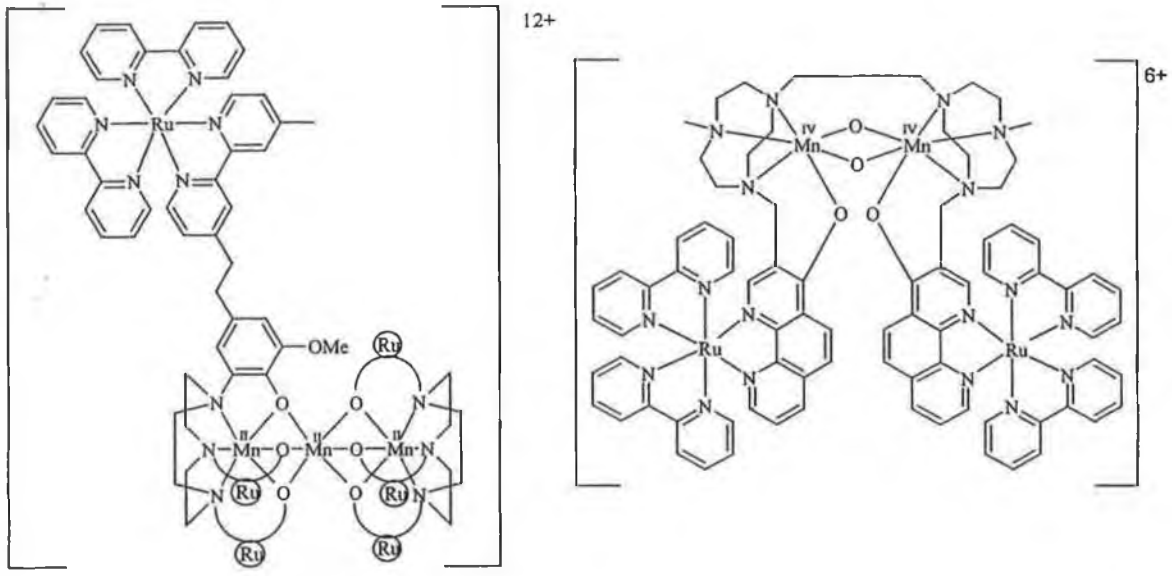

Fig. 1.25 Structures of some Ru-Mn systems

Photoinduced electron transfer from the manganese cluster to the photooxdised ruthenium centre was subsequently studied by spectroscopic and electrochemical means[107]. It was found that in the case of systems containing Mn(II) centres, electron transfer occurred from the manganese to the ruthenium, whereas when the manganese was in the +4 state, electron transfer occurred from the phenolate ligand coordinated to the manganese to the ruthenium centre. This was postulated as being due to the high charge on the manganese. The lifetime of the charge separated state featuring the phenoxyl radical was found to be surprisingly long due to the inaccessibility of the phenoxyl radical, as a result of steric hindrance, and the presence of the adjacent electron donating methoxy group.

Due to the promising results obtained from these experiments which have been carried out over the past few years, it was hoped to synthesise a similar system in

which the triad would be covalently linked via a pyridyl triazole spacer. This would have altered photochemical and electrochemical properties and might even give a better model system for the water oxidation which occurs in Photosystem II.

1.6 Scope of This Thesis

This thesis concerns itself primarily with the systematic approach to the design, synthesis and subsequent characterization of a series of novel ruthenium polypyridyl complexes, to be used as models for artificial photosynthesis. Two different types of model systems are investigated, each demonstrating different processes which occur in natural photosynthesis.

The first set of models which were studied were intended to provide some insight into the mechanism by which electron transfer from a manganese cluster to P_{680} results in the oxidation of water. This was done by designing a range of novel pyridyl triazoles bearing terminal synthons. These were prepared and characterised by standard means. Their ruthenium(II) bisbipyridyl (and bis-d_8-bipyridyl) complexes were also prepared. These were characterised by spectroscopic and electrochemical techniques showing typical properties. A corresponding series of pyrazyl triazoles and their ruthenium complexes were similarly prepared and characterised. A comparison of the two series showed the expected changes upon replacing the pyridine with a pyrazine in the bridging ligands. The synthons were then employed to introduce electron donors, such as manganese clusters or tyrosine in order to study the possibility of electron transfer to the photo oxidised ruthenium centre. Again, a comparison of the pyridine compounds with the pyrazine compounds gave some insight into the importance of the driving force for the reactions. This project was carried out in collaboration with Prof. B. Åkkermark in Stockholm and Prof. J. J. Girerd in Paris.

The second approach was carried out under the supervision of Prof. J. H. Fuhrhop in Berlin. This involved a study of the possibility of electron transfer in a membrane bound system. In order to achieve this, a novel lipid membrane was synthesised. This lipid contained a terminal bipyridyl moiety. It was hoped to be able to have this lipid form self assembled monolayers on a suitable surface, which had been treated with a porphyrin. The subsequent pores in the membrane, caused by the presence of the porphyrin on the surface, could then be closed by complexation of the bipyridyl with a suitable metal such as ruthenium. Should this be successful, the interaction between the ruthenium and the porphyrin could be investigated. Model complexes of various intermediates in the synthesis of the lipid were also prepared and characterised by spectroscopic and electrochemical means. The study of the system on a suitable surface will be carried out by others in Berlin and is not discussed here.

1.7 Bibliography

[1] Bolton, J. R.; *Solar Energy Materials and Solar Cells*, **38**, (1995), 543

[2] Yachandra, V. K.; DeRose, V. J.; Latimer, M. J.; Mukerji, I.; Sauer, K.; Klein, M. P.; *Science*, **260**, (1993), 675

[3] Lawlor, D. W.; *Photosynthesis*, 2nd Edition, Longman Scientific & Technical, (1993)

[4] Hall, D. O.; Rao, K. K.; *Photosynthesis*, 3rd Edition, Edward Arnold Ltd., (1981)

[5] Barber, J.; Andersson, B.; *Nature*, **370**, (1994), 31

[6] Deienhofer, J. P.; Epp, O.; Miki, K.; Huber, R.; Michel, H.; *Nature*, **318**, (1985), 618

[7] Norris, J. R.; Gast, P.; *J. Photochem Photobiol. A Chem.*, **29**, (1985), 185

[8] Graige, M. S.; Paddock, M. L.; Bruce, J. M.; Feher, G.; Okamura, M. Y.; *J. Am. Chem. Soc.*, **118**, (1996), 9005

[9] http://www.bc.ic.ac.uk

[10] Lagoutte, B.; Mathis, P.; *Photochemistry and Photobiology*, **49**, (1989), 833

[11] Rompel, A.; Andrews, J. C.; Cinco, R. M.; Wemple, M. W.; Christou, G.; Law, N. A.; Pecoraro, V. L.; Sauer, K.; Yachandra, V. K.; Klein, M. P.; *J. Am. Chem. Soc.*, **119**, (1997), 4465

[12] Boxer, S. G.; Goldstein, R. A.; Lockhart, D. J.; Middendorf, T. R.; Takiff, L.; *J. Phys. Chem.*, **93**, (1989), 8280

[13] Gust, D.; Moore, T. A.; *Science*, **244**, (1989), 35

[14] Lay, P. A.; Mau, A. W. H.; Sasse, W. H. F.; Creaser, I. I.; Gahan, L. R.; Sargesson, A. M.; *Inorg. Chem.*, **22**, (1983), 2347

[15] Cotton, F. A.; Wilkinson, G.; *Advanced Inorganic Chemistry*, 5th Edition, Wiley, Chichester, (1988)

[16] Paris, J. P.; Brandt, W. W.; *J. Am. Chem. Soc.*, **81**, (1959), 5001

[17] Durham, B.; Caspar, J. K.; Nagle, T. J.; Meyer, T. J.; *J. Am. Chem. Soc.*, **104**, (1982), 4803

[18] Balzani, V.; Juris, A.; *Coord. Chem. Rev.*, **211**, (2001), 97

[19] Paul, P.; Tyagi, B.; Bilakhiya, A. K.; Dastidar, P.; Suresh, E.; *Inorg. Chem.*, **39**, (2000), 14

[20] Cargill Thompson, A. M. W.; Jeffery, J. C.; Liard, D. J.; Ward, M. D.; *J. Chem. Soc. Dalton Trans.*, (1996), 879

[21] Juris, A.; Balzani, V.; Barigelletti, F.; Campagna, S.; Belser, P.; Von Zelewsky, A.; *Coord. Chem. Rev.*, **84**, (1988), 85

[22] Demas, J.; Crosby, G.; *J. Am. Chem. Soc.*, **93**, (1971), 2840

[23] Barigelleti, F.; Belser, P.; Von Zelewski, A.; Juris, A.; Balzani, V.; *J. Phys. Chem. B*, **89**, (1985), 3680

[24] Veletsky, N. I.; Dementiev, I. A.; Ershov, A. Y.; Nikol'skii, A. B.; *J. Photochem. Photobiol. A Chem.*, **89**, (1995), 99

[25] Van Houten, J.; Watts, R. J.; *J. Am. Chem. Soc.*, **98**, (1976), 4853

[26] Creutz, C.; Chou, M.; Netzel, T.; Okumura, M.; Sutin, W.; *J. Am. Chem. Soc.*, **102**, (1980), 1309

[27] Barigelletti, F.; DeCola, L.; Balzani, V.; Hage, R.; Haasnoot, J.; Reedijk, J.; Vos, J. G.; *Inorg. Chem.*, **30**, (1991), 641

[28] Anderson, P. A.; Deacon, G. B.; Haarmann, K. H.; Keene, F. R.; Meyer, T. J. Reitsma, D. A.; Skelton, B. W.; Strouse, G. F.; Thomas, N. C.; Treadway, J. A.; White, A. H.; *Inorg. Chem.*, **34**, (1995), 6145

[29] Allen, G. H.; White, R. P.; Rillema, D. P.; Meyer, T. J.; *J. Am. Chem. Soc.*, **106**, (1984), 2613

[30] Juris, A.; Campagna, S.; Balzani, V.; Gremaud, G.; Von Zelewski, A.; *Inorg. Chem.*, **27**, (1988), 3652

[31] Barigelletti, F.; Juris, A.; Balzani, V.; Belser, P.; Von Zelewski, A.; *Inorg. Chem.*, **26**, (1987), 4115

[32] Rau, S.; Büttner, T.; Temme, C.; Ruben, M.; Görls, H.; Walther, D.; Duati, M.; Fanni, S.; Vos, J. G.; *Inorg. Chem.*, **39**, (2000), 1621

[33] Steel, P. J.; Lahousse, F.; Marzin, C.; *Inorg. Chem.*; **22**, (1983), 1488

[34] Fanni, S.; DiPietro, C.; Serroni, S.; Campagna, S.; Vos, J. G.; *Inorg. Chem. Commun.*, **3**, (2000), 42

[35] Ernst, S.; Kaim, W.; *Inorg. Chem.*, **28**, (1989), 1520

[36] Barigelletti, F.; Juris, A.; Balzani, V.; Belser, P.; Von Zelewski, A.; *Inorg. Chem.*, **22**, (1983), 3335

[37] Hage, R.; Haasnoot, J. G.; Nieuwenhuis, H. A.; Reedijk, J.; DeRidder, D. J. A.; Vos, J. G.; *J. Am. Chem. Soc.*, **112**, (1990), 9245

[38] Hage, R.; Haasnoot, J. G.; Nieuwenhuis, H. A.; Reedijk, J.; Wang, R.; Vos, J. G.; *J. Chem. Soc. Dalton Trans.*, (1991), 3271

[39] Wang, R.; Vos, J. G. Schmehl, R. H. Hage, R.; *J. Am. Chem. Soc.*, **114**, (1992), 1964

[40] Hage, R.; Prins, R.; Haasnoot, J. G.; Reedijk, J.; Vos, J. G.; *J. Chem. Soc. Dalton Trans.*; (1987), 1389

[41] Collin, J. P.; Guillerez, S.; Sauvage, J. P.; *J. Chem. Soc. Chem. Commun.*, (1989), 776

[42] Demas, J. N.; Harris, E. W.; McBride, R. P.; *J. Am. Chem. Soc.*, **99**, (1977), 3547

[43] Harriman, A.; Hissler, M.; Khatyr, A.; Zissel, R.; *J. Chem. Soc. Chem. Commun.*, (1999), 735

[44] Duati, M.; Fanni, S.; Vos, J. G.; *Inorg. Chem. Commun.*, **3**, (2000), 68

[45] Ryan, E. M.; Wang, R.; Vos, J. G.; Hage, R.; Haasnoot, J.; *Inorg. Chim. Acta*, **208**, (1993), 49

[46] Balzani, V.; Juris, A.; Venturi, M.; Camapgna, S.; Seroni, S.; *Chem. Rev.*, **96**, (1996), 759

[47] Cárdenas, D. J.; Gaviña, P.; Sauvage, J. P.; *J. Am. Chem. Soc.*, **119**, (1997), 2656

[48] Belser, P.; Von Zelewsky, A.; Frank, M.; Seel, C.; Vögtle, F.; DeCola, L.; Barigelletti, F.; Balzani, V.; *J. Am. Chem. Soc.*, **115**, (1993), 4076

[49] Atwood, J. L.; *Comprehensive Supramolecular Chemistry*, 1st Ed., Pregamon, (1996)

[50] Grubert, L.; Jacobi, D.; Buck, K.; Abraham, W.; Mugge, C.; Krause, E.; *Eur. J. Org. Chem.*, **20**, (2001), 3921

[51] Amabilino, D. B.; Sauvage, J. P.; *Chem. Commun.*, (1996), 2441

[52] Baxter, P. N.; Lehn, J. M.; Kneisel, B. O.; Baum, G.; Fenske, D.; *Chem. Eur. J.*, **5**, (1999), 113

[53] Ishow, E.; Credi, A.; Balzani, V.; Spandola, F.; Mandolini, L.; *Chem. Eur. J.*, **5**, (1999), 984

[54] DeSilva, A. P.; Gunaratne, H. Q. N.; Gunnlaugsson, T.; Huxley, A. J. M.; McCoy, C. P.; Rademacher, J. T.; Rice, T. E.; *Chem. Rev.*, **97**, (1997), 1515

[55] Beer, P. D.; Dent, S. W.; *Chem. Commun.*, (1998), 825

[56] Barigelletti, F.; Flamigni, L.; Calogero, G.; Hammarström, L.; Sauvage, J. P.; Collin, J. P.; *Chem. Commun.*, (1998), 2333

[57] Carraway, E. R.; Demas, J. N.; DeGraff, B. A.; Bacon, J. R.; *Anal. Chem.*, **63**, (1991), 337

[58] DeSilva, A. P.; Rice, T. E.; *Chem. Commun.*, (1999), 163

[59] Benniston, A. C.; Mackie, P. R.; Harriman, A.; *Angew. Chem. Int. Ed.*, **37**, (1998), 354

[60] Hu, Y. Z.; Bossman, S. H.; Van Loyen, D.; Schwarz, O.; Dürr, H.; *Chem. Eur. J.*, **5**, (1999), 1267

[61] Gust, D.; Moore, T. A.; Moore, A. L.; *Acc. Chem. Res.*, **34**, (2001), 40

[62] Denti, G.; Campagna, S.; Serroni, S.; Ciano, M.; Balzani, V.; *J. Am. Chem. Soc.*, **114**, (1992), 2944

[63] Puntoriero, F.; Serroni, S.; Licciardello, A.; Venturi, M.; Juris, A.; Ricevuto, V.; Campagna, S.; *J. Chem. Soc. Dalton Trans.*, (2001), 1035

[64] Liddell, P. A.; Kuciauskas, D.; Sumida, J. P.; Nash, B.; Nguyen, D.; Moore, A. L.; Moore, T. A.; Gust, D.; *J. Am. Chem. Soc.*; **119**, (1997), 1400

[65] Johnson, D. G.; Niemczyk, M. P.; Minsek, D. W.; Wiederrecht, G. P.; Svec, W. A.; Gaines, G. L.; Wasielewski, M. R.; *J. Am. Chem. Soc.*, **115**, (1993), 5692

[66] Hage, R.; *Ph.D. Thesis*, Rijksuniversiteit te Leiden, (1991)

[67] Larson, S. L.; Elliott, C. M.; Kelley, D. F.; *Inorg. Chem.*, **35**, (1996), 2070

[68] Rutherford, T. J.; Keene, F. R.; *Inorg. Chem.*, **36**, (1997), 2872

[69] Sauvage, J. P.; Collin, J. P.; Chambron, J. C.; Guillerez, S.; Coudret, C.; *Chem. Rev.*, **94**, (1994), 993

[70] Kelso, L. S.; Smith, T. A.; Schultz, A. C.; Junk, P. C.; Warrener, R. N.; Ghiggino, K. P.; Keene, F. R.; *J. Chem. Soc. Dalton Trans.*, (2000), 2599

[71] Armspach, D.; Constable, E. C.; Diederich, F.; Housecroft, C. E.; Nierengarten, J. F.; *Chem. Commun.*, (1996), 2009

[72] Opperman, K. A.; Mecklenburg, S. L.; Meyer, T. J.; *Inorg. Chem.*, **33**, (1994), 5295

[73] Klumpp, T.; Linsenmann, M.; Larson, S. L.; Limoges, B. R.; Bürssner, D.; Krissinel, E. B.; Elliott, C. M.; Steiner, U. E.; *J. Am. Chem. Soc.*, **121**, (1999), 1076

[74] Hu, Y. Z.; Tsukiji, S.; Shinkai, S.; Oishi, S.; Hamachi, I.; *J. Am. Chem. Soc.*, **122**, (2000), 241

[75] DeArmond, M. K.; Fried, G. A.; *Progress in Inorganic Chemistry*, Vol. 44, (1997), John Wiley & Sons Inc.

[76] Gaines, G. L.; Behnken, P. E.; Valenty, S. J.; *J. Am. Chem. Soc.*, **100**, (1978), 6549

[77] Sprintschnik, G.; Sprintschnik, H.; Kirsch, P. P.; Whitten, D. G.; *J. Am. Chem. Soc.*, **99**, (1977), 4947

[78] Hammarström, L.; Norrby, T.; Stenhagen, G.; Mårtensson, J.; Åkermark, B.; Almgren, M.; *J. Phys. Chem. B*, **101**, (1997), 7494

[79] Dismukes, G. C.; *Science*, **292**, (2001), 446

[80] Zouni, A.; Witt, H. T.; Kern, J.; Fromme, P.; Krauss, N.; Saenger, W.; Orth, P.; *Nature*, **409**, (2001), 739

[81] Kok, B.; Forbush, B.; McGloin, M.P.; *Photochem. Photobiol.*, **11**, (1970), 457

[82] Ruettinger, W.; Ho, D. M.; Dismukes, G. C.; *Inorg. Chem.*, **38**, (1999), 1036

[83] Kirk, M. L.; Chan, M. K.; Armstrong, W. H.; Solomon, E. I.; *J. Am. Chem. Soc.*, **114**, (1992), 10342

[84] Blondin, G.; Davydov, R.; Philouze, C.; Charlot, M. F.; Styring, S.; Åkermark, B.; Girerd, J. J.; Boussac, A.; *J. Chem. Soc. Dalton Trans.*, (1997), 4069

[85] Siegbahn, P. E. M.; Crabtree, R. H.; *J. Am. Chem. Soc.*, **121**, (1999), 117

[86] Blomberg, M. R. A.; Siegbahn, P. E. M.; Styring, S.; Babcock, G. T.; Åkermark, B; Korall, P.; *J. Am. Chem. Soc.*, **119**, (1997), 8285

[87] Limburg, J.; Szalzai, V. A.; Brudvig, G. W.; *J. Chem. Soc. Dalton Trans.*; (1999), 1353

[88] Rüttinger, W.; Dismukes, G. C.; *Chem. Rev.*, **97**, (1997), 1

[89] Naruta, Y.; Sasayama, M. A.; Sasaki, T.; *Angew. Chem. Int. Ed. Engl.*, **33**, (1994), 1839

[90] Yagi, M.; Kaneko, M.; *Chem. Rev.*, **101**, (2001), 21

[91] Gersten, S. W.; Samuels, G. J.; Meyer, T. J.; *J. Am. Chem. Soc.*, **104**, (1982), 4029

[92] Chronister, C. W.; Binstead, R. A.; Ni, J.; Meyer, T. J.; *Inorg. Chem.*, **36**, (1997), 3814

[93] Lebeau, E. L.; Adeyemi, S. A.; Meyer, T. J.; *Inorg. Chem.*, **37**, (1998), 6476

[94] Yagi, M.; Takahashi, Y.; Ogino, I.; Kaneko, M.; *J. Chem. Soc. Faraday Trans.*, **93**, (1997), 3125

[95] Sun, L.; Hammarström, L.; Norrby, T.; Berglund, H, Davydov, R.; Andersson, M.; Börje, A.; Korall, P.; Philouze, C.; Almgren, M.; Styring, S.; Åkermark, B.; *Chem. Commun.*, (1997), 607

[96] Sun, L.; Berglund, H.; Davydov, R.; Norrby, T.; Hammarström, L.; Korall, P.; Börje, A.; Philouze, C.; Berg, K.; Tran, A.; Andersson, M.; Stenhagen, G.; Mårtensson, J.; Almgren, M.; Styring, S.; Åkermark, B.; *J. Am. Chem. Soc.*, **119**, (1997), 6996

[97] Berglund-Baudin, H.; Sun, L.; Davydov, R.; Sundahl, M.; Styring, S.; Åkermark, B.; Almgren, M.; Hammarström, L.; *J. Phys. Chem. A*, **102**, (1998), 2512

[98] Styring, S.; Sun, L.; Hammarström, L.; Davydov, R.; Almgren, M.; Andersson, M.; Berglund, H.; Börje, A.; Korall, P.; Norrby, T.; Philouze, C.; Åkermark, B.; *Proc. Indian Acad. Sci.*, **109**, (1997), 389

[99] Berg, K. E.; Tran, A.; Raymond, M. K.; Abrahamsson, M.; Wolny, J.; Redon, S.; Andersson, M.; Sun, L.; Styring, S.; Hammarström, L.; Toftlund, H.; Åkermark, B.; *Eur. J. Inorg. Chem.*, (2001), 1019

[100] Magnuson, A.; Berglund, H.; Korall, P.; Hammarström, L.; Åkermark, B.; Styring, S.; Sun, L.; *J. Am. Chem. Soc.*, **119**, (1997), 10720

[101] Sun, L.; Burkitt, M.; Tamm, M.; Raymond, M. K.; Abrahamsson, M.; LeGourriérec, D.; Frapart, Y.; Magnuson, A.; Huang Kenéz, P.; Brandt. P.; Tran, A.; Hammarström, L.; Styring, S.; Åkermark, B.; *J. Am. Chem. Soc.*, **121**, (1999), 6834

[102] Magnuson, A.; Frapart, Y.; Abrahamsson, M.; Horner, O.; Åkermark, B.; Sun, L.; Girerd, J. J.; Hammarström, L.; Styring, S.; *J. Am. Chem. Soc.*, **121**, (1999), 89

[103] Hammarström, L.; Sun, L.; Åkermark, B.; Styring, S.; *Catalysis Today*, **58**, (2000), 57

[104] Hammarström, L.; Sun, L.; Åkermark, B.; Styring, S.; *Biochim. Biophys. Acta*, **1365**, (1998), 193

[105] Sun, L.; Hammarström, L.; Åkermark, B.; Styring, S.; *Chem. Soc. Rev.*, **30**, (2001), 36

[106] Burdinski, D.; Bothe, E.; Wieghardt, K.; *Inorg. Chem.*, **39**, (2000), 105

[107] Burdinski,. D.; Wieghardt, K.; Steenken, S.; *J. Am. Chem. Soc.*, **121**, (1999), 10781

Chapter 2

Experimental Procedures

2.1 Materials and Reagents

All synthetic reagents were of commercial grade and no further purification was employed. Solvents used during reactions were also of reagent grade and were not purified prior to use unless otherwise stated. The solvents used for spectroscopic and electrochemical measurements were of spectrophotometric grade

2.2 Nuclear Magnetic Resonance Spectroscopy

^{1}H-NMR and ^{13}C-NMR spectra were obtained using a Bruker AC400 (400MHz and 100MHz respectively) instrument. Measurements were generally carried out in d_6-DMSO, unless otherwise stated. Chemical shifts were recorded relative to TMS. The spectra were converted from their free induction decay (FID) profiles using XWINNMR software.

The 2-D COSY (correlated spectroscopy) experiments involved the accumulation of 128 FIDs of 16 scans. Digital filtering was sine-bell squared and the FID was zero filled in the F1 dimension. Acquisition parameters were F1 = ± 500 Hz, F2 = 1000Hz and $t_{½}$ = 0.001 s. The cycle time delay was 2 s.

2.3 High Performance Liquid Chromatography (HPLC)

Analytical cation exchange chromatography was used for the analysis of the ruthenium complexes. HPLC was carried out using a JVA analytical HPLC system, consisting of a Varian Prostar pump, a Varian Prostar photodiode array detector, a 20µl injector loop and a HiChrom Partisil P10SCX-3095 cation exchange column. The detection wavelength used was 280nm, where both complexes and ligands absorb strongly. The mobile phase used was acetonitrile:water 80:20 (v/v) containing 0.08M $LiClO_4$ at a flow rate of 1.8 cm^3/min. (It should be noted that care must be taken when working with perchlorates, as they are potentially **explosive** when in contact with combustible material!)

2.4 Absorption and Emission Spectroscopy

UV/Vis spectra were carried out using a Shimadzu UV3100 UV-Vis-NIR spectrophotometer interfaced to an Elonex PC575 personal computer.

Emission spectra were obtained both at room temperature and at low temperature (77K, cooled with liquid nitrogen) using a Perkin-Elmer LS50B luminescence spectrometer equipped with a Dell PC166 personal computer employing Perkin-Elmer FL Winlab custom built software. Excitation and emission slit widths of 10 nm were used for all measurements except at low temperature, where an emission slit width of 2.5nm was used.

Ground and excited state pK_a's were measured by manipulating the observed intensity changes in the relevant spectra as a function of pH. The inflection points of

the subsequent graphs were estimated by differentiating the best-fit sigmoidal curve calculated using Microcal Origin. The excitation wavelength was chosen from a suitable isosbestic point determined from the absorption acid/base titration. The samples were prepared by dissolution in a few drops of a suitable organic solvent followed by dilution to 100 cm^3 with Britton-Robinson buffer (0.04M H_3BO_3, 0.04M H_3PO_4, 0.04M CH_3COOH). The pH of the solution was adjusted by the addition of concentrated sulphuric acid or concentrated sodium hydroxide solution and measured using a Corning 240 digital pH meter.

2.5 Electrochemical Measurements

Measurements were carried out in dry acetonitrile with tetraethylammoniumperchlorate as electrolyte. A 3mm glassy carbon electrode encased in Teflon was used as the working electrode, a platinum wire as the counter electrode and saturated calomel electrode (SCE) served as the reference electrode. All measurements were carried out on approximately the 1mM scale with 0.1M TEAP and were degassed with nitrogen unless otherwise stated. During scans, a gentle flow of nitrogen was maintained above the solvent surface to prevent absorption of atmospheric oxygen. Cyclic voltammetric (CV) measurements were carried out using a CH Instruments Memphis 660 potentiostat interfaced to an Elonex PC575 personal computer and manipulated with Model 660 CH software.

2.6 Luminescent Lifetime Measurements

The lifetime measurements of the ruthenium complexes were carried out with the assistance of Marco Duati and Wesley Browne. The instrument used was an Edinburgh Analytical Instruments single photon counter, in a T setting. The lamp was an nF900, in a nitrogen setting, the monochromators were J-yA models, the detector was a single photon photomultiplier detection system, model S 300, with an MCA card type Norland N5000 and a PC interface Cd900 serial. Data correlation and manipulation was carried out using the program F900, Version 5.13.

The measurements were performed in acetonitrile, basified with triethylamine and acidified with trifluoroacetic acid. The samples were excited using 337 nm as excitation wavelength and the lifetimes were collected in the maxima of the emission.

2.7 Infra Red Spectroscopy

Infra red spectra of ligands were measured in a KBr disc on a Perkin Elmer 2000 FTIR spectrometer.

2.8 Elemental Analysis

C, H, N elemental analyses were carried out by the Microanalytical Laboratory of University College Dublin, using an Exador analytical CE440.

It must not be forgotten that the presence of the deuterium needed to be taken into account when calculating elemental analysis ratios. When determining the percentage of hydrogen in a sample, the number of water molecules, and not the weight of water, formed from the sample is measured. As a result, the amount of water formed from a sample remains the same after deuteration, even though the mass of water formed has changed. Therefore, when calculating the theoretical amount of hydrogen in a sample, one treats deuterium as if it were hydrogen. However, the molecular mass of the compound has increased upon deuteration and this must be taken into account for in the calculation of the percentage hydrogen. This is best illustrated by the example below, using bpy and d_8-bpy:

In general: $\%E = [Mass_E \div M.W._C] \times 100$ (E=element, C=compound)

bpy: $\%H = [\mathbf{(8 \times 1)} \div \{(10 \times 12) + \mathbf{(8 \times 1)} + (2 \times 14)\}] \times 100 = 5.16$

d_8-bpy: $\%H = [\mathbf{(8 \times 1)} \div \{(10 \times 12) + \mathbf{(8 \times 2)} + (2 \times 14)\}] \times 100 = 4.91$

2.9 Deuteration

The deuteration of ligands was carried out in a general purpose dissolution bomb P/N 4744, including Teflon cup and cover, purchased from Scientific Medical Products. Pd/C and D_2O (99%) were obtained from Aldrich.

The percentage deuteration was calculated by means of a simple NMR experiment. By dissolving a known amount (in moles) of undeuterated ligand in a known amount of a suitable NMR solvent, a ratio of the peak integration of the ligand to the peak integration of the solvent may be found. After obtaining a spectrum of the same amount (again in moles – assuming complete deuteration when calculating the

increased mass) of the perdeutero ligand in the same amount of solvent, another ratio may be obtained. Comparison of the ratios then leads to a measurement of the percentage of atoms, which were successfully deuterated.

2.10 Mass Spectrometry

Mass spectra of the compounds synthesised in the Freie Univerität, Berlin, Germany (Chapter 6), were obtained by the Mass Spectrometry Department of the Institut für Organische und Physikalische Chemie der Freien Universität, Berlin, Germany. Those of the compounds reported in Chapter 5 were kindly measured by Mr. Maurice Burke in Dublin City University.

2.11 X-Ray Crystallography

The crystal structure of the ligand pyTol was obtained in collaboration with Dr. Sven Rau and Dr. Helmar Gurls in the Friedrich Schiller Universität, Jena, Germany

Chapter 3

The Synthesis and Characterisation of Ruthenium (II) Complexes Containing Novel 3-(2'-Pyridyl)1,2,4-Triazole Ligands

3.1 Introduction

Manganese is present in the naturally occurring PSII, where it functions as an electron donor to an oxidised photosensitiser, prior to the oxidation of water. Interest in the use of manganese as an electron donor in synthetic artificial photosynthetic systems is on the increase[1]. As mentioned in Section 1.3, ruthenium polypyridyl complexes make ideal photosensitisers for use in artificial photosynthetic systems. However the range of known covalently linked ruthenium-manganese systems remains small. In an attempt to provide a better understanding of the processes which may occur between ruthenium and manganese centres, an investigation into the synthesis and characterisation of novel ruthenium complexes, which may be used to produce ruthenium-manganese systems, has been carried out. The results of this work shall be discussed in the next three chapters. In this chapter, the synthesis and characterisation of a number of novel ligands and their ruthenium complexes shall be discussed.

The key element in designing a covalently linked ruthenium manganese system is the correct choice of bridging ligand. This is the linkage between the two systems and therefore it must possess two separate coordination sites, one for each of the metals. Its synthesis must be carefully planned to limit the number of isomers formed upon complexation and to ensure stability of the system for the duration of the synthesis. In this case, it was decided to first create a ruthenium polypyridyl precursor and to work towards the incorporation of manganese by the modification of one of the ligands to include extra binding sites. Due to the inherent difficulties associated with the synthesis of manganese complexes, this route was chosen, as the manganese is

not introduced into the complex until the final step. Many manganese complexes are paramagnetic; thus limiting the potential for NMR spectroscopy for the rest of the synthesis. In general, manganese complexes are relatively unstable and may not survive certain standard synthetic procedures, such as column chromatography. Procedures such as this, which are basic techniques, may result in the loss or alteration of the ligand system, which is co-ordinated to the manganese. On the other hand, ruthenium complexes are known to be stable under a wide range of conditions. For example, during the synthesis of metal dendrimer systems, the ruthenium complexes are often treated as if they are organic ligands[2]. This is known as the "complex as ligands" approach and demonstrates how ruthenium complexes may undergo a wide range of reactions, without suffering adverse effects.

Having decided to build the ruthenium photosensitiser, prior to the inclusion of manganese, the factors influencing the choice of ligands to be prepared must be discussed. Of all of the bimetallic Ru-Mn systems previously prepared, none have addressed the issue of the location of the ruthenium excited state. All but one[3] of the published Ru-Mn dyads are based on $[Ru(bpy)_3]^{2+}$ derivatives. In the case of these complexes, the excited state may be located on any of the three bpy ligands. Should the excited state be localised on the bpy that serves as the bridging ligand, then electron transfer from the electron donor may not occur – the excited state simply decays as per normal. This reduces the efficiency of the system.

This problem may easily be addressed by the use of mixed ligand ruthenium complexes. It has been decided to utilise pyridyl triazoles instead of one of the bpy ligands due to the advantageous properties of their complexes. $[Ru(bpy)_2ptr]^+$,

(where ptr = pyridyl triazole), and its related complexes have been extensively studied[4,5]. It has been shown that in all cases, the excited state is always located on one of the bpy ligands and never on the pyridyl triazole[6]. This has remarkable implications on the preparation of donor-acceptor dyads. Through the modification of the pyridyl triazole ligand to incorporate an electron donor, well-defined vectorial electron transfer may be obtained[7]. Since the excited state is never located on the bridging ligand, there is nothing to prevent electron transfer to proceed smoothly from the donor to the photo oxidised ruthenium centre.

The triazole also has another important feature which may be exploited if necessary. With a pK_a of approximately 4, the proton on the triazole is quite acidic. Under normal circumstances, it is deprotonated when complexed. It may be reversibly protonated if required, resulting in dramatic changes in the properties of the complex. Protonation increases the oxidation potential of the metal centre, due to the reduction of its σ-donor nature. The absorption and emission spectra are also blue shifted[6]. Accordingly, the properties of the complexes may be tuned by simply altering the pH. This makes pyridyl triazoles, such as those shown in *Fig. 3.1*, ideal precursors for the preparation of Ru-Mn dyads.

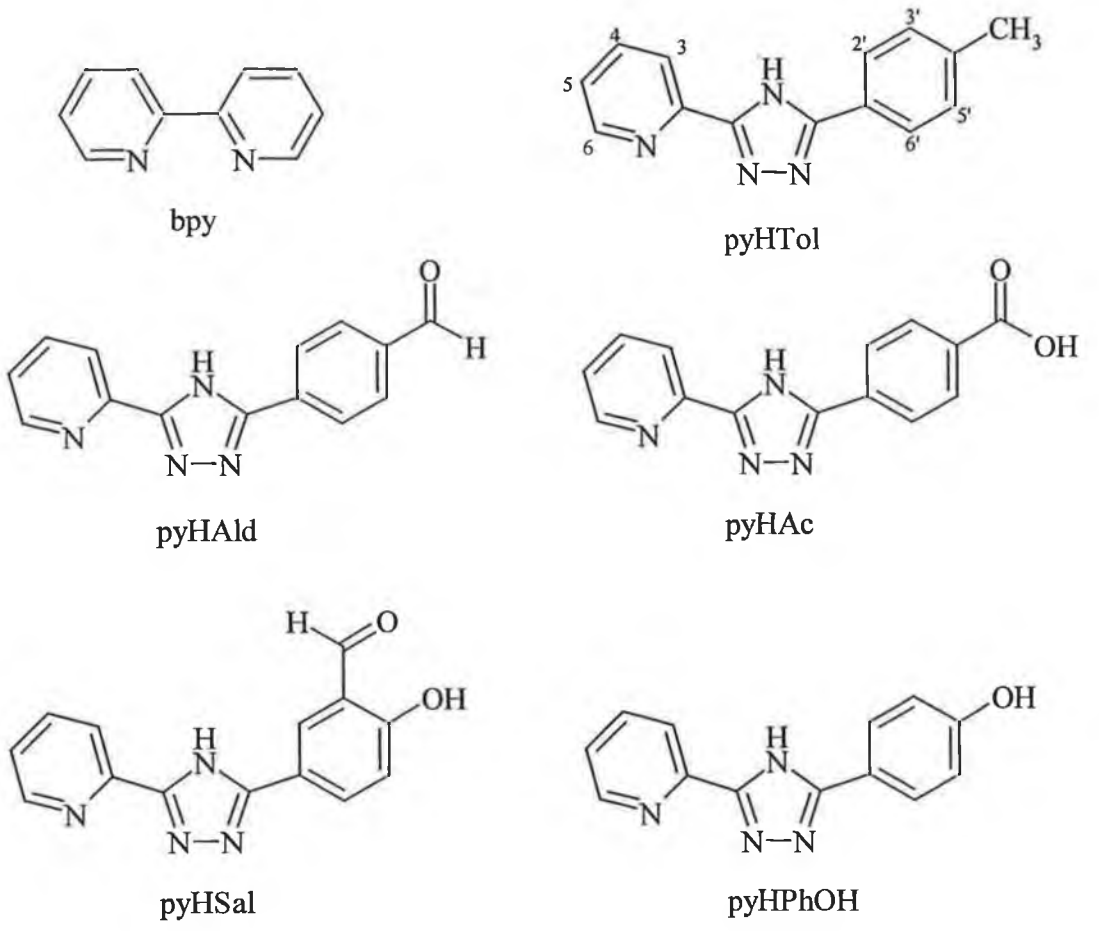

Fig. 3.1 List of ligands cited in this chapter

As can be seen from the figure above, the novel ligands prepared here all adhere to the criteria outlined earlier. They are pyridyl triazole derivatives, so as to exploit not only their useful acid-base chemistry, but also the knowledge of the location of the excited state in their ruthenium complexes. Each ligand also contains a terminal synthon, necessary for the reaction to incorporate the manganese chelating ligands, once the ruthenium complex has been prepared. Using them as bridging ligands would result in the excited state actually being directed away from the manganese electron donor.

3.2 Synthetic Procedures

3.2.1 Synthesis of Ligands

3-(2'-pyridyl), 5-(4''-tolyl), 1,2,4-triazole (pyHTol)

A solution of 27 g (0.199 mol) p-toluic acid and 2 cm^3 concentrated sulphuric acid in 100 cm^3 of absolute ethanol was refluxed for 6 hours. After removal of the excess ethanol under reduced pressure, 50 cm^3 of water was added to the residue and this extracted 3 times with 75 cm^3 of dichloromethane. The extract was neutralised by washing once with a saturated solution of sodium bicarbonate and subsequently dried with magnesium sulphate, before removal of the solvent. The resulting 33 g (0.199 mol) of ester were dissolved in 30 cm^3 of DMF. 72 g (2 mol - 10 eq) of hydrazine monohydrate were added and the solution stirred at room temperature overnight. Crystallisation of the product was induced by scratching the flask with a glass rod. The hydrazide was collected by vacuum filtration, washed with a small amount of ice-cold methanol and dried in the vacuo. The 19 g (0.126 mol) of hydrazide obtained were added to a solution of 13.1 g (0.126 mol) of cyanopyridine and 0.6 g of sodium in 100 ml of methanol, which had been refluxing for 3 hours. This was refluxed with vigorous stirring for a further 2 hours. The yellow precipitate formed was collected by vacuum filtration, washed with a small amount of cold ethanol and dried *in vacuo*. The acylamidrazone was cyclical to the triazole by refluxing in 150 cm^3 ethylene glycol for 1 hour. Upon cooling, the product was crashed out with ice, filtered, washed with cold ethanol and dried *in vacuo*. The

resulting compound was sufficiently pure so as not to warrant further purification. Overall yield: 19.7 g (0.083 mol). 42% based on p-toluic acid. M.p. 202-204°C

^{1}H NMR (400 MHz, $(CD_3)_2SO$)) δ in ppm 8.70 (d, 1H, J=6Hz, H6), 8.16 (d, 1H, J=8Hz, H3), 8.01 (m, 3H, H4, H3', H5'), 7.53 (m, 1H, H5), 7.31 (d, 2H, J=8Hz, H2', H6'), 2.35 (s, 3H, CH_3)

^{13}C NMR (100 MHz, $(CD_3)_2SO$)) δ in ppm 160.15, 153.48, 149.93, 145.74, 141.86, 138.42, 129.73, 127.10, 126.24, 125.19, 121.75, 21.29

IR (KBr) 3421cm^{-1} Triazole N-H stretch, 3027cm^{-1} Aromatic C-H stretch, 1599 cm^{-1} C=N stretch, 825 cm^{-1} C-H out of plane bend, 746 cm^{-1} C-H out of plane bend (pyridine)

Elemental Analysis for $C_{14}H_{12}N_4$: Calc: C 71.17, H 5.12, N 23.71, Found: C 69.77, H 5.01, N 23.27

3-(2'-pyridyl), 5-(4''-formylphenyl), 1,2,4-triazole (pyHAld)

2 g (8.5 mmol) of pyHTol were dissolved in 30 cm^3 of 6M HNO_3 at 85°C. A solution of 17.5 g (34mmol - 4 eq) of ceric ammonium nitrate in 90 cm^3 6M HNO_3 was added over 20 minutes. This was then refluxed overnight at 85°C, resulting in a decolourisation of the solution. When cooled to room temperature, it was poured onto 200 cm^3 of ice water and left to stand for 7 hours at 0-4°C. The precipitate was collected by vacuum filtration, washed with water and diethyl ether before being dried *in vacuo*. The resulting compound was sufficiently pure and required no further purification. Yield: 1.95 g (7.8 mmol) 91.7%. M.p. 231-234°C (decomposition)

^{1}H NMR (400 MHz, $(CD_3)_2SO$)) δ in ppm 10.06 (s, 1H, CHO), 8.77 (d, 1H, J=6Hz, H6), 8.30 (m, 3H, H3, H3', H5'), 8.21 (t, 1H, J=7Hz, H4), 8.07 (d, 2H, J=8Hz, H2', H6'), 7.71 (t, 1H, J=5Hz, H5)

^{13}C NMR (100 MHz, $(CD_3)_2SO$)) δ in ppm 193.08, 159.45, 155.87, 148.31, 145.43, 140.63, 137.03, 135.12, 130.54, 126.96, 126.15, 122.57

IR data: [KBr] Triazole N-H stretch 3448cm^{-1}, Aromatic C-H stretch 3032 cm^{-1}, Aldehyde C-H stretch 2728 cm^{-1}, C=O stretch 1684 cm^{-1}, C=N stretch 1610 cm^{-1}, 1576 cm^{-1}, C-H out of plane bend (pyridine) 752cm^{-1}

Elemental analysis: Calc: C 67.19, H 4.03, N 22.39, Found: C 66.97, H 4.04, N 22.22

3-(2'-pyridyl), 5-(4''-carboxylic acid phenyl), 1,2,4-triazole. $Na^+.3H_2O$ (pyHAc)

2 g (8.5 mmol) of pyHTol were dissolved in 30 cm^3 of concentrated sulphuric acid. 3.6 g (12.7mmol) of solid potassium dichromate were added over 30 minutes. The exothermic reaction mixture was stirred vigorously for 2 hours, after which it was poured onto 100 cm^3 of crushed ice and left to stand for 2 hours at 0-4°C. The product was obtained by vacuum filtration, washed with water and dried *in vacuo*. The brown powder was recrystalised by dissolution in aq. NaOH and reprecipitation by the addition of conc. HCl. Yield: 1.7 g (6.5mmol) 75%. M.p. >250°C

^{1}H NMR (400 MHz, $(CD_3)_2SO$)) δ in ppm 8.78 (d, 1H, J=6Hz, H6), 8.36 (m, 2H, H3, H4), 8.21 (d, 2H, J=8Hz, H3' H5'), 8.09 (d, 2H, J=8Hz, H2', H6'), 7.77 (t, 1H, J=5Hz, H5)

^{13}C NMR (100 MHz, $(CD_3)_2SO$) δ in ppm 168.00, 158.54, 155.65, 146.98, 145.35, 142.28, 132.45, 131.62, 127.20, 126.75, 125.08, 123.53

IR (KBr) 3410cm^{-1} Triazole N-H stretch, 3090 cm^{-1} Aromatic C-H stretch, 1699 cm^{-1} C=O stretch, 1580 cm^{-1} C=N stretch, 1280 cm^{-1} C-O stretch, 1003 cm^{-1} O-H out of plane bend, 733 cm^{-1} C-H out of plane bend (pyridine)

Elemental analysis for $C_{14}H_{15}N_4O_5Na$: C 49.13, H 4.42, N 16.37, Found: C 49.23, H 3.58, N 16.24

3-(2'-pyridyl), 5-(4''-salicylyl), 1,2,4-triazole (pyHSal).H_2O

2 g (8.4 mmol) of pyHPhOH[16] and 5 g (34mmol - 4 eq) of hexamethylenetetramine were refluxed for 6 hours in 80 cm^3 of a 1:1 ratio of acetic acid and trifluoroacetic acid. After being left to stand at room temperature overnight, the solution was poured onto 150 cm^3 of ice. The pH of the solution was raised to pH 4 with NaOH. The precipitate formed was collected by vacuum filtration, washed with water and diethyl ether and dried *in vacuo*. The product formed did not require further purification. Yield: 2 g (7.4 mmol) 88%. M.p. 212-215°C

^1H NMR (400 MHz, $(CD_3)_2SO$)) δ in ppm 11.1 (s, 1H, OH), 10.40 (s, 1H, CHO), 8.77 (d, 1H, J=6Hz, H6), 8.44 (s, 1H, H2'), 8.26 (m, 2H, H3, H5'), 8.07 (t, 1H, J=7Hz, H4), 7.59 (t, 1H, J=5Hz, H5), 7.21 (d, 1H, J=8Hz, H6')

^{13}C NMR (100 MHz, $(CD_3)_2SO$) δ in ppm 198.38, 158.78, 154.57, 153.19, 152.14, 138.88, 137.70, 135.40, 131.28, 128.78, 127.78, 124.73, 121.82, 117.30

IR (KBr) 3083 cm^{-1} Aromatic C-H stretch, 2849 cm^{-1} Aldehyde C-H stretch, 1654 cm^{-1} C=O stretch, 1610 cm^{-1} C=N stretch, 1428 cm^{-1} C-H stretch, 754 cm^{-1} C-H out of plane bend (pyridine)

Elemental analysis for $C_{13}H_{12}N_4O_3$: C 59.15, H 4.26, N 19.71, Found: C 60.01, H 4.00, N 19.66

D_8-2,2'-Bipyridyl[8]

3 g (18 mmol) of 2,2'-bipyridyl and 0.2 g of a Pd/charcoal catalyst were added to 20 cm^3 of D_2O in a Teflon coated bomb. The bomb was stoppered tightly and placed in an oven at 200°C for 3 days. After this time, the bomb was removed and allowed to cool slightly. While still warm, the catalyst was filtered off and washed well with diethyl ether. The aqueous and organic layers of the filtrate were separated and the aqueous layer extracted three times with ether. The organic layers were combined and dried over magnesium sulphate before being evaporated to dryness *in vacuo*. The partially deuterated bpy was placed in the bomb again with fresh Pd/C and D_2O, and the procedure repeated. Yield 2.2 g (73%)

NMR analysis showed the product to be 99.8% Atom D (See Section 3.3.1.2)

IR (KBr) 2250cm^{-1} C-D Vibrations

3.2.2 Synthesis of the Ruthenium Complexes

***Cis*-[$Ru(bpy)_2Cl_2$].$2H_2O$**[9]

7.8 g (30 mmol) of $RuCl_3.3H_2O$ and 1.8 g (43 mmol) of LiCl were heated to reflux in 60 cm^3 of DMF, with nitrogen bubbling constantly through the solution. 9.4 g (58

mmol) of bpy were added in three portions over 30 minutes. The resulting mixture was refluxed with constant nitrogen bubbling for another 5 hours. After cooling, it was poured into 200 cm^3 of acetone and left at –4°C for 16 hours. The dark purple $[Ru(bpy)_2Cl_2].2H_2O$ was filtered *in vacuo* and washed with copious amounts of cold water, before being dried *in vacuo*. Yield: 8.9 g (17.1 mmol) 59%

^1H NMR (400 MHz, $(CD_3)_2SO$) δ in ppm 9.95 (d, 1H, H6), 8.62 (d, 1H, H3), 8.47 (d, 1H, H3'), 8.04 (t, 1H, H4), 7.75 (t, 1H, H5), 7.66 (t, 1H, H4'), 7.50 (d, 1H, H6'), 7.09 (t, 1H, H5')

[Ru(bpy)$_2$pyTol](PF$_6$)

0.29 g (1.2 mmol) of pyHTol were dissolved in 50 cm^3 of ethanol/water (1:1). Addition of 0.52 g (1 mmol) of $[Ru(bpy)_2Cl_2].2H_2O$ resulted in a deep purple coloured solution. After refluxing for 45 minutes, the colour had faded to a dark orange solution. This was refluxed for a further 5 hours, after which the solvent was removed with the rotary evaporator. The solid was redissolved in 10 cm^3 of water. Dropwise addition of a saturated solution of ammonium hexafluorophosphate brought about the precipitation of an orange solid, which was filtered, washed with small amounts of water and diethyl ether and dried *in vacuo*.

The impure complex obtained was purified by column chromatography on neutral alumina, with acetonitrile/methanol (98:2) as eluent. Subsequent recrystalisation of the major fraction in acetone/water (2:1) resulted in a dark red solid.

Yield: 0.6 g (0.75 mmol) 75%

^{1}H NMR (400 MHz, $(CD_3)_2SO$) δ in ppm 8.75 (m, 4H, 4xbpy H3), 8.09 (m, 5H, H3, 4xbpy H4), 7.95 (td, 1H, J_1=1Hz, J_2=7Hz, H4), 7.86 (d, 1H, J=6Hz, bpy H6), 7.82 (d, 1H, J=6Hz, bpy H6), 7.76 (m, 3H, H3', H5', bpy H6), 7.67 (d, 1H, J=6Hz, bpy H6), 7.53 (m, 3H, 3xbpy H5), 7.47 (m, 2H, H6, bpy H5), 7.24 (td, 1H, J_1=2Hz, J_2=6Hz, H5), 7.13 (d, 2H, J=8Hz, H2', H6'), 2.27 (s, 3H, CH_3)

Elemental Analysis for $C_{34}H_{28}N_8RuPF_6$: Calc: C 51.47, H 3.43, N 14.12, Found: C 51.28, H 3.42, N 13.97

[Ru(bpy)$_2$pyAld](PF$_6$).2H$_2$O

0.75 g (3.0 mmol) of pyHAld were dissolved in 100 cm^3 of ethanol/water (1:1). Addition of 1.1 g (2.3 mmol) of $[Ru(bpy)_2Cl_2].2H_2O$ resulted in a deep purple coloured solution. This was refluxed for 5 hours, after which the solvent was removed with the rotary evaporator. The solid was redissolved in 10 cm^3 of water. Dropwise addition of a saturated solution of ammonium hexafluorophosphate brought about the precipitation of an orange solid, which was filtered, washed with small amounts of water and diethyl ether and dried *in vacuo*.

The impure complex obtained was purified by column chromatography on neutral alumina, with acetonitrile as eluent. Subsequent recrystalisation of the major fraction in acetone/water (2:1) resulted in a dark red solid.

Yield: 1.2 g (1.5 mmol) 65%

^{1}H NMR (400 MHz, $(CD_3)_2SO$) δ in ppm 9.96 (s, 1H, CHO), 8.76 (m, 4H, 4xbpy H3), 8.09 (m, 7H, H3, H3', H5', 4xbpy H4), 8.01 (td, 1H, J_1=1Hz, J_2=7Hz, H4), 7.89 (m, 3H, H2', H6', bpyH6), 7.85 (d, 1H, J=6Hz, bpy H6), 7.79 (d, 1H, J=6Hz, bpy

H6), 7.69 (d, 1H, J=6Hz, bpyH6), 7.55 (m, 4H, H6, 3xbpy H5), 7.47 (m, 1H, bpy H5), 7.30, (td, 1H, J_1=1Hz, J_2=6Hz, H5)

^{13}C NMR (100 MHz, $(CD_3)_2SO$) δ in ppm 192.59, 157.30, 137.34, 137.00, 135.55, 130.59, 126.22

Elemental analysis for $C_{34}H_{30}N_8O_3RuPF_6$: Calc: C 48.41, H 3.46, N 13.28, Found: C 48.61, H 3.26, N 13.03

[Ru(bpy)$_2$pyAc](PF$_6$).4H$_2$O

0.75 g (2.8 mmol) of pyHAc were dissolved in 100 cm^3 of ethanol/water (1:1). Addition of 1.0 g (2.2 mmol) of $[Ru(bpy)_2Cl_2].2H_2O$ resulted in a deep purple coloured solution. This was refluxed for a further 5 hours, after which the solvent was removed under reduced pressure. The red solid was redissolved in 10 cm^3 of water. Dropwise addition of a saturated solution of ammonium hexafluorophosphate brought about the precipitation of an orange solid, which was filtered, washed with small amounts of water and diethyl ether and dried *in vacuo*.

The impure complex obtained was purified by flash chromatography on neutral silica gel, with acetonitrile/methanol/saturated aqueous solution of KNO_3 (80:20:1) as eluent. Subsequent recrystalisation of the major fraction in acetone/water (2:1) resulted in a dark red solid. Yield: 1.1 g (1.3 mmol) 61%

^{1}H NMR (400 MHz, $(CD_3)_2SO$) δ in ppm 8.76 (m, 4H, 4xbpy H3), 8.08 (m, 5H, H3, 4xbpy H4), 7.99 (m, 3H, H4, H3', H5'), 7.91 (d, 2H, J=8Hz, H2', H6'), 7.87 (d, 1H, J=6Hz, bpy H6), 7.82 (d, 1H, J=6Hz, bpy H6), 7.77 (d, 1H, J=6Hz, bpy H6), 7.69 (d, 1H, J=6Hz, bpy H6), 7.50 (m, 4H, 3xbpy H5, H6), 7.44 (m, 1H, bpy H5), 7.28 (td, 1H, J_1=6Hz, J_2=1Hz, H5)

Elemental Analysis for $C_{34}H_{34}N_8O_6RuPF_6$: Calc: C 45.59, H 3.71, N 12.51, Found: C 45.62, H 3.09, N 12.23

[Ru(bpy)$_2$pySal](PF$_6$).3H$_2$O

0.75 g (2.8 mmol) of pyHSal were dissolved in 100 cm^3 of ethanol/water (1:1). Addition of 1.0 g (2.2 mmol) of $[Ru(bpy)_2Cl_2].2H_2O$ resulted in a deep purple coloured solution. This was heated at reflux for 5 hours, after which time the solvent was removed under reduced pressure. The solid was redissolved in 10 cm^3 of water. Dropwise addition of a saturated solution of ammonium hexafluorophosphate brought about the precipitation of an orange solid, which was filtered, washed with small amounts of water and diethyl ether and dried *in vacuo*.

The impure complex obtained was purified by column chromatography on neutral alumina, with acetonitrile as eluent. Subsequent recrystalisation of the major fraction in acetone/water (2:1) resulted in a dark red solid.

Yield: 1.05 g (1.3 mmol) 58%

^{1}H NMR (400 MHz, $(CD_3)_2SO$) δ in ppm 10.29 (s, 1H, CHO), 8.77 (m, 4H, 4xbpy H3), 8.08 (m, 6H, H3, H3', 4xbpy H4), 8.02 (m, 2H, H4, H5'), 7.86 (d, 1H, J=6Hz, bpy H6), 7.81 (d, 1H, J=6Hz, bpy H6), 7.76 (d, 2H, J=6Hz, 2xbpy H6), 7.55 (m, 5H, H6, 4xbpy H5), 7.32 (td, 1H, J_1=1Hz, J_2=6Hz, H5), 7.04 (d, 1H, J=8Hz, H6')

Elemental Analysis for $C_{34}H_{32}N_8O_5RuPF_6$: Calc: C 46.53, H 3.56, N 12.76, Found: C 46.80, H 3.02, N 12.54

[$Ru(bpy)_2pyPhOH](PF_6)$

0.75 g (3.1 mmol) of pyHPhOH were dissolved in 100 cm^3 of ethanol/water (1:1). Addition of 1.2 g (2.3 mmol) of $[Ru(bpy)_2Cl_2].2H_2O$ resulted in a deep purple coloured solution. This was refluxed for 5 hours, after which the solvent was removed using the rotary evaporator. The solid was redissolved in 10 cm^3 of water. Dropwise addition of a saturated solution of ammonium hexafluorophosphate brought about the precipitation of an orange solid, which was filtered, washed with small amounts of water and diethyl ether and dried *in vacuo*.

The impure complex obtained was purified by column chromatography on neutral alumina, with acetonitrile/methanol (98:2) as eluent. Subsequent recrystalisation of the major fraction in acetone/water (2:1) resulted in a dark red solid.

Yield: 1.25 g (1.5 mmol) 67%

^1H NMR (400 MHz, $(CD_3)_2SO$) δ in ppm 9.48 (s, 1H, OH), 8.79 (m, 4H, 4xbpy H3), 8.09 (m, 5H, H3, 4xbpy H4), 7.95 (t, 1H, J=7Hz, H4), 7.87 (d, 1H, J=6Hz, bpy H6), 7.83 (d, 1H, J=6Hz, bpy H6), 7.77 (d, 1H, J=6Hz, bpy H6), 7.71 (m, 2H, H3', H5', bpy H6), 7.54 (m, 5H, H6, 4xbpy H5), 7.24 (t, 1H, J=6Hz, H5), 6.73 (d, 2H, J=8Hz, H2', H6')

^{13}C NMR (100 MHz, $(CD_3)_2SO$) δ in ppm 163.69, 160.85, 157.61, 157.37, 157.27, 156.91, 156.64, 151.38, 151.13, 137.01, 127.80, 127.38, 126.88, 124.12, 123.59, 122.31, 121.39, 115.76

Elemental Analysis for $C_{33}H_{25}N_8ORuPF_6$: Calc: C 49.82, H 3.17, N 14.08, Found: C 49.53, H 3.16, N 13.94

[Ru(d_8-bpy)$_2$Cl$_2$].2H$_2$O[9]

2.75 g (10.5 mmol) of $RuCl_3.3H_2O$ were added to 20 cm^3 of DMF. This was brought to reflux with a constant stream of argon bubbling through the reaction mixture. 3.5 g (21 mmol) of d_8-bpy were then added to the reaction mixture in three portions over 30 minutes. After refluxing for a further 6 hours, the mixture was allowed to cool to room temperature, poured onto 75 cm^3 of acetone and stored in the freezer overnight. The black mixture was filtered and the filtrate replaced in the freezer for a further 24 hours. The precipitate was washed with copious amounts of cold water until the washings were almost colourless, then with diethyl ether and finally dried *in vacuo*. A second fraction of the desired complex could be filtered from the filtrate which had been placed in the freezer, and washed and dried in the same manner, to give a total yield of 2.4 g (43%)

Purity was assessed by HPLC control and by the lack of peaks in ^{1}H NMR.

[Ru(d_8-bpy)$_2$pyTol](PF$_6$).H$_2$O

40 mg (0.17 mmol) of pyHTol and 75 mg (0.14 mmol) of [Ru(d_8-bpy)$_2$Cl$_2$].2H$_2$O were refluxed for 5 hours in 10 cm^3 of ethanol/water (1:1). After this time, the solvent was reduced to ~3 cm^3 in vacuo. Dropwise addition of an aqueous saturated solution of NH_4PF_6 brought about the precipitation of the orange complex, which was filtered off, washed with cold water and diethyl ether and dried *in vacuo*. The complex was purified by column chromatography on neutral alumina with

CH_3CN/MeOH (98:2) as eluent. Subsequent recrystalisation from acetone/water (2:1) yielded the complex in a yield of 75 mg (67%).

^1H NMR (400 MHz, $(CD_3)_2SO$) δ in ppm 8.11 (d, 1H, J=8Hz, H3), 7.95 (td, 1H, J_1=1Hz, J_2=7Hz, H4), 7.77 (d, 2H, J=8Hz, H3', H5'), 7.47 (d, 1H, J=6Hz, H6), 7.24, (td, 1H, J_1=1Hz, J_2=6Hz, H5), 7.13 (d, 2H, J=8Hz, H2', H6'), 2.26, (s, 1H, CH_3)

^{13}C NMR (100 MHz, $(CD_3)_2SO$) δ in ppm 164.64, 161.54, 157.32, 156.91, 151.67, 151.02, 136.47, 129.56, 128.67, 125.86, 20.93

Elemental Analysis for $C_{34}H_{13}N_8D_{16}ORuPF_6$: Calc. C 49.35, H 3.53, N 13.54, Found: C 49.67, H 3.33, N 13.69

[Ru(d_8-bpy)$_2$pyAld](PF$_6$).2H$_2$O

42 mg (0.17 mmol) of pyHAld and 75 mg (0.14 mmol) of [Ru(d_8-bpy)$_2$Cl$_2$].2H$_2$O were refluxed for 5 hours in 10 cm^3 of ethanol/water (1:1). After this time, the solvent was reduced to ~3 cm^3 in vacuo. Dropwise addition of an aqueous saturated solution of NH_4PF_6 brought about the precipitation of the orange complex, which was filtered off, washed with cold water and diethyl ether and dried *in vacuo*. The complex was purified by column chromatography on neutral alumina with CH_3CN/MeOH (98:2) as eluent. Subsequent recrystalisation from acetone/water (2:1) yielded the complex in a yield of 64 mg (56%).

^1H NMR (400 MHz, $(CD_3)_2SO$) δ in ppm 9.97 (s, 1H, CHO), 8.18 (d, 1H, J=8Hz, H3), 8.10 (d, 2H, J=8Hz, H3', H5'), 8.01 (t, 1H, J=7Hz, H4), 7.90 (d, 2H, J=8Hz, H2', H6'), 7.53 (d, 1H, J=5Hz, H6), 7.30 (t, 1H, J=6Hz, H5)

Elemental Analysis for $C_{34}H_{13}N_8D_{16}O_3RuPF_6$: Calc. C 47.51, H 3.40, N 13.04, Found: C 47.84, H 2.99, N 13.06

[Ru(d_8-bpy)$_2$pyAc](PF$_6$).2H$_2$O

45 mg (0.17 mmol) of pyHAc and 75 mg (0.14 mmol) of [Ru(d_8-bpy)$_2$Cl$_2$].2H$_2$O were refluxed for 5 hours in 10 cm^3 of ethanol/water (1:1). After this time, the solvent was reduced to ~3 cm^3 in vacuo. Dropwise addition of an aqueous saturated solution of NH_4PF_6 brought about the precipitation of the orange complex, which was filtered off, washed with cold water and diethyl ether and dried *in vacuo*. The complex was purified by column chromatography on neutral silica with CH_3CN/H_2O/sat. aq. KNO_3 (80:20:1) as eluent. After removal of the solvent from the relevant fractions, the solid was redissolved in water, precipitated as the PF_6 salt as before and filtered off. Subsequent recrystalisation from acetone/water (2:1) yielded the complex in a yield of 52 mg (44%).

^{1}H NMR (400 MHz, $(CD_3)_2SO$) δ in ppm 8.15 (d, 1H, J=8Hz, H3), 7.99 (m, 3H, H4, H3', H5'), 7.91 (d, 2H, J=8Hz, H2', H6'), 7.49 (d, 1H, 6Hz, H6), 7.28 (td, 1H, J_1=6Hz, J_2=1Hz, H5)

Elemental Analysis for $C_{34}H_{13}N_8D_{16}O_4RuPF_6$: Calc. C 46.65, H 3.34, N 12.80, Found: C 46.78, H 3.21, N 12.72

[Ru(d_8-bpy)$_2$pySal](PF$_6$).2H$_2$O

50 mg (0.19 mmol) of pyHSal and 84 mg (0.16 mmol) of [Ru(d_8-bpy)$_2$Cl$_2$].2H$_2$O were refluxed for 5 hours in 10 cm^3 of ethanol/water (1:1). After this time, the solvent was reduced to ~3 cm^3 in vacuo. Dropwise addition of an aqueous saturated solution of NH_4PF_6 brought about the precipitation of the orange complex, which was filtered off, washed with cold water and diethyl ether and dried *in vacuo*. The complex was purified by column chromatography on neutral silica with CH_3CN/H_2O/sat. aq. KNO_3 (80:20:1) as eluent. Subsequent recrystalisation from acetone/water (2:1) gave the complex in a yield of 60 mg (45%).

^{1}H NMR (400 MHz, $(CD_3)_2SO$) δ in ppm 10.89 (s, 1H, OH), 10.29 (s, 1H, CHO), 8.08 (m, 2H, H3, H3'), 8.02 (m, 2H, H4, H5'), 7.55 (d, 1H, J=6Hz, H6), 7.32 (td, 1H, J_1=1Hz, J_2=6Hz, H5), 7.04 (d, 1Hz, J=8Hz, H6')

^{13}C NMR (100 MHz, $(CD_3)_2SO$) δ in ppm 211.57

Elemental Analysis for $C_{34}H_{13}N_8D_{16}O_4RuPF_6$: Calc. C 46.64, H 3.34, N 12.80, Found: C 46.48, H 3.02, N 13.29

[Ru(d_8-bpy)$_2$pyPhOH](PF$_6$).H$_2$O

50 mg (0.21 mmol) of pyHPhOH and 94 mg (0.18 mmol) of [Ru(d_8-bpy)$_2$Cl$_2$].2H$_2$O were refluxed for 5 hours in 10 cm^3 of ethanol/water (1:1). After this time, the solvent was reduced to ~3 cm^3 in vacuo. Dropwise addition of an aqueous saturated solution of NH_4PF_6 brought about the precipitation of the orange complex, which was filtered off, washed with cold water and diethyl ether and dried *in vacuo*. The complex was purified by column chromatography on neutral silica with

CH_3CN/H_2O/sat. aq. KNO_3 (80:20:1) as eluent. After removal of the solvent from the relevant fractions, the solid was redissolved in water, precipitated as the PF_6 salt as before and filtered off. Subsequent recrystalisation from acetone/water (2:1) yielded the complex in a yield of 91 mg (64%).

^1H NMR (400 MHz, $(CD_3)_2SO$) δ in ppm 9.47 (s, 1H, OH), 8.10 (d, 1H, J= 8Hz, H3), 7.95 (t, 1H, J=7Hz, H4), 7.70 (d, 2H, J=8Hz, H3', H5'), 7.48 (d, 1H, J=5Hz, H6), 7.24 (t, 1H, J=6Hz, H5), 6.73 (d, 2H, H2', H6')

^{13}C NMR (100 MHz, $(CD_3)_2SO$) δ in ppm 164.58, 161.34, 157.33, 157.21, 156.91, 151.68, 150.99, 138.01, 123.25, 121.03, 115.67

Elemental Analysis for $C_{33}H_{11}N_8D_{16}O_2RuPF_6$: Calc. C 47.79, H 3.28, N 13.51, Found: C 48.02, H 2.98, N 13.38

3.3 Results and Discussion

3.3.1 Synthesis

As the aim of the work discussed in this chapter was to synthesise a range of ligands, (shown in *Fig. 3.1*), whose complexes could later be coupled with potential ligands for manganese complexation, (such as those in *Fig. 3.2*). The majority of manganese chelating ligands, which have been shown to be capable of holding manganese in a high enough oxidation state for water oxidation to occur, are amine ligands. Of the many possible structures, porphyrins and pyridine derived ligands are probably the most widely used. The use of phenolates as manganese ligands has also been investigated, in the hope that the negatively charged oxygen would stabilise higher oxidation states.

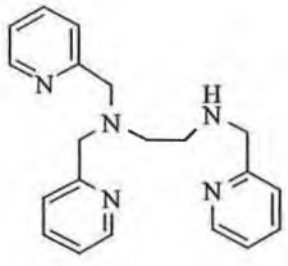

Trispicen

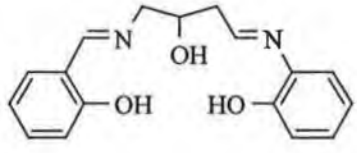

2-OH-Salpn

Fig.3.2 Examples of manganese chelating ligands[10,11]

3.3.1.1. Synthesis of the Ligands

Whilst the structures of the various potential manganese ligands to be used later in the course of this work vary significantly, they all contain terminal amine moieties. In order to couple these effectively with the ruthenium complexes, the correct synthons had to be introduced on the ruthenium pyridyl triazole ligands. It was decided to prepare ligands bearing carbonyl functionalities, (pyHAld and pyHAc). These would be capable of forming imine and amide bonds with the amine ligands. As previously stated, phenolates are also excellent ligands for high oxidation state manganese complexes. Bearing this in mind, it was decided to incorporate a hydroxyl group into one of the pyridyl triazoles, (pyHSal). A pyridyl triazole ligand bearing a terminal phenol, (pyHPhOH), was also prepared, as this would make an ideal candidate for the introduction of new binding sites via a Mannich reaction.

It can be seen that the ligands mentioned above are pyridyl triazoles, as previously explained. However, a phenyl spacer has also been introduced into the ligands. The inclusion of the phenyl spacer was decided upon for two main reasons. Firstly, a wide range of cheap benzoic acid derivatives (used in the synthesis of the ligands) is available. Secondly, the introduction of various functionalities into the phenyl ring can easily be achieved and, with five available sites on the phenyl ring, the number of possible functionalities far outnumbers the number of possibilities available on the triazole ring.

Before attempting to synthesise these ligands, a model compound was prepared (pyHTol). The synthesis of this ligand is shown in *Fig. 3.3*. The lack of highly

reactive functional groups in this ligand makes it an ideal model compound to investigate the synthesis of pyridyl triazoles and the physical properties of the resulting ruthenium complexes. However, it also served another vital role, since the compound is a starting material for other derivatised ligands. The approach to the synthesis of the acid (pyHAc) and aldehyde (pyHAld) ligands from this starting material was very attractive. Selective oxidation of the methyl group could lead to the formation of the acid or the aldehyde.

1,2,4-Triazoles are a well-documented class of compounds[15]. Fused triazoles, such as benzotriazole, and substituted triazoles, such as pyridyl triazoles are easily accessible, generally by means of condensation reactions. Earlier methods to their synthesis[12] relied on high temperature reactions involving acid hydrazides and amides, or at slightly lower temperatures in the case of acid hydrazides and thioamides. Other work brought about the advantageous route to triazoles, which proceeds via acylamidrazones[13,14] – which cyclise spontaneously with loss of water upon heating (see *Scheme 1*). Nowadays, there are many routes to the synthesis of triazoles. In the case of pyridyl triazoles, two methods in particular are of interest, due the commercial availability of the required starting compounds. These two schemes are shown below.

Scheme 1:

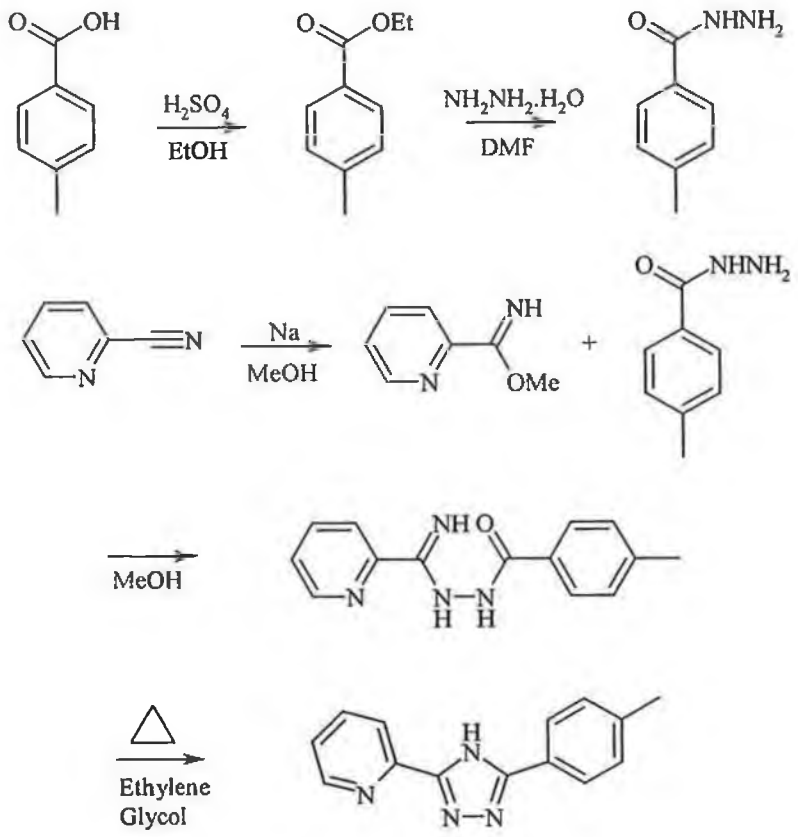

Scheme 2:

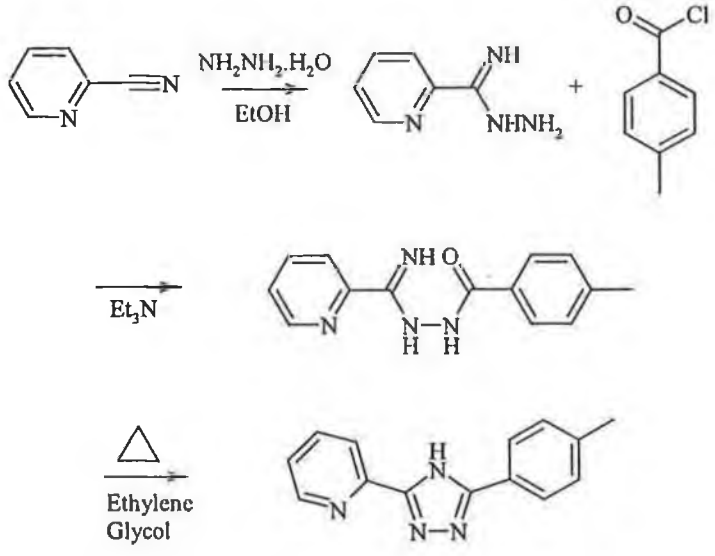

Fig. 3.3. Reaction schemes for the synthesis of pyridyl triazole ligands

Both of the schemes shown above have been used to prepare a wide range of pyridyl triazoles bearing an assortment of groups in the 5-position of the triazole[15]. Generally speaking, one tends to choose the method based on the commercial availability of the starting acid, ester, hydrazide or acid chloride. However, of the two methods shown, *Scheme 1* was chosen over *Scheme 2* in this case, for the ease of its stepwise reactions. Acid chlorides are highly reactive species and require care and attention during their use, whereas acids, esters and hydrazides are all much more robust compounds, requiring little special care. The yields for the two routes are comparable (almost 50% overall for the total synthesis). Very few difficulties were encountered during this synthesis. However, there is one point regarding *Scheme* 2, which is worth mentioning. The use of base in the reaction with the acid chloride is necessary to ensure sole formation of the triazole. The base is used to neutralise the HCl formed in the course of the reaction with the hydrazide. Without this, the HCl salt of the uncyclised compound may also be formed. Cyclisation of this salt may result in the formation of the oxadiazole via loss of ammonia, as well as the triazole which occurs via loss of water. This has been shown before for similar systems[15]. The two compounds are, however, easily separable.

The synthesis of pyHTol via *Scheme* 1 resulted in a highly pure compound being isolated from the cyclisation reaction mixture. In fact, small white crystals were isolated. The quality of these crystals was increased by recrystalisation from hot DMSO. After 2 weeks, larger clear crystals had formed in the solution. These were filtered and washed with water to remove excess DMSO before being studied by x-ray diffraction in FSU Jena, Germany. A planar structure showing typical bond lengths and angles was obtained (See Appendix A). It can be seen that the N2 of the

triazole is protonated and not the N4, as was shown in the structures of the ligands (*Fig. 3.*1). This is shown in *Fig. 3.4* below, along with some selected bond lengths in *Table 3.1*.

Bond	Length (Å)
N(1) – C(1)	1.338
N(1) – C(2)	1.366
N(2) – C(1)	1.335
N(3) – C(2)	1.342
N(2) – N(3)	1.362

Table 3.1 Selected bond lengths in pyHTol

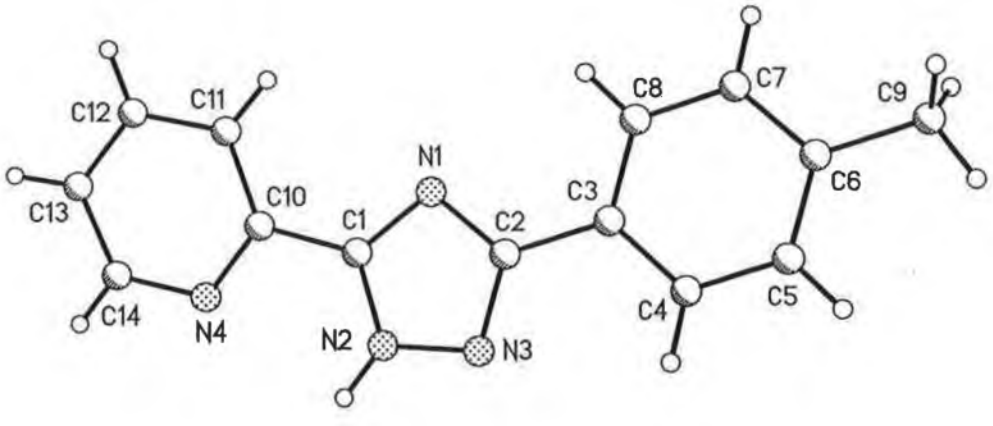

Fig. 3.4 Crystal structure of pyHTol showing crystallographer's numbering of atoms

Having successfully prepared the model compound, attention was turned to the modification of this ligand and the synthesis of other ligands (shown in *Fig. 3.1*).

The ligand pyHPhOH had previously been prepared by T. E. Keyes[16]. The method used for its synthesis was the same as that used for the preparation of pyHTol, but starting from the corresponding hydrazide. It did not require purification after cyclisation either, but was isolated in a pure form.

Synthesis of the acid derivative pyHAc from the tolyl precursor proceeded as expected. Pyridyl triazoles are very resilient compounds and survive reactions with quite severe reagents. Aware of this fact, it was possible to choose quite a harsh oxidation method to bring about this conversion. The conditions used were those applied in the oxidation of 4,4'-dimethyl-2,2'-bipyridine[17]. Although the use of potassium dichromate is not encouraged due to its detrimental effects to the environment; the small scale of the reaction, its high yield and ease of the work up of the reaction all made it an unavoidably attractive option. Unfortunately, reprecipitation of the product by varying the pH resulted in the formation of the sodium salt of the acid, as seen by elemental analysis. This did not however prove to be a problem for the later synthesis of the ruthenium complex.

The oxidation of pyHTol to the aldehyde posed many problems. Oxidations to the aldehyde are generally problematic. If the oxidising agent used is too strong; the acid may be formed, but use of too mild an oxidant may result in only the alcohol being formed. This greatly limits the range of appropriate oxidising agents. Another possibility is to try to reduce the acid back to the aldehyde. However, this again presents the problem of possible alcohol formation, should the reducing agent or conditions employed be too strong. These two routes are shown in *Fig. 3.5* and shall be discussed in turn.

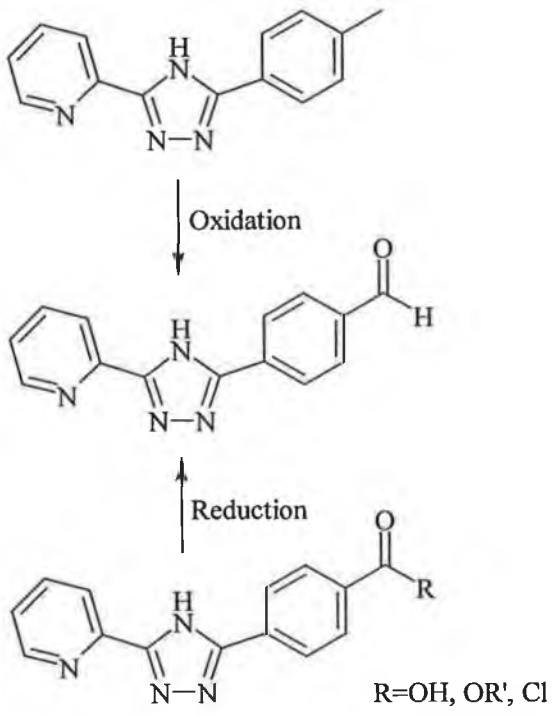

Fig. 3.5 Possible synthetic routes to pyHAld

Much work has been carried out on the synthesis of aromatic aldehydes, starting from methyl-substituted or carboxylic acid derivatives. Although reductions are generally more difficult to carry out than oxidations, the availability of selective reducing agents makes them a viable option. Aromatic esters have been shown to be easily reducible to the corresponding aldehyde by reaction with diisobutylaluminium hydride[18]. The reaction, which is best carried out in at low temperatures in non-polar, aprotic solvents, gives high yields (80-90%) for aliphatic aldehydes, but only gives moderate to good yields (48-70%) for aromatic aldehydes. This yield could be slightly improved upon by use of the sodium salt of diisobutylaluminium hydride.

Acid chlorides present themselves as more suitable precursors to aldehydes. They too may be reduced selectively to the aldehyde without significant production of the

alcohol derivative. Sodium borohydride has even been shown to produce high yields of aldehydes with little (~10%) production of the corresponding alcohol, when used under the correct conditions[19]. The reaction must be carried out in DMF at low temperature. Raising the reaction temperature or use of different solvents results in a higher yield of alcohol and sometimes no formation of aldehyde.

One of the most versatile methods for the reduction of acid chlorides to aldehydes is the Rosenmund reduction[20]. This is a highly selective reduction, only reducing acid chlorides[21]. It involves catalytic hydrogenation in the presence of a hydrogen chloride acceptor. The catalyst is usually palladium based, such as Pd-C, Pd-$BaSO_4$ or Pd-C poisoned with quinoline-S. The standard Pd-C catalyst has been shown to be an excellent catalyst for use with aliphatic acid chlorides, whereas it is much more efficient when poisoned with quinoline-S, for use with aromatic acid chlorides[22]. With yields typically in the region of 70 - 95%, this approach appears to be one of the best methods for the reduction of acid chlorides to aldehydes.

Just as there are many methods for the reduction of various compounds to aldehydes, there are even more for the oxidation of terminal methyl groups to the corresponding aldehydes. These usually involve treatment of the compound with various metal salts. In the course of this work it was decided to proceed, if possible, by this route. Silver(II) is an excellent oxidant, with silver(II) oxide having proven itself to be an extremely selective reagent[23]. It is capable of not only oxidising terminal methyl groups to the corresponding aldehyde, but it can also oxidise terminal alcohols selectively to aldehydes.

MnO_2 is also reportedly capable of oxidising methyl groups directly to aldehydes. This reaction in sulphuric acid was attempted on pyHTol, but no oxidation products were obtained after refluxing for two days. Similarly, SeO_2 and benzeneselenic anhydride[24,25] have been shown to be effective in the oxidation of methyl groups of even electron poor species. Indeed, selenium dioxide is commonly used to yield the mono aldehyde from the oxidation of 4,4'-dimethyl-2,2'-bipyridine[26]. This reaction on PyHTol also proved to be fruitless. Exhaustive attempts under a wide range of conditions, involving the variation of temperature, solvent and water content, came to no avail. Chromium(VI) oxide in acetic anhydride may also be used to bring about the oxidation of a methyl group to the aldehyde[27]. It does this by means of a two-step reaction. Firstly, the diacetate derivative of the methyl group is obtained. This may then be hydrolysed to the aldehyde. Unfortunately, this procedure also failed to oxidise PyHTol. No diacetate was formed in the course of the reaction and therefore no aldehyde.

Having attempted these various oxidation reactions without success, it was decided to employ a less frequently used method. Cerium (IV) salts are known to be excellent oxidising agents and their use in analytical chemistry has been well documented. However, they have not been used extensively on a preparative scale[28]. Work done on the oxidising ability of ceric ammonium nitrate has pointed to the fact that it is a useful agent for the oxidation of methyl groups, on a variety of species, to the corresponding aldehydes[29]. Even, strongly deactivated systems have undergone reaction to give quantitative yields. This salt proved itself to be invaluable in the course of this project, as it succeeded to produce the aldehyde where many other reagents had failed. The high purity of the compound isolated and the simplicity of

the reaction add to the appeal of this procedure. The compound obtained was seen to be pure by NMR and required no further purification. The ceric ammonium nitrate reaction demonstrates well how effective Ce(IV) is as a selective oxidising agent[30]. No side products are formed during the reaction and there appears to be little or no complexation of the cerium with pyHTol, despite its strong chelating properties.

Four equivalents of the cerium salt were used during the experiment. The necessity of four Ce(IV) for every one oxidisable methyl group has been reported by L.K. Sydnes *et al*[31]. As shown in *Fig. 3.6*, he postulates that the reaction proceeds via the formation of a cation radical, followed by irreversible proton abstraction. Subsequent oxidation of the radical yields the cation, which reacts with an anion, such as NO_3^-, and is finally oxidised to the aldehyde.

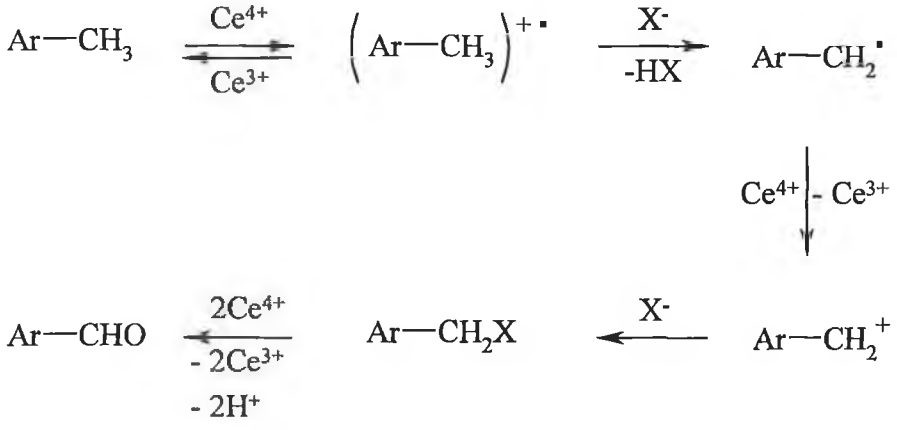

Fig.3.6 Proposed mechanism for the oxidation of a methyl to a formyl group with Ce(IV)[31]

Synthesis of a salicylaldehydyl ligand such as pyHSal presents another problem – whether one should start from the aldehyde and introduce a hydroxyl group, or start from the phenol and formylate it. These two possibilities are represented in *Fig. 3.7*.

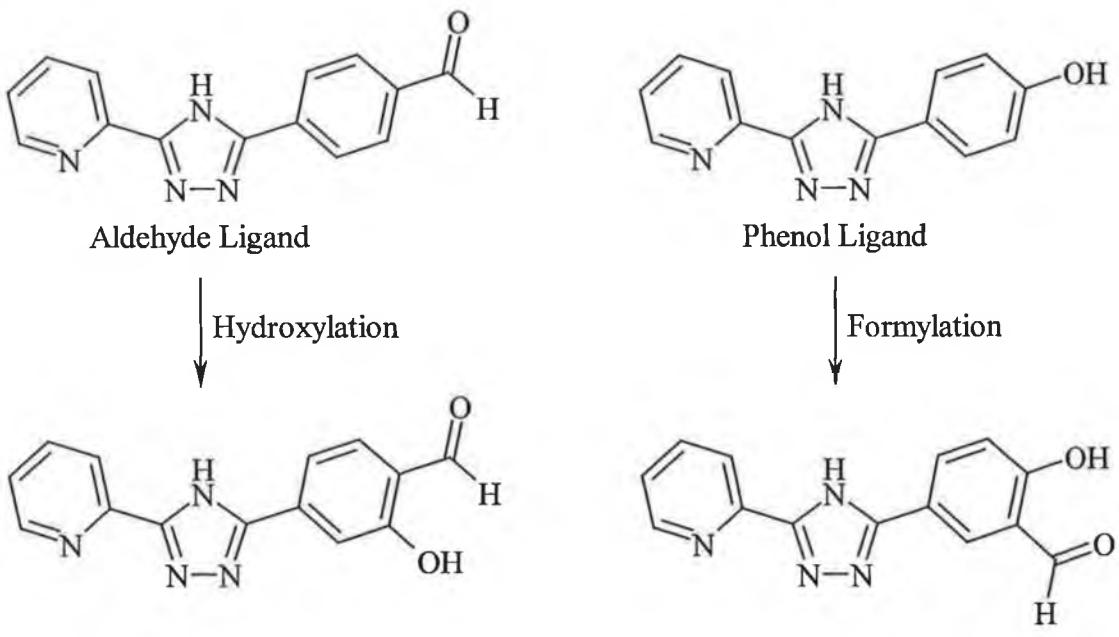

Fig. 3.7 Possible synthetic routes to pyHSal

Although the two forms of pyHSal shown above differ in the relative positions of the hydroxyl and formyl functionalities in relation to the triazole, the preparation of either of the two isomers would be satisfactory. As it is intended to later react the formyl group with a suitable amine ligand, with the aim of chelating manganese, the exact positions of the two functional groups are not overly important, since they present only a slight difference in the orientation of the manganese complex with respect to the ruthenium complex. If one assumes that the phenol will be directly involved in the complexation of the manganese, then it can be seen that in both cases the manganese will be directed away from the ruthenium centre, while its actual

position and distance from the ruthenium do not vary significantly. This is shown in *Fig. 3.8* below.

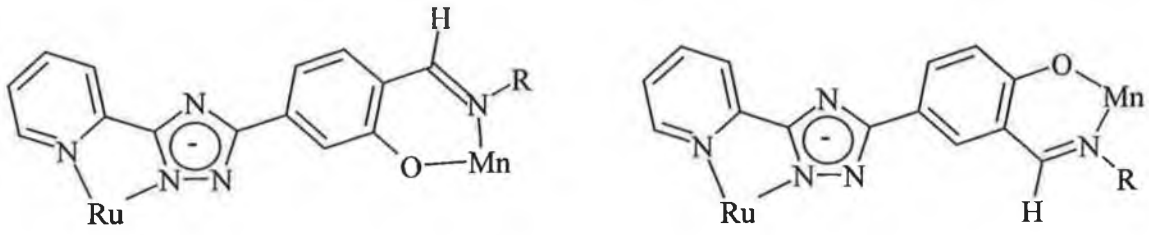

Fig. 3.8 Possible orientations of Ru and Mn for dyads based on the potential isomers of pyHSal

The first approach to the synthesis of a salicylaldehydyl ligand was the hydroxylation approach. This was tried on pyHTol. Methods for direct hydroxylation of aromatic rings are usually quite drastic. In many cases they involve the use of HF or superacids. From a safety and environmental point of view, these should be avoided. However, milder methods such as the use of triflic acid and sodium perborate provide an alternative, if less efficient approach to this reaction[32]. despite numerous attempts, this procedure proved to be incapable of successfully hydroxylating PyHTol.

It was then decided to introduce the hydroxy group by other means. The idea to prepare suitable nitro-toluene derived pyridyl triazoles, followed by the conversion of the nitro into the hydroxyl group seemed attractive. Initial attempts to achieve this, by the reaction of benzaldoxime, sodium hydride and 3-(2'-pyridyl), 5-(4''-nitro- 3''-tolyl), 1,2,4-triazole in dry DMSO[33], proved to be fruitless. Reduction of the nitro group to the amine derivative with $SnCl_2$[34], to be followed by hydrolysis to

the phenol, also proved problematic, due to the low yield from the reduction step. Separation of the tin by-products, the amine and unreacted nitro compound was inefficient and time consuming. At this point it was decided to investigate the possibility of direct formylation of the phenol.

Of the many possibilities[35,36], the Duff formylation[37,38] seemed to be an obvious choice for this procedure. It has been shown that hexamethylene tetraamine (hexamine) reacts with phenols in acidic medium to yield the salicylaldehyde derivative[39]. Although the exact mechanism of this reaction is uncertain[40], it appears that the reaction proceeds via addition of the hexamine onto the aromatic ring of the phenol. This then isomerises and undergoes hydrolysis to yield the aldehyde (See *Fig. 3.9* below)[41].

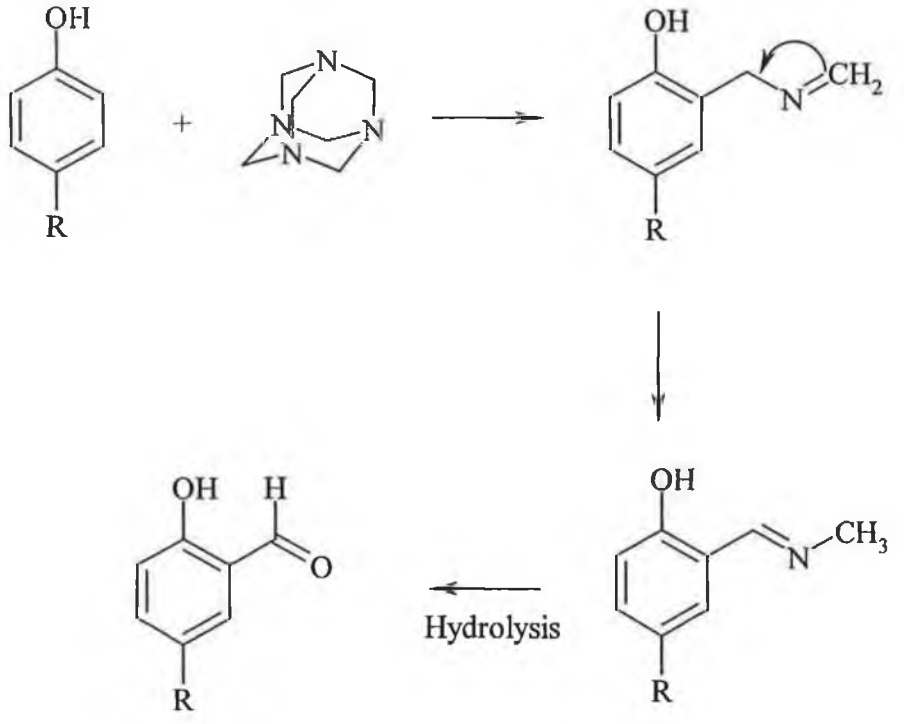

Fig. 3.9 Proposed reaction pathway for Duff formylation

This reaction has since been modified slightly. While initial reports focused on the reaction in acetic acid, the reaction is nowadays more commonly carried out in trifluoroacetic acid or a mixture of trifluoroacetic acid and acetic acid[42]. The choice of solvent may influence the products obtained from the reaction[43]. Use of dry trifluoroacetic acid may result in a high yield of diformylated phenol[44], while a 1:1 mixture of acetic acid and trifluoroacetic acid generally results in a high yield of monoformylated phenol. In the case of PyHSal, only the monoformylated derivative was required, so the latter reaction conditions were chosen. Again, a high yield was obtained for the reaction. Isolation of the product by forced precipitation upon raising of the pH of the reaction mixture resulted in a pure compound being isolated. As was the case with all of the ligands synthesised here, it required no further purification.

Despite the many initial problems encountered during the syntheses of the ligands referred to in this chapter, the eventual pathways found to their synthesis are both straightforward and give high yields of pure compounds. PyHTol, pyHAld, pyHPh and pyHSal have all been isolated from the reaction mixtures in pure enough forms so as not to require any further purification. However, should one so wish, all of these ligands may be recrystallised from hot ethanol. PyHTol and PyHAld may also be recrystallised from DMSO, where upon they form crystals. The crystal structure of PyHTol has been obtained by single crystal x-ray diffraction of a crystal grown by this method.

3.3.1.2 Synthesis of Deuterated Compounds

Deuteration of the 2,2'-bipyridyl was carried out according to a literature procedure[8]. After 3 days in the bomb at 200°C, it was found that approximately 90% atom deuteration had been achieved. Even after longer reaction times, this ratio failed to improve significantly. After isolation of the partially deuterated compound and its reaction with fresh D_2O and Pd/C for a second 3 days in the bomb, it was found that approximately 99.7% atom deuteration was obtainable. The percentage deuteration was calculated as a result of simple NMR experiments, see Section 2.9.

The presence of d_8-bpy in some of the complexes did not alter their synthesis or purification in any way.

3.3.1.3 Synthesis of Ruthenium Complexes

Synthesis of the ruthenium complexes proceeded without difficulty. The preparation of the dichloride complexes, $[Ru(bpy)_2Cl_2].2H_2O$ and $[Ru(d_8\text{-}bpy)_2Cl_2].2H_2O$, was carried out according to literature procedures[9]. It is a problematic reaction, sometimes leading to the formation of carbonyl containing complexes (e.g. $[Ru(bpy)_2COCl]Cl$), due to the degradation of DMF, which must be removed. Another problem, which may occur, is the formation of an oil during the recrystalisation from acetone. This can sometimes be resolved by the dropwise addition of the oil to rapidly stirring diethyl ether, resulting in its precipitation as a fine powder. Reaction of these dichlorides with the ligands in refluxing ethanol/water resulted in the initial replacement of the chlorides by solvent

molecules and subsequently by the ligands. As the reactions proceeded, the initial deep violet colour of the $[Ru(bpy)_2Cl_2]$ solution was gradually replaced by the deep orange/red colour of the pyridyl triazole complexes. The chloride counter ion was replaced by the precipitation of the complex as the PF_6^- salt, as these are soluble in many organic solvents but not in water. This greatly eases their purification and characterisation.

The preparations of the RuN_6 complexes were monitored by cation exchange HPLC (See *Table 3.2*). This was also used to determine the purity of the complexes, as HPLC is capable of separating coordination isomers[45]. Coordination isomers arise because the triazole contains two potential coordination sites. The N2 isomer seems to be predominately formed over the N4, when a large substituent, e.g. a phenyl ring, is present on the triazole ring. This is due to steric effects resulting from more interaction of the bpy ligands with the phenyl ring in the case of the N4 isomer, which limit its rotation. This was observed by simple molecular modelling using **Hyperchem®**[i], in which approximate geometry optimisation calculations were performed. The results of these are shown in *Fig. 3.10*. However, in the case of PyHAc, PyHSal and pyHPhOH, the possibility of coordination of the ruthenium via the hydroxyl group is also a potential problem. In reality, this does not tend to happen, with the triazole and pyridine being favoured due to their formation of more stable complexes.

[i] As no parameters for Ru were available, Cl was chosen as the central atom of the complexes. However, bond lengths and angles were found to be comparable to those found for crystal structures for similar ruthenium complexes[15]

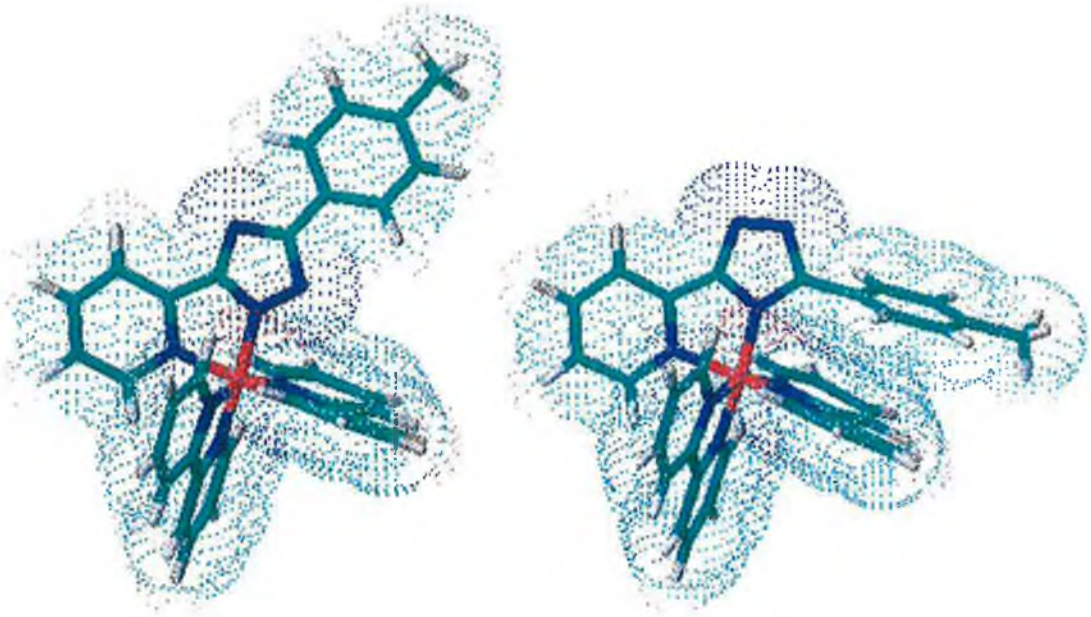

Fig. 3.10 Three dimensional representations of the N2 (left) and N4 (right) isomers of $[Ru(bpy)_2pyTol]^{2+}$

Compound	Retention Time
$[Ru(bpy)_2pyTol](PF_6)$	2.1 mins
$[Ru(bpy)_2pyAld](PF_6)$	2.6 mins
$[Ru(bpy)_2pyAc](PF_6)$	4.2 mins
$[Ru(bpy)_2pySal](PF_6)$	3.2 mins
$[Ru(bpy)_2pyPhOH](PF_6)$	3.1 mins

Table 3.2. Retention times of Ru(II) complexes with a flow rate of 1.8 cm^3*/min of 0.08M* $LiClO_4$ *in* $MeCN/H_2O$ *(80:20)*

HPLC analysis of crude reaction mixtures was indicative of the conditions necessary to purify them by column chromatography. The retention times of the complexes can be seen to correlate to their mobility on neutral alumina. The purification of the

complexes of pyHTol and pyHAld were carried out on neutral alumina, with acetonitrile/methanol (98:2) as eluent. The complexes of pyHSal and pyHPhOH could also be columned on neutral alumina, as before. However, due to the more polar nature of their functional groups, they tended to bind more to the alumina, resulting in poorer separation and lower yields. They could also be purified by flash chromatography on silica, with acetonitrile/water/aq. KNO_3 (80:20:1) as eluent. The complex of pyHAc could only be purified on silica, as it appeared to bind irreversibly with alumina.

In all cases however, pure samples of the complexes were obtainable in their deprotonated triazole forms, as shown by CHN elemental analysis. These were then used to characterise the compounds (Section 3.3.2 below) and for the synthesis of a range of larger, more complicated supramolecular assemblies (See Chapter 6).

3.3.2 Characterisation

The ruthenium complexes prepared have been studied by a variety of techniques. Emission and absorption spectra as well as the excited state lifetimes of the various metal complexes have been measured. The pK_a's of the triazole in each of the complexes in both the ground and excited states have also been determined. In the electrochemical analysis, both the oxidation of the metal centre and the ligand based reductions have been measured. All of these properties are of interest when designing a dinuclear system. The absorption spectrum is of importance because it indicates how much of the solar spectrum is absorbed by the compound and to what extent. For optimal efficiency, the complex should be capable of absorbing as much

light as possible across a broad band of the visible spectrum. The pK_a's are also important since they demonstrate the potential to alter the characteristics of the complex by varying the pH. One of the most important properties of these complexes is the oxidation potential of the metal centre. Upon introduction of the manganese centre, this will provide the driving force for the electron transfer between the two metal. The driving force of the electron transfer reaction has to be such that efficient transfer takes place, resulting in a long-lived charge separation state.

3.3.3 NMR Spectroscopy

NMR spectroscopy has proven itself to be an invaluable tool in the analysis of the products prepared in this section. While the spectra of the ligands were straightforward to interpret, spectra of complexes proved to be much more complex, requiring both 2D NMR experiments and deuteration studies[46] in order to fully explain the spectra. Carbon spectra proved to be of little use in aiding in the elucidation of the structures of the complexes. Where sufficient sample was available, these were measured and are included in section 3.2.2. However, due to the near-equivalency of the various pyridine based carbon, they were found to be difficult to resolve. Even after large numbers of scans (>4000), it was not always possible to see evidence of quaternary carbons. Examples of typical spectra obtained for the free ligand, bpy complex (1D and 2D) and deuterated bpy complex is given in *Figs. 3.11, 3.12, 3.13 and 3.14* respectively.

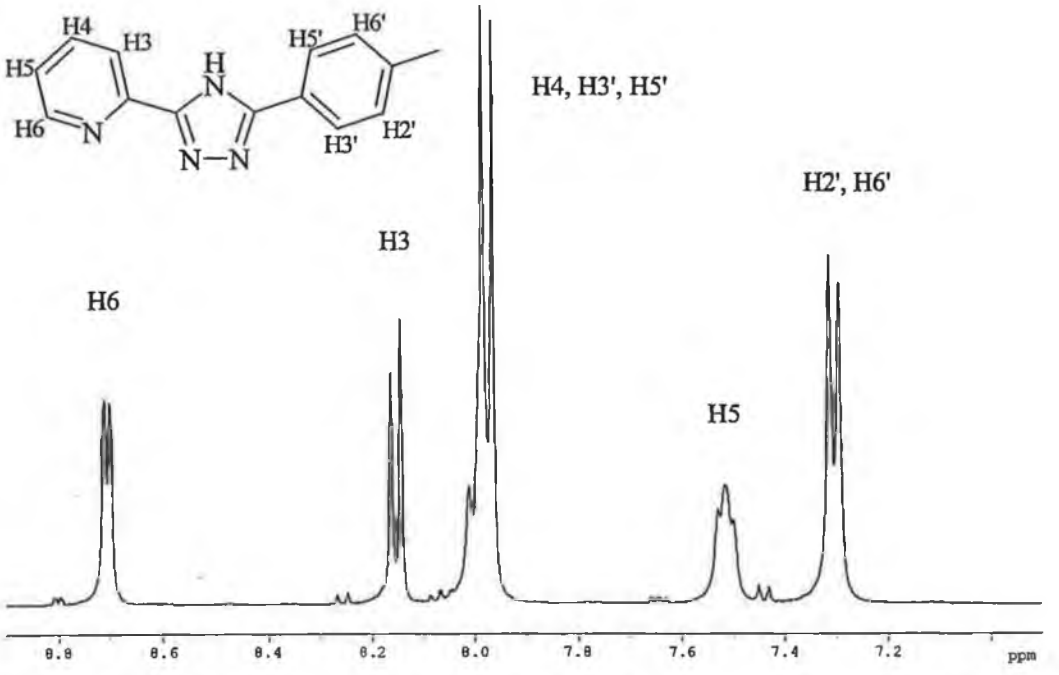

Fig. 3.11 ^{1}H NMR spectrum of pyHTol in d_6-DMSO showing the nomenclature of the various protons

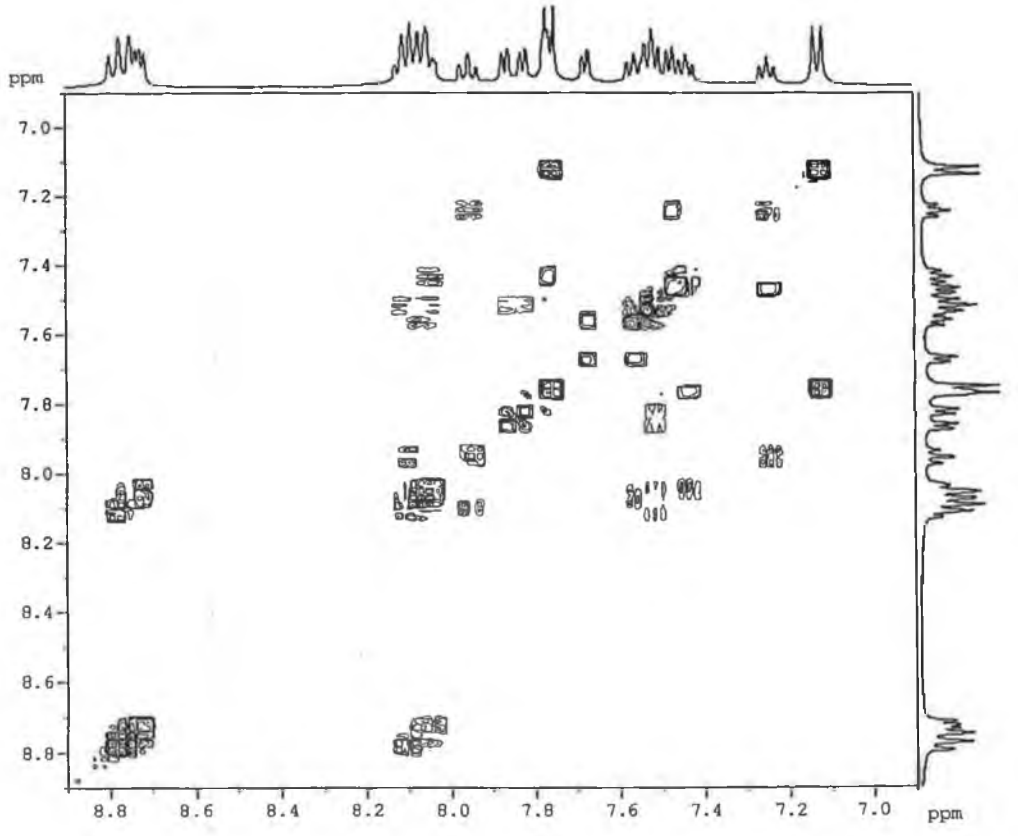

Fig. 3.12 2D COSY spectrum of [Ru(bpy)$_2$pyTol](PF$_6$) in d_6-DMSO

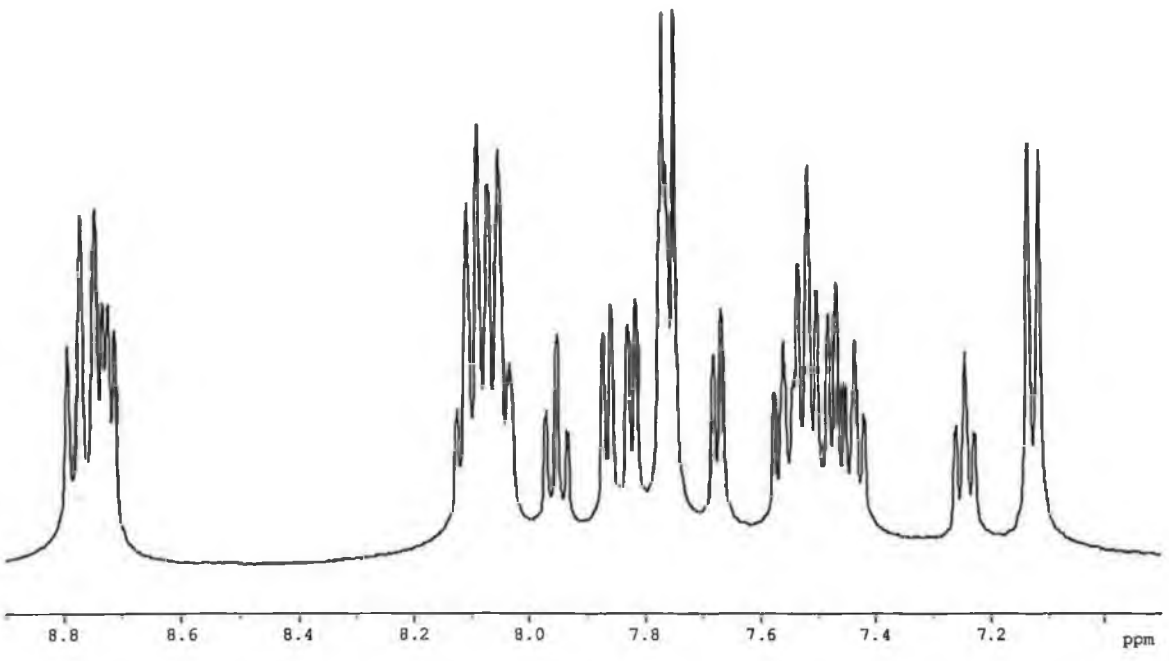

Fig. 3.13 ^1H NMR spectrum of [Ru(bpy)$_2$pyTol](PF$_6$) in d_6-DMSO

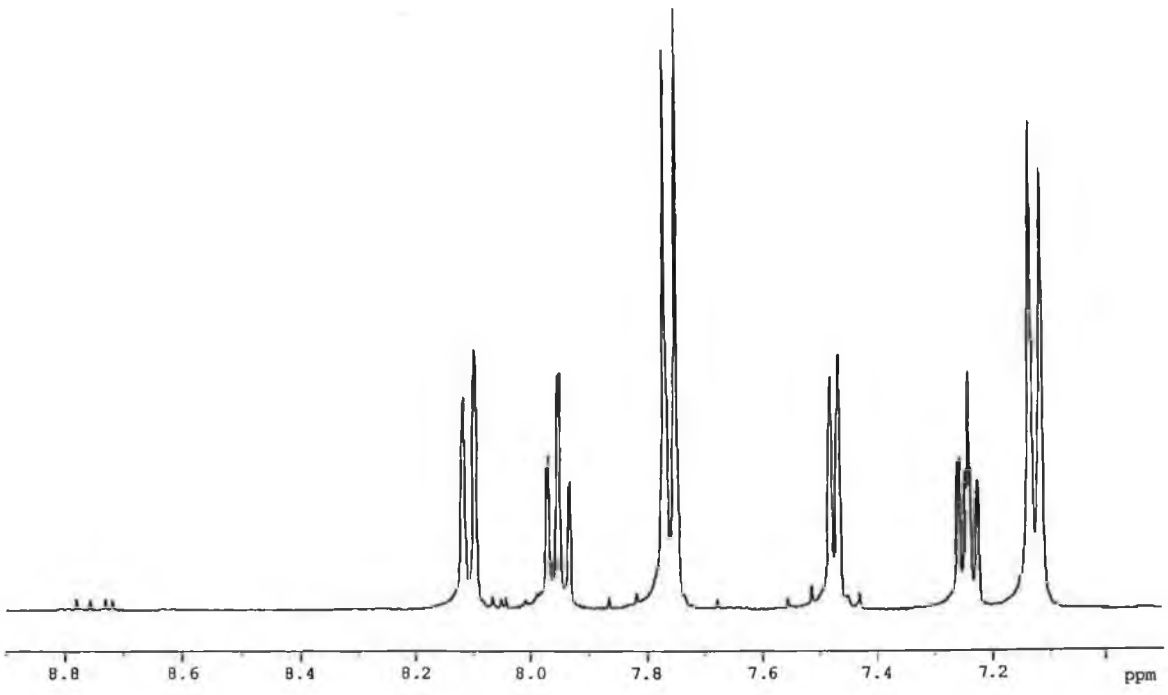

Fig. 3.14 ^1H NMR spectrum of [Ru(d_8-bpy)$_2$pyTol](PF$_6$) in d_6-DMSO

During the synthesis of the ligands, NMR proved to be extremely useful. Not only did it provide a quick and easy way to check the purity of the ligands, it also showed

instantly whether the various functional group conversions had worked or not. Oxidation of the methyl group resulted in the disappearance of the methyl signal at 2.3 (in the case of pyHAc) and its replacement by a new signal at 10 (in the case of pyHAld). Similarly, formylation of pyHPhOH resulted in a loss of symmetry of the phenyl ring to give two doublets and a singlet and a new signal at 10.5 corresponding to the new formyl group.

A number of points may be quickly seen from the previous spectra. The purity of the ligand isolated from the reaction mixture is obvious from the NMR of the crude product shown above. Upon coordination the spectrum becomes much more complex, with a total of 24 aromatic protons. The COSY spectrum clearly shows the coupling of the various protons in the complex. However, due to the large amount of coupling evident, assignment is still a cumbersome process. However, the NMR of the d_8-bpy complex sheds a great deal of light on the elucidation. With all of the bipyridine signals gone, it is possible to see clearly where all of the ligand signals are. The shifts caused by complexation are also evident. Of course, the pyridine protons feel the influence of the metal centre much more strongly than those of the phenyl ring and are therefore shifted more dramatically.

A summary of the chemical shifts of the ligands in their free and complexed forms is given in *Table 3.3*.

Name	H3	H4	H5	H6
$[Ru(bpy)_2pyTol]^+$	8.11 (8.16)	7.95 (8.01)	7.24 (7.53)	7.47 (8.70)
$[Ru(bpy)_2pyAld]^+$	8.18 (8.30)	8.01 (8.21)	7.30 (7.71)	7.53 (8.67)
$[Ru(bpy)_2pyAc]^+$	8.15 (8.36)	7.99 (8.36)	7.28 (7.77)	7.49 (8.78)
$[Ru(bpy)_2pyPhOH]^+$	8.10 (8.28)	7.95 (8.00)	7.24 (7.54)	7.48 (8.76)
$[Ru(bpy)_2pySal]^+$	8.08 (8.26)	8.02 (8.07)	7.32 (7.59)	7.55 (8.77)

Table 3.3 Comparison of chemical shifts of ligand protons in their complexed and free (in parentheses) forms, measured in d_6-DMSO

It can be seen that the H6 proton experiences the greatest shift upon coordination. This is probably due to its spatial orientation, which directs it towards one of the pyridine rings of one of the bpy ligands (See *Fig. 3.10*). The ring current effect, which it feels, results in a large downfield shift (> 1ppm)[47]. All of the other protons are shifted slightly due to the altered electron density on the ligand after coordination. The introduction of the various substituents onto the phenyl ring induces only small changes in the shifts of the pyridine protons because of the presence of the negatively charged triazole between the two rings.

3.3.4 UV/Vis Absorption and Emission Spectroscopy

The electronic absorption spectra of this range of complexes are quite similar, showing small shifts in the positioning of the various bands. The UV/Vis absorption spectra are dominated by two intense bands. The first and most intense (ε=5.5x10^4

$M^{-1}cm^{-1}$ at 285nm in the case of $[Ru(bpy)_2pyTol](PF_6)$) is located in the region of 250-300nm and is due to the π-π^* transitions based on the bpy and pyridyl triazole ligands[48]. However, it is the second major band which is of most interest here. It lies at approximately 440-450nm and is agreed to arise from a singlet $d\pi$-π^* metal-to-ligand charge-transfer (^{1}MLCT). It is a very intense band with extinction coefficients (ε) typically in the range of $10^4M^{-1}cm^{-1}$. In all of the cases here, the MLCT of the deprotonated species is red-shifted with respect to that of $[Ru(bpy)_3]^{2+}$, since exact position of this band is governed by the nature of the ligands present[49]. Strong σ-donor ligands result in an electron rich ruthenium centre and a shift of the absorption wavelength to lower energy. All of the complexes studied in this chapter are pyridyl triazole derivatives. The coordinated triazole may be protonated or deprotonated, resulting in different absorption spectra[50]. A deprotonated triazole is a strong σ-donor, whilst the protonated form is a weaker σ-donor. This is evident in the position of the MLCT, which is blue-shifted from 483nm to 443nm in the case of $[Ru(bpy)_2pyTol]^{+/2+}$ upon protonation. Subsequently isosbestic points at 286 nm, 303 nm, 313 nm, 391 nm and 451 nm are evident.

Deuteration of ligands has been shown not to have any effect on either the position or the intensity of the MLCT of ruthenium (II) complexes[51]. The extinction coefficients of the $[Ru(d_8\text{-}bpy)_2Ligand]^{2+}$ complexes prepared here were not measured, as they are the same as for the undeuterated complexes[52]. In both cases, the energy of the transition (t_{2g} - π^*) is unaffected by replacement of the bpy hydrogens with deuterium atoms. A list of the positions and intensities of the various MLCT bands is presented in *Table 3.4*. *Fig. 3.15* shows a comparison of the

absorption spectra of $[Ru(bpy)_2pyAld]^+$ and $[Ru(bpy)_2pyHAld]^{2+}$ (protonated by the addition of 1 drop of trifluoroacetic acid to the solution) in acetonitrile.

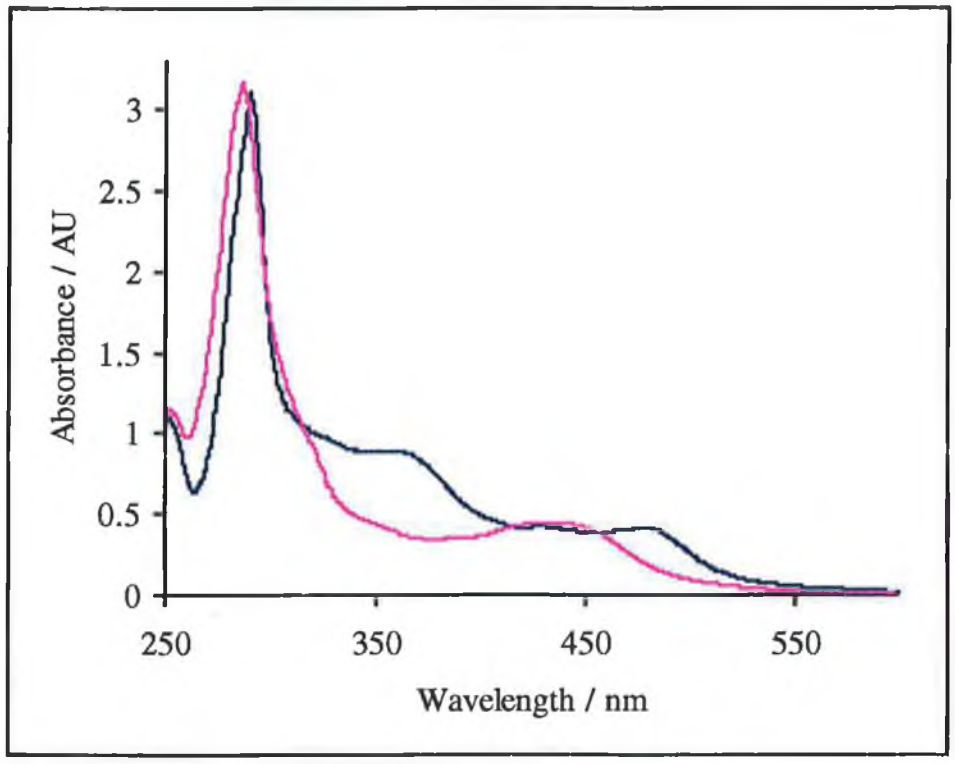

Fig. 3.15 UV/Vis Absorption spectra of 3.4 x 10^{-5}M solutions of $[Ru(bpy)_2pyAld]^+$ (blue) and $[Ru(bpy)_2pyHAld]^{2+}$ (pink) in acetonitrile

In the emission spectra, weaker emission than $[Ru(bpy)_3]^{2+}$ is observed for the ruthenium complexes studied at room temperature. The position of the emission is red shifted with respect to $[Ru(bpy)_3]^{2+}$ (612 nm) when the triazole is deprotonated, but located at a similar wavelength when protonated (685 nm vs. 622nm in the case of $[Ru(bpy)_2pyTol]^{+/2+}$ with an isoemissive point at 644 nm) . The shift to lower energy when deprotonated is easily explained[53]. The negative charge on the triazole

ligand increases electron density on the ruthenium centre. Consequently, the t_{2g} – MLCT energy gap is reduced, resulting in a lower emission energy (because emission originates from the lowest excited state). An example of the room temperature emission spectra of $[Ru(bpy)_2pyAc]^+$ in its deprotonated and protonated forms is given in *Fig. 3.16*, and a summary of the positions of the emission of the various complexes in *Table 3.4*.

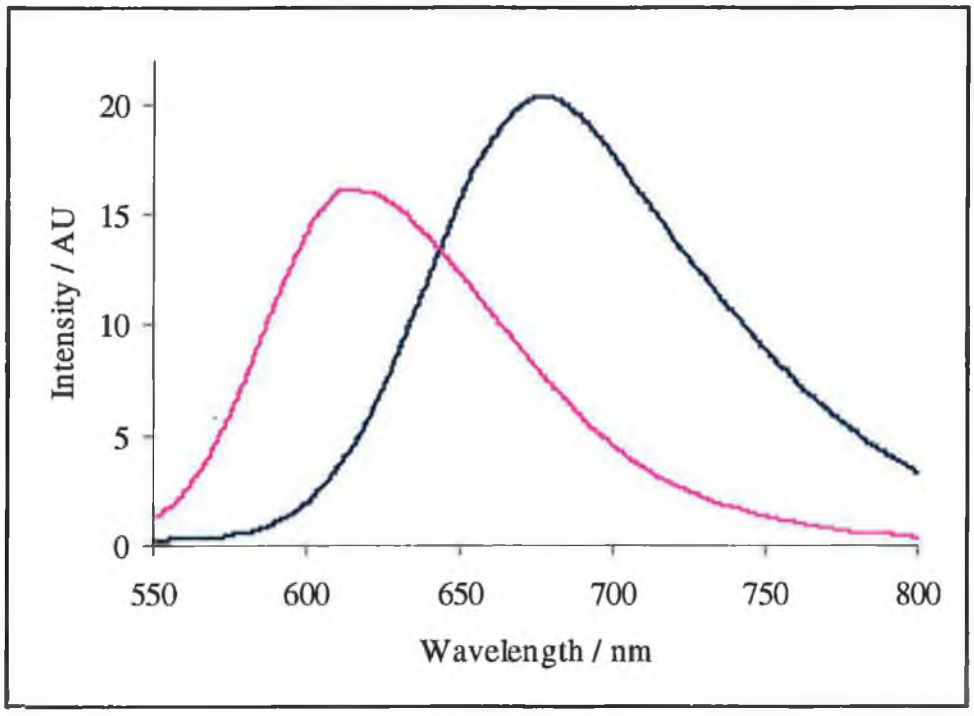

Fig. 3.16. Emission spectra of 3.4x 10^{-5}M solutions of $[Ru(bpy)_2pyAc]^+$ (blue) and $[Ru(bpy)_2pyHAc]^{2+}$ (pink) in acetonitrile at 300K

Measurements at low temperature (77K) in an alcoholic glass resulted in both a blue-shift and an increase in intensity of the emission, similar to those found for other systems[54]. A change in the shape of the emission spectrum to a spectrum exhibiting vibrational structure was also observed due to the relaxation via bpy based vibrations. The blue-shift of the emission maximum is due to rigidchromism,

whereby solvent dipoles are immobile on the timescale of the excited state and cannot reorganise as a result of the change in electronic configuration of the excited complex[55]. A resultant increase in emission energy is observed. The increase in the intensity of the spectrum may also be explained. As previously mentioned (Chapter 1.2) the excited state may decay either via emission (k_r) or via radiationless routes (k_{nr}). Due to the rigid matrix, vibrational decay via Ru-N vibrations is reduced. Similarly, quenching of the excited state by oxygen is also reduced, due to the inability of the oxygen to migrate to the location of the excited state in the frozen solvent. The third reason for the increase in intensity is due to the inaccessibility of the ^{3}MC state. At room temperature, this may be thermally accessible, resulting in deactivation of the excited state. However, at 77K, there is not enough thermal energy to access this energy level, thus eliminating another deactivation pathway.

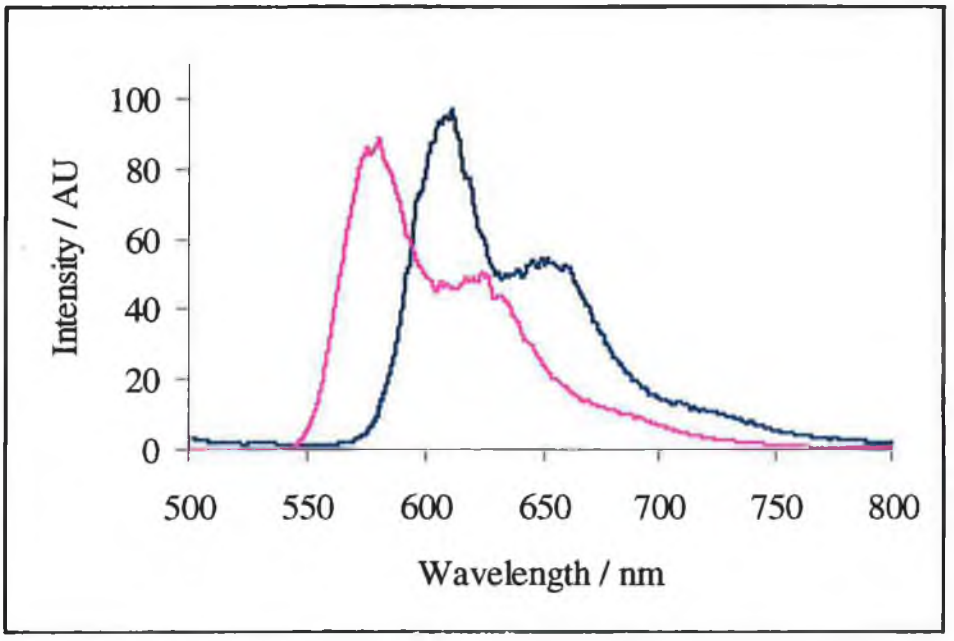

Fig. 3.17. Emission spectra of $[Ru(bpy)_2pyAc]^+$ (blue) and $[Ru(bpy)_2pyHAc]^{2+}$ (pink) in ethanol/methanol (4:1) at 77K

The positions of the low temperature emission energies are summarised in *Table 3.4*. The 77K emission spectra of $[Ru(bpy)_2pyAc]^+$ in its protonated and deprotonated forms are given in *Fig. 3.17*. There were many difficulties encountered in producing spectra with reproducible intensities, as this was dependent on the quality of the alcoholic glass formed, but the figure above is representative of the spectra obtainable.

Compound	**Absorption/nm** ($\varepsilon/10^4$ $M^{-1}cm^{-1}$)	**Emission/nm** (300K)	**Emission/nm** (77K)
$[Ru(bpy)_2pyTol]^+$	483 (0.99)	685	609
$[Ru(bpy)_2pyHTol]^{2+}$	443 (1.01)	622	577
$[Ru(bpy)_2pyAld]^+$	478 (1.16)	677	614
$[Ru(bpy)_2pyHAld]^{2+}$	434 (1.32)	616	577
$[Ru(bpy)_2pyAc]^+$	479 (1.08)	670	609
$[Ru(bpy)_2pyHAc]^{2+}$	441 (1.35)	612	578
$[Ru(bpy)_2pySal]^+$	453 (1.13)	664	608
$[Ru(bpy)_2pyHSal]^{2+}$	443 (1.20)	669	577
$[Ru(bpy)_2pyPhOH]^+$	481 (0.98)	688	613
$[Ru(bpy)_2pyHPhOH]^{2+}$	429 (1.28)	622	578

Table 3.4. Spectroscopic data for ruthenium complexes measured in acetonitrile (300K) or ethanol/methanol 4:1 (77K) at concentrations of approximately 3 x 10^{-5}M

3.3.5 Luminescent Lifetime Measurements

The aim of this part of the investigation was to aid in the characterisation and location of the excited state. As previously stated (Section 3.1) the location of the excited state is of prime importance from a supramolecular interaction point of view. Should the excited electron be located on the bridging ligand between the ruthenium and manganese centres, then the chances of electron transfer occurring from the manganese to the ruthenium are greatly diminished. Therefore it is vital to confirm that the excited state is indeed located on a bpy ligand and not on the pyridyl triazole bridging ligand.

Due to the σ-donor nature of the triazolate ligand, one would naturally expect that the excited state would be located on the bpy ligands and not the pyridyl triazole. Two spectroscopic methods are employed here to verify that the excited state is indeed located there: luminescent lifetime measurements and pK_a titrations (Section 3.3.6). It has previously been shown that the location of the excited state may found by means of selective deuteration, as deuteration of the ligand on which the excited state lies results in an increase of the luminescent lifetime[56].

The luminescent lifetime of each of the ruthenium complexes prepared has been measured by means of single photon counting. Lifetimes were measured at room temperature both prior to and after degassing the samples with nitrogen. The lifetimes of the deprotonated complexes were found to be in the region of 50-250ns, with errors estimated to be in the region of 10%. However, the lifetimes of the protonated species are not included here. Typically they were <10ns and could not

be measured to a great degree of accuracy using the instrumentation available. A list of the lifetimes of the complexes in their deprotonated forms is presented in *Table. 3.5.*

Compound	Aerated Lifetime / ns	Deaerated Lifetime / ns
$[Ru(bpy)_2pyTol]^+$	50	95
$[Ru(d_8\text{-}bpy)_2pyTol]^+$	51	118
$[Ru(bpy)_2pyAld]^+$	64	168
$[Ru(d_8\text{-}bpy)_2pyAld]^+$	69	225
$[Ru(bpy)_2pyAc]^+$	63	160
$[Ru(d_8\text{-}bpy)_2pyAc]^+$	66	202
$[Ru(bpy)_2pySal]^+$	54	182
$[Ru(d_8\text{-}bpy)_2pySal]^+$	74	269
$[Ru(bpy)_2pyPhOH]^+$	45	85
$[Ru(d_8\text{-}bpy)_2pyPhOH]^+$	46	93

Table 3.5 Luminescent lifetime data (± 10%) for ruthenium complexes measured at room temperature in acetonitrile both prior to and after efficient deaerating

No clear pattern can be seen regarding the influence of the substituent on the lifetime of the excited state. However, it should be noted that phenols are capable of acting as electron donors. In Photosystem II, tyrosine – a phenol, serves as an electron donor to P_{680}. This may explain the reduced lifetime of $[Ru(bpy)_2pyPhOH]^+$. More work would need to be carried out on this complex in order to determine whether or not the excited state is being quenched by the phenol.

The data presented in *Table 3.5* are typical of other previously reported pyridyl triazole complexes[57]. As previously stated, should the ligand on which the excited state is located be deuterated, then an increase in the lifetime should be observed. This is due to a reduction of the non-radiative decay due to C-H vibrations. In the case of the degassed samples, the lifetime increases by 10 – 40%[58]. This is indicative of the excited state being located on the bpy ligands and not on the pyridyl triazole ligands. This feature is not evident in the aerated samples most likely as quenching by oxygen has a more drastic effect on the lifetime than deactivation by C-H vibration.

3.3.6 Acid-Base Properties

The possibility of protonation of the coordinated triazole opens up the whole area of pK_a titrations. This technique is a useful tool in the location of excited states. By measurement of the ground and excited state pK_a's of the triazole one can deduce whether or not the excited state is located on the triazole-containing ligand or not[59].

Assuming the excited state is located on the bpy's, then the ruthenium will have a charge of +3. This higher charge on the metal will lead to easier deprotonation of the triazole. This will be noted in the pK_a titration as a more acidic ligand. Conversely, should the excited electron reside on the pyridyl triazole, then deprotonation would be significantly more difficult, due to the negative charge already resident on the triazole. This scenario would give a more basic excited state pK_a value. Thus, by

comparing ground and excited state pK_a's, one has a simple yet effective method for determining the location of the excited state in a mixed ligand system such as this.

All of the complexes studied show typical ground state pK_a's for triazoles (see *Table 3.6*). Their variation results from differences in the substituent on the phenyl ring. Although some distance away, its effect on the triazole is still noticeable. Strongly electron-withdrawing groups (such as in the case of pyHAc) lower the pK_a, while electron donating groups (such as in the case of pyHTol) increase it. The ground and excited state pK_a's of the unsubstituted pyridyl triazole (pytr) are included for comparison[47]. The value of the pK_a (± 0.1) was found from the point of inflection of the curve obtained upon plotting absorbance at a suitable wavelength versus the pH of the solution (see *Fig. 3.18*). The point of inflection of the corresponding curve for the emission gives the pH_i value (±0.1) (see *Fig. 3.19*). However, this does not equal the excited state pK_a because of the different lifetimes of the protonated and deprotonated species. By use of equation 3.1, one may calculate pK_a^* from pH_i and the lifetimes of the protonated (τ_a) and deprotonated (τ_b) species. Since the lifetimes of the protonated species could not be measured, the Förster equation (equation 3.2) has been used to estimate pK_a^*. This equation relates the excited state pK_a to the ground state pK_a, the emission maxima (in wavenumbers) of the protonated (ν_a) and deprotonated (ν_a) species and the temperature[60].

$$\mathbf{pK_a^* = pH_i + \log (\tau_a / \tau_b)} \qquad \textbf{eqn. 3.1}$$

$$\mathbf{pK_a^* = pK_a + 0.625(\nu_b - \nu_a) / T} \qquad \textbf{eqn. 3.2}$$

The results of the ground and excited state pK_a titrations are summarised in *Table 3.6*. For the calculation of the excited state pK_a's using equation 3.2, the emission maxima at 77K were used.

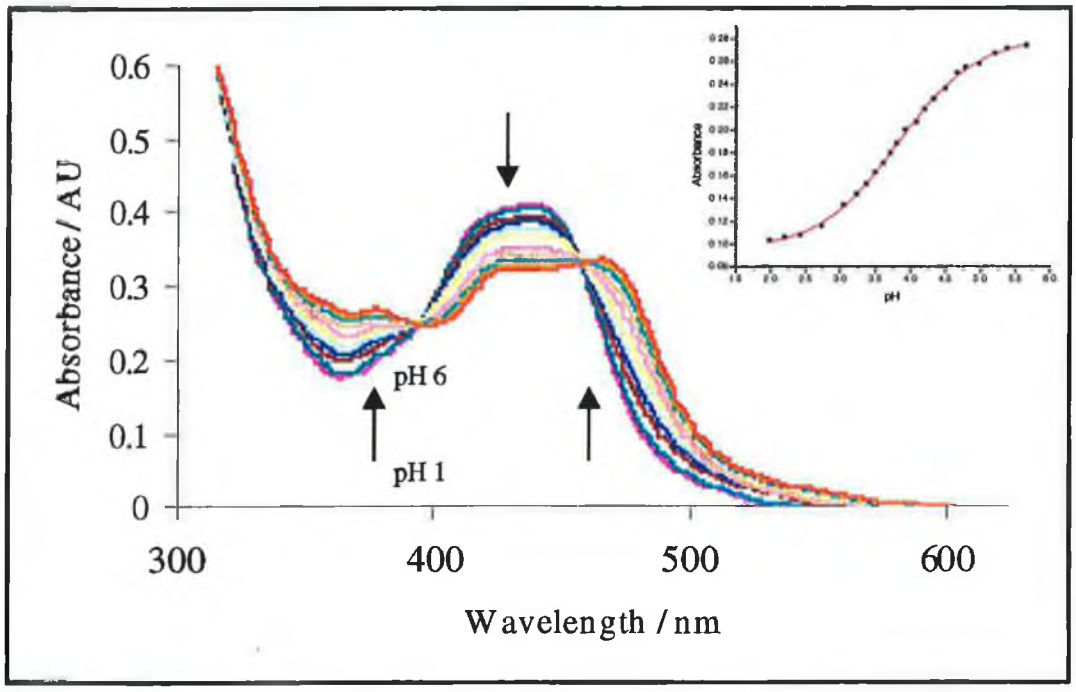

Fig. 3.18. Ground state pK_a titration (pH1 - pH6) of $[Ru(bpy)_2pyTol]^+$ in Britton Robinson buffer. Inset – Plot of absorbance at 480nm versus increasing pH, with fitted curve

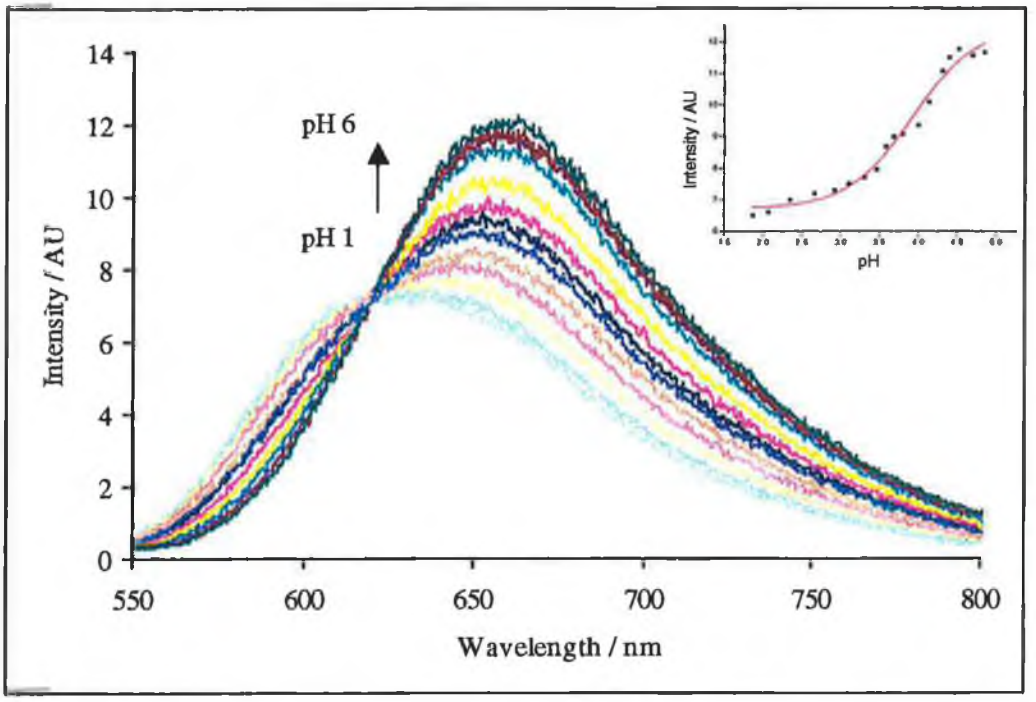

Fig. 3.19 Excited state pK_a titration (pH1 – pH6) of $[Ru(bpy)_2pyTol]^+$ in Britton Robinson buffer, excited at 451nm. Inset – Plot of Intensity versus increasing pH, with fitted curve

Complex	pK_a	pH_i	pK_a^*
$[Ru(bpy)_2pyTol]^+$	4.4	2.2	2.2
$[Ru(bpy)_2pyAld]^+$	3.4	2.0	1.2
$[Ru(bpy)_2pyAc]^+$	3.3	1.9	1.0
$[Ru(bpy)_2pySal]^+$	3.9	1.9	1.4
$[Ru(bpy)_2pyPhOH]^+$	3.8	1.8	1.2
$[Ru(bpy)_2pytr]^+$	4.1	2.7	3.4

Table 3.6 Ground and excited state pK_a titration results, measured in Britton Robinson buffer (Error: ±0.1)

These results obtained show the general trend that the co-ordinated pyridyl triazole is more acidic in the excited state than in the ground state. This is an important observation, since it shows that they are spectator ligands and do not actively participate in the emission processes. Again, this backs up what one would expect from pyridyl triazole ligands[59]. Due to the strong σ-donor nature of the triazolate, the lowest excited state must be bpy based. Thus, both luminescent lifetime measurements and pK_a titrations show that the excited state in all of these complexes is located on the bpy ligands and not on the pyridyl triazole ligands.

3.3.7 Electrochemical Properties

Electrochemistry is another important technique which may be employed in the study of the electronic properties of the complexes. As deuteration only affects excited state lifetimes and not electronic structures, these complexes were not studied here. It was of prime importance to study the oxidation potential of the ruthenium centre, since this would provide the driving force for any electron transfer reactions in supramolecular systems, which may later be prepared. The reduction potentials are an indication of the location of the excited state, as it should be located on the most easily reduced ligand.

Triazoles are σ-donors, so they increase electron density on a metal centre. Therefore, complexes containing triazoles should have lower oxidation potentials than those of the corresponding bipyridine based complexes. Pyridine and related compounds are strong π-acceptors, so they reduce the electron density on a metal centre and thus result in an increased oxidation potential.

Ruthenium pyridyl triazole complexes have an interesting acid base chemistry, as already shown by the pK_a titrations. Under normal conditions, the triazole is deprotonated. However, upon protonation of the triazole with one drop of 0.1M triflic acid in acetonitrile, a marked increase in the oxidation potential of the ruthenium centre was observed (see *Fig. 3.20*). This is explained by the fact that the protonation of the triazole decreases its σ-donor capabilities[57]. It no longer increases electron density on the metal centre as significantly as before. The net result of this is that the oxidation potential increases dramatically. In fact, the oxidation potential for ruthenium in a pyridyl triazole complex in acidic medium is almost comparable with that of $[Ru(bpy)_3]^{2+}$.

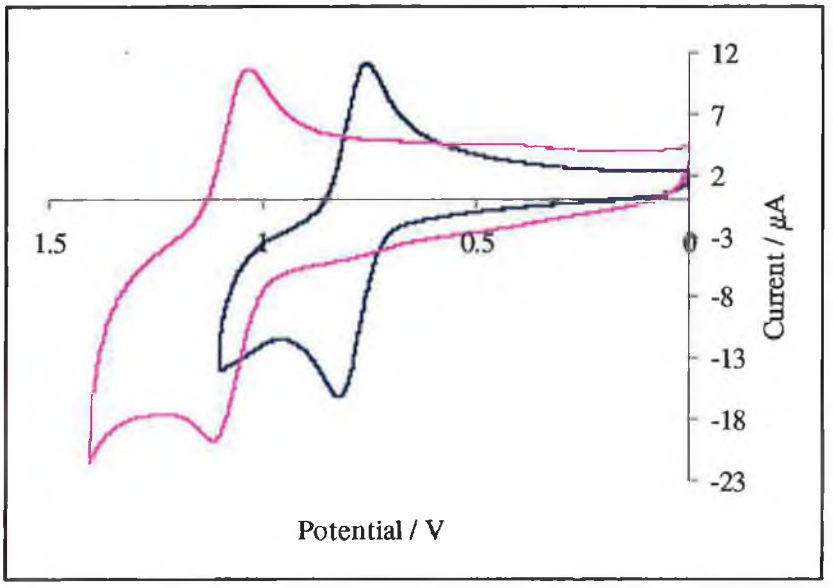

Fig. 3.20 Oxidation waves of $[Ru(bpy)_2pyTol]^+$ (blue) and $[Ru(bpy)_2pyHTol]^{2+}$ (pink) in 0.1M TEAP in MeCN, measured at $100mVs^{-1}$ versus SCE

All of the compounds show the expected shift to higher oxidation potential upon protonation of the triazole (see *Table 3.7*). Even $[Ru(bpy)_2pyPhOH]^+$, which exhibits

the smallest shift, still shifts by approximately 100mV. The oxidations are reversible. Typical peak-peak separations were of the order of 60-90mV. It should be noted, that each of the oxidation potentials of the deprotonated species is insufficient for water oxidation. However these model compounds may still be used in electron transfer experiments, using other donors. A photoexcited ruthenium centre would still be capable of oxidising a phenothiazine or suitable manganese complex, for example. This issue is dealt with in further detail in Chapter 4, in which pyrazine triazole ligands and complexes are prepared and characterised.

Compound	Oxidation / V (vs. SCE)	Reduction / V (vs. SCE)
$[Ru(bpy)_2pyTol]^+$	0.79	-1.29, -1.52, -1.94 (irr.)
$[Ru(bpy)_2pyTol]^{2+}$	1.08	-1.33, -1.54
$[Ru(bpy)_2pyAld]^+$	0.78	-1.47, -1.74
$[Ru(bpy)_2pyHAld]^{2+}$	1.12	-1.46, -1.75
$[Ru(bpy)_2pyAc]^+$	0.79	-1.51, -1.75
$[Ru(bpy)_2pyHAc]^{2+}$	1.10	-1.52, -1.77
$[Ru(bpy)_2pySal]^+$	0.89	-1.34, -1.54, -1.85 (irr.)
$[Ru(bpy)_2pyHSal]^{2+}$	1.16	----------
$[Ru(bpy)_2pyPhOH]^+$	1.04	-1.52, -1.76
$[Ru(bpy)_2pyHPhOH]^{2+}$	1.13	-1.46, -1.77

Table 3.7 Redox potentials for ruthenium complexes in 0.1M TEAP in MeCN, measured at 100mVs^{-1} versus SCE

The reduction potentials found for the complexes are in close agreement with those found previously for similar complexes. In those cases, as well as in the case of those mentioned here, reduction is assumed to be bpy based, due to the positions in which the peaks come. In the case of $[Ru(bpy)_2pyTol]^+$, the first two reduction waves are typical bpy reductions, but the third reduction comes at a much more negative potential as a result of the strong σ-donor properties of the triazolate[49]. After protonation of the triazole, reduction waves became more difficult to measure, disappearing altogether in one case (*Table 3.7*). A typical cyclic voltammogram of a

complex containing a deprotonated triazole, displaying bpy based reduction waves is shown in *Fig. 3.21.*

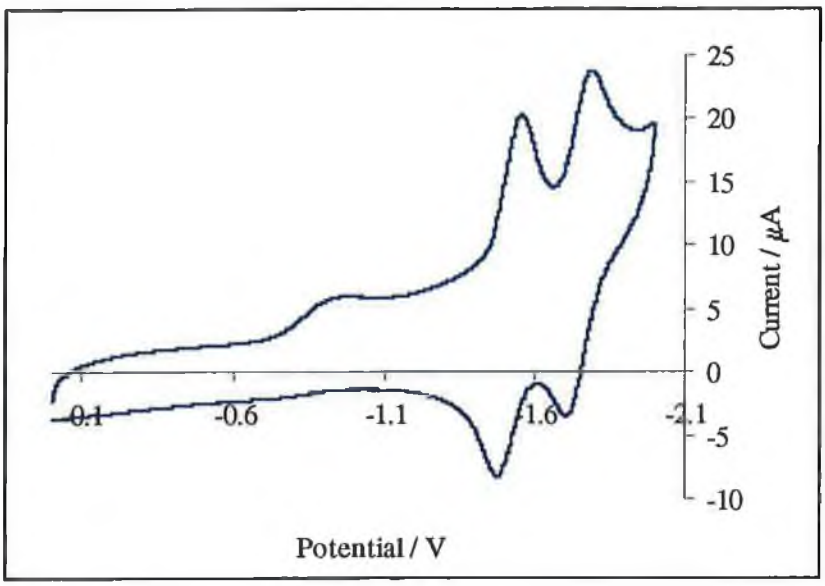

Fig. 3.21 Reduction waves of $[Ru(bpy)_2pyAc]^+$ in 0.1M TEAP in MeCN, measured at $100mVs^{-1}$ versus SCE

3.4 Conclusion

A range of novel pyridyl triazole ligands has been prepared and characterised. The synthesis of a model compound (pyHTol) was first carried out by standard means. This ligand was then be modified by selectively oxidising the methyl group to an aldehyde (with Ce(IV)) and an acid (with Cr(VI)). Similarly, a salicylaldehyde derivative was prepared by means of a Duff formylation of a phenol containing ligand. Each of these bidentate ligands make ideal starting materials for supramolecular systems, in particular for covalently linked Ru-Mn systems, due to their terminal functional groups.

To ensure that these ligands were suitable for use in this study, they were subsequently complexed with both $[Ru(bpy)_2Cl_2].2H_2O$ and $[Ru(d_8\text{-}bpy)_2Cl_2].2H_2O$. The mononuclear complexes thus formed were purified by column chromatography. Characterisation by elemental analysis, NMR and HPLC aided in the elucidation of their structures, which were found to be as expected.

Spectroscopic studies show that the σ-donor nature of the triazolate result in a red shift of both the absorption and emission spectra when compared to $[Ru(bpy)_3]^{2+}$. This has been explained as being due to the increased electron density on the Ru centre, which in turn reduces the energy of the MLCT transition.

Luminescent lifetimes, pK_a titrations and electrochemical studies all point towards the fact that the excited state of the complexes lies on the bpy ligands and not on the pyridyl triazole ligands. This is again due to the σ-donor properties of the triazole ligands. However, due to this feature of their chemistry, the oxidation potential of the ruthenium centre in each of the complexes has been reduced significantly with respect to $[Ru(bpy)_3]^{2+}$. Although this may make them unsuitable for use as photosensitisers in Ru-Mn water oxidation catalysts, they may still be used in conjunction with a wide range of electron donors in order to study the electron transfer reactions This may be remedied by use of pyrazyl triazole ligands (see Chapter 4), which are known to have higher oxidation potentials. These complexes may be seen as model complexes, which should aid in the synthesis, purification and characterisation of the pyrazine complexes.

3.5 Bibliography

[1] Sun, L.; Hammarström, L.; Åkermark, B.; Styring, S.; *Chem. Soc. Rev.*, **30**, (2001), 36

[2] Puntoriero, F.; Serroni, S.; Licciardello, A.; Venturi, M.; Juris, A.; Ricevuto, V.; Campagna, S.; *J. Chem. Soc. Dalton Trans.*, (2001), 1035

[3] Burdinski, D.; Bothe, E.; Wieghardt, K.; *Inorg. Chem.*, **39**, (2000), 105

[4] Giuffrida, G.; Calogero, G.; Guglielmo, G.; Ricevuto, V.; Ciano, M.; Campagna, S.; *Inorg. Chem.*, **1993**, 32, 1179

[5] Hughes, H. P.; Vos, J. G.; *Inorg. Chem.*, **1995**, 34, 4001

[6] Barigelletti, F.; DeCola, L.; Balzani, V.; Hage, R.; Haasnoot, J.; Reedijk, J.; Vos, J. G.; *Inorg. Chem.*, **1989**, 28, 4344

[7] Fanni, S.; Keyes, T. E.; Campagna, S.; Vos, J. G.; *Inorg. Chem.*, **1998**, 37, 5933

[8] Keyes, T. E.; Weldon, F.; Müller, E.; Pechy, P.; Grätzel, M.; Vos, J. G.; *J. Chem. Soc. Dalton Trans.*, **1995**, 2705

[9] B.P.Sullivan, D.J. Salmon, T.J.Meyer, *Inorg. Chem.*, **1978**, 17, 3334

[10] Horner, O.; Anxolabhere-Mallart, E.; Charlot, M. F.; Tchertanov, L.; Guillem, J.; Mattioli, C. A.; Boussac, A.; Girerd, J. J.; *Inorg. Chem.*, **1999**, 38, 1222

[11] Caudle, M. T.; Riggs-Gelasco, P.; Gelasco, A. K.; Penner-Hahn, J. E.; Pecoraro, V. L.; *Inorg. Chem.*, **1996**, 35, 3577

[12] Weidinger, H.; Kranz, J.; *Chem. Ber.*, **1963**, 96, 1064

[13] Potts, K. T.; *J. Chem. Soc.*, **1954**, 3461

[14] Liljegren, D. R.; Potts, K. T.; *J. Chem. Soc.*; **1961**, 518

[15] Hughes, D.; *Ph.D. Thesis*, Dublin City University, **2000**

[16] Keyes, T.E.; *Ph.D. Thesis*, Dublin City University, **1994**

[17] Garelli, N.; Vierling, P.; *J. Org. Chem.*, **1992**, 57, 3046

[18] Zakharkin, L. I.; Khorlina, I. M.; *Tetrahedron Lett.*, **1962**, 619

[19] Babler, J. H.; Invergo, B. J.; *Tetrahedron Lett.*, **1981**, 11

[20] Peters, J. A.; Van Bekkum, H.; *Recl. J. Royal Neth. Chem. Soc.*, **1981**, 100, 21

[21] Bold, G.; Steiner, H.; Moesch, L.; Walliser, B.; *Helv. Chim. Acta*, **1990**, 73, 405

[22] Burgstahler, A. W.; Weigel, L. O.; Shaefer, C. G.; *Synthesis*, **1976**, 767

[23] Syper, L.; *Tetrahedron Lett.*, **1967**, 4193

[24] Barton, H. R. D.; Hui, R. A. H. F.; Lester, D. J.; Ley, S. V.; *Tetrahedron Lett.*, **1979**, 3331

[25] Barton, D. H. R.; Hui, R. A. H. F.; Ley, S. V.; *J. Chem. Soc. Perkin Trans. I*; **1982**, 2179

[26] Geren, L.; Hahm, S.; Durham, B.; Millett, F.; *Biochem*, **1991**, 30, 9450

[27] Furniss, B. S.; Hannaford, A. J.; Smith, P. W. G.; Tatchell, A. R.; *Vogel's Textbook of Practical Organic Chemistry*, 5th Ed. , **1989**, Longman Scientific and Technical

[28] Makhon'kov, D. I.; Cheprakov, A. V.; Rodkin, M. A.; Mil'chenko, A. Y.; Beletskaya, I. P.; *J. Org. Chem. USSR*, **1986**, 22, 24

[29] Syper, L.; *Tetrahedron Lett.*, **1966**, 4493

[30] Marrocco, M.; Brilmyer, G.; *J. Org. Chem.*, **1983**, 48, 1487

[31] Sydnes, L. K.; Hansen, S. H.; Burkow, I. C.; Saethre, L. J.; *Tetrahedron*, **1985**, 41, 5205

[32] Prakash, G. K. S.; Krass, N.; Wang, Q.; Olah, G. A.; *Synlett*, **1991**, 39

[33] Knusden, R. D.; Snyder, H. R.; *J. Org. Chem.*, **1974**, 39, 3343

[34] Bellamy, F. D.; Ou, K.; *Tetrahedron Lett.*, **1984**, 839

[35] Arduini, A.; Fanni, S.; Manfredi, G.; Pochini, A.; Ungaro, R.; Sicuri, A. R.; Ugozzoli, F.; *J. Org. Chem.*, **1995**, 60, 1448

[36] Thoer, A.; Denis, G.; Delmas, M.; Gaset, A.; *Synth. Commun.*, **1988**, 18, 2095

[37] Duff, J. C.; Bills, E. J.; *J. Chem. Soc.*, **1932**, 1987

[38] Duff, J. C.; Bills, E. J.; *J. Chem. Soc.*, **1934**, 1305

[39] Baker, W.; McOmie, J. F. W.; Miles, D.; *J. Chem. Soc.*; **1953**, 820

[40] Smith, W. E.; *J. Org. Chem.*, **1972**, 37, 3972

[41] Ogata, Y.; Kawasaki, A.; Sugiura, F.; *Tetrahedron*, **1968**, 24, 5001

[42] Mathew, T. V.; Chauhan, V. S.; *Ind. J. Chem.*, **1987**, 26B, 1071

[43] Lindoy, L. F.; Meehan, G. V.; Svenstrup, N.; *Synthesis*, **1998**, 1029

[44] Larrow, J. F.; Jacobsen, E. N.; *J. Org. Chem.*, **1994**, 59, 1939

[45] Buchanan, B. E.; McGOvern, E.; Harkin, P.; Vos, J. G.; *Inorg. Chim. Acta*, **1988**, 154, 1

[46] Chirayil, S.; Thummel, R. P.; *Inorg. Chem.*, **1989**, 28, 812

[47] Hage, R.; *Ph.D. Thesis*, Rijksuniversiteit te Leiden, **1991**

[48] Brauns, E.; Jones, S. W.; Clark, J. A.; Molnar, S. M.; Kawanishi, Y.; Brewer, K. J.; *Inorg. Chem.*, **1997**, 36, 2861

[49] Barigelletti, F.; DeCola, L.; Balzani, V.; Hage, R.; Haasnoot, J. G.; Reedijk, J.; Vos, J. G.; *Inorg. Chem.*, **1991**, 30, 641

[50] Wang, R.; Vos, J. G.; Schmehl, R. H.; Hage, R.; *J. Am. Chem. Soc.*, **1992**, 114, 1964

[51] O'Brien, L.; *Ph.D. Thesis*, Dublin City University, **2001**

[52] O'Connor, C. M.; *Ph.D. Thesis*, Dublin City University, **2000**

[53] Keyes, T. E.; Vos, J. G.; Kolnaar, J. A.; Haasnoot, J. G.; Reedijk, J.; Hage, R.; *Inorg. Chim. Acta*, **1996**, 245, 237

[54] Serroni, S.; Campagna, S.; Denti, G.; Keyes, T. E.; Vos. J. G.; *Inorg. Chem.*, **1996**, 35, 4513

[55] Wrighton, M.; Morse, D. L.; *J. Am. Chem. Soc.*, **1974**, 96, 996

[56] Haga, M.; Ali, M. M.; Koseki, S.; Fujimoto, K.; Yoshimura, A.; Nozaki, K.; Ohno, T.; Nakajima, K.; Stufkens, D. J.; *Inorg. Chem.*, **1996**, 35, 3335

[57] Ryan, E. M.; Wang, R.; Vos, J. G.; Hage, R.; Haasnoot, J. G.; *Inorg. Chim. Acta*, **1993**, 208, 49

[58] VanHouten, J.; Watts, R. J.; *J. Am. Chem. Soc.*, **1975**, 97, 3843

[59] Bucahanan, B. E.; Vos, J. G.; Kaneko, M.; Van der Putten, W. J. M.; Kelly, J. M.; Hage, R.; de Graff, R. A. G.; Prins, R.; Haasnoot, J. G.; Reedijk, J.; *J. Chem. Soc. Dalton Trans.*, **1990**, 2425

[60] Vos, J. G.; *Polyhedron*, **1992**, 11, 2285

Chapter 4

The Synthesis and Characterisation of Ruthenium (II) Complexes Containing Novel 3-(2'-Pyrazyl)1,2,4-Triazole Ligands

4.1 Introduction

As has been seen in Chapter 3, a range of novel pyridyl triazoles and their corresponding ruthenium complexes have been prepared and characterised. Each contains a suitable terminal synthon, for later reaction with a variety of amine-based ligands, which may be used to form complexes with manganese. It is hoped that vectorial electron transfer from the manganese to the ruthenium may be observed for these bimetallic complexes. In this way, they would emulate some of the initial processes that occur in PSII.

During the characterisation of these complexes it was noted that the oxidation potential of the ruthenium typically ranged between 0.8-0.9V, when the triazole was deprotonated, 1.1-1.2V, when the triazole was protonated. This feature leads to the possibility of the complexes being used as pH dependent molecular switches. Should these complexes be used as biomimetic models of P_{680} in PSII, then their oxidation potential becomes of prime importance, as this provides the driving force behind any possible electron transfer reactions[1]. While the potentials above may be sufficient to oxidise many manganese complexes, they may not be sufficient to easily oxidise tyrosine, which is also of vital importance in PSII. Tyrosine, with an oxidation potential of ~0.9V vs. SCE[2], has been used as an intermediate electron donor between manganese and ruthenium in supramolecular assemblies, as in PSII. The possibility of electron transfer taking place is thus highly pH dependent. A more useful supramolecular complex would be capable of displaying electron transfer over a wide pH range. This search for a more versatile photosensitiser has lead to the compounds discussed in this chapter to be prepared.

Since the driving force for the electron transfer reaction appeared to be insufficient using pyridyl triazoles, the complexes had to be modified so as to increase the oxidation potential of the metal centre to a potential greater than 0.85V (vs. SCE). Due to its favourable properties, ruthenium was maintained as the central metal of the complexes. Alteration of the ligand sphere would have to bring about the changes necessary. In the original complexes only two types of ligand were directly bound to the ruthenium, i.e. bpy and pyridyl triazole. By altering one or both of these, it was hoped to sufficiently increase the oxidation potential of the metal without losing the properties that seemed appealing in the original complexes (Chapter 3).

As previously stated, ligands may be grouped into one of two classes: σ-donors or π-acceptors. σ-Donors increase electron density on the metal centre resulting in a decrease in the oxidation potential, whilst π-acceptors reduce the electron density and hence increase the oxidation potential. Due to their advantageous properties, it was decided to retain the triazoles, which only left the option of somehow increasing the π-acceptor attributes of the pyridine or bpy ligands. Introduction of functional groups onto bpy ligands, such as Br or CF_3, result in an increase in the electron withdrawing nature of the ligand[3,4]. Unfortunately, these may require lengthy synthetic routes and could cause problems in the later synthesis of larger supramolecular assemblies. Instead, it was decided to replace the pyridine of the pyridyl triazole with pyrazine, a well-known strong π-acceptor.

Many pyrazine containing complexes have been prepared and characterised. Its use as a bridging ligand in its own right has been thoroughly investigated[5,6,7], with the Creutz-Taube ion being one of the most famous ruthenium complexes prepared[8]. It

also features regularly in a variety of bridging ligands[9,10], especially in the area of metal complex dendrimers[11]. Less work has been carried out on pyrazine triazoles[12]. However, from what is known about them and their ruthenium complexes, they too provide an ideal starting point for the synthesis of ruthenium-manganese systems.

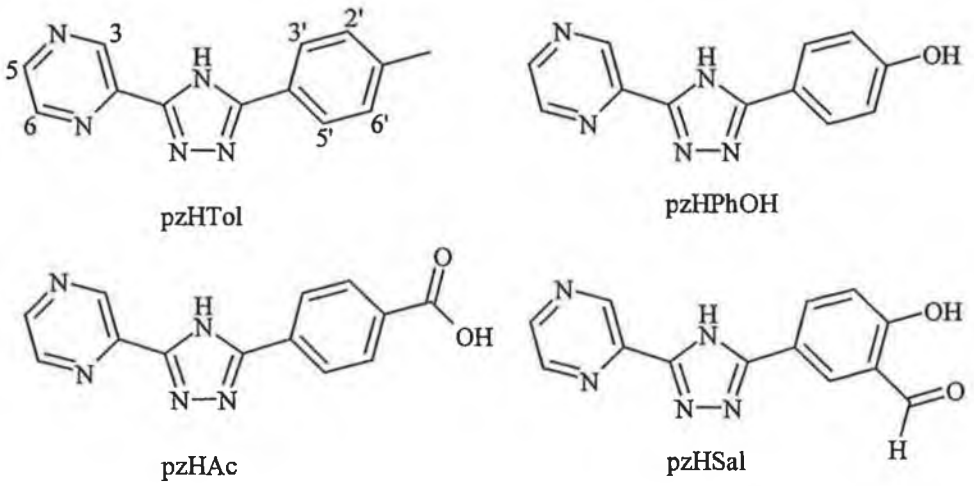

Fig. 4.1 Structures of novel ligands cited in this chapter

In *Fig. 4.1* above, the structures of the novel pyrazine ligands prepared are given. These are analogous to those prepared in Chapter 3. As before, their ruthenium complexes have also been prepared and studied in the same systematic method as their pyridine analogues.

4.2 Synthetic Procedures

4.2.1 Synthesis of Ligands

3-(2'-pyrazyl), 5-(4''-tolyl), 1,2,4-triazole (pzHTol)

17 g (0.11 mol) of p-toluic hydrazide (See Section 3.2.1 – synthesis of pyHTol) were added to a solution of 12 g (0.11 mol) of cyanopyrazine and 0.5 g of sodium in methanol, which had been heating at reflux for 3 hours. This was heated at reflux with vigorous stirring for a further hour. The yellow precipitate formed was collected by vacuum filtration, washed with a small amount of cold ethanol and dried *in vacuo*. The acylamidrazone was cyclised to the triazole by heating at reflux in 110 cm^3 ethylene glycol for 1 hour. Upon cooling, the product was crashed out with ice, filtered, washed with cold ethanol and dried *in vacuo*. The resulting compound was sufficiently pure so as not to warrant further purification. Overall yield: 16.8 g (0.071 mol). 62% based on p-toluic hydrazide. M.p. 245-247°C

^{1}H NMR (400 MHz, $(CD_3)_2SO$)) δ in ppm 9.33 (d, 1H, J=1Hz, H3), 8.77 (m, 2H, H5, H6), 8.00 (d, 2H, J= 8Hz, H3', H5'), 7.34 (d, 2H, J=8Hz, H2', H6'), 2.36 (s, 3H, CH_3)

^{13}C NMR (100 MHz, $(CD_3)_2SO$)) δ in ppm 145.66, 144.82, 142.94, 140.00, 129.86, 126.39, 21.30

IR (KBr) 3420cm^{-1} Triazole N-H stretch, 3033cm^{-1} Aromatic C-H stretch, 1615 cm^{-1} C=N stretch, 822 cm^{-1} C-H out of plane bend, 746 cm^{-1} C-H out of plane bend (pyrazine)

Elemental Analysis for $C_{13}H_{11}N_5$: Calc: C 65.80, H 4.67, N 29.52, Found: C 65.17, H 4.67, N 29.24

3-(2'-pyrazyl), 5-(4''-hydroxyphenyl), 1,2,4-triazole (pzHPhOH)

7.4 g (0.048 mol) of p-hydroxy benzoic hydrazide were added to a solution of 5.1 g (0.048 mol) of cyanopyrazine and 0.2 g of sodium in 50 cm^3 of methanol, which had been heating at reflux for 3 hours. This was heated at reflux with vigorous stirring for a further 2 hours. The yellow precipitate formed was collected by vacuum filtration, washed with a small amount of cold ethanol and dried *in vacuo*. The acylamidrazone was cyclised to the triazole by heating at reflux in 50 cm^3 ethylene glycol for 1 hour. Upon cooling, the product was crashed out with ice, filtered, washed with cold ethanol and dried *in vacuo*. The resulting compound was sufficiently pure so as not to warrant further purification. Overall yield: 7.6 g (0.032 mol). 66% based on p-hydroxytoluic hydrazide. M.p. >250°C

^1H NMR (400 MHz, $(CD_3)_2SO$)) δ in ppm 9.96 (br, 1H, OH), 9.32 (d, 1H, J=1Hz, H3), 8.76 (d, 2H, H5, H6), 7.94 (d, 2H, J=8Hz, H3', H5'), 6.92 (d, 2H, J=8Hz, H2', H6')

^{13}C NMR (100 MHz, $(CD_3)_2SO$)) δ in ppm 144.82, 142.95, 129.35, 128.18, 116.68, 116.06

IR (KBr) 3117cm^{-1} O-H stretch, 1615 cm^{-1} C=N stretch, 761 cm^{-1} C-H out of plane bend (pyrazine)

Elemental Analysis for $C_{12}H_9N_5O$: Calc: C 60.25, H 3.79, N 29.27, Found: C 59.27, H 3.84, N 28.14

3-(2'-pyrazyl), 5-(4''-carboxylic acid phenyl), 1,2,4-triazole.3H_2O (pzHAc)

1 g (4.2 mmol) of pzHTol were dissolved in 15 cm^3 of concentrated sulphuric acid. 1.9 g (6.3 mmol - 1.5 eq) of solid potassium dichromate were added over 1 hour. The exothermic reaction mixture was stirred vigorously for 3 hours, after which it was poured onto 100 cm^3 of crushed ice. The pH of the solution was raised to pH 4 with conc. aq. NaOH and left to stand for 2 hours at 0-4°C. The product was obtained by vacuum filtration, washed with water and dried in vacuo. Yield: 0.82 g (3.1 mmol) 73%. M.p. >250°C

^1H NMR (400 MHz, $(CD_3)_2SO$)) δ in ppm 9.33 (d, 1H, J=1Hz, H3), 8.77 (m, 2H, H5, H6), 8.20 (d, 2H, J=8Hz, H3', H5'), 8.07 (d, 2H, J=8Hz, H2', H6')

^{13}C NMR (100 MHz, $(CD_3)_2SO$) δ in ppm 167.28, 159.72, 155.18, 146.04, 144.86, 142.87, 133.75, 131.82, 130.47, 126.88, 126.45

IR (KBr) 3420cm^{-1} Triazole N-H stretch, 3071 cm^{-1} Aromatic C-H stretch, 1697 cm^{-1} C=O stretch, 1616 cm^{-1} C=N stretch, 1288 cm^{-1} C-O stretch, 989 cm^{-1} O-H out of plane bend, 737 cm^{-1} C-H out of plane bend (pyrazine)

Elemental analysis for $C_{13}H_{15}N_5O_5$: C 48.60, H 4.71, N 21.80, Found: C 48.59, H 3.98, N 21.69

3-(2'-pyrazyl), 5-(4''-salicylyl), 1,2,4-triazole.1.5H_2O (pzHSal)

1 g (4.2 mmol) of pzHPhOH and 2.5 g (16.8 mmol - 4 eq) of hexamethylene-tetramine were heated at reflux for 6 hours in 20 cm^3 of a 1:1 ratio of acetic acid and trifluoroacetic acid. After being left to stand at room temperature overnight, the

solution was poured onto 100 cm^3 of ice. The pH of the solution was raised to pH 4 with NaOH and left to stand in the fridge overnight. The precipitate formed was collected by vacuum filtration, washed with water and diethyl ether and dried *in vacuo*. The product formed did not require further purification. Yield: 0.68 g (2.6 mmol) 62%. M.p. 223°C (decomp.)

^{1}H NMR (400 MHz, $(CD_3)_2SO$)) δ in ppm 10.35 (s, 1H, CHO), 9.33 (d, 1H, J=1Hz, H3), 8.78 (br, 2H, H5, H6), 8.39 (d, 1H, J=2Hz, H3'), 8.23 (dd, 1H, J_1=2Hz, J_2=8Hz, H5') 8.07 (d, 1H, J=6Hz, H6')

^{13}C NMR (100 MHz, $(CD_3)_2SO$) δ in ppm 199.23, 156.65, 145.77, 143.29, 134.11, 127.01, 118.45

IR (KBr) 3403 cm^{-1} Triazole N-H stretch, 3074 Aromatic C-H stretch, 2869 cm^{-1} Aldehyde C-H stretch, 1662 cm^{-1} C=O stretch, 1615 cm^{-1} C=N stretch, 1425 cm^{-1} C-H stretch, 758 cm^{-1} C-H out of plane bend (pyrazine)

Elemental analysis for $C_{13}H_{12}N_5O_{3.5}$: C 53.06, H 4.11, N 23.80, Found: C 52.50, H 3.58, N 23.48

4.2.2 Synthesis of the Ruthenium Complexes

$[Ru(bpy)_2pzTol](PF_6).2H_2O$

80 mg (0.34 mmol) of pzHTol were dissolved in 15 cm^3 of ethanol/water (1:1). Addition of 0.15 g (0.29 mmol) of $[Ru(bpy)_2Cl_2].2H_2O$ resulted in a deep purple coloured solution. After heating at reflux for 45 minutes, it had faded to a dark orange solution. This was heated at reflux for a further 5 hours, after which the

solvent was removed with the rotary evaporator. The solid was redissolved in 5 cm^3 of water. Dropwise addition of a saturated solution of ammonium hexafluorophosphate brought about the precipitation of an orange solid, which was filtered, washed with small amounts of water and diethyl ether and dried *in vacuo*. The impure complex obtained was purified by column chromatography on neutral alumina, with acetonitrile/methanol (98:2) as eluent. Subsequent recrystallisation of the major fraction in acetone/water (2:1) resulted in a dark red solid. Yield: 0.18 g (0.23 mmol) 78%

^{1}H NMR (400 MHz, $(CD_3)_2SO$) δ in ppm 9.25 (d, 1H, J=1Hz, H3), 8.76 (m, 4H, 4xbpy H3), 8.36 (d, 1H, J=3Hz, H6), 8.12 (m, 4H, 4xbpy H4), 7.99 (d, 1H, J=6Hz, bpy H6), 7.80 (m, 4H, H3', H5', 2xbpy H6), 7.66 (dd, 1H, J_1=3Hz, J_2=1Hz, H5), 7.60 (m, 5H, bpy H6, 4xbpy H5), 7.17 (d, 2H, J=8Hz, H2', H6')

^{13}C NMR (100 MHz, $(CD_3)_2SO$) δ in ppm 153.21, 152.92, 146.83, 142.54, 138.61, 130.03, 129.00, 128.88, 126.85, 125.43, 124.79, 124.62, 21.67

Elemental Analysis for $C_{33}H_{30}N_9O_2RuPF_6$: Calc: C 47.72, H 3.64, N 15.18, Found: C 47.97, H 3.17, N 15.18

[Ru(bpy)$_2$pzPhOH](PF$_6$).2H$_2$O

70 mg (0.29 mmol) of pzHPhOH were dissolved in 10 cm^3 of ethanol/water (1:1). Addition of 125 mg (0.24 mmol) of $[Ru(bpy)_2Cl_2].2H_2O$ resulted in a deep purple coloured solution. This was heated at reflux for 5 hours, after which the solvent was removed using the rotary evaporator. The solid was redissolved in 3 cm^3 of water. Dropwise addition of a saturated solution of ammonium hexafluorophosphate brought about the precipitation of an orange solid, which was filtered, washed with

small amounts of water and diethyl ether and dried *in vacuo*. The impure complex obtained was purified by column chromatography on neutral silica, with acetonitrile/water/aq. KNO_3 (80:20:1) as eluent. Subsequent recrystallisation of the major fraction in acetone/water (2:1) resulted in a dark red solid. Yield: 0.14 g (0.17 mmol) 72%

^{1}H NMR (400 MHz, $(CD_3)_2SO$) δ in ppm 9.54 (br, 1H, OH), 9.23 (d, 1H, J=1Hz, H3), 8.78 (m, 4H, 4xbpy H3), 8.33 (d, 1H, J=3Hz, H6), 8.11 (m, 4H, 4xbpy H4), 7.98 (d, 1H, J=6Hz, bpy H6), 7.81 (d, 1H, J=6Hz, bpy H6), 7.76 (d, 1H, J=6Hz, bpy H6), 7.72 (d, 2H, J=8Hz, H3', H5'), 7.64 (dd, 1H, J_1=3Hz, J_2=1Hz, H5), 7.60 (m, 2H, bpy H6, bpy H5), 7.50 (m, 3H, 3xbpy H5), 6.74 (d, 2H, J=8Hz, H2', H6')

^{13}C NMR (100 MHz, $(CD_3)_2SO$) δ in ppm 157.03, 151.65, 127.23, 115.51

Elemental Analysis for $C_{32}H_{28}N_9O_3RuPF_6$: Calc: C 46.16, H 3.39, N 15.14, Found: C 45.93, H 2.84, N 15.54

[Ru(bpy)$_2$pzAc](PF$_6$).3H$_2$O.(CH$_3$)$_2$CO

100 mg (0.37 mmol) of pzHAc were dissolved in 15 cm^3 of ethanol/water (1:1). Addition of 160 mg (0.31 mmol) of $[Ru(bpy)_2Cl_2].2H_2O$ resulted in a deep purple coloured solution. This was heated at reflux for a further 5 hours, after which the solvent was removed with the rotary evaporator. The red solid was redissolved in 5 cm^3 of water. Dropwise addition of a saturated solution of ammonium hexafluorophosphate brought about the precipitation of an orange solid, which was filtered, washed with small amounts of water and diethyl ether and dried *in vacuo*. The impure complex obtained was purified by flash chromatography on neutral silica gel, with acetonitrile/water/saturated aqueous solution of KNO_3 (80:20:1) as eluent.

Subsequent recrystallisation of the major fraction in acetone/water (2:1) resulted in a dark red solid. Yield: 90 mg (0.11 mmol) 36%

^{1}H NMR (400 MHz, $(CD_3)_2SO$) δ in ppm 9.28 (d, 1H, J=1Hz, H3), 8.80 (m, 4H, 4xbpyH3), 8.38 (d, 1H, J=3Hz, H6), 8.14 (m, 4H, 4xbpy H4), 8.01 (m, 3H, H3', H5', bpy H6), 7.94 (d, 2H, J=8Hz, H2', H6'), 7.82 (d, 2H, J=6Hz, bpy H6), 7.78 (d, 2H, J=6Hz, bpy H6), 7.68 (dd, 1H, J_1=3Hz, J_2=1Hz, H5), 7.61 (m, 5H, bpy H6, 4xbpy H5)

^{13}C NMR (100 MHz, $(CD_3)_2SO$) δ in ppm 167.56, 157.40, 157.09, 156.98, 151.67, 147.95, 146.03, 137.86, 137.48, 130.12, 127.83, 125.56

Elemental Analysis for $C_{36}H_{36}N_9O_6RuPF_6$: Calc: C 46.16, H 3.87, N 13.46, Found: C 45.69, H 2.95, N 13.07

[Ru(bpy)$_2$pzSal](PF$_6$).2H$_2$O

75 mg (0.28 mmol) of pzHSal were dissolved in 10 cm^3 of ethanol/water (1:1). Addition of 115 g (0.22 mmol) of $[Ru(bpy)_2Cl_2].2H_2O$ resulted in a deep purple coloured solution. This was heated at reflux for a total of 5 hours, after which the solvent was removed with the rotary evaporator. The solid was redissolved in 3 cm^3 of water. Dropwise addition of a saturated solution of ammonium hexafluorophosphate brought about the precipitation of an orange solid, which was filtered, washed with small amounts of water and diethyl ether and dried *in vacuo*. The impure complex obtained was purified by column chromatography on silica, with acetonitrile/water/sat. aq. KNO_3 (80:20:1) as eluent. Subsequent

recrystallisation of the major fraction in acetone/water (2:1) resulted in a dark red solid. Yield: 110 mg (1.3 mmol) 60%

^{1}H NMR (400 MHz, $(CD_3)_2SO$) δ in ppm 10.97 (s, 1H, OH), 10.27 (s, 1H, CHO), 9.27 (d, 1H, J=1Hz, H3), 8.76 (m, 4H, 4xbpyH3), 8.36 (d, 1H, J=3Hz, H6), 8.14 (m, 5H, H3', 4xbpy H4), 8.05 (dd, 1H, J_1=2Hz, J_2=8Hz, H5'), 7.98 (d, 1H, J=6Hz, bpy H6), 7.80 (m, 2H, 2xbpyH6), 7.66 (dd, 1H, J_1=3Hz, J_2=1Hz, H5), 7.59 (m, 5H, bpy H6, 4xbpy H5), 7.01 (d, 1H, J=8Hz, H6')

Elemental Analysis for $C_{33}H_{28}N_9O_4RuPF_6$: Calc: C 46.05, H 3.28, N 14.65, Found: C 46.51, H 3.77, N 14.79

[Ru(d_8-bpy)$_2$pzTol](PF$_6$).H$_2$O

30 mg (0.13 mmol) of pzHTol and 50 mg (0.093 mmol) of [Ru(d_8-bpy)$_2$Cl$_2$].2H$_2$O were heated at reflux for 5 hours in 10 cm^3 of ethanol/water (1:1). After this time, the solvent was reduced to ~3 cm^3 in vacuo. Dropwise addition of an aqueous saturated solution of NH_4PF_6 brought about the precipitation of the orange complex, which was filtered off, washed with cold water and diethyl ether and dried *in vacuo*. The complex was purified by column chromatography on neutral alumina with CH_3CN/MeOH (98:2) as eluent. Subsequent recrystallisation from acetone/water (2:1) yielded the complex in a yield of 48 mg (62%).

^{1}H NMR (400 MHz, $(CD_3)_2SO$) δ in ppm 9.25 (d, 1H, J=1Hz, H3), 8.36 (d, 1H, J=3Hz, H6), 7.80 (d, 2H, J=8Hz, H3', H5'), 7.66 (dd, 1H, J_1=3Hz, J_2=1Hz, H5), 7.17 (d, 2H, J=8Hz, H2', H6'), 2.29 (s, 3H, CH_3)

Elemental Analysis for $C_{34}H_{13}N_8D_{16}ORuPF_6$: Calc. C 47.84, H 3.41, N 15.21, Found: C 48.15, H 3.63, N 14.85

[Ru(d_8-bpy)$_2$pzPhOH](PF$_6$).3H$_2$O

30 mg (0.13 mmol) of pzHPhOH and 50 mg (0.093 mmol) of [Ru(d_8-bpy)$_2$Cl$_2$].2H$_2$O were heated at reflux for 5 hours in 10 cm^3 of ethanol/water (1:1). After this time, the solvent was reduced to ~3 cm^3 in vacuo. Dropwise addition of an aqueous saturated solution of NH_4PF_6 brought about the precipitation of the orange complex, which was filtered off, washed with cold water and diethyl ether and dried *in vacuo*. The complex was purified by column chromatography on silica with CH_3CN/H_2O/sat. aq. KNO_3 (80:20:1) as eluent. After removal of the solvent from the relevant fractions, the solid was redissolved in water, precipitated as the PF_6 salt as before and filtered off. Subsequent recrystallisation from acetone/water (2:1) yielded the complex in a yield of 37 mg (49%).

^{1}H NMR (400 MHz, $(CD_3)_2SO$) δ in ppm 9.54 (s, 1H, OH), 9.23 (d, 1H, J=1Hz, H3), 8.33 (d, 1H, J=3Hz, H6), 7.72 (d, 2H, J=8Hz, H3', H5'), 7.64 (dd, 1H, J_1=3Hz, J_2=1Hz, H5), 6.74 (d, 2H, J=8Hz, H2', H6')

Elemental Analysis for $C_3H_{14}N_9D_{16}O_4RuPF_6$: Calc. C 44.36, H 3.49, N 14.55, Found: C 44.35, H 2.78, N 14.38

[Ru(d_8-bpy)$_2$pzAc](PF$_6$).3H$_2$O

30 mg (0.11 mmol) of pzHAc and 50 mg (0.093 mmol) of [Ru(d_8-bpy)$_2$Cl$_2$].2H$_2$O were heated at reflux for 5 hours in 10cm^3 of ethanol/water (1:1). After this time, the

solvent was reduced to ~3 cm^3 in vacuo. Dropwise addition of an aqueous saturated solution of NH_4PF_6 brought about the precipitation of the orange complex, which was filtered off, washed with cold water and diethyl ether and dried *in vacuo*. The complex was purified by column chromatography on silica with CH_3CN/H_2O/sat. aq. KNO_3 (80:20:1) as eluent. After removal of the solvent from the relevant fractions, the solid was redissolved in water, precipitated as the PF_6 salt as before and filtered off. Subsequent recrystallisation from acetone/water (2:1) yielded the complex in a yield of 27 mg (35%).

^1H NMR (400 MHz, $(CD_3)_2SO$) δ in ppm 9.28 (d, 1H, J=1Hz, H3), 8.38 (d, 1H, J=3Hz, H6), 7.99 (d, 2H, J=8Hz, H3', H5'), 7.94 (d, 2H, J=8Hz, H2', H6'), 7.68 (dd, 1H, J_1=3Hz, J_2=1Hz, H5)

^{13}C NMR (100 MHz, $(CD_3)_2SO$) δ in ppm 164.25, 160.20, 156.93, 130.13, 125.55

Elemental Analysis for $C_{33}H_{14}N_9D_{16}O_5RuPF_6$: Calc. C 44.31, H 3.38, N 14.09, Found: C 44.74, H 3.74, N 13.86

[Ru(d_8-bpy)$_2$pzSal](PF$_6$).2H$_2$O

50 mg (0.19 mmol) of pzHSal and 70 mg (0.16 mmol) of $[Ru(d_8\text{-bpy})_2Cl_2].2H_2O$ were heated at reflux for 5 hours in 10 cm^3 of ethanol/water (1:1). After this time, the solvent was reduced to ~3 cm^3 in vacuo. Dropwise addition of an aqueous saturated solution of NH_4PF_6 brought about the precipitation of the orange complex, which was filtered off, washed with cold water and diethyl ether and dried *in vacuo*. The complex was purified by column chromatography on silica with CH_3CN/H_2O/sat. aq.

KNO_3 (80:20:1) as eluent. Subsequent recrystallisation from acetone/water (2:1) gave the complex in a yield of 55 mg (50%).

^1H NMR (400 MHz, $(CD_3)_2SO$) δ in ppm 10.97 (s, 1H, OH), 10.27 (s, 1H, CHO), 9.27 (d, 1H, J=1Hz, H3), 8.36 (d, 1H, J=3Hz, H6), 8.10 (d, 1H, J=2Hz, H3'), 8.05 (dd, 1H, J_1=2Hz, J_2=8Hz, H5'), 7.66 (dd, 1H, J_1=3Hz, J_2=1Hz, H5), 7.01 (d, 1Hz, J=8Hz, H6')

Elemental Analysis for $C_{33}H_{12}N_9D_{16}O_4RuPF_6$: Calc. C 45.22, H 3.22, N 14.38, Found: C 44.83, H 2.83, N 14.02

4.3 Results and Discussion

4.3.1 Synthesis

All of the ligands and complexes prepared here contain suitable synthons for the incorporation of other amine ligands, which may later be used to bind manganese. The terminal functional groups chosen are the same as those chosen for the corresponding pyridyl triazole ligands prepared earlier. It was hoped that the synthesis would proceed as before. Purification of the complexes was expected to be slightly more difficult due to the free nitrogen of the pyrazine which would be expected to interact strongly with the stationary phase, during chromatography.

4.3.1.1 Synthesis of the Ligands

The synthesis of the model compound pzHTol was carried out by the same method as was used for the synthesis of pyHTol (See *Scheme 1, Fig 3.3*), starting from cyanopyrazine instead of cyanopyridine. As this method was concerned with the formation of the triazole, it was expected to work equally well for both pyridine and pyrazine derivatives. The crucial step, where a difference between the pyridine and pyrazine may have been noticeable, was during the addition of the hydrazide to the iminoether. No appreciable difference in reaction time or yield for this step was evident, showing that in both cases, the nitrile is equally activated towards nucleophilic addition by the methoxide, and subsequently by the hydrazide. As before, cyclisation of the acyl amidrazone thus formed was brought about by heating at reflux for 1 hour in ethylene glycol.

Similarly, the preparation of pzHPhOH was carried out in the same manner. Again, neither compounds required purification after cyclisation of the triazole. Each reaction produced ligands that were pure by NMR, with only the presence of water as an impurity. Having successfully prepared these two novel ligands, attention was turned to the synthesis of other desirable ligands from them. As before, it was hoped to prepare an aldehyde, an acid and a salicylaldehyde derivative.

The preparation of an aldehyde ligand, analogous to pyHAld, once again proved to be a source of frustration. Initial efforts to oxidise the methyl group, using ceric ammonium nitrate, by a similar means as for pyHTol, were problematic. Even after increasing the concentration of the acid and lengthening the reaction time, only a meagre yield of approximately 15% prior to necessary purification was achievable. Neither SeO_2[13] nor CrO_3[14] managed to oxidise the methyl group to the aldehyde. It was then decided not to pursue the matter any further.

The oxidation of the methyl group to the corresponding carboxylic acid proceeded well. The initial reaction between the ligand and the potassium dichromate[15] appeared to be more vigorous than for the corresponding pyridine derivative. The temperature of the solution quickly rose to almost 60°C. To reduce the possibility of the mixture boiling or bumping, the addition was slowed to a rate such that any further addition did not cause the temperature of the solution to exceed 60°C. While working up the reaction, the difference between the two ligands (pyHAc and pzHAc) became evident. The pH of the solution had to be raised to pH 4 before any precipitation of the product began, unlike in the case of pyHTol. This did not cause any problems and did not reduce the purity of the ligand obtained.

Again, the Duff formylation[16] was chosen as the method to introduce the formyl group into the phenol of pzHPhOH. Similar reaction conditions to those used to make pyHSal were employed. No changes in the means of isolation of the compound were needed and a comparable yield was obtained.

The synthesis of the four ligands prepared here proceeded without any major problems. Unfortunately, the fifth ligand (bearing an aldehyde group) was not prepared due to problems in its synthesis. It can be seen that changing the pyridine for a pyrazine does not usually have any drastic effects on the conditions needed to alter the substituents on the phenyl ring.

4.3.1.2 Synthesis of the Ruthenium Complexes

The ruthenium complexes of the pyrazine ligands prepared proceeded in a similar manner to the preparation of the complexes of the corresponding pyridine ligands. Again, the standard procedure of heating at reflux in ethanol/water was undertaken. As the reactions proceeded, the colour changed from a deep violet colour to a dark blood red solution upon completion. Reaction times were typically in the order of 5 hours. By following the reactions by cation exchange HPLC, as before, it was possible to monitor the progress of the complexation. Within short periods of time (~30 min) much of the $[Ru(bpy)_2Cl_2]$ had been consumed, but longer reaction times resulted in higher yields.

Again, the HPLC proved to be useful in giving an insight into how the purification of the complexes by column chromatography would proceed. From the HPLC traces, it

was possible to see that the main impurities in the products isolated were unreacted starting materials and small amounts of coordination isomers. As previously explained (Section 3.3.1.2), the formation of coordination isomers comes about due to the different binding sites at N2 and N4 of the triazole. For the complexes prepared in this section, very little of the N4 isomer was formed due to the steric hindrance of the phenyl ring attached to the triazole. However, due to their altered properties, because of the difference of the σ-donor capabilities of the N2 and N4, the N4 isomers had to be removed from the desired (N2 bound) complexes.

HPLC retention times (see *Table 4.1*) of the complexes gave an indication of the method of purification that would be needed. Those with short retention times were separable on alumina and those with longer retention times on silica. All of the retention times were longer than those of the corresponding pyridine complexes, due to the extra free nitrogen in the pyrazine ring. However, the same trend, observed for the pyridyl triazole complexes, held true for these complexes. The complex of pzHTol had the shortest retention time and was purified by column chromatography on alumina, using acetonitrile and methanol as eluent. The other three complexes were purified on silica, using acetonitrile/water/sat. aq. KNO_3 as eluent. The complex of pzHPhOH was the easiest to elute and that of pzHAc the most difficult. While it was possible to use alumina for the complexes of pyHPhOH and pyHSal, it proved inefficient here due to the very low R_f values of the complexes on alumina and the streaky bands which were obtained. $[Ru(bpy)_2pzAc]^+$ proved to be difficult to purify. Only a very short column could be used, as it tended to bind quite strongly with the silica resulting in a low yield for the reaction. As before, no difference

between complexes containing bpy or d_8-bpy was evident during synthesis or purification.

Compound	Retention Time
$[Ru(bpy)_2pzTol]^+$	2.5 mins
$[Ru(bpy)_2pzPhOH]^+$	3.3 mins
$[Ru(bpy)_2pzAc]^+$	4.5 mins
$[Ru(bpy)_2pzSal]^+$	3.6 mins

Table 4.1 HPLC retention times of Ru(II) complexes with a flow rate of 1.8 cm^3/min of 0.08M $LiClO_4$ in $MeCN/H_2O$ (80:20)

C, H, N, elemental analysis of the complexes has been obtained and indicate that in each case only one counter ion is present as the triazole is deprotonated.

4.3.2 Characterisation

This series of complexes were made with the intention of increasing the oxidation potential of the ruthenium centre so as to increase the driving force for electron transfer from tyrosine or a manganese complex to the photo-oxidised ruthenium centre. Therefore, it is essential that they be studied properly to confirm that the changes in their structure have indeed improved the driving force for the electron transfer reaction.

All of the ligands prepared were characterised by NMR and IR spectroscopy. All of the complexes have been studied by a range of techniques. NMR spectroscopy has been used to confirm the purity and the structure of the complexes. UV/Vis spectroscopy gives a quick and easy way to see the influence of the pyrazine on the metal centre. Similarly, an investigation into the emission of these complexes gives us vital information about the location and energy of the excited state. pK_a titrations and luminescence studies also aid in the confirmation of the location of the excited state. However, electrochemistry provides the definitive analysis of the change in the oxidation potential of the metal centre.

4.3.3 NMR Spectroscopy

Having previously made the series of pyridyl triazole ligands and complexes mentioned in Chapter 3, the synthesis and characterisation of the pyrazine analogues was not expected to provide any major complications. Since all of the protons in the NMR spectra for the pyridyl triazoles had been assigned, assignment of the protons for the pyrazine ligands could be achieved by a simple comparison of the spectra[17]. In fact, spectra of the pyrazine compounds were actually more straightforward to assign since they have one proton less. While 2-substituted pyridine gives four multiplets in the NMR, 2-substituted pyrazine gives a multiplet and two doublets. This is particularly evident in the spectrum of pzHTol (*Fig. 4.2*). On close inspection of the spectra, long-range coupling was evident between the protons in the 3 and 5 positions. This resulted in the apparent singlet for H3 being split into a doublet. However, the magnitude of this coupling was generally in the region of 1Hz and was

sometimes difficult to observe, relying on very sharp spectra for it to be clear. However, as it also resulted in the splitting of the doublet for H5 into a double of doublets, this aided tremendously in the assignment of the protons.

As before, the introduction of the various functional groups into the ligands was observed by NMR. The attempted oxidation of the methyl group to the aldehyde was checked by NMR, as it should result in the disappearance of the CH_3 signal and the appearance of a new signal at approx. 10ppm for the aldehyde. The estimation of a 15% yield for the reaction was based on the relative intensities of the aldehyde peak to that of the methyl peak. Similarly, the oxidation to the acid resulted in the complete disappearance of the methyl peak at 2.2ppm. The formylation of pzHPhOH again caused a dramatic alteration to the NMR spectrum. The symmetry of the phenyl ring was lost and a new signal for the aldehyde was observed at 10.5ppm. Unfortunately quaternary carbons were often too weak to be visible in ^{13}C NMR, but all C-H carbons were found.

The assignment of the protons in the ruthenium complexes was not as cumbersome as for those of the pyridyl triazole complexes. The splitting patterns and positions of the bpy protons had already been established. These were not expected to change significantly on going from the pyridyl triazole complex to the pyrazyl triazole complex. This was found to be the case. The shifts of the signals from the triazole ligands upon coordination, due to interaction with the metal centre and ring currents from bpy ligands, have already been established. These were not expected to be greatly different for the pyrazine ligands compared to the pyridine ligands. Also, the signals obtained for the pyrazine are quite distinguishable from those of bpy due to

their unique shapes. The doublet (H3) and the doublet of doublets (H5) are unlike any other signals in the spectrum. Even the large doublets from the phenyl rings are clearly evident. However, at a first glance, the spectrum of one of the ruthenium complexes (*Fig. 4.3*) still appears confusing. The use of 2D spectroscopy (*Fig. 4.4*) and the comparison with spectra obtained for d_8-bpy complexes (*Fig. 4.5*) aids in the confirmation of the assignment of the protons.

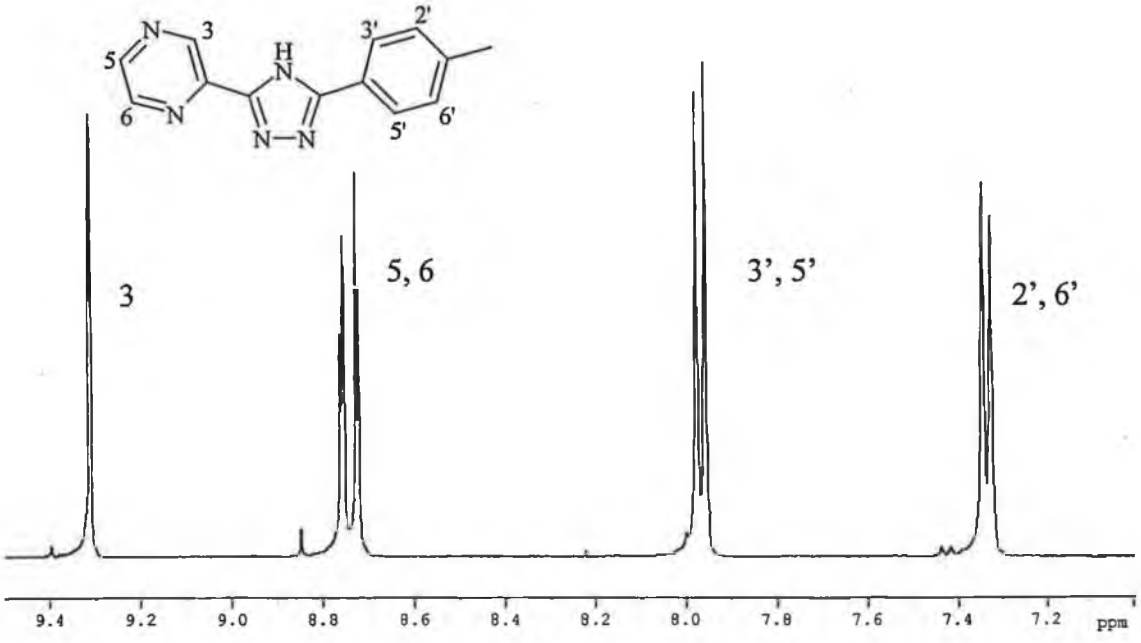

Fig. 4.2 ^{1}H NMR spectrum of pzHTol in d_6-DMSO. Inset – structure of pzHTol showing numbering of protons

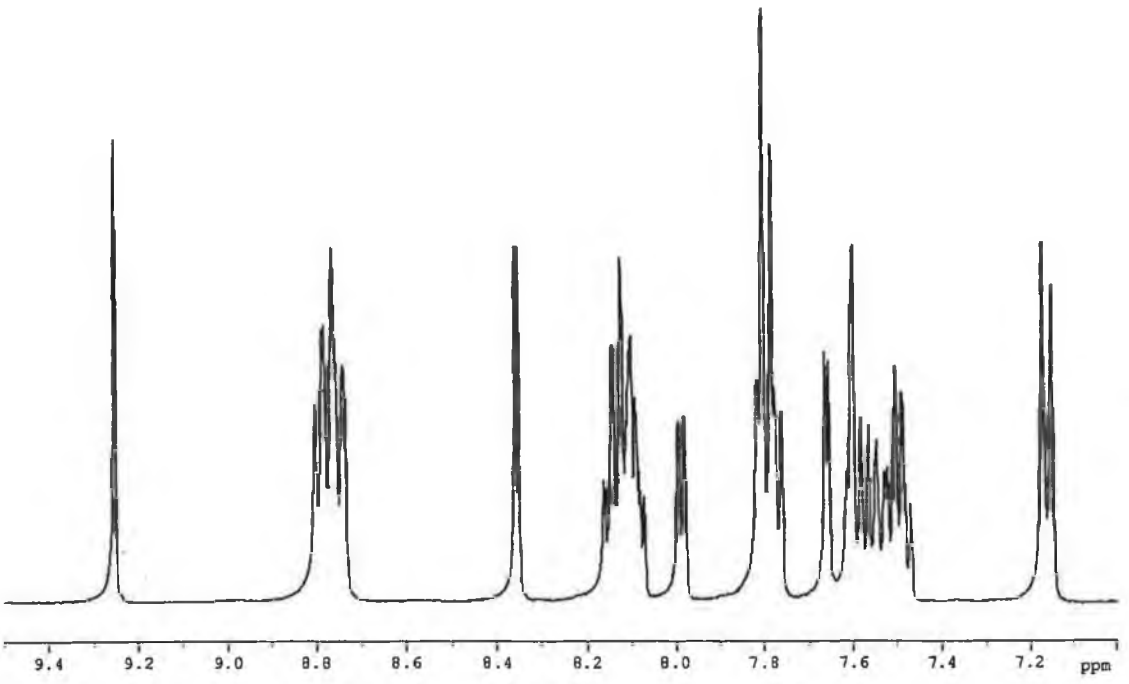

Fig. 4.3 ^{1}H NMR spectrum of $[Ru(bpy)_2pzTol](PF_6)$ in d_6-DMSO

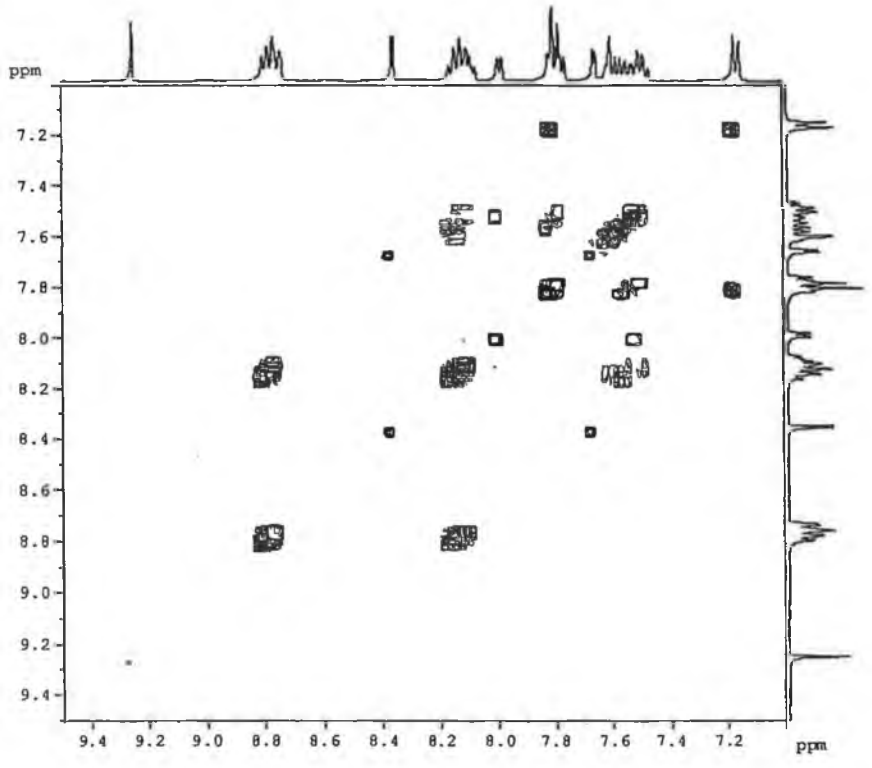

Fig. 4.4 2D COSY spectrum of $[Ru(bpy)_2pzTol](PF_6)$ in d_6-DMSO

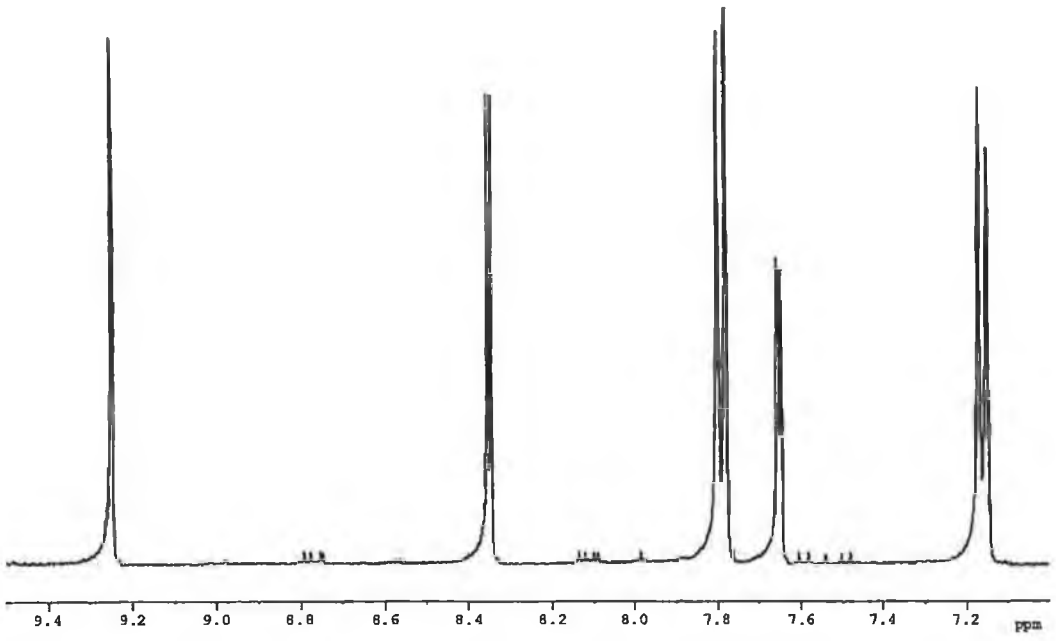

Fig. 4.5 ^1H NMR spectrum of [Ru(d_8-bpy)$_2$pzTol](PF$_6$) in d_6-DMSO

Name	H3	H5	H6
[Ru(bpy)$_2$pzTol]$^+$	9.25 (9.33)	7.66 (8.77)	8.36 (8.77)
[Ru(bpy)$_2$pzAc]$^+$	9.28 (9.33)	7.68 (8.77)	8.38 (8.77)
[Ru(bpy)$_2$pzPhOH]$^+$	9.23 (9.32)	7.64 (8.76)	8.33 (8.76)
[Ru(bpy)$_2$pzSal]$^+$	9.27 (9.33)	7.66 (8.78)	8.36 (8.78)

Table 4.2 Comparison of chemical shifts of ligand protons in their complexed and free (in parentheses) forms, measured in d_6-DMSO

It is seen that the shift upon coordination is similar in all complexes. H3 remains almost unchanged. However, H6 and H5 are shifted upfield upon coordination. In section 3.3.3 it was stated that the cause for the shift of H6 is due to its interaction with the ring current of a neighbouring bpy ring. This holds true again for the

pyrazine complexes. It should be noted that the shift is no longer so great and that H5 actually undergoes a larger upfield shift. The reason for this is not known, but appears to be constant for all pyrazine triazole complexes.

4.3.4 UV/Vis Absorption and Emission Spectroscopy

The uv/vis absorption spectra of the complexes have been measured in acetonitrile. Two major bands dominate. The band in the region of 280nm (ε=6.5x10^4 M^{-1}cm^{-1}) results from ligand based π–π^* transitions[18]. These are similar to those found for all ruthenium (II) polypyridyl complexes. The other intense band arises from the d-π^* metal to ligand charge transfer (MLCT)[19]. This transition occurs in the region of 450nm, similar to that of $[Ru(bpy)_3]^{2+}$. They are highly intense bands, possessing extinction coefficients typically of 1.3x10^4 M^{-1}cm^{-1} (see *Table 4.3*), and result in the complexes' deep red colour.

In section 3.3.4, the positioning of the MLCT bands for complexes containing pyridyl triazoles was found to be between 450 – 480nm. The strong σ-donor nature of the deprotonated triazole increases electron density on the metal centre, thus reducing the energy of the MLCT. However, in the case of the pyrazyl triazole complexes, the situation becomes more complex. Pyrazine is known to be a strong π-acceptor. This causes a reduction of electron density on the metal centre and hence an increase in the energy of the MLCT[18]. Combining this with the effect of the triazole actually seems to result in a cancelling of the two effects. The MLCT is now found in the region of 455nm. Upon protonation of the triazole, by the addition of one drop of 0.1M CF_3COOH in acetonitrile, MLCT's tended to shift to

approximately 445nm for pyridyl triazoles. Again, in the case of pyrazyl triazoles, the π-accepting nature of the pyrazine seems to be the source of the difference. The change in wavelength is no longer as dramatic, with an average shift of just 15nm to give an MLCT band at 440nm (see *Table 4.3*). Isosbestic points at 305 nm, 325 nm, 405 nm and 465 nm were evident. An example of the difference between the protonated and deprotonated forms of the complexes is shown in *Fig. 4.6* below.

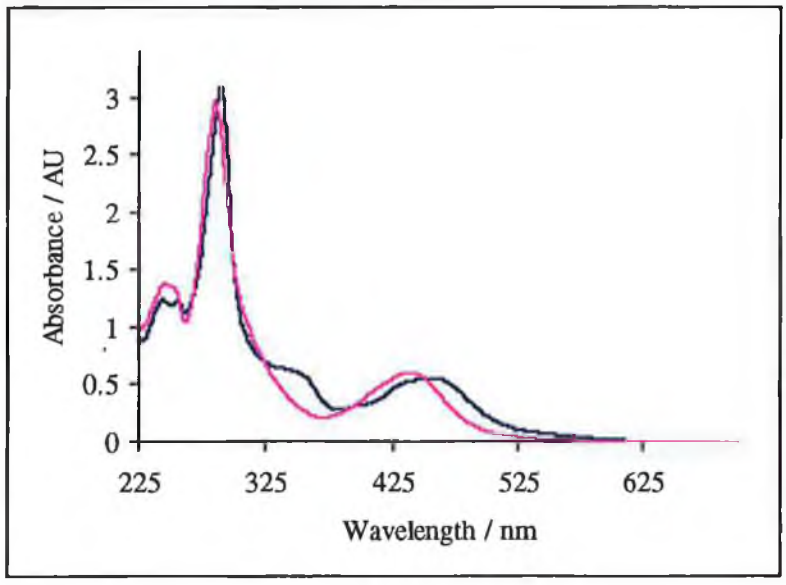

Fig. 4.6 UV/Vis absorption spectra of 3.8 x 10^{-5} M solutions of $[Ru(bpy)_2pzTol]^+$ (blue) and $[Ru(bpy)_2pzHTol]^{2+}$ (pink) in acetonitrile

Compound	Absorption / nm ($\varepsilon/10^4$ $M^{-1}cm^{-1}$)	Emission / nm (300K)	Emission / nm (77K)
$[Ru(bpy)_2pzTol]^+$	455 (1.29)	665	606
$[Ru(bpy)_2pzHTol]^{2+}$	439 (1.42)	674	613
$[Ru(bpy)_2pzPhOH]^+$	455 (1.15)	671	613
$[Ru(bpy)_2pzHPhOH]^{2+}$	440 (1.15)	675	614
$[Ru(bpy)_2pzAc]^+$	456 (1.15)	656	601
$[Ru(bpy)_2pzHAc]^{2+}$	443 (1.15)	666	613
$[Ru(bpy)_2pzSal]^+$	455 (1.42)	661	609
$[Ru(bpy)_2pzHSal]^{2+}$	440 (1.50)	670	611

Table 4.3 Spectroscopic data for ruthenium complexes measured in acetonitrile (300K) or ethanol/methanol 4:1 (77K) at concentrations of approximately 3 x 10^{-5}M

All of the complexes prepared here emit in acetonitrile at room temperature. Although not as strong an emission is observed as for $[Ru(bpy)_3]^{2+}$, the emission was easily measured. The trends observed for the emission spectra differed from those observed for absorption spectra and for pyridyl triazoles. Pyridyl triazole complexes generally emitted at ~680nm when deprotonated and ~620nm when protonated. Here, however, the pyrazyl triazole complexes emit at ~665nm when deprotonated and ~670nm when protonated (see *Fig. 4.7* and *Table 4.3*). This reduction in emission energy upon protonation contrasts the increase in energy observed in the absorption spectra, indicating that the nature of the emitting species may not be straightforward as before.

In carrying out the measurements, it was important to ensure that only the triazole was protonated and not the pyrazine. The emission intensity has been shown to be greatly dependent on the degree of protonation. At high pH, emission is weak. Upon protonation of the triazole the emission increases significantly. However, increasing the acidity further results in the protonation of the pyrazine that is characterised by the lack of emission[19].

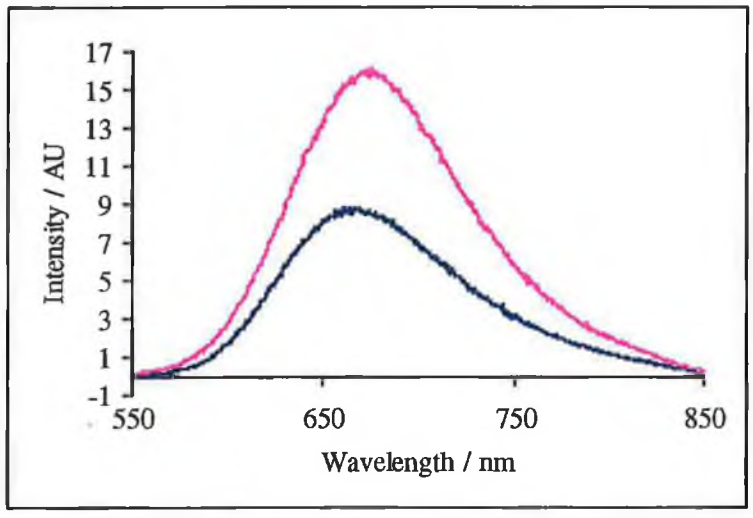

Fig. 4.7 Emission spectra of 4.8x 10^{-5}M solutions of $[Ru(bpy)_2pzTol]^+$ (blue) and $[Ru(bpy)_2pzHTol]^{2+}$ (pink) in acetonitrile at 300K, excited at 465nm

Measurement of the emission at 77K in an alcoholic glass revealed similar spectra to those of the pyridyl triazole complexes. As before, a shift to shorter wavelength was observed as well as an increase in intensity. The increase in the intensity was strongly dependent on the quality of the glass formed upon cooling, which in turn was dependent on the water content of the solvents. The deprotonated forms displayed a change in the shape of the emission spectrum arising from relaxation via bpy based vibrations. This was not observed for the protonated species.

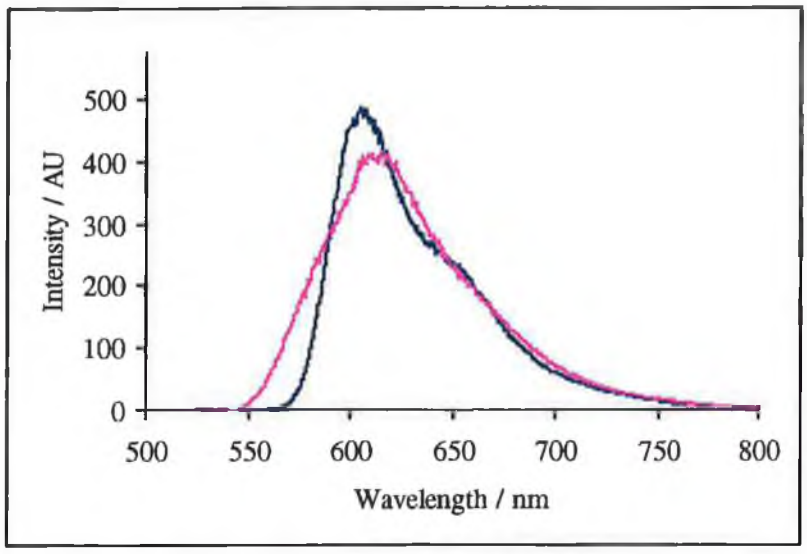

Fig. 4.8 Emission spectra of $[Ru(bpy)_2pzTol]^+$ (blue) and $[Ru(bpy)_2pzHTol]^{2+}$ (pink) in ethanol/methanol (4:1) at 77K

4.3.5 Luminescent Lifetime Measurements

Once again, it is hoped that the study of the luminescent lifetimes of a series of complexes will lead to the location of the excited state. In section 3.3.5 it was shown that, for pyridyl triazole complexes, the excited state is always located on one of the bpy ligands and never on the pyridyl triazole. This was found by noting the increase in lifetime upon deuteration of the bpy ligands – indicative of the photoexcited electron being located there. However, this could also be deduced logically. Emission should always stem from the LUMO. Of the two ligands in question, bpy or pyridyl triazole, bpy is lower in energy, since pyridine is a weaker σ-donor and a stronger π-acceptor than a triazole[20]. Therefore it should be easier to promote an electron onto a bpy (2 pyridines) than a pyridyl triazole (1 pyridine, 1 triazole), and the emission should be bpy-based.

The series of complexes studied in this section are somewhat more complicated. Pyrazine is known to be a very strong π-acceptor. The combination of this with a triazole results a ligand that possesses both excellent σ-donor and π-acceptor properties. Whichever one of these two properties dominates will determine the location of the excited state. In its deprotonated form, the triazolate is an extremely strong donor and its effect is clearly evident in the visible spectrum of the complex (*Fig. 4.6*). A slight red shift of the MLCT is still present. Upon protonation its properties appear to be overshadowed by the pyrazine with a slight blue shift of the MLCT with respect to $[Ru(bpy)_3]^{2+}$. This would indicate that at high pH, the excited state is probably located upon a bpy ligand, but on protonation of the triazole, the location of the excited state is unclear, being possibly located on the pyrazyl triazole[21].

Therefore, a study of the lifetimes of the complexes was necessary in order to determine the site of the emitting state. As before, the presence of the excited state on a deuterated bpy ligand would result in a significant increase in the lifetime. In the deprotonated form, this measurement was not expected to provide and major problems. On the other hand, lifetimes of protonated complexes were expected to be troublesome to measure. As previously stated, (section 4.3.4), protonation of the pyrazine results in a decrease of the emission. While care must be taken to ensure that each triazole (pK_a~4) is completely protonated and each pyrazine (pK_a~-1.8) completely deprotonated, a compromise may be found. By preparing samples for measurement from equal amounts of complex dissolved in equal amounts of a suitably concentrated stock solution of CF_3COOH in acetonitrile, one may deduce that each complex is protonated to approximately the same extent. In general,

samples of a complex and its deuterated analogue were prepared and measured at the same time to ensure similar conditions. The results obtained are shown below in *Table 4.4.*

Complex	Aerated Lifetime / ns		Deaerated Lifetime / ns	
	Deprotonated	Protonated	Deprotonated	Protonated
$[Ru(bpy)_2pzTol]^+$	68	170	176	293
$[Ru(d_8\text{-}bpy)_2pzTol]^+$	73	167	230	332
$[Ru(bpy)_2pzPhOH]^+$	59	206	126	558
$[Ru(d_8\text{-}bpy)_2pzPhOH]^+$	62	285	164	708
$[Ru(bpy)_2pzAc]^+$	79	134	171	269
$[Ru(d_8\text{-}bpy)_2pzAc]^+$	76	150	242	320
$[Ru(bpy)_2pzSal]^+$	73	157	196	271
$[Ru(d_8\text{-}bpy)_2pzSal]^+$	71	139	220	275

Table 4.4 Luminescent lifetime data (±10%) for ruthenium pyrazyl triazole complexes measured at ~10^{-4}M in MeCN or 10^{-3}M CF_3COOH in MeCN

All compounds show an increase in lifetime upon protonation of the triazole. In the case of the complexes of pzHPhOH, this increase is particularly large and requires more work to determine the reason for this. For degassed samples of complexes with deprotonated triazoles, a definite trend is evident upon deuteration of the bpy ligands. The observed increases of 20-40% are greater than possible experimental error. This is indicative of the excited state being located on the bpy ligands, similar

to the case for the pyridyl triazole complexes. As before, this only became evident after degassing the samples, thus removing the possibility of oxygen quenching.

However, at lower pH, the location of the excited state is not quite as clear-cut[22]. The complexes of three of the ligands, pzHTol, pzHAc and pzHPhOH, show an increase in the lifetime in the region of 20-40% upon deuteration. This is similar to before and would indicate that bpy is again the location of the excited state. However, the complexes of pzHSal show no significant change upon deuteration. The increase of 4ns is negligible and within the 10% experimental error associated with these measurements. This would indicate that the excited state is probably located on the pyrazyl triazole ligand and not on the bpy. One would expect all pyrazyl triazoles to behave in a similar manner. However, the presence of a salicylaldehyde group at low pH is sufficient to alter the properties of the ligand enough to result in the excited state being located on it.

Despite this anomalous result, one may tentatively state that the excited state is generally located on the bpy ligands in pyrazyl triazole complexes. However, pKa and electrochemical measurements shall be used to confirm this in the coming sections.

4.3.6 Acid-Base Properties

As was shown in section 3.3.6, a measurement of the ground and excited state acid/base properties of a complex can lead to the determination of the location of the

excited state. This is due to the fact that the acidity of a proton is dependent on the electron density present on the ligand to which it is attached[23,24,25]. By increasing the electron density on the ligand (excited state located on the ligand), the proton becomes less acidic. By reducing electron density on the ligand (spectator ligand coordinated to a more positive metal centre), the acidity of the proton increases. It was hoped that this phenomenon could again be exploited in the search for the location of the excited state, this time of pyrazine complexes.

Whilst the excited state pK_a of pyridyl triazole complexes could only be calculated by the Förster equation (equation 4.2), due to their short lifetimes, both methods (equations 4.1, 4.2) could be used to calculate pK_a^* of the pyrazine complexes.

$$\mathbf{pK_a^* = pH_i + \log(\tau_a / \tau_b)} \qquad \textbf{eqn. 4.1}$$

$$\mathbf{pK_a^* = pK_a + 0.625(\nu_b - \nu_a) / T} \qquad \textbf{eqn. 4.2}$$

The results obtained are summarised in *Table 4.5* below.

Compound	pK_a	pH_i	pK_a^* (1)	pK_a^* (2)
$[Ru(bpy)_2pzTol]^+$	3.1	5.9	6.1	3.5
$[Ru(bpy)_2pzPhOH]^+$	3.1	-----	----	3.2
$[Ru(bpy)_2pzAc]^+$	2.7	3.7	3.9	3.4
$[Ru(bpy)_2pzSal]^+$	2.9	----	----	3.0
$[Ru(bpy)_2pztr]^+$	3.7[19]	3.9[19]	3.8[19]	3.5[26]

Table 4.5 Ground (± 0.1) and excited state (± 0.2) pK_a titration results, measured in Britton Robinson buffer. pK_a^* (1) calculated using equation 4.1, pK_a^* (2) calculated using equation 4.2. (pztr=pyrazyl triazole)

The measurement of the complexes in their ground state did not generate any difficulties. Clean isosbestic points were observed at 324 nm, 370 nm, 455 nm and 485 nm. An example of the changes in the spectra and a plot of the changes in absorbance are shown in *Fig. 4.9*. It can be seen that the differences between the spectra of the species at pH1 and pH5 are not as great as those observed for complexes of pyridyl triazoles (Section 3.3.6). This resulted in a decrease in the accuracy of the measurement, as can be seen from the graph of absorbance versus pH. A best-fit curve was added to clarify the graph. This curve was differentiated in order to solve for the position of the point of inflection.

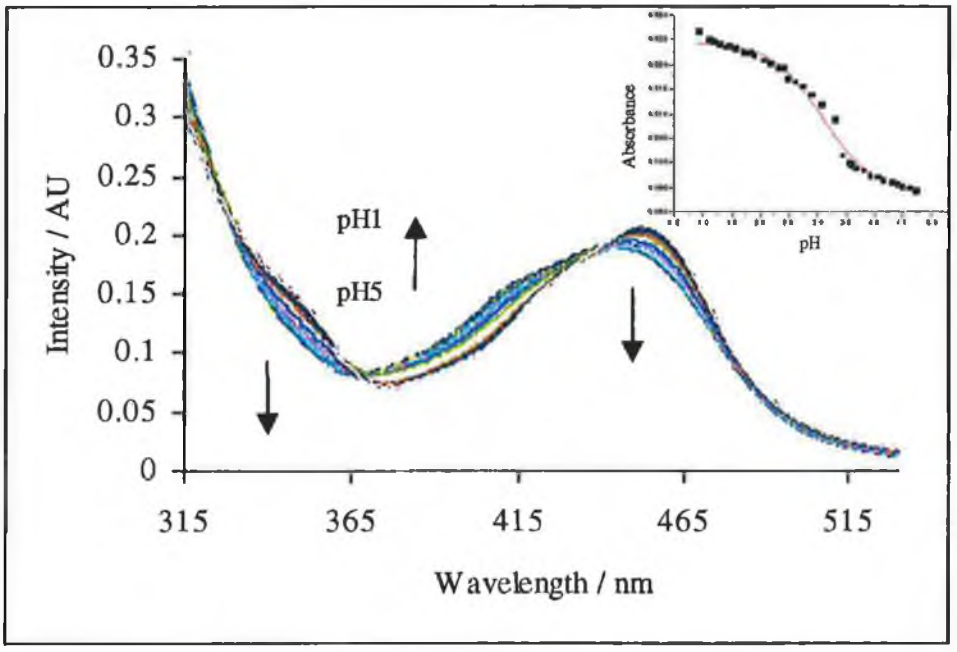

Fig. 4.9 Ground state pK_a titration (pH1 – pH5) of $[Ru(bpy)_2pzTol]^+$ in Britton Robinson buffer. Inset – Plot of absorbance at 450nm versus increasing pH

The emission spectra proved to be very problematic. The intensity of the emission in aqueous solution was found to be extremely low with noise being a common

problem (see *Fig. 4.10*). Again, the changes in the spectra over the chosen pH range were found to be significantly less than those found for the corresponding pyridine complexes. A combination of these two factors introduced more possible errors into the calculations. This can be seen quite clearly from the graph of intensity versus pH in *Fig. 4.10*. Therefore, the pH_i values obtained must be seen as merely indicators of the value and not accurate constants. Unfortunately no values of pH_i were obtained for the complexes of pzHPhOH and pzHSal. Neither compound emitted strongly enough or displayed enough of a change in emission for the value of pH_i to be found.

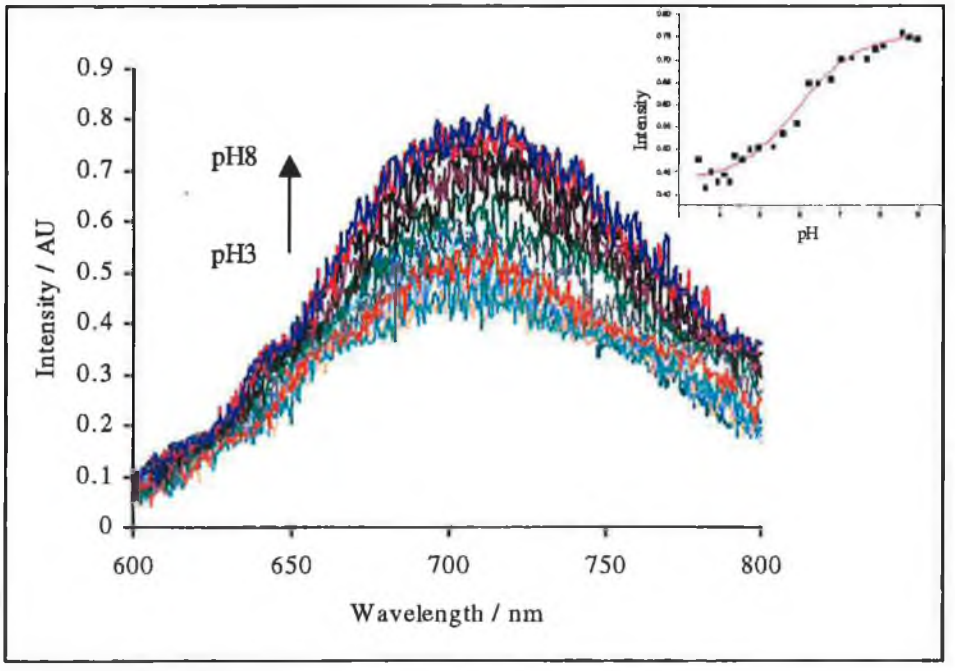

Fig. 4.10 Excited state pK_a titration (pH3 – pH8) of $[Ru(bpy)_2pzTol]^+$ in Britton Robinson buffer. Inset – Plot of absorbance at 700nm versus increasing pH

A comparison of the ground and excited state pK_a values with those obtained for $[Ru(bpy)_2pztr]^{2+}$ indicates that the introduction of the various substituted phenyl rings into the ligand has altered its electronic structure slightly. In the ground state a change of ~ 0.7 in the pK_a was observed, but in the excited state this difference was

only ~0.1. This may be due to stabilisation of the deprotonated species because of the possibility of delocalisation of charge on the phenyl ring.

By comparing the ground and excited state pK_a's of each complex, one can see that the excited state value is generally higher than the ground state. This indicates that the photoexcited electron resides on pyrazyl triazole ligand and not on the bpy. Only a small increase in the pK_a is seen, but this is enough for us to draw this conclusion. This is in contrast to the results obtained for pyridyl triazole complexes. It is also in contradiction to the results obtained from the luminescent lifetime measurements of the complexes and their deuterated analogues. As a result, still more studies are necessary to clarify this problem.

4.3.7 Electrochemical Properties

Just as the change from a pyridine to a pyrazine was evident from spectroscopic studies, so too were the effects of the pyrazine visible from electrochemical studies on the series of complexes presented here. Ruthenium complexes of pyrazyl triazoles are known to have higher oxidation potentials than those of the corresponding pyridyl triazoles[20]. This is an important property of the metal complex, especially if one wishes to use these complexes as photosensitisers in supramolecular assemblies. This redox potential will provide the driving force behind any possible electron transfer reactions. Therefore it is important to gain some information about the strength of this potential driving force before preparing supramolecular systems.

Typically an increase of approximately 100-150mV in the oxidation potential is expected on going from the pyridine complex to the pyrazine complex. As can be seen from *Table 4.6*, (compare to *Table 3.7*), this is true in most cases. However, the complex of pzHPhOH does not adhere to this pattern. In fact, its oxidation potential is 100mV lower than that of its pyridine analogue. There is no evidence to explain the reason for this based on absorption and emission spectroscopy, although it does possess a long luminescence lifetime. It is possible that the phenol is causing some more complex intramolecular processes. Further work would be required to understand the exact reasons behind these strange properties. Another very peculiar fact about this complex is the lack of change upon protonation of the triazole. Each of the other complexes displays an increase in oxidation potential of about 150mV (see *Fig. 4.11*). This is in sharp contrast to the 300mV increase noted for pyridyl triazole complexes.

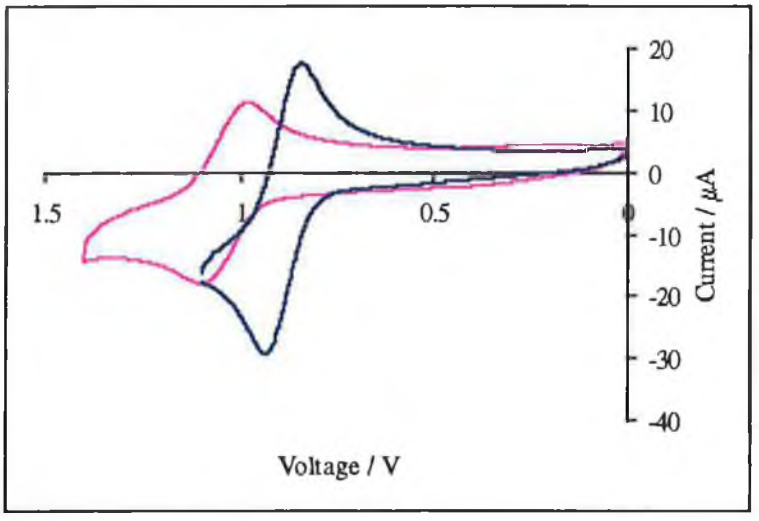

Fig. 4.11 Oxidation waves of $[Ru(bpy)_2pzTol]^+$ (blue) and $[Ru(bpy)_2pzHTol]^{2+}$ (pink) in 0.1M TEAP in MeCN, measured at 100mVs^{-1} versus SCE

Compound	Oxidation / V (vs. SCE)	Reduction / V (vs. SCE)
$[Ru(bpy)_2pzTol]^+$	0.89	-1.45, -1.67, -1.96 (irr.)
$[Ru(bpy)_2pzTol]^{2+}$	1.04	-----
$[Ru(bpy)_2pzPhOH]^+$	0.93	-1.46, -1.72 (irr.)
$[Ru(bpy)_2pzHPhOH]^{2+}$	0.93	-----
$[Ru(bpy)_2pzAc]^+$	0.94	-1.45, -1.66, -1.93 (irr.)
$[Ru(bpy)_2pzHAc]^{2+}$	1.11	-----
$[Ru(bpy)_2pzSal]^+$	0.89	-1.46, -1.72 (irr.)
$[Ru(bpy)_2pzHSal]^{2+}$	1.03	-----

Table 4.6 Redox potentials for ruthenium complexes in 0.1M TEAP in MeCN, measured at 100mVs^{-1} versus SCE

The reduction potentials of the deprotonated complexes were also measured and are presented in *Table 4.6* and *Fig. 4.12*. Those of the protonated complexes were not measured. The addition of acid to the solution was found to result in a drastic decrease in the intensity of all reduction peaks. As a result they could not be measured with any degree of accuracy and are not included. However, the data obtained provides us with some useful knowledge. In each case the first two reduction peaks are typical for bpy reductions[27]. The third (irreversible) peak, visible in only two examples, is probably a pyrazyl triazole reduction by analogy to other complexes[17,28]. This very simple observation leads us to the conclusion that, in the deprotonated form, the excited state is located on the bpy as it has the lower

reduction potential. This is in agreement with what was found from luminescent lifetime studies (Section 4.3.5).

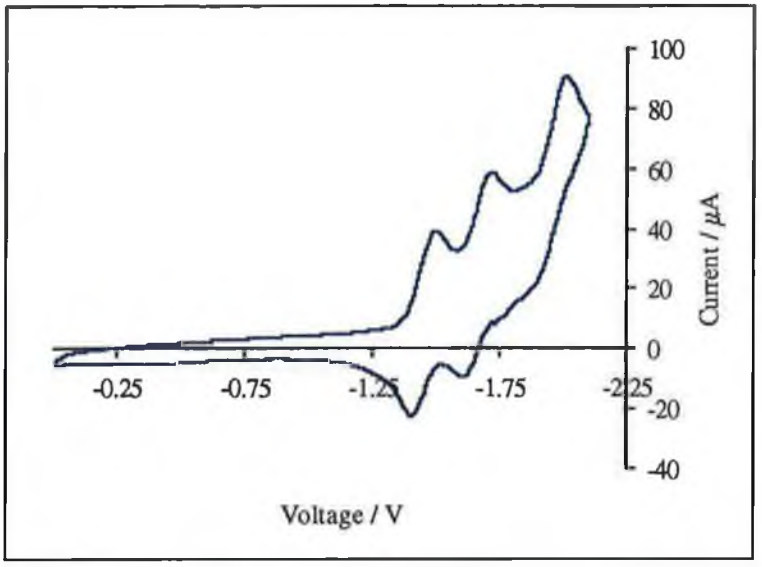

Fig. 4.12 Reduction waves of $[Ru(bpy)_2pzTol]^+$ in 0.1M TEAP in MeCN, measured at $100mVs^{-1}$ versus SCE

4.4 Conclusion

A range of novel pyrazyl triazole ligands and their ruthenium complexes has been successfully prepared and characterised. The synthesis of the triazole ligands was carried out in a similar manner to before. Yields were comparable to those obtained for the pyridine analogues. The modification of the ligands proved to be slightly more difficult, with the pyrazine equivalent of pyHAld not being isolated at all. The preparation of the complexes proceeded as before. Purification of the acid complex $[Ru(bpy)_2pzAc]^+$ was less efficient than before due to its extremely polar nature causing it to bind to the silica gel.

The complexes were characterised by a variety of means. NMR spectroscopy again illustrated the change in chemical shift caused by complexation with the metal. Typical pyrazine signals were obtained, with long range coupling being evident.

UV/Vis spectra displayed all the typical elements of ruthenium polypyridyl complexes. Intense MLCT bands in the region of 450nm dominate the spectra. These are blue shifted with respect to the pyridine complexes due to the increase in the π-acceptor nature of the pyrazine. This was also apparent in the emission spectra of the complexes. As before, protonation of the triazole resulted in these values shifting as a direct consequence of the reduction in the triazole's σ-donor nature. Electrochemistry showed the effect the introduction of pyrazine has upon the oxidation potentials of the metal centre, by increasing them to values in the region of 0.9V (vs. SCE), which may be increased still further by protonation of the triazole. Although no reduction potentials for the protonated complexes were obtainable, one

would expect the first reduction to shift to a less negative value, thereby keeping the energy gap between the oxidation potential and the first reduction potential constant. This would be in line with the fact that no significant change in the emission wavelength was observed after protonation of the triazole.

In the case of pyrazyl triazoles, it was found that the location of the excited state is a contentious issue. The four compounds here were all studied by the same techniques previously used to assign the location of the excited state. Initial measurements on the luminescent lifetimes of the h_8-bpy and d_8-bpy complexes indicated that the excited state was bpy-based. However, upon protonation of the triazole, the excited state appears to reside on the pyrazyl triazole of $[Ru(bpy)_2pzHSal]^{2+}$, but on the bpy of the other 3 complexes. Ground and excited state pK_a measurements indicated that the excited state is based on the pyrazine ligand in all cases. Electrochemistry pointed towards the first reduction being bpy-based, when the triazole is deprotonated. It was not possible to measure the reduction potentials in acidic media.

Consequently, the location of the excited state may not be definitely be assigned yet. One may assume, however, that at high pH it shall be bpy-based, but at low pH it may be pyrazyl triazole based. This would be in accordance with results obtained by others. Further studies, such as resonance Raman, would aid in this problem[4,29]. However, these complexes do appear to make ideal starting materials for supramolecular systems, due to their well behaved properties.

4.5 Bibliography

[1] Sjödin, M.; Styring, S.; Åkkermark, B.; Sun, L.; Hammarström, L.; *J. Am. Chem. Soc.*, **2000**, 122, 3932

[2] Magnusson, A.; Frapart, Y.; Abrahamsson, M.; Horner, O.; Åkkermark, B.; Sun, L.; Girerd, J. J.; Hammarström, L.; Styring, S.; *J. Am. Chem. Soc.*, **1999**, 121, 89

[3] Anderson, P. A.; Anderson, R. F.; Furue, M.;, Junk, P. C.; Keene, F. R.; Patterson, B. T.; Yeomans, B. D.; *Inorg. Chem.*, **2000**, 39, 2721

[4] Mabrouk, P. A.; Wrighton, M. S.; *Inorg. Chem.*, **1986**, 25, 526

[5] Iengo, E.; Zangrando, E.; Mestroni, S.; Fronzoni, G.; Stener, M.; Allesio, E.; *J. Chem. Soc. Dalton Trans.*, **2001**, 1338

[6] Coe, B. J.; Meyer, T. J.; White, P. S.; *Inorg. Chem.*, **1995**, 34, 593

[7] Cruetz, C.; Chou, M. H.; *Inorg. Chem.*, **1987**, 26, 2995

[8] Creutz, C.; Taube, H.; *J. Am. Chem. Soc.*, **1973**, 95, 1086

[9] Sherbourne, J.; Scott, S. M.; Gordon, K. C.; *Inorg. Chim. Acta*, **1997**, 260, 199

[10] Kirsch-De Mesmaeker, A.; Jacquet, L.; Masschelein, A.; Vanhecke, F.; Heremans, K.; *Inorg. Chem.*, **1989**, 28, 2465

[11] Puntoriero, F.; Serroni, S.; Licciardello, A.; Venturi, M.; Juris, A.; Ricevuto, V.; Campagna, S.; *J. Chem. Soc. Dalton Trans.*, (2001), 1035

[12] Hage, R.; Lempers, H. E. B.; Haasnoot, J. G.; Reedijk, J.; Weldon, F. M.; Vos. J. G.; *Inorg. Chem.*, **1997**, 36, 3139

[13] Geren, L.; Hahm, S.; Durham, B.; Millett, F.; *Biochem*, **1991**, 30, 9450

[14] Furniss, B. S.; Hannaford, A. J.; Smith, P. W. G.; Tatchell, A. R.; *Vogel's Textbook of Practical Organic Chemistry*, 5th Ed. , **1989**, Longman Scientific and Technical

[15] Garelli, N.; Vierling, P.; *J. Org. Chem.*, **1992**, 57, 3046

[16] Ogata, Y.; Kawasaki, A.; Sugiura, F.; *Tetrahedron*, **1968**, 24, 5001

[17] Hage, R.; Haasnoot, J. G.; Reedijk, J.; Wang, R.; Vos, J. G.; *Inorg. Chem.*, **1991**, 30, 3263

[18] Steel, P. J.; Constable, E. C.; *J. Chem. Soc. Dalton, Trans.*; **1990**, 1389

[19] Hage, R.; Haasnoot, J.; Nieuwenhuis, H. A.; Reedijk, J.; Wang, R.; Vos, J. G.; *J. Chem. Soc. Dalton Trans.*, **1991**, 3271

[20] Hage, R.; *Ph. D. Thesis*, **1991**, Rijksuniversiteit te Leiden

[21] Keyes, T. E.; O'Connor, C. M.; O'Dwyer, U.; Coates, C. G.; Callaghan, P.; McGarvey, J. J.; Vos, J. G.; *J. Phys. Chem. A*, **1999**, 8915

[22] Fanni, S.; Keyes, T. E.; O'Connor, C. M.; Hughes, H.; Wang, R.; Vos, J. G.; *Coord. Chem. Rev.*, **2000**, 208, 77

[23] Hicks, C.; Ye, G.; Levi, C.; Gonzales, M.; Rutenburg, I.; Fan, J.; Helmy, R.; Kassis, A.; Gafney, H. D.; *Coord. Chem. Rev.*, **2001**, 211, 207

[24] Giordano, P. J.; Bock, C. R.; Wrighton, M. S.; Interrante, L. V.; Williams, R. F. X.; *J. Am. Chem. Soc.*, **1977**, 99, 7612

[25] Nazeeruddin, Md. K.; Zakeeruddin, S. M.; Humphrey-Baker, R.; Kaden, T. A.; Grätzel, M.; *Inorg. Chem.*, **2000**, 39, 4542

[26] O'Connor, C. M; *Ph.D. Thesis*, **1999**, Dublin City University

[27] Thummel, R. P.; Lefoulon F.; Chirayil, S.; *Inorg. Chem.*, **1987**, 26, 3072

[28] Nieuwenhuis, H. A.; Haasnoot, J. G.; Hage, R.; Reedijk, J.; Snoeck, T. L.; Stufkens, D. J.; Vos, J. G.; *Inorg. Chem.*, **1991**, 30, 48

[29] Coates, C. G.; Keyes, T. E.; Hughes, H. P.; Jayaweera, P. M.; McGarvey, J. J.; Vos, J. G.; *J. Phys, Chem. A*, **1998**, 102, 5013

Chapter 5

Ruthenium Pyridyl and Pyrazyl Triazole Complexes as Building Blocks for Supramolecular Systems

5.1 Introduction

Photosystem II is a highly complex system, incorporating a wide range of elements such as quinones, porphyrins and carotenoids. From the initial irradiation of a porphyrin in the antenna to the oxidation of water and to the reduction of CO_2, numerous stepwise electron transfer reactions take place. Each of these is essential to enable the system to function effectively. However, as of yet, no complete understanding of the mechanism of photosynthesis has been found. In order to comprehend the processes well enough to mimic them successfully for our own benefit in a controlled environment, photosynthesis must be broken down into a series of reactions. By studying each of these reactions and preparing suitable models, one may learn more about what is necessary to utilise the concepts for our own good. In this chapter, the synthesis of a series of mimics of PSII shall be discussed. In particular, these compounds should be capable of mimicking the electron transfer from manganese, possibly via tyrosine, to a suitable photosensitiser.

Thus far, only a very small number of either Ru-Mn[1] or Ru-Tyr[2,3] systems have been reported in the literature. Almost all have been based on the well known $[Ru(bpy)_3]^{2+}$ complex. While this appears to be an attractive starting point, due to the widespread knowledge of its electronic and redox properties and the range of known bipyridine derived bridging ligands, it is not without problems. The location of the excited state in $[Ru(bpy)_3]^{2+}$ is not well defined. Photoexcitation could lead to an electron being localised on any of three bpy ligands. This is also the case for complexes containing one modified bpy ligand. As shall be discussed in greater detail in Chapter 6, often

the variation of the group introduced into a bpy ligand does not greatly alter the electronic properties of a complex of the form $[Ru(bpy)_2bpy']^{2+}$. Therefore it is difficult to determine the exact location of the excited state – it may be on any of the ligands. When one wishes to use these ligands as bridging ligands between a donor and acceptor, it is hoped that the excited electron is not located on the bridging ligand. If it is, then recombination occurs before the possibility of electron transfer (*Fig. 5.1*).

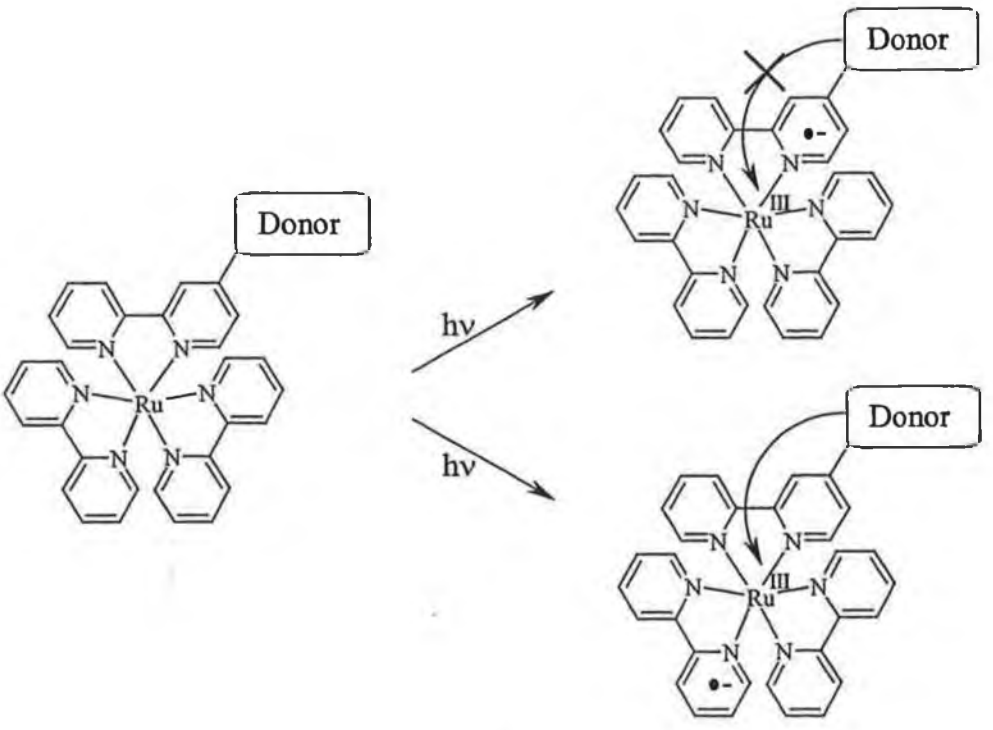

Fig. 5.1 Electron transfer possibilities in from an electron donor to $[Ru(bpy)_3]^{2+}$

In summary, although a variety of dyads based on a $[Ru(bpy)_3]^{2+}$ sensitiser and a manganese complex or tyrosine donor have been prepared and studied (see Section 1.5), none have addressed the problem of the excited state being possibly located on the bridging ligand. With the wide range of ligands and complexes prepared in Chapter 3 and Chapter 4, it should be possible to synthesise a range of dyads or

triads in which the excited state is definitely not located on the bridging ligand. This should help minimise the possibility of recombination prior to electron transfer and reduce the risk of any subsequent back electron transfer.

Each of the complexes bearing terminal synthons is ideally suited for reaction with typical manganese chelating ligands[4,5]. The acid compounds $[Ru(bpy)_2pyAc]^+$ and $[Ru(bpy)_2pzAc]^+$ are obviously suited to the formation of amides. The aldehyde compounds $[Ru(bpy)_2pyAld]^+$, $[Ru(bpy)_2pySal]^+$ and $[Ru(bpy)_2pzSal]^+$ are perfect starting materials for the formation of imine linkages. The phenols $[Ru(bpy)_2pyPhOH]^+$ and $[Ru(bpy)_2pzPhOH]^+$ present themselves as potential substrates for aromatic Mannich reactions[6]. Due to the wide range of manganese chelating ligand systems available (*Fig. 5.2*), it may be possible to prepare a range of Ru-Mn systems in which the manganese is in a variety of chemical environments.

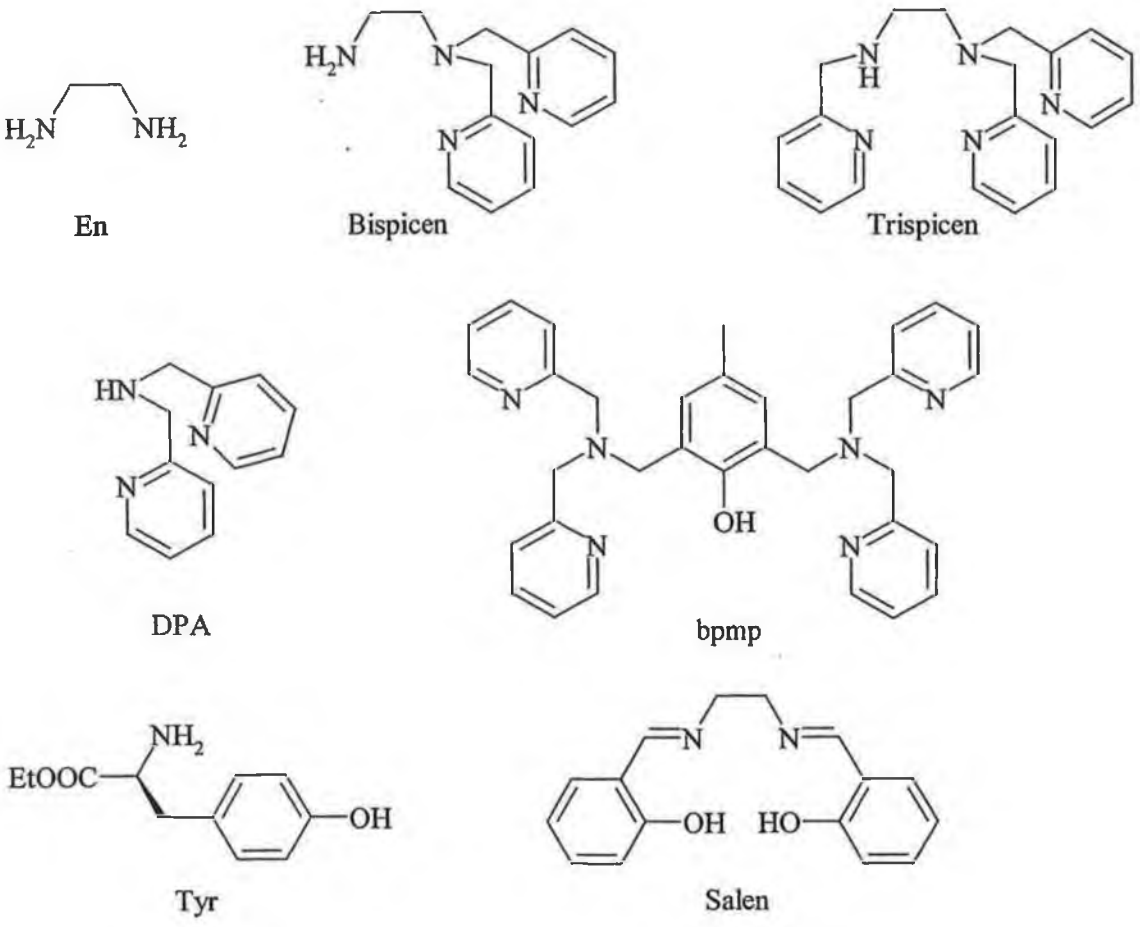

Fig. 5.2 List of ligands and abbreviations cited in this chapter

Using the ligands shown above, it is hoped to be able to prepare a wide range of ruthenium complexes, such as those shown in *Fig. 5.3* overleaf.

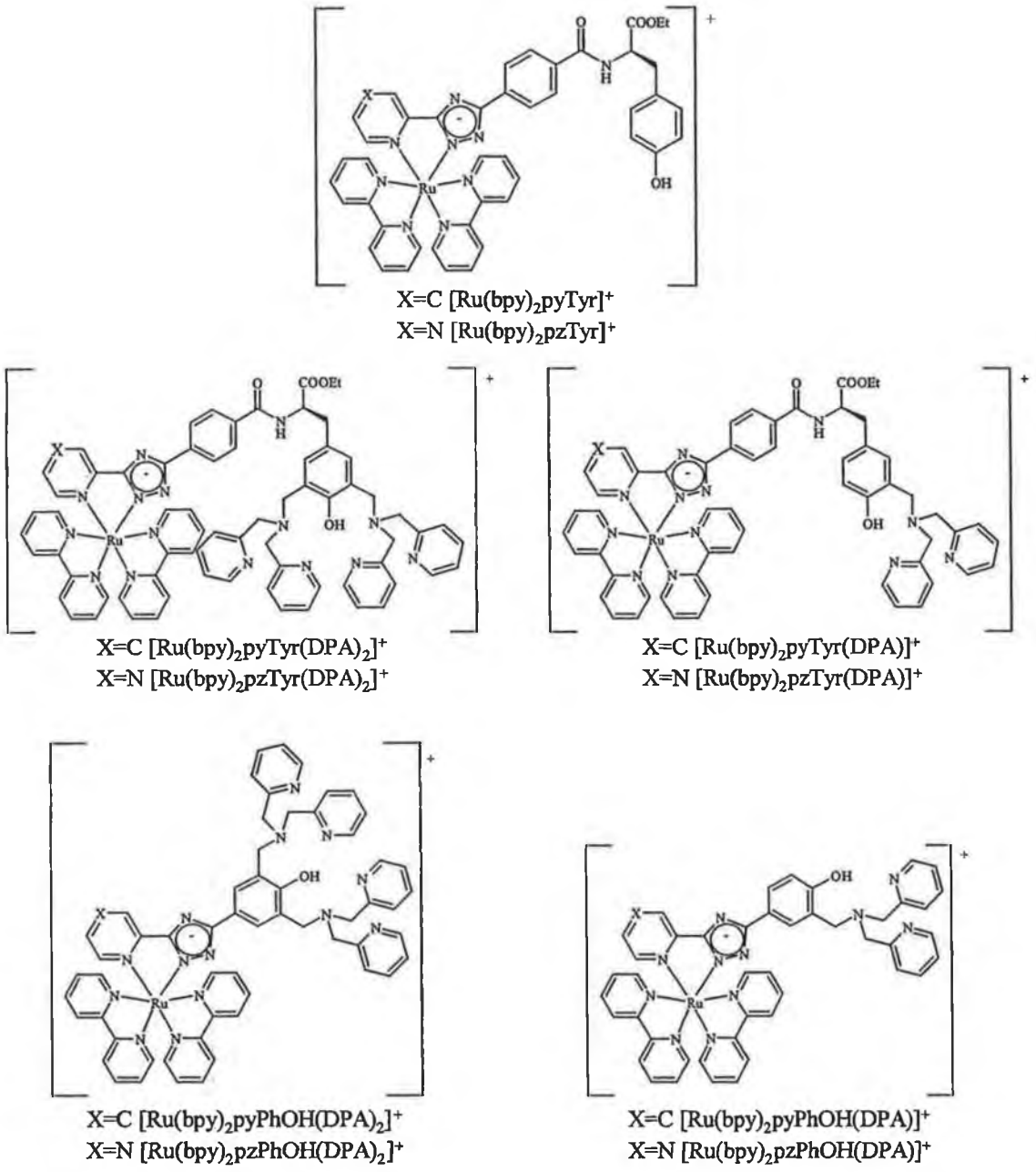

Fig. 5.3 Structures and names of novel ruthenium complexes cited in this chapter

5.2 Synthetic Procedures

[Ru(bpy)$_2$pyTyr](PF$_6$).H$_2$O

600 mg (0.7 mmol) of [Ru(bpy)$_2$pyAc](PF$_6$) were refluxed under argon in 30 cm^3 of thionyl chloride for 3 hours. After the thionyl chloride had been removed, the bright red residue was redissolved in 25 cm^3 of dry dichloromethane. 100 mg of sodium bicarbonate and 190 mg of L-tyrosine ethyl ester hydrochloride were added and the mixture stirred under argon at room temperature overnight. The mixture was subsequently filtered and the solvent removed on the rotary evaporator to yield a bright red solid. This was purified by column chromatography on silica using acetonitrile/water/sat. aq. KNO_3 (80:20:1) as eluent. The acetonitrile was removed under reduced pressure. Addition of a saturated solution of NH_4PF_6 brought about the precipitation of the complex, which was filtered and dried *in vacuo* to yield 600 mg (0.65mmol) 90%

^{1}H NMR (400 MHz, $(CD_3)_2SO$) δ in ppm 9.28 (br, 1H, NH), 8.80 (m, 5H, 4xbpy H3, OH), 8.11 (m, 5H, 4xbpy H4, H3), 8.03 (td, 1H, J_1=6Hz, J_2=1Hz, H4), 7.99 (d, 2H, J=8Hz, H3', H5'), 7.92 (d, 1H, bpy H6), 7.83 (m, 4H, 2xbpyH6, H2', H6'), 7.75 (t, 1H, bpy H6), 7.57 (m, 4H, 3xbpy H5, H6), 7.50 (t, 1H, bpy H5), 7.33 (td, 1H, J_1=6Hz, J_2=1Hz, H5), 7.12 (d, 2H, J=8Hz, Tyr Ar CH), 6.69 (d, 2H, J=8Hz, Tyr Ar CH), 4.57 (m, 1H, C*H*COOEt), 4.12 (q, 2H, J=7Hz, C*H*$_2$CH$_3$), 3.05 (m, 2H, C*H*$_2$Ph), 1.18 (t, 3H, J=7Hz, CH$_2$C*H*$_3$)

Elemental Analysis for $C_{45}H_{40}N_9O_5RuPF_6$: Calc: C 52.32, H 3.90, N 12.20, Found: C 52.26, H 3.87, N 11.99

[Ru(bpy)$_2$pzTyr](PF$_6$).2H$_2$O

200 mg (0.23 mmol) of [Ru(bpy)$_2$pzAc](PF$_6$) were refluxed under argon in 10 cm^3 of thionyl chloride for 3 hours. After the thionyl chloride had been removed, the bright red residue was redissolved in 10 cm^3 of dry dichloromethane. 35 mg of sodium bicarbonate and 65 mg of L-tyrosine ethyl ester hydrochloride were added and the mixture stirred under argon at room temperature overnight. The mixture was subsequently filtered and the solvent removed on the rotary evaporator to yield a bright red solid. This was purified by column chromatography on silica using acetonitrile/water/sat. aq. KNO_3 (80:20:1) as eluent. The acetonitrile was removed under reduced pressure. Addition of a saturated solution of NH_4PF_6 brought about the precipitation of the complex, which was filtered and dried *in vacuo* to yield 140 mg (0.15 mmol) 63%

^{1}H NMR (400 MHz, $(CD_3)_2SO$) δ in ppm 9.27 (s, 1H, H3), 9.22 (br, 1H, NH), 8.78 (m, 5H, 4xbpy H3, OH), 8.39 (d, 1H, J=3Hz, H6), 8.09 (m, 4H, 4xbpy H4), 7.95 (m, 3H, H3', H5', bpy H6), 7.77 (m, 4H, H2', H6', 2xbpy H6), 7.68 (d, 1H, J=3Hz, H5), 7.50 (m, 5H, bpy H6, 4xbpy H5), 7.07 (d, 2H, J=8Hz, Tyr Ar CH), 6.64 (d, 2H, J=8Hz, Tyr Ar CH), 4.73 (m, 1H, C*H*COOEt), 4.14 (q, 2H, J=7Hz, C*H*$_2$CH$_3$), 2.99 (m, 2H, C*H*$_2$Ph), 1.21 (t, 3H, J=7Hz, CH$_2$C*H*$_3$)

Elemental Analysis for $C_{44}H_{41}N_{10}O_6RuPF_6$: Calc: C 50.24, H 3.93, N 13.32, Found: C 50.35, H 3.84, N 12.67

N,N Di(2-picolyly)amine.3HCl[7]

To a stirred solution of 4.3 g (0.04 mol) of pyridine-2-carboxaldehyde dissolved in 20 cm^3 of dry methanol, 4.3 g (0.04 mol) of 2(aminomethyl)-pyridine were added dropwise. 5 g of sodium borohydride were added to the reaction mixture in small portions over 45 minutes, while maintaining the temperature at 0-4°C. After stirring for 3 hours at room temperature, the mixture was filtered. The filtrate was cooled in ice and the pH of the solution lowered to pH 1 with concentrated HCl (highly exothermic reaction!). The suspension was filtered once more. 120 cm^3 of ethanol and 40 cm^3 of diethyl ether were added and the solid left to precipitate out at room temperature for 3 days to yield 8.94 g (0.029 mol) 72%. (The free base, which turned black over long periods, was prepared as required by dissolving the salt in alkaline water and extracting into chloroform)

^{1}H NMR (400 MHz, ($CDCl_3$)) δ in ppm 8.51 (d, 2H, 2xH6), 7.60 (t, 2H, 2xH4), 7.31 (d, 2H, 2xH3), 7.10 (t, 2H, 2xH5), 2.55 (s, 4H, 2xCH_2)

[Ru(bpy)$_2$pyPhOH(DPA)$_2$](PF$_6$)

A solution containing 250 mg (0.31 mmol) of [Ru(bpy)$_2$pyPhOH](PF$_6$), 230 mg (3.7 eq.) of DPA and 37 mg (3.9 eq.) of paraformaldehyde in 10 cm^3 of ethanol/water (7:3) and one drop of conc. acetic acid was heated at reflux for 4 days. After this time a dark red oil had separated from the rest of the solution. After cooling to room temperature, the mixture was partitioned between dichloromethane and water. The organic layer was washed with dil. aq. $NaHCO_3$ and evaporated to dryness *in vacuo*. This red solid was purified first by column chromatography on silica

(MeCN/H_2O/sat. aq. KNO_3 – 80:20:1). The main fraction was reduced in volume to ~10 cm^3 *in vacuo* and reprecipitated by the addition of aq. NH_4PF_6. This precipitate was recrystalised twice from acetone/toluene (1:1). The glassy solid obtained, containing both mono- and disubstituted products, was then purified further by repeated size exclusion chromatography using a 30 cm long Sephadex LH-20 column, with methanol as eluent. After removal of the solvent, the red solid was redissolved in dichloromethane, washed with dil. aq. $NaHCO_3$ and evaporated to dryness *in vacuo* to yield 80 mg (26%) of the monosubstituted complex $[Ru(bpy)_2pyPhOH(DPA)](PF_6)$. No significant quantity of the disubstituted complex was obtained.

^1H NMR (400 MHz, $((CD_3)_2CO)$) δ in ppm 8.61 (m, 2H, 2xbpy H3), 8.50 (m, 2H, 2xbpy H3), 8.38 (d, 2H, 2xPy H), 7.85 (m, 11H, 4xbpy H4, 3xbpy H6, H3, H4, H3', H5'), 7.65 (d, 1H, bpy H6), 7.58 (td, 2H, 2xPy H), 7.53 (d, 1H, H6), 7.40 (m, 4H, 3xbpy H5, Py H), 7.26 (m, 2H, 2xPy H), 7.06 (m, 3H, Py H, bpy H5, H5), 6.84 (d, 1H, J=8Hz, H6'), 3.67 (s, 2H, PhCH_2N), 3.71 (s, 4H, CH_2Py)

MS (EI) m/z 862 $(M\text{-}PF_6)^+$, 663 $(M\text{-}PF_6\text{-}DPA)^+$

[Ru(bpy)$_2$pzPhOH(DPA)$_2$](PF$_6$)

A solution containing 180 mg (0.22 mmol) of $[Ru(bpy)_2pzPhOH](PF_6)$, 170 mg (3.8 eq.) of DPA and 28 mg (4.2 eq.) of paraformaldehyde in 10 cm^3 of ethanol/water (7:3) and one drop of conc. acetic acid was heated at reflux for 4 days. After this time a dark red oil had separated from the rest of the solution. After cooling to room temperature, the mixture was partitioned between dichloromethane and water. The

organic layer was washed with dil. aq. $NaHCO_3$ and evaporated to dryness *in vacuo*. This was recrystalised twice from acetone/toluene (1:1). The glassy solid obtained, containing both mono- and disubstituted products, was then purified further by repeated size exclusion chromatography using a 30 cm long Sephadex LH-20 column, with methanol as eluent. After removal of the solvent, the red solid was redissolved in dichloromethane, washed with dil. aq. $NaHCO_3$ and evaporated to dryness *in vacuo* to yield 90 mg (41%) of the monosubstituted complex $[Ru(bpy)_2pzPhOH(DPA)](PF_6)$. Approximately 15 mg of the desired disubstituted complex, still impure, was also obtained.

^1H NMR (400 MHz, $((CD_3)_2CO)$) δ in ppm 9.23 (d, 1H, J=1Hz, H3), 8.76 (t, 2H, 2xbpy H3), 8.67 (t, 2H, 2xbpy H3), 8.55 (d, 2H, 2xPy H), 8.49 (d, 1H, Py H), 8.29 (d, 1H, J=3Hz, H6), 8.11 (m, 7H, H3', 4xbpy H4, H5', bpy H6), 7.83 (m, 3H, 2xbpy H6, Py H), 7.74 (m, 2H, bpy H6, H5), 7.56 (m, 2H, 2xbpy H5), 7.50 (m, 2H, 2xbpy H5), 7.41 (d, 2H, 2xPy H), 7.25 (m, 2H, 2xPy H), 6.78 (d, 1H, J=8Hz, H6'), 3.85 (m, 4H, CH_2Py), 3.80 (s, 2H, $PhCH_2N$)

MS (EI) Monosubstituted Complex m/z 863 $(M\text{-}PF_6)^+$, 664 $(M\text{-}PF_6\text{-}DPA)^+$

Disubstituted Complex m/z 1073 $(M\text{-}PF_6)^+$, 875 $(M\text{-}PF_6\text{-}DPA)^+$, 677 $(M\text{-}PF_6\text{-}2DPA)^+$

[Ru(bpy)$_2$pyTyr(DPA)$_2$](PF$_6$)

A solution containing 250 mg (0.31 mmol) of $[Ru(bpy)_2pyTyr](PF_6)$, 230 mg (3.7 eq.) of DPA and 37 mg (3.9 eq.) of paraformaldehyde in 10 cm^3 of ethanol/water (7:3) and one drop of conc. acetic acid was heated at reflux for 4 days. After this

time a dark red oil had separated from the rest of the solution. After cooling to room temperature, the mixture was partitioned between dichloromethane and water. The organic layer was washed with dil. aq. $NaHCO_3$ and evaporated to dryness *in vacuo*. This red solid was purified by column chromatography on silica, firstly using $MeCN/H_2O$/sat. aq. KNO_3 (80:20:1) to remove any unreacted $[Ru(bpy)_2pyTyr]^{2+}$. The column was then washed with $MeCN/H_2O$/2M CH_3COOH (80:20:5). Subsequently, a red band was eluted using $MeCN/H_2O$/sat. aq. K_2CO_3 (70:30:10). This fraction was reduced in volume to ~10cm^3 *in vacuo* and reprecipitated by the addition of aq. NH_4PF_6. This precipitate was recrystalised from acetone/toluene (1:1). The red solid obtained was redissolved in dichloromethane, washed with dil. aq. $NaHCO_3$ and evaporated to dryness *in vacuo* to yield 80 mg (26%) which appeared to contain both mono- and disubstituted products.

MS (FAB+) m/z 1438 $(M+H)^+$, 1292 $(M-PF_6)^+$

5.3 Results and Discussion

5.3.1 Synthesis

The idea of the treatment of metal complexes as organic compounds is a well-known concept. It is used frequently in the preparation of large supramolecular systems such as dendrimers[8]. Here too, it was decided to employ this concept in the preparation of these larger, potential Ru-Mn precursors. In this section it was decided to investigate the feasibility of subjecting pyridyl or pyrazyl triazole complexes to a variety of common organic synthetic procedures. Adopting this strategy was made even more tantalising by the fact that it would appear to make the synthesis of Ru-Mn systems less complicated (see *Fig. 5.4 overleaf*).

Should one prepare a bridging ligand with two or more different free coordination sites (in *Fig. 5.4* - green), a wide range of isomers would be formed upon the introduction of the first metal centre (Ru)(in *Fig. 5.*4 - red). This would result in a range of complexes in which the ruthenium is in a variety of different chemical environments. A lengthy purification process would be necessary, leading to the loss of valuable ruthenium. By preparing a suitable ruthenium complex, with no free binding sites, a pure sample may be obtained by standard chromatographic means. Introduction of new binding sites into the complex, by whatever means necessary, would remove the possibility of the formation of isomers. This is a more time efficient and less costly approach.

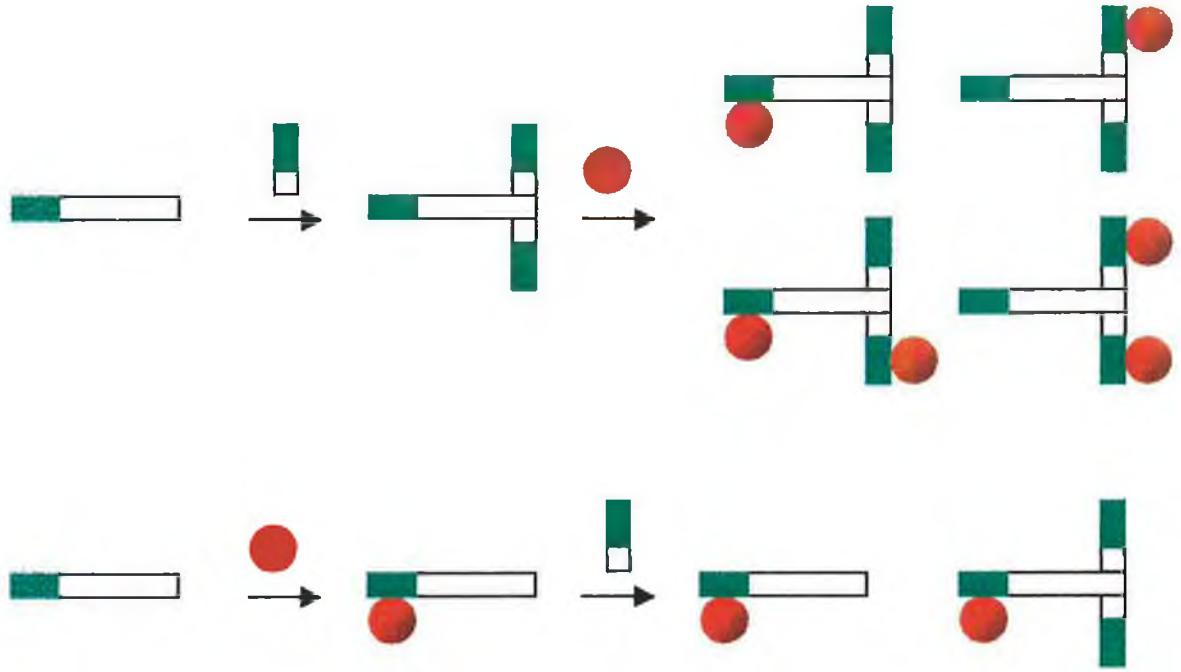

Fig. 5.4 Possible routes to the synthesis of metal complexes containing free coordination sites

The range of complexes prepared in previous chapters are ideal starting complexes for the synthesis of larger supramolecular systems as they contain suitable synthons for the introduction of new binding sites into the complex, while having the desired properties of a ruthenium pyridyl or pyrazyl triazole complex.

The first modified complexes prepared were the two tyrosine containing complexes $[Ru(bpy)_2pyTyr](PF_6)$ and $[Ru(bpy)_2pzTyr](PF_6)$ (See *Fig. 5.3*). These were assumed to be the most straightforward complexes to prepare and purify, as they required simply the formation of an amide linkage between tyrosine ethyl ester and the relevant acid complex, $[Ru(bpy)_2pyAc]^{2+}$ or $[Ru(bpy)_2pzAc]^{2+}$. Initial attempts to introduce this linkage were unsuccessful. The mild method chosen for the reaction

was the use of DCC as a coupling agent[9]. No tyrosine containing complexes were obtained and the unreacted DCC proved to be difficult to remove by chromatographic means. It was then decided to proceed via the acid chloride, as reported by Magnuson *et al.*[10] This was found to function well, with high yields obtained (See Section 5.2.1). HPLC analysis indicated >95% conversion to the amide. Separation of the amide complexes the unreacted acid complexes was straightforward, using the same procedure on silica as used for the purification of many of the precursor complexes in Chapters 3 and 4. Excellent separation was obtained between the two complexes and satisfactory elemental analysis of the tyrosine containing complexes was obtained.

Having shown that ruthenium complexes containing triazolate ligands are sufficiently robust to undergo a straightforward amide coupling, it was decided to venture into the area of elongation of the bridging ligand to incorporate new coordination sites. The introduction of DPA (dipicolylamine) arms into complexes *via* a Mannich reaction was investigated. Mannich reactions are common in organic chemistry[11]. They provide a simple, effective route to the aminomethylation of compounds containing an active hydrogen.

The presence of either an acid or base may catalyse Mannich reactions. The method used here is the acid catalysed method. As can be seen from the proposed reaction mechanism (*Fig.5.5*)[12], the reaction proceeds in two steps. The initial process involves the acid catalysed formation of the imine from formaldehyde and the amine being introduced (DPA in this case). The electrophilic carbon attacks at the site of the active hydrogen, forming a new C-C bond, with the loss of a proton to the acidic

solution. This gives the new tertiary amine shown, which may subsequently react further to form the disubstituted product.

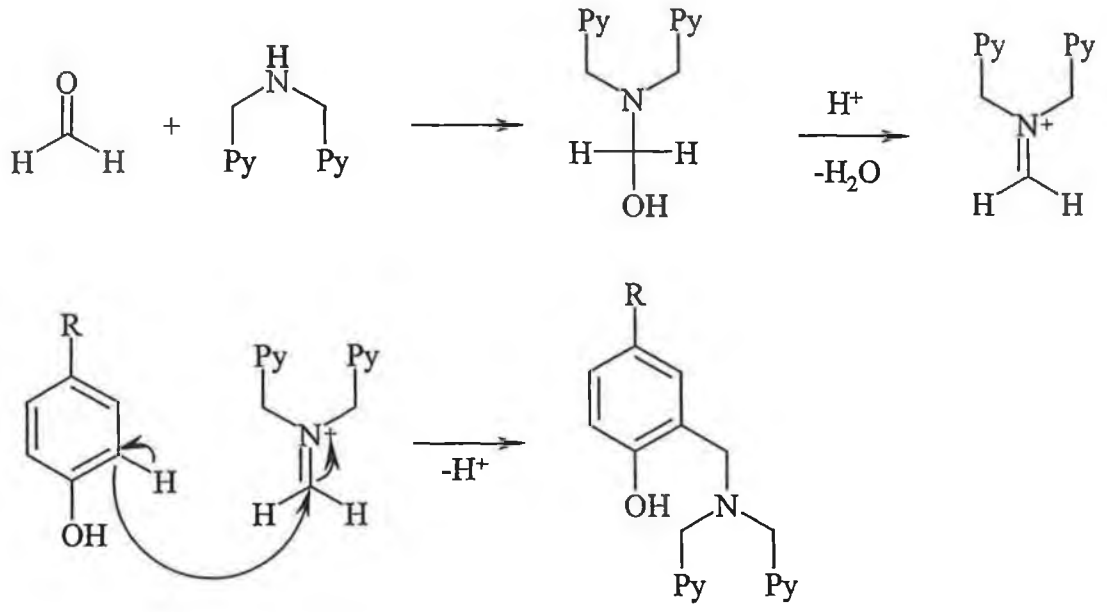

Fig. 5.5 Proposed reaction mechanism for Mannich reaction[12]

As well as many monosubstituted phenols, a wide range of both symmetrically and asymmetrically disubstituted phenols have been prepared by means of this reaction[13,14]. This one pot reaction is far more economical than the traditional method for aminomethylation of phenols, i.e. formylation, reduction to the alcohol, substitution of the benzylic hydroxyl groups for a chlorine, followed by substitution of this chloride by an amine.

In the investigation of the reaction of the suitable ruthenium complexes prepared earlier, it was decided to try to prepare the disubstituted compound, using DPA as the amine. By introducing two DPA arms into a phenolic complex, a 2,6-bis[bis(2-methylpyridyl)aminomethyl]-4-methylphenol system could be obtained. The ligand, commonly abbreviated to bpmp, is a highly versatile chelating moiety. It is capable

of forming a wide range of dinuclear complexes with metals such as copper, iron or manganese (see *Fig. 5.6* below)[15]. The presence of the phenol facilitates the formation of a bridging μ-oxo between the metal centres[16]. It should be noted that EPR studies on the manganese cluster in PSII indicate the presence of μ-oxo bridges between the metal centres[17]. Another interesting feature in these bpmp complexes is the presence of two free binding sites on each of the coordinated metals. These are often taken up by bridging acetate ligands, thus increasing the interaction between the metals, but they may be replaced with other ligands if necessary[18].

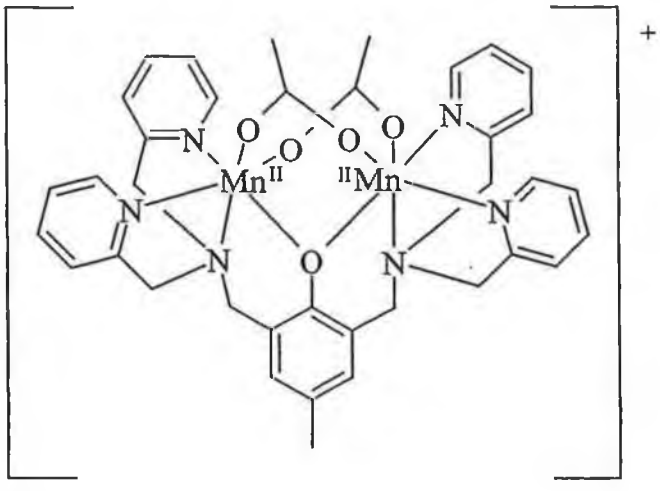

Fig. 5.6 Structure of [(bpmp)$Mn_2(OAc)_2$]$^+$

Initial attempts at the aminomethylation of [Ru(bpy)$_2$pyTyr](PF$_6$) were carried out under the supervision of Prof. B. Åkkermark and Dr. L. Sun in the KTH Stockholm, using a method previously used to carry out this transformation on a [Ru(bpy)$_3$]$^{2+}$ derivative[19]. Although the reaction itself is straightforward to carry out, it was not possible to monitor the progress of the reaction well. HPLC analysis was not possible, as the aminomethylated complexes did not elute from the cation exchange

column, even at high salt concentrations. Similarly, while TLC showed the presence of any unreacted tyrosine containing complex, it said nothing about the degree of substitution. All substituted complexes remained on the baseline, even under drastic (strongly acidic/basic) conditions. However, after 4 days, consumption of $[Ru(bpy)_2pyTyr](PF_6)$ appeared to have ceased. At this stage a dark oil had formed in the reaction mixture. Column chromatography proved extremely difficult to perform. Unreacted $[Ru(bpy)_2pyTyr](PF_6)$ was easily removed using the usual eluent of MeCN/Water/Sat. aq. KNO_3 (80/20/1). However, none of the modified complex could be obtained by this method. By washing the column with acidified aqueous acetonitrile and subsequently with basicified aqueous acetonitrile, an ion exchange column of sorts was prepared[19]. This removed most of the substituted complex from the silica, but did not separate the mono- and disubstituted isomers. Recrystalisation from acetone/toluene removed any traces of unreacted DPA, but did not appear to improve the ratio of monosubstituted : disubtituted complexes. Attempts to carry out this reaction on the pyrazine equivalent, $[Ru(bpy)_2pzTyr](PF_6)$ were unsuccessful. It proved to be almost impossible to remove the complex from silica, even by the method described above. A small amount of an impure compound in a yield of ~5% was obtained. Attempts to purify the complexes by size exclusion chromatography, using Sephadex LH-20[20], proved highly inefficient. Due to the large size of these compounds, the size difference between $[Ru(bpy)_2pyTyr]^+$, $[Ru(bpy)_2pyTyr(DPA)]^+$ and $[Ru(bpy)_2pyTyr(DPA)_2]^+$ was not sufficient to bring about satisfactory separation. Although no clean NMR spectra of $[Ru(bpy)_2pyTyr(DPA)_2]^+$ were obtained, its presence was confirmed by mass spectrometry. A sample of this impure complex was investigated as a possible precursor to a Ru-Mn trimer (Section 5.3.3).

It was hope that it may be possible to separate the different isomers after complexation with manganese, due to their different charges.

While the purification of the substituted tyrosine derivatives $[Ru(bpy)2pyTyr(DPA)_x](PF_6)$ (x=1,2) was extremely taxing, the preparation of the derivatives of $[Ru(bpy)_2pyPhOH](PF_6)$ and $[Ru(bpy)_2pzPhOH](PF_6)$ (See *Fig. 5.3*) was more rewarding. Initial attempts to purify the complexes by column chromatography on silica did improve the purity of the product, by removing starting reagents, but again did not separate the mono and disubstituted products. It was decided to reinvestigate the use of LH-20 as a means of purification. Due to the smaller size of the complexes, it was hoped that the presence of one or two DPA arms would result in a sufficient size difference in order for the isomers to be separated by size exclusion chromatography. This was found to be the case. Although the separation of the complexes was not very well resolved, by repeatedly columning very small quantities (<10mg) of the complex, small amounts of relatively clean products were obtainable.

Interestingly, in the case of both $[Ru(bpy)_2pyPhOH]^+$ and $[Ru(bpy)_2pzPhOH]^+$, the main product of the reaction was the monosubstituted isomer, of the form $[Ru(bpy)_2XPhOH(DPA)](PF_6)$ (X=py, pz). Comparatively small amounts of the disubstituted isomers were isolated. It is not though that the presence of the triazolate would decrease the rate of the Mannich reaction. The lack of formation of the disubstituted complex is most likely due to steric effects. For the tyrosine containing complexes, the phenol is not hindered in its rotation. However, the complexes based on pyPhOH and pzPhOH are much shorter. As a result, the DPA arms may interact

with the bpy ligands upon rotation of the phenol. Higher yields of the disubstituted complexes may be obtainable through still longer reaction times with even higher concentrations of formaldehyde and DPA. This theory has yet to be investigated.

Having demonstrated the usefulness of the phenol and acid complexes prepared earlier, attention was turned to the complexes containing terminal aldehydes. Reductive amination of these complexes could introduce a variety of potential manganese chelating ligands[21]. A preliminary investigation of the reaction between $[Ru(bpy)_2pyAld](PF_6)$ and trispicen[22] (*Fig. 5.2*) in acidic methanol in the presence of $NaBH_3CN$ showed no reaction. A similar reaction between $[Ru(bpy)_2pySal](PF_6)$ and bispicen[21] (*Fig. 5.2*) was also attempted. It was hoped that this reaction would lead to a system (*Fig. 5.7*) capable of producing a manganese core similar to the well-defined structure, previously used as an electron donor to a photooxidised ruthenium centre[23]. Unfortunately this too failed to produce any of the desired complex.

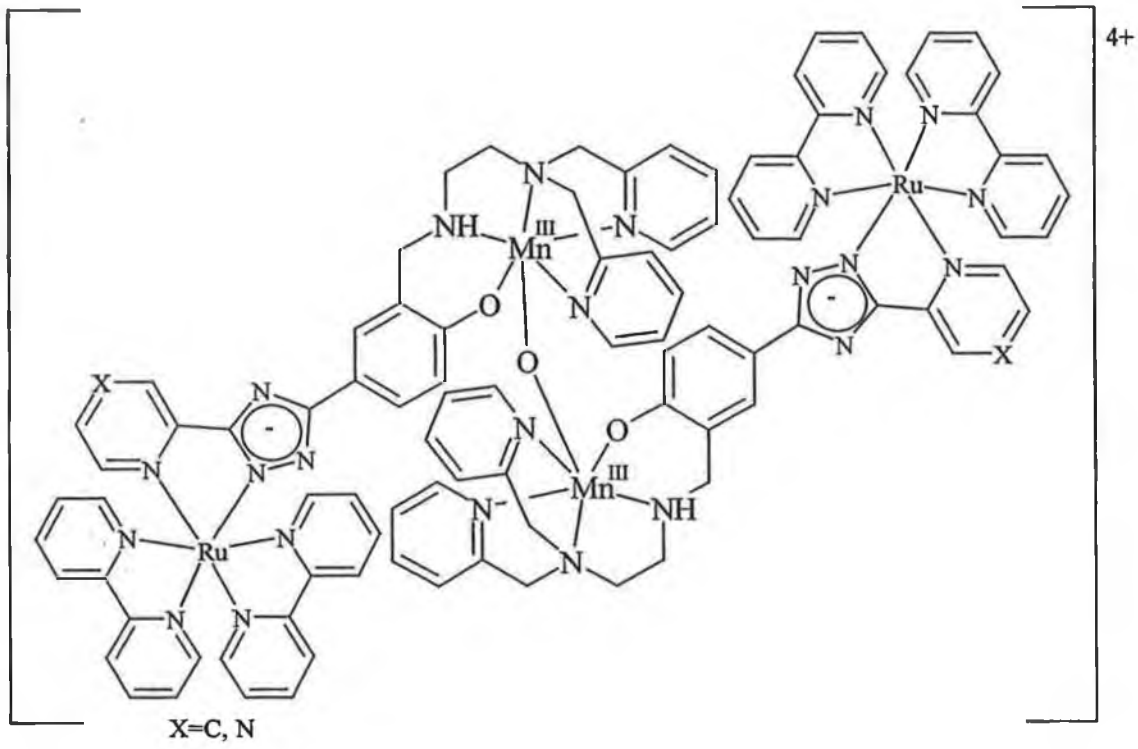

Fig. 5.7 Desired Ru-Mn system from the reaction of $[Ru(bpy)_2pySal]^+$ with bispicen

Using $[Ru(bpy)_2pzSal](PF_6)$, the preparation of a salen-like compound was attempted. Complexes of salen are widely used in a variety of catalytic cycles[24]. Salen derivatives are often prepared by heating a salicylaldehyde derivative and a suitable diamine in ethanol or acetonitrile[25], or by means of a Mannich reaction[26]. In this case, the ruthenium complex served as the aldehyde. This was treated with 0.5 equivalents of en in boiling methanol. The reaction was also attempted in ethanol and acetonitrile. None of these solvents gave substantial amounts of the desired compound. However, size exclusion chromatography of the reaction mixture did indicate the presence of two species of significantly different size, one of which was larger than the original ruthenium complex.

From these investigations into the use of ruthenium complexes bearing terminal aldehydes as precursors to Ru-Mn systems, one can conclude that the aldehyde is significantly deactivated towards nucleophilic attack. This is most likely due to the proximity of the triazolate. As a result, normal methods for the formation of imines do not function well. Other approaches to aid their formation must yet be attempted. Titanium complexes, such as $TiCl_4$[27] or $Ti(OiPr)_4$[28], have displayed catalytic ability in the formation and stabilisation of imines and their use in these reactions should be investigated.

5.3.2 NMR Spectroscopy

^1H NMR spectroscopy was of major importance in the synthesis of the Tyr complexes ($[Ru(bpy)_2pyTyr](PF_6)$, $[Ru(bpy)_2pzTyr](PF_6)$). The introduction of the amide linkages resulted in two distinct doublets for the aromatic protons of Tyr. At ~7.1 and ~6.6 ppm, these did not overlap with any other signals, and so give a good indication of the purity of the complex. A multiplet was obtained for each of the two signals for the CH and CH_2 of the Tyr. The ester group, protecting the carboxylic acid of Tyr, was clearly visible, showing clean splitting of the signals for the CH_2 and CH_3. The presence of an amide linkage and not an ester linkage, via the phenolic oxygen, was confirmed by NMR. One NH signal and one OH signal were found in the aromatic region, confirmed by D_2O exchange and assigned by comparison with a similar complex[10]. Had the ester been formed, then a signal with an integral of two, corresponding to an NH_2 would have been observed.

Due to the lack of a suitable solvent system for TLC and HPLC analysis, ^{1}H NMR spectroscopy was found to be the only method to examine the purity of the extended complexes containing DPA. This added to the cumbersome nature of their purification. The presence of both pyridines and a phenol in close proximity caused problems in the NMR. The complexes were found to be extremely pH sensitive, with signals shifting greatly, or even doubling, depending on water content and pH. In an effort to minimise this problem, all samples were washed with an aqueous solution of sodium bicarbonate, extracted into dichloromethane and evaporated to dryness prior to measurement. This resulted in much cleaner spectra, with only one signal for each proton.

A indication of the degree of substitution of the complexes was found by examining the region 6.5 - 7.5 ppm. Asymmetric complexes (monosubstituted) lose their symmetry and typically produce a doublet with an integral of 1 at ~6.8 ppm. Disubstituted complexes should result in the formation of a singlet with an integral of 2.

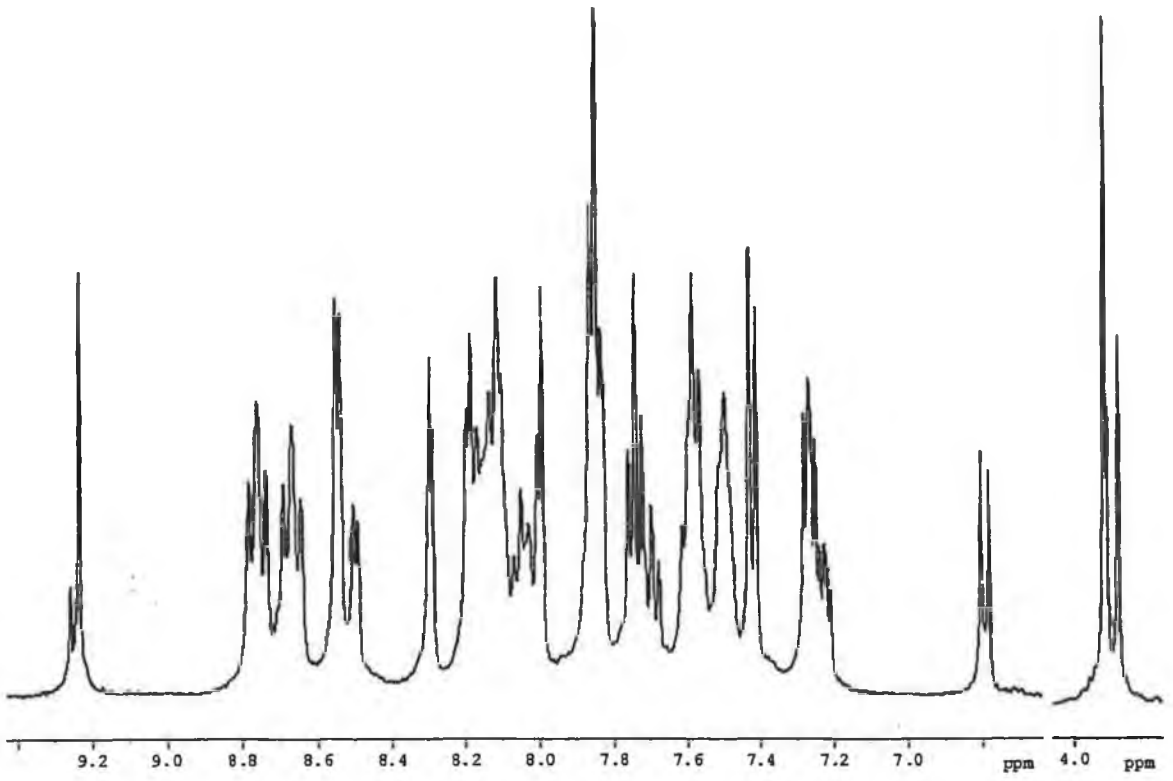

Fig. 5.8 ^1H NMR spectrum of $[Ru(bpy)_2pzPhOH(DPA)](PF_6)$ in d_6-acetone

Assignment of the protons has only been tentatively carried out. As the compounds are still not totally pure, it is difficult to be absolutely sure as to the positions of the protons. The possibility of the presence of impurities interferes with integration, and comparison with other spectra is also problematic as slight changes in the moisture content of the sample or solvent result in different spectra. This is probably due to the degree of hydrogen bonding between the phenol and the pyridines[19], which will vary according to the water content and pH. However, despite this, the ^1H NMR spectrum of $[Ru(bpy)_2pzPhOH(DPA)](PF_6)$, shown in *Fig. 5.8* above, gives an indication of the sort of spectra obtainable for these compounds. The purity of this complex may be estimated from the signal for H3 of the pyrazine at ~9.2 ppm. The reason for the small adjacent peak is not clear, it is possibly some disubstituted

impurity or perhaps a pH problem. Despite repeated recrystalisation and repeated chromatographic separations, this peak remains present.

5.3.3 A Ruthenium-Tyrosine-Manganese Triad

In this section, the preparation and characterisation of a Ru-Tyr-Mn_2 system (*Fig. 5.9*) shall be described. As previously mentioned, $[Ru(bpy)_2pyTyr(DPA)_2](PF_6)$ was prepared by a Mannich reaction on $[Ru(bpy)_2pyTyr](PF_6)$. Unfortunately, purification proved to be extremely taxing, yielding an impure mixture containing roughly equal amounts of both the mono- and disubstituted complexes. It was thought that by complexing manganese with this impure compound, it may be possible to isolate the subsequent Ru-Tyr-Mn_2 and Ru-Tyr-Mn complexes. The work presented in this section was carried out by Sebastien Blanchard under the supervision of Prof. J. J. Girerd in Paris.

Introduction of manganese into the impure complex containing DPA arms ($[Ru(bpy)_2pyTyr(DPA)_2](PF_6)$) was quite straightforward. Treatment of the complex with manganese (II) acetate in an alcoholic solution for a short period of time[29] yielded the desired compound, which was precipitated out by the addition of aq. NH_4PF_6 and filtered off.

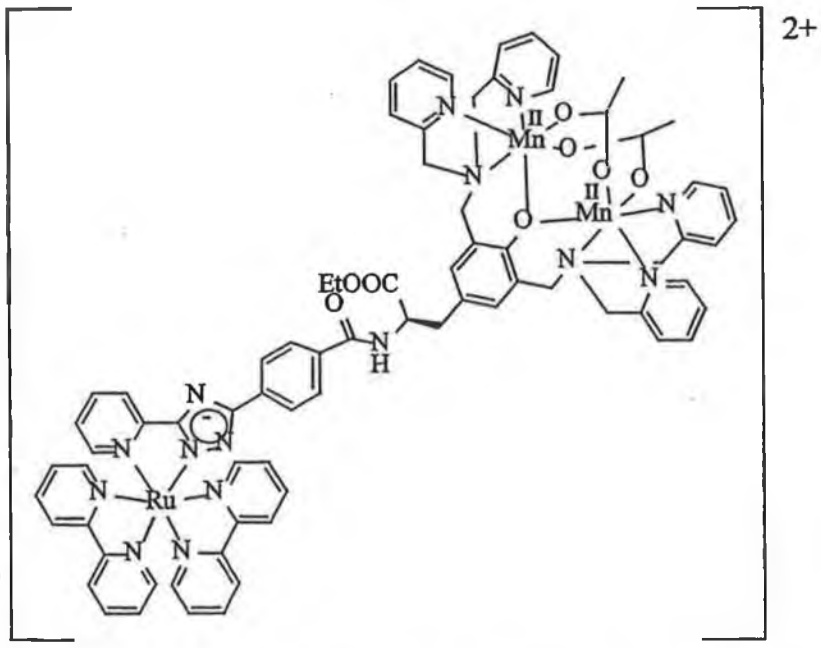

Fig. 5.9 Structure of the desired [Ru-Tyr-Mn_2]$^{2+}$ complex

The complex (*Fig. 5.9*) obtained as outlined above was characterised by mass spectrometry, EPR spectroscopy and magnetic susceptibility measurements. Mass spectrometry showed the presence of the desired [Ru-Tyr-Mn_2]$^{2+}$ species at m/z = 760 (mass of [Ru-Tyr-Mn_2]$^{2+}$ = 1519.4 gmol^{-1}). In order to simplify its characterisation, a model complex - [(bpmp)Mn_2(OAc)$_2$]$^+$ (*Fig. 5.6*), was prepared and characterised.

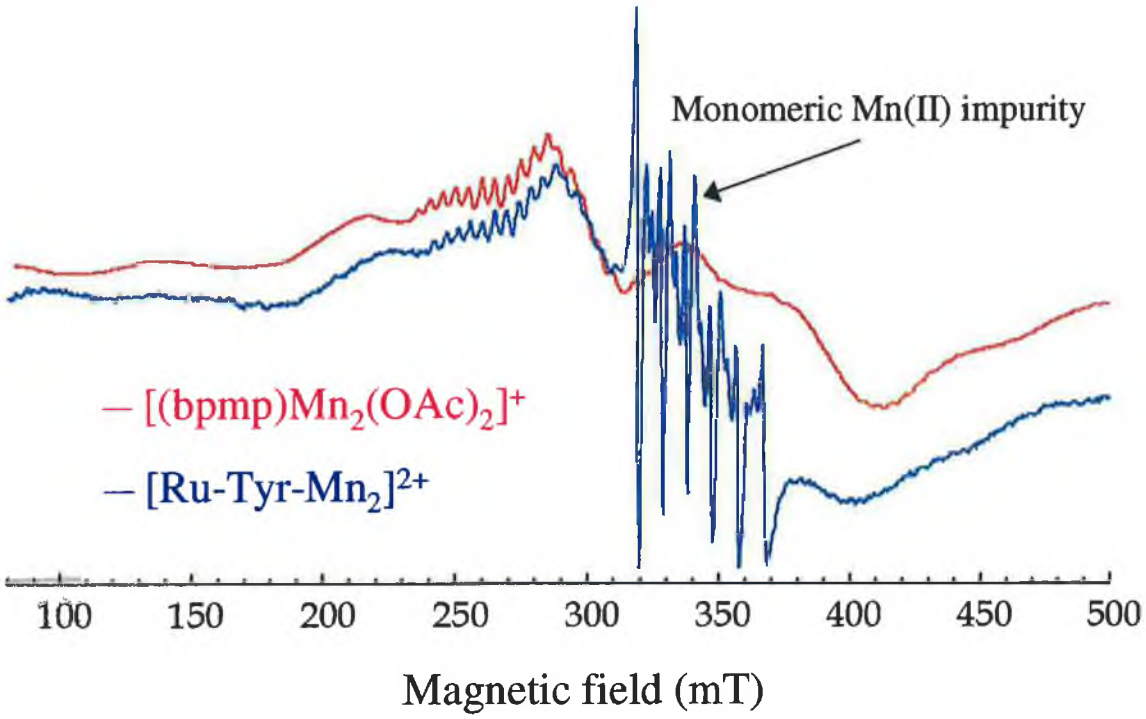

Fig. 5.10 X-Band EPR spectra of $[Ru\text{-}Tyr\text{-}Mn_2]^{2+}$ and $[(bpmp)Mn_2(OAc)_2]^{+}$ at 100K in acetonitrile, irradiated at 9.42GHz

EPR is a very sensitive probe of the magnetic environment of the electronic spin of a molecule (just as the chemical shift in NMR is sensitive to the surrounding of the nuclear spin). Therefore, if the manganese centres are in the same chemical environment in the two complexes, one would expect similar spectra. In the case shown in *Fig. 5.10* above, it can be seen that the impure $[Ru\text{-}Tyr\text{-}Mn_2]^{2+}$ gives two overlapping signals. The broad band is due to the Mn_2 compound (similar to $[(bpmp)Mn_2(OAc)_2]^{+}$), whilst the sharp hyperfine lines (at 300-350 mT) are due to the Mn_1 complex of $[Ru(bpy)_2pyTyr(DPA)](PF_6)$. The broad band is typical of a coupled Mn(II) dimer, in which the electronic spins of each Mn (S=5/2) are interacting to give rise to a unique spin system. The hyperfine structure that can be seen between 250 and 300 mT is due to the interaction of this electronic spin with the nuclear spin (I=5/2) of two identical Mn(II) atoms.

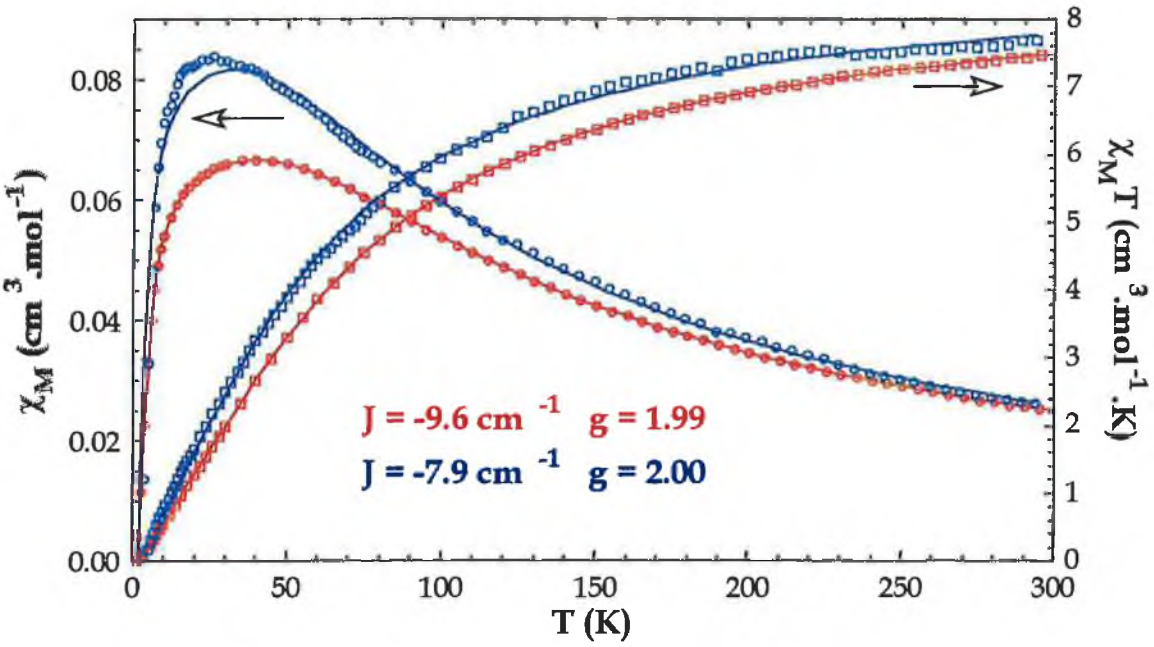

Fig. 5.11 Magnetic susceptibility measurements for [Ru-Tyr-Mn_2]$^{2+}$ (blue) and [(bpmp)$Mn_2(OAc)_2$]$^+$ (red)

Magnetic susceptibility measurements on the model complex and [Ru-Tyr-Mn_2]$^{2+}$ indicate antiferromagnetic (i.e. antiparallel spins in the fundamental state) behaviour, indicated by the decreasing values of $\chi_M T$. J values of –9.6 cm^{-1} and –7.9 cm^{-1} indicate quite a strong degree of interaction between the manganese centres. This is typical of oxo and acetate bridged metal centres[30,31]. Again it should be noted that the values obtained for [Ru-Tyr-Mn_2]$^{2+}$ closely match those obtained for the model complex [(bpmp)$Mn_2(OAc)_2$]$^+$. This is an good indication that the di-manganese complex has been formed and is of the same structure as the known [(bpmp)$Mn_2(OAc)_2$]$^+$. The slight difference in the J values for [Ru-Tyr-Mn_2]$^{2+}$ with respect to the model complex may be due to the presence of the [Ru-Tyr-Mn]$^+$ impurity.

5.4 Conclusion

The synthesis of complexes capable of mimicking the initial processes in PSII, *viz.* the electron transfer from a manganese cluster *via* a tyrosine moiety to a photo-oxidised porphyrin (P_{680}), is not a trivial task. Firstly a suitable photosensitiser must be chosen. This must then be modified to incorporate suitable electron donors without disturbing the desired properties of the photosensitiser. In the course of the work presented here, a series of ruthenium pyridyl- and pyrazyl triazole complexes were used as the precursors to larger supramolecular systems. Each of these complexes had been designed with to possess desired electronic properties and terminal synthons so as they may serve as building blocks for larger structures.

Starting with two complexes bearing terminal carboxylic acids, covalently linked photosensitiser-tyrosine systems were prepared *via* an acid chloride. The treatment of metal complexes as organic molecules is becoming more common and was shown to work well in this case. These complexes have yet to undergo studies into investigating the possibility of electron transfer to the ruthenium centre. The rate of electron transfer is known to be pH dependent. These ruthenium complexes are also known to have pH dependent properties. A study of the electron transfer would have to take both of these facts into account. Although this is not covered in this work, it is thought that a comparison between the results obtainable for the pyridine based compounds with those obtainable for the pyrazine based compounds will give a good insight into the importance of the driving force behind electron transfer reactions.

Using these tyrosine derivatives and two phenolic complexes, $[Ru(bpy)_2pyPhOH](PF_6)$ and $[Ru(bpy)_2pzPhOH](PF_6)$, aromatic Mannich reactions

were carried out to incorporate DPA ligands into the complexes. The success of this reaction varied. In some cases, a 1:1 ratio of the mono- to disubstituted complexes was achieved; in others the formation of the monosubstituted isomer was almost exclusive. Unfortunately, although the reactions appeared to be quite successful, purification was extremely problematic. The combination of the charged complex with the presence of many free nitrogens resulted in compounds which bound strongly to both silica and alumina. Size exclusion chromatography did prove to be quite successful in isolating relatively pure samples of $[Ru(bpy)_2pyPhOH(DPA)](PF_6)$ and $[Ru(bpy)_2pzPhOH(DPA)](PF_6)$, but did not function well for $[Ru(bpy)_2pyTyr(DPA)_2](PF_6)$.

Analysis of the products obtained from the Mannich reactions could only be tentatively attempted. None of the products could be isolated in a pure form. While mass spectrometry indicated the presence of the desired products, ^1H NMR spectroscopy showed them to be still quite impure. Due to the mixtures of products, no ^{13}C NMR spectra, IR spectra, CHN analysis, electrochemical or photophysical measurements were carried out.

Reactions with complexes bearing terminal aldehydes were unsuccessful. Despite attempts with three different amines, very little, if any, of the desired product seemed to form. It is thought that the aldehyde is strongly deactivated by the triazolate. The possibility of catalysis by titanium complexes may provide a solution to the problem.

Using an impure sample of $[Ru(bpy)_2pyTyr(DPA)_2](PF_6)$, containing the mono- and disubstituted complexes, a research group in Paris has succeeded in preparing a Ru-

Tyr-Mn_2 system, similar to that prepared by L. Sun *et al*[1]. Initial experiments involving mass spectrometry, EPR spectroscopy and magnetic susceptibility measurements have shown that the desired complex is present and shows similar properties to those of a model complex $[(bpmp)Mn_2(OAc)_2]^+$.

Thus, one may conclude, that metal complexes may indeed be treated as organic molecules. Difficulties arise in the purification of the compounds, but by using less traditional methods such as size exclusion chromatography, these may be overcome. As a result, a wide range of supramolecular systems, such as Ru-Tyr-Mn_2, may be built up from smaller metal complexes.

5.5 Bibliography

[1] Sun, L.; Hammarström, L.; Åkkermark, B.; Styring, S.; *Chem. Soc. Rev.*, **2001**, 30, 36

[2] Sjödin, M.; Styring, S.; Åkkermark, B.; Sun, L.; Hammarström, L., *J. Am. Chem. Soc.*, **2000**, 122, 3932

[3] Suzuki, M.; Sano, M.; Kimura, M.; Hanabusa, K.; Shirai, H.; *Eur. Poly. J.*, **1999**, 35, 221

[4] Howard, T.; Telser, J.; DeRose, V. J.; *Inorg. Chem.*, **2000**, 39, 3379

[5] Horner, O.; Girerd, J. J.; Philouze, C.; Tchertanov, L.; *Inorg. Chim. Acta*, **1999**, 290, 139

[6] Blicke, F. F.; McCarthy, F. J.; *J. Org. Chem.*, **1959**, 24, 1061

[7] Gruenwedel, D. W.; *Inorg. Chem.*, **1968**, 7, 495

[8] Puntoriero, F.; Serroni, S.; Licciardello, A.; Venturi, M.; Juris, A.; Ricevuto, V.; Campagna, S.; *J. Chem. Soc. Dalton Trans.*, **2001**, 1035

[9] Klausner, Y. S.; Bodansky, M.; *Synthesis*, **1972**, 453

[10] Magnuson, A.; Berglund, H.; Korall, P.; Hammarström, L.; Åkkermark, B.; Styring, S.; Sun, L.; *J. Am. Chem. Soc.*, **1997**, 119, 10720

[11] Tramontini, M.; Angiolini, L.; *Tetrahedron*, **1990**, 46, 1791

[12] Cummings, T. F.; Shelton, J. R.; *J. Org. Chem.*; **1960**, 25, 419

[13] Lubben, M.; Feringa, B.; *J. Org. Chem.*; **1994**, 59, 2227

[14] Lukyanenko, N. G.; Pastushok, V. N.; Bordunov, A. V.; Vetrogon, V. I,; Vetrogon, N, I.; Bradshaw, J. S.; *J. Chem. Soc. Perkin Trans. I*, **1994**, 1489

[15] Ghiladi, M.; McKenzie, C. J.; Meier, A.; Powell, A. K.; Ulstrup, J.; Wocaldo, S.; *J. Chem. Soc. Dalton. Trans.*, **1997**, 4011

[16] Nagata, T.; *Chem. Lett.*, **1997**, 127

[17] Blondin, G.; Davydov, R.; Philouze, C.; Charlot, M. F.; Styring, S.; Åkkermark, B.; Girerd, J. J.; Boussac, A.; *J. Chem. Soc. Dalton Trans.*, **1997**, 4069

[18] Ghiladi, M.; Åkkermark, B.; *J. Inorg. Biochem.*, **1999**, 74, 140

[19] Sun, L.; Burkitt, M.; Tamm, M.; Raymond, M. K.; Abrahamsson, M.; LeGourriérec, D.; Frapart, Y.; Magnuson, A.; Kenéz, P. H.; Brandt, P.; Tran, A.; Hammarström, L.; Styring, S.; Åkkermark, B.; *J. Am. Chem. Soc.*, **1999**, 121, 6834

[20] Lees, A.C.; Evrard, B.; Keyes, T.E.; Vos, J.G.; Kleverlaan, C.J.; Alebbi, M.; Bignozzi, C.A.; *Eur. J. Inorg. Chem.*, **1999**, 12, 2309

[21] Horner, O.; Anxolabéhère-Mallart, E.; Charlot, M. F.; Tchertanov, L.; Guilhem, J.; Mattioli, T.; Boussac, A.; Girerd, J. J.; *Inorg. Chem.*, **1999**, 38, 1222

[22] Generously donated by O. Horner and J. J. Girerd, Université de Paris-Sud, Orsay, France

[23] Magnuson, A.; Frapart, Y.; Abrahamsson, M.; Horner, O.; Åkkermark, B.; Sun, L.; Girerd, J. J.; Hammarström, L.; Styring, S.; *J. Am. Chem. Soc.*, **1999**, 121, 89

[24] Shyu, H. L.; Wei, H. H.; Wang, Y.; *Inorg. Chim. Acta*, **1999**, 290, 8

[25] Morris, G.A.; Zhou, H.Y.; Stern, C.L.; Nguyen, S.T.; *Inorg. Chem.*, **2001**, 40, 3222

[26] Tshuva, E.Y.; Gendeziuk, N.; Kol, M.; *Tetrahedron Lett.*, **2001**, 42, 6405

[27] Barney, C. L.; Huber, E. W.; McCarthy, J. R.; *Tetrahedron Lett.*, **1990**, 31, 5547

[28] Bhattacharyya, S.; *Tetrahedron Lett.*, **1994**, 35, 2401

[29] Guidote, A. M.; Ando, K.; Kurusu, Y.; Nagao, H.; Masuyama, Y.; *Inorg. Chim. Acta*, **2001**, 314, 27

[30] Sakiyama, H.; Sugawara, A.; Sakamoto, M.; Unoura, K.; Inoue, K.; Yamasaki, M.; *Inorg. Chim. Acta*, **2000**, 310, 163

[31] Higuchi, C.; Sakiyama, H.; Okawa, H.; Fenton, D. E.; *J. Chem. Soc. Dalton Trans.*, **1995**, 4015

Chapter 6

The Synthesis and Characterisation of a Novel Lipid and its Ruthenium Complex

6.1 Introduction

Bolaamphiphiles, or "bolas" for short, are long hydrocarbon chain compounds with a polar head and tail group[1,2,3]. They get their name from the shape of the molecule – a long thin wire joining two bulkier end groups. In this way they are shaped like the weapon of the South American indians, which consisted of a leather rope with a weight fixed to each end. Bolas are well known to aggregate in water. They may form stacks of layers of bolas, vesicles or any other form of complex aggregation[4]. The exact form of the aggregation depends on the type of bola used. Different head and tail groups will produce different intermolecular interactions and, hence, different forms of aggregation. Similarly, a long chain will introduce a higher degree of flexibility into the bola, so more complex arrangements may be formed. By controlling the length of the chain, the nature of the head groups and the environment in which they are to be studied, highly organised assemblies may be obtained[5,6].

If the conditions chosen are exactly right, then the bolas may self-assemble into the structure desired[7]. This form of synthesis is called synkinesis, and is generally used to create highly ordered lipid membranes[8,9]. If one wishes to study these membranes, it is often useful to immobilise them on a suitable surface, such as gold. Bolas with terminal SH groups readily self-assemble on gold surfaces. The thiol binds strongly with the gold, leaving the other head group free at the end of the lipid[10]. If a large excess of bola is used and left to immobilise for long enough, then one can assume that the whole surface is covered by thiol-gold bonds. This can be proven by various spectroscopic methods. All of the hydrocarbon chains of the bolas will then be

directed out into space. These may be totally randomly arranged or possibly highly organised, again depending on the nature of the chain and the end groups[11].

Take for example the two cases illustrated in *Fig. 6.1.* below. The first case is that of a long chain hydrocarbon with one terminal thiol. As can be seen, the hydrocarbon chains are totally in disarray with no pattern to the structure. Indeed, they possess a fluid-like freedom to move. The second case is that of a long chain hydrocarbon with terminal amide groups. One of the amides contains a thiol. In this case, the chains all stand straight on end. This is due to the hydrogen bonding between the amide linkages. In order to maximise this interaction, the chains tilt slightly to reduce the distance from the carbonyl to the NH of the amide[12].

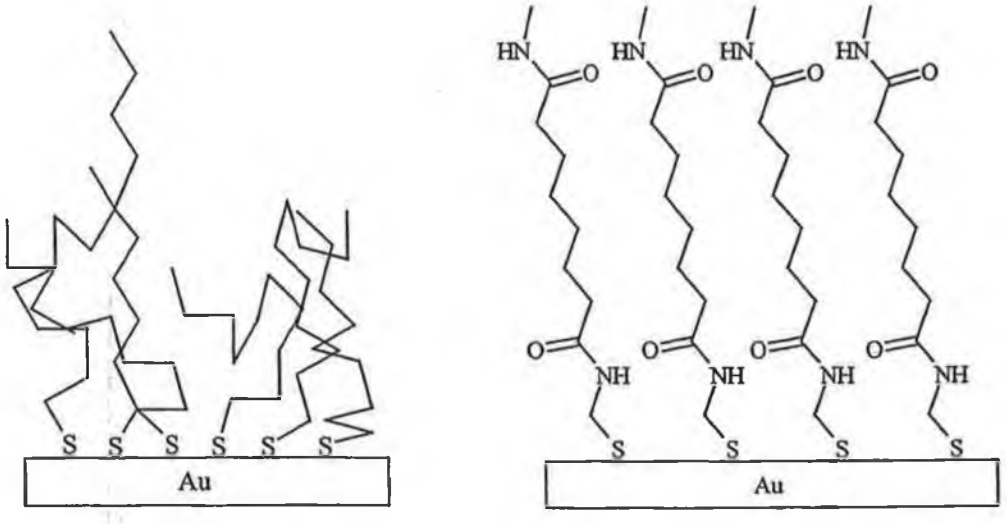

Fig. 6.1. Two types of monolayer assembly on a gold surface

As can be seen from the picture, the introduction of amide linkages into a bola greatly increases its order and rigidity on a gold surface. These then form robust

membranes of definite thickness. It should be noted however, that for this specific type of organisation to be successful, there must be an even number of carbon atoms between the two amide groups. If there is an odd number of carbon atoms in the chain, then the angle of tilt necessary to bring the lower amides closer together will actually bring the upper amides further apart and introduce fluidity into the edge of the membrane. This is illustrated in *Fig. 6.2.*

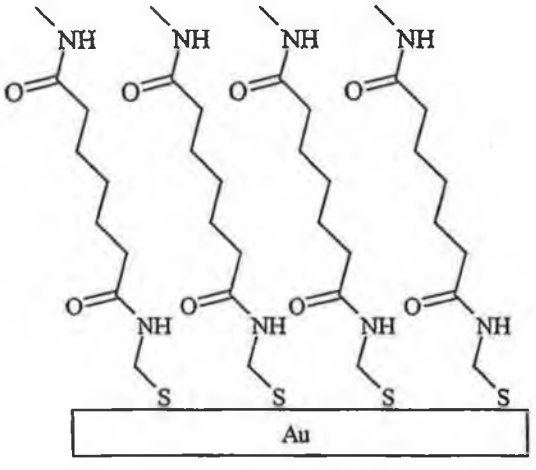

Fig. 6.2. Monolayer with odd number of carbons in chain

If the surface upon which the bolas are being absorbed is not a homogenous gold surface, then an interesting structure may be formed. For example, if the gold surface is first treated with a solution of a tetraphenyl porphyrin bearing carboxylate or thiol groups, then a new type of surface is obtained. It is no longer a pure gold surface, but a gold surface with "islands" of porphyrins scattered randomly across the surface. *Fig. 6.3.* demonstrates how this surface would then appear.

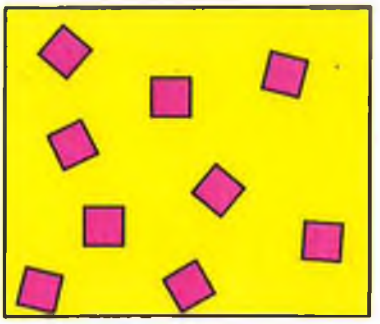

Fig. 6.3. Gold surface treated with porphyrin

If one now tries to functionalise the surface by adding a suitable bola (such as the diamide shown above), then this may only bind to the naked gold. Where it does bind, it will form a similar rigid membrane as before, but wherever there is a porphyrin lying flat on the surface, there will be a hole in the membrane[13]. It can be thought of as a porphyrin surrounded by a "fence", as in *Fig. 6.4.* Since one can tell exactly how thick the membrane is, the surface can then be described as having a membrane coating with pores of specific depth.

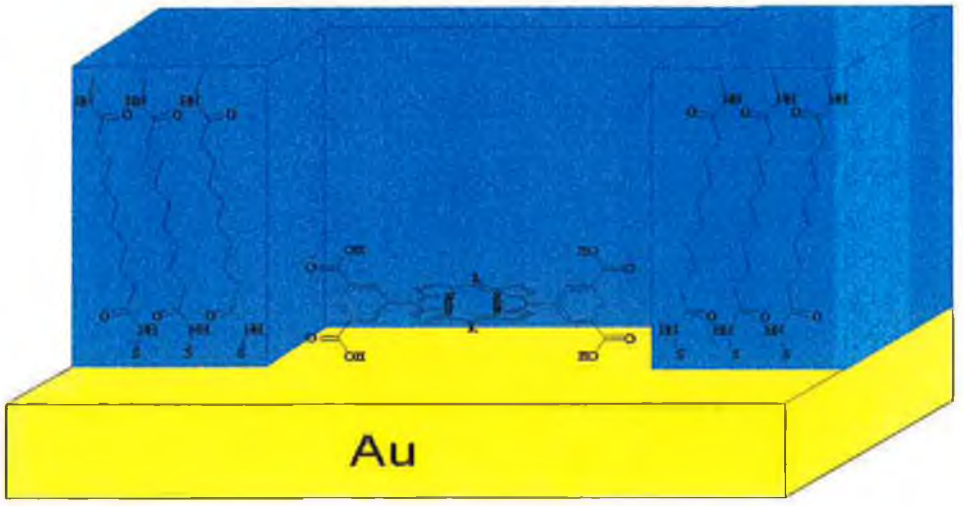

Fig. 6.4. A porphyrin at the bottom of a membrane pore

If a fluorescent porphyrin is used at the base of the pore, then this provides an easy method to detect the diffusion of different substances into the pore. For example, a quencher diffusing into the hole would gradually decrease the fluorescence of the porphyrin until all of the pores were full. Another method to investigate diffusion into the hole, would be to use redox active molecules[14]. A suitable compound would only be detected if it could get close enough to the surface to register a current. In the case of ferricyanide, a current is measured if it comes close enough to the porphyrin, but no current is measured if it is outside of the pore[15].

If the bola was to contain a functional group other than those necessary for self-assembly, this could then be reacted, in situ, to modify the fence[16]. However, only reactive sites on bolas which are at the border of the gaps in the membrane can react[17]. This is again due to the extreme rigidity of the membrane, i.e. all of the other reactive sites within the membrane are inaccessible to any reagents. In this way, they are similar to proteins which have specific reaction sites. Under the correct conditions, suitable reagents could be placed in these pores where they will be able to react with each other. This reaction inside the pore could also be seen to function as a molecular switch. A reaction, such as an addition to a double bond, would change the size of the gap – making it narrower. This could be followed by spectroscopic or electrochemical means. A bulky molecule which only just fitted into the gap before the reaction may not now make it all the way to the bottom of the pore. This point is illustrated best by *Fig. 6.5.* overleaf.

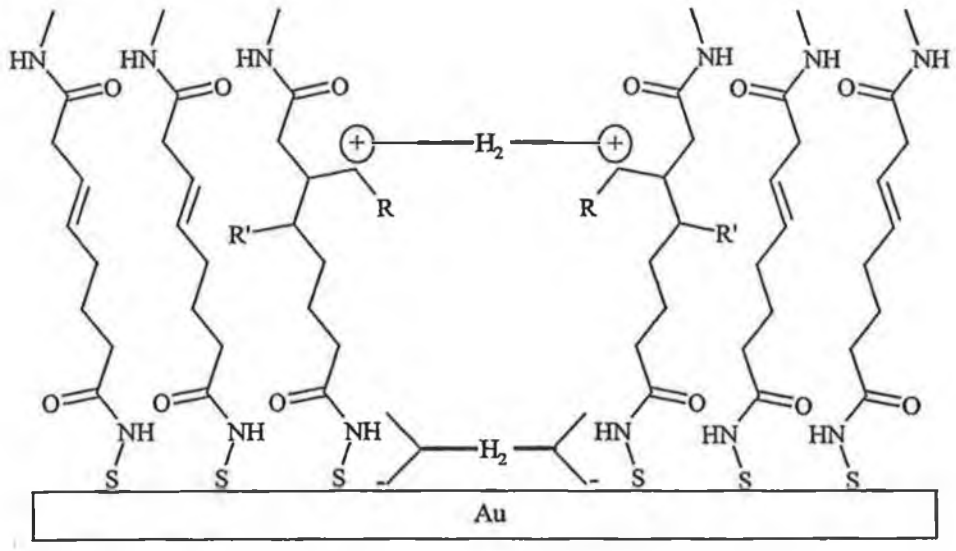

Where:

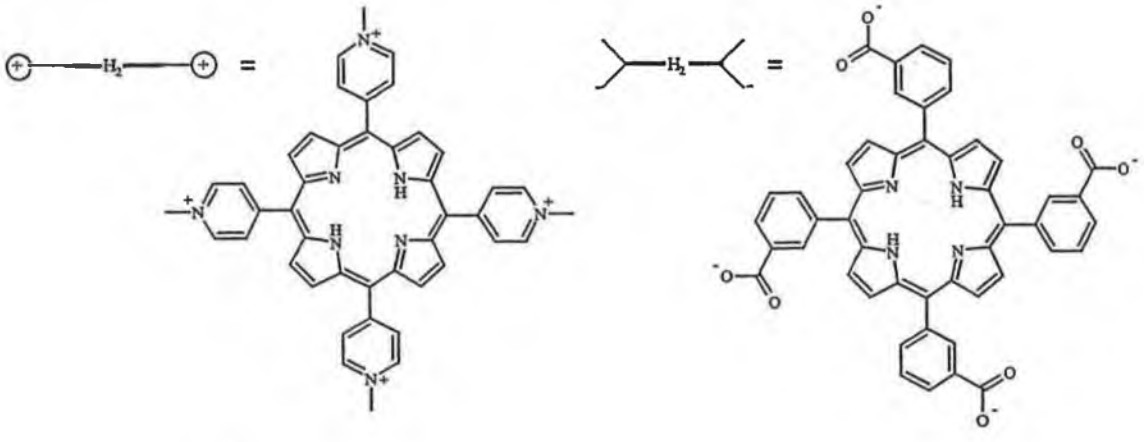

Fig. 6.5. A pore stoppered by a porphyrin after an addition to a double bond

This has already been investigated to some extent. It has been found that not only can the width of the pore be decreased at a desired depth, but that the gap can be "stoppered" at this point by adding another porphyrin which can enter the hole, but not get past the reaction site. If the new functionality in the membrane wall may bind (by any means) with the incoming porphyrin, then it will be held rigidly in place. In this way, two non-covalently bound porphyrins may be positioned a defined distance from one another. Energy transfer between the two porphyrins may then be studied if

the distance is short enough. If the distance is too large, then a suitable "shuttle" must be encased in the pore before sealing it with the second porphyrin. This could then mediate the energy transfer between the two porphyrins. Under suitable conditions, it is also possible to remove the stopper when desired.

The aim of the work presented here is to synthesise a novel bola, containing amide linkages and a terminal metal chelating ligand. It was hoped that the possibility of closing a membrane pore by means of complexation with a suitable metal might later be investigated. The upper part of the membrane should contain a 2,2'-bipyridyl derivative in a suitable orientation with respect to the membrane. It should be then possible to complex this with an appropriate metal in order to seal the pore, as bipyridines have been shown to form stable complexes with a variety of transition metals under mild conditions. A 5-substituted bipyridine was decided upon, as it would allow the easiest access for a metal to the pore, whilst being well positioned to close the gap tightly once the metal has complexed. It is hoped that $[Ru(bpy)_2Cl_2].2H_2O$ might be used to close the gap as in *Fig. 6.6.* This would make an excellent model system for artificial photosynthesis. The fact that the exact positions of the ruthenium centre and the surface bound porphyrin are known means that accurate rates of energy/electron transfer rates between them may be determined. Should this work, then a range of systems with various lengths of lipids may be made and measured.

The lipid chosen also contains a double bond. This feature provides the added possibility to close the pore beneath the final position of the ruthenium or other metal

centre. It may then be possible to assemble a triad with the ruthenium in the uppermost position, a porphyrin embedded midway in the membrane and another porphyrin on the gold surface beneath.

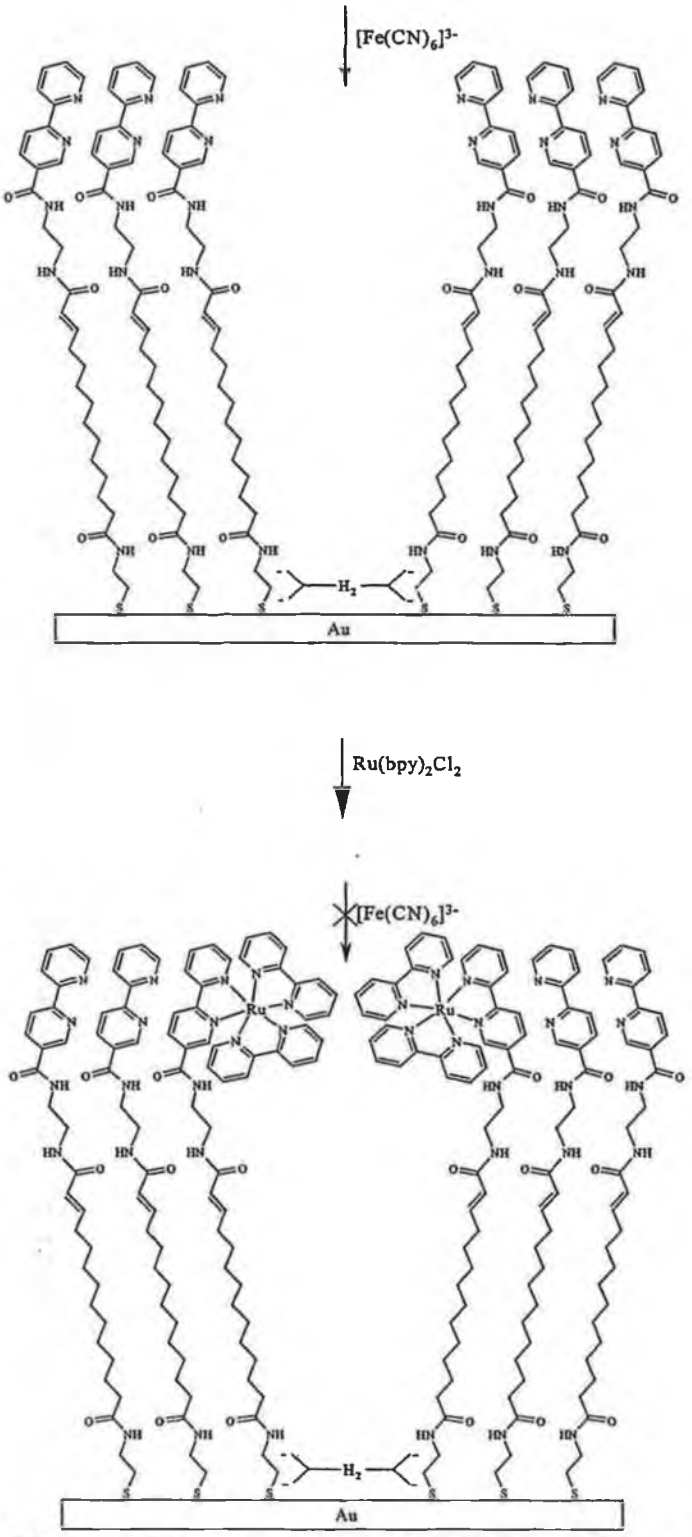

Fig. 6.6. Schematic representation of the closure of the membrane

As can be seen from the figure on the previous page, the closure of the gap would firstly be studied by the use of ferricyanide. This would give a quick and accurate indication as to whether the pore is open or closed. Unfortunately there is an important potential problem with this system. This problem would be incurred upon closing the membrane pore. In order for ruthenium to bind to a bpy, heat is required. Although the reaction proceeds cleanly and efficiently in a reaction flask, it may prove more difficult on a surface. Conditions would have to be monitored closely to ensure that the thiol-gold bond did not break. If this did become a problem, then a different metal would have to be used. One with a lower 10Dq value would bind quicker and easier and would also be easier to remove at the end. However, the photochemical and electrochemical properties would also have to be suitable. Metals such as Os may form extremely stable complexes, with ideal electronic properties for this study, but they require drastic conditions in order to form these complexes. The heat required would possibly be too severe for the membrane to survive on the gold surface. Conversely, metals such as Fe or Cu readily complex with bpy, but the complexes formed are unstable due to the weak M-N bonds formed. However, ruthenium seems to be most suited for this work as it should be possible to form the complex with the surface bound bola under quite mild conditions to produce a system stable enough to be studied without any problems.

In this chapter the synthesis of a novel lipid will be presented. It differs from the compound shown in *Fig. 6.6*, in that it does not contain the terminal thiol containing amide. However, this acid could still be attached to a TiO_2 surface. This work will be undertaken by Prof. Fuhrhop's research group. At a later date, the terminal amide

may be introduced and the system immobilised on a gold surface. The lipid prepared here has been characterised by the standard methods. As well as the synthesis and characterisation of this bola, the synthesis and characterisation of various model ruthenium complexes will also be discussed. The complexes prepared are those of some selected intermediates in the synthesis of the bola. They have been investigated to determine the effect of different substituents, in the 5-position of bpy, on the spectroscopic and electrochemical properties of $[Ru(bpy)_3]^{2+}$. The results obtained should be of assistance in the analysis of the system upon its immobilisation on a surface.

6.2 Synthetic Procedures

6.2.1 Synthesis of the Lipid Membrane

Benzyl 12-Hydroxydodecanoate[17] (i)

A solution of 10 g (26.3 mmol) of 12-hydroxydodecanoic acid in 120 cm^3 of DMF was treated with 5.1 g (50.9 mmol) of potassium bicarbonate and 9.12 g (53.2 mmol) of benzyl bromide and stirred for 24h. The solvent was removed under reduced pressure. The resulting mixture was partitioned between ethyl acetate and aqueous HCl. The organic phase was separated, washed with water and dried with sodium sulphate. Removal of the solvent in vacuo resulted in a solid, which was recrystalised in methanol to afford white crystals in a yield of 8.50 g. (60%)

^{1}H NMR (250 MHz, $CDCl_3$) δ in ppm 1.36 (m, 14H, 7 x CH_2), 1.57 (m, 4H, 2 x CH_2), 2.38 (t, 2H, CH_2COO), 3.63 (t, 2H, CH_2OH), 5.11 (s, 2H, CH_2Ph), 7.38 (s, 5H, aromat).

^{13}C NMR (63 MHz, $CDCl_3$) δ in ppm 24.8, 25.6, 28.9, 29.0, 29.3, 29.4, 29.5, 32.6, 34.2, 62.7, 65.9, 128.0, 128.4, 136.0, 173.6

MS (EI) m/z 306 $(M)^+$, 278 $(M\text{-}CO)^+$

12-Oxo-dodecanoic acid benzyl ester[17] (ii)

3.23 g (15 mmol) of pyridinium chlorochromate was suspended in 100 cm^3 of dichloromethane and 3.5 g (10 mmol) of the benzyl ester (i) was rapidly added at room temperature. After 1.5 hours the oxidation was complete (followed by TLC). The black reaction mixture was diluted with 300 cm^3 of anhydrous ether, the solvent was decanted, and the black solid was washed twice with ether. The product was isolated simply by filtration of the organic extracts through Florisil and evaporation of the solvent at reduced pressure to afford the product in a yield of 3.15 g. (90%)

^1H NMR (250 MHz, $CDCl_3$) δ in ppm 1.35 (m, 12H, 6 x CH_2), 1.57 (m, 4H, 2 x CH_2), 2.40 (m, 4H, CH_2COO, CH_2OH), 5.10 (s, 2H, CH_2Ph), 7.40 (s, 5H, aromat), 9.77 (s, 1H, CHO).

^{13}C NMR (63 MHz, $CDCl_3$) δ in ppm 21.9, 24.8, 29.0, 29.1, 29.2, 34.2, 43.7, 65.9, 128.0, 128.4, 136.0, 173.5, 202.8

MS (EI) m/z 304 $(M)^{+\cdot}$, 276 $(M\text{-}CO)^+$

Tetradec-2-enedioic acid 14-benzyl ester 1-*tert*-butyl ester[17] (iii)

1.32 g (32.9 mmol) of sodium hydride was suspended in 100 cm^3 of THF at 0°C under an argon atmosphere. 7.38 g (32.9 mmol) of *tert*-butyl P, P-dimethylphosphono acetate was added dropwise at this temperature. After the evolution of H_2 bubbles had ceased (30 mins), a solution of 10 g (32.9 mmol) of the aldehyde (ii) in 50 cm^3 THF was added slowly. The resulting mixture was stirred for 24 hours. The solvent was removed under reduced pressure and the residue taken up

with water. After extraction with four portions of ether and subsequent drying, a white solid was obtained. This was recrystalised from hexane to give 9.80 g of the desired product. (74%)

^{1}H NMR (250 MHz, $CDCl_3$) δ in ppm 1.30 (m, 12H, 6 x CH_2), 1.44 (s, 9H, $(CH_3)_3C$), 1.58 (m, 4H, 2 x CH_2), 2.30 (m, 4H, 2 x CH_2), 5.10 (s, 2H, CH_2Ph), 5.73 (d, 1H, J=11Hz, vinyl α-H), 6.87 (dt, 1H, J_1=11 J_2=3Hz, vinyl β–H), 7.41 (s, 5H, aromat).

^{13}C NMR (63 MHz, $CDCl_3$) δ in ppm 24.8, 28.0, 28.1, 28.5, 28.7, 28.9, 29.0, 29.1, 29.3, 31.9, 34.2, 65.9, 79.8, 122.8, 128.0, 128.4, 136.0, 148.0, 166.7, 173.5.

MS (FAB, neg., Xe) m/z 682$(M)^-$, 653$(M\text{-}CO)^-$

Tetradec-2-enedioic acid 14-benzyl ester[17] (iv)

5 g (14.5 mmol) of the *tert*-butyl ester (iii), 100 cm^3 of toluene and 0.5 g of p-toluenesulphonic acid were heated to reflux for 30 mins and subsequently stirred at room temperature overnight. After removal of the toluene, 300 cm^3 of 5% aqueous potassium bicarbonate solution was added and stirred for 10 minutes. The white precipitate was filtered off and the filtrate was acidified to pH 3 with dil. HCl. The resulting suspension was extracted with chloroform, dried with magnesium sulphate, dried in vacuo and finally recrystalised with chloroform/hexane. 3.95 g of white crystals were obtained. (81%)

^{1}H NMR (250 MHz, $CDCl_3$) δ in ppm 1.33 (m, 12H, 6 x CH_2), 1.48 (m, 2H, CH_2), 1.61 (m, 2H, CH_2), 2.20 (m, 2H, CH_2), 2.38 (t, 2H, CH_2COO), 5.10 (s, 2H, CH_2Ph),

5.73 (d, 1H, J=11Hz, vinyl α-H), 6.87 (dt, 1H, J_1=11 J_2=3Hz, vinyl β-H), 7.41 (s, 5H, aromat), 11.60 (m, 1H, COOH).

^{13}C NMR (63 MHz, $CDCl_3$) δ in ppm 24.8, 27.7, 28.5, 29.0, 29.1, 29.2, 29.3, 29.4, 32.2, 34.2, 66.0, 120.4, 128.0, 128.4, 136.0, 152.2, 172.0, 173.6.

MS (FAB,pos.,Xe) m/z 347$(M)^+$, 329$(M\text{-}OH)^+$

1-(2-oxo-2-[2]pyridyl-ethyl)-pyridinium iodide[18] (v)

A solution of 52.5 g (0.21 mol) of iodine in 150 cm^3 dry pyridine was added over 30 minutes to a solution of 25 g (0.21 mol) of 2-acetylpyridine in 100 cm^3 of dry pyridine. After heating for 3 hours at 100°C under a nitrogen atmosphere, the resulting black mixture was allowed to stand at room temperature overnight. The pyridinium salt was filtered off and recrystalised from hot ethanol to yield 54 g (80%) as a beige powder.

^{1}H NMR (250 MHz, $(CD_3)_2CO$) δ in ppm 6.76 (s, 2H, CH_2), 7.83 (m, 1H, pyH3), 8.132 (m, 2H, pyH2, pyH1), 8.45 (t, 2H, J=4.5Hz, py^+H3, py^+H5), 8.90 (m, 2H, pyH4, py^+H4), 9.20 (d, 2H, J=4.5Hz, py^+H6)

^{13}C NMR (63 MHz, $(CD_3)_2CO$) δ in ppm 68.34, 123.38, 129.48, 130.41, 139.23, 147.86, 148.02, 150.92, 152.07, 192.41

5-Methyl 2,2′-bipyridine[19,20,21] (vi)

54 g (0.17mol) of the pyridinium salt (v) and 50 g (3.9 eq) of ammonium acetate were dissolved in 320 cm^3 of formamide at 60°C. After the addition of 17 g of an 85% solution of methacrolein in one portion, the resulting solution was stirred for 6 hours at 60°C. This was then extracted with diethyl ether. Removal of the solvent in vacuo yielded a brown oil which was resuspended in water and extracted with hexane. The organic phases were combined and dried with magnesium sulphate prior to evaporation of the solvent to afford 21.8 g (78%) as a yellow oil.

^1H NMR (250 MHz, $CDCl_3$) δ in ppm 2.34 (s, 3H, CH_3), 7.20 (dd, 1H, pyH5'), 7.55 (d, 1H, pyH4), 7.72 (dd, 1H, pyH4'), 8.35 (d, 1H, pyH3), 8.41 (d, 1H, pyH3'), 8.47 (s, 1H, pyH6), 8.59 (d, 2H, pyH6')

^{13}C NMR (63 MHz, $CDCl_3$) δ in ppm 18.18, 120.43, 120.62, 123.21, 133.23, 136.66, 137.27, 148.96, 149.49, 153.50, 156.1

2, 2′-Bipyridyl-5-carboxylic acid[22] (vii)

21.8 g (0.128 mol) of the methyl bpy (vi) was suspended in 200 cm^3 of water at 70°C. To this was added 41 g (0.25 mol) of solid $KMnO_4$ over 3 hours. A second portion of 41 g (total 0.5 mol) was added over a further 3 hours at 90°C. After all of the $KMnO_4$ had been consumed, the dark brown mixture was filtered while hot and the precipitate washed with two portions of hot water. The combined filtrate and washings were concentrated *in vacuo* to approximately 40 cm^3. Slow addition, with

external cooling, of 25% aq. HCl brought about the precipitation of the acid in a yield of 76%.

m.p. 195°C (decomp.)

^{1}H NMR (250 MHz, $(CD_3)_2SO_2$) δ in ppm 7.82 (m, 1H, pyH5'), 8.37 (m, 3H, pyH4'), 8.55 (m, 1H, pyH3), 8.60 (m, 2H, pyH4, pyH3'), 8.86 (d, 1H, pyH6'), 9.12 (s, 1H, pyH6)

^{13}C NMR (63 MHz, $(CD_3)_2SO_2$) δ in ppm 122.12, 123.81, 139.61, 143.30, 146.10, 149.93, 150.29, 153.46, 166.15

(2-Amino-ethyl)-carbamic acid *tert*-butyl ester[23,24] (viii)

12.7 g (0.055 mol) of "BOC- Anhydride" in 75 cm^3 of dioxane were added over two and a half hours to an ice cold solution of 25 g (0.41 mol) of ethylene diamine in 75 cm^3 of dioxane. This was then stirred overnight while warming slowly to room temperature. Removal of the solvent under reduced pressure yielded a yellow oil. Trituration of this oil with water produced a white precipitate which was filtered off before extracting the filtrate with dichloromethane. The organic phases were dried with magnesium sulphate and subsequently the solvent evaporated to give a clear oil in a yield of 7.5 g (83%).

^{1}H NMR (250 MHz, $CDCl_3$) δ in ppm 1.22, (s, 9H, $(CH_3)_3$), 2.50 (t, 2H, CH_2), 2.92 (m, 2H, C*H*$_2$NHBOC), 3.47 (s, 2H, NH_2), 5.41 (br, 1H, NHBOC)

^{13}C NMR (63 MHz, $CDCl_3$) δ in ppm 27.9, 41.47, 43.06, 66.59, 155.95

2, 2′-Bipyridyl-5-carboxylic acid (2-amino-ethyl)-carbamic acid *tert*-butyl ester (ix)

5 g (25 mmol) of the bipyridine acid (vii) were heated to reflux in 100 cm^3 of freshly distilled thionyl chloride for 3 hours. This was then evaporated to complete dryness in vacuo. The formation of the acid chloride was assumed to be complete and was used immediately. 4 g (25 mmol) of the mono Boc-protected ethylene diamine and a catalytic amount of 4-(N, N dimethylamino)pyridine were dissolved in 50 cm^3 of dry dichloromethane and this solution added slowly to a stirred suspension of the acid chloride in 250 cm^3 of dry dichloromethane. This was then left to stir at room temperature overnight. The now dark solution was washed with aq. NaOH and then with water, before being dried to an orange oil in vacuo. Addition of diethyl ether brought about the precipitation of a white solid which was filtered off and dried *in vacuo* to afford 4.3 g (50%).

m.p. 187-189°C

^{1}H NMR (250 MHz, $CDCl_3$) δ in ppm 1.41 (s, 9H, $(CH_3)_3$), 3.46 (m, 2H, CH_2NHBOC), 3.57 (m, 2H, CH_2), 5.09 (t, 1H, NHBOC), 7.42 (t, 1H, pyH5'), 7.65 (br, 1H, NH), 7.83 (t, 1H, pyH4'), 8.25 (d, 1H, pyH3'), 8.48 (m, 2H, pyH4, pyH6'), 8.69 (d, 1H, pyH3), 9.11 (s,1H, pyH6)

^{13}C NMR (63 MHz, $CDCl_3$) δ in ppm 28.32, 39.94, 42.31, 80.10, 120.51, 121.68, 124.20, 129.36, 135.64, 136.98, 148.15, 149.22, 155.20, 157.76, 158.24, 165.89

MS EI (80eV) m/z 342 $(M)^+$

2, 2′-Bipyridyl-5-carboxylic acid (2-amino-ethyl)-amide (x)

3.3 g of the protected bipyridyl amine (ix) were dissolved in 18 cm^3 of a 3M HCl solution in ethyl acetate and stirred at room temperature for 1 hour. After evaporating the mixture to dryness on the rotary evaporator and washing with diethyl ether, the resulting solid was redissolved in aqueous sodium hydroxide and extracted three times with chloroform. The chloroform fractions were combined, dried over magnesium sulphate and evaporated in vacuo to give 2.2 g (86%) as a yellow waxy solid.

^{1}H NMR (250MHz, $CDCl_3$) δ in ppm 2.87 (t, 2H, C$H_2$$NH_2$), 3.48 (m, 2H, C$H_2$NH), 7.32 (t, 1H, pyH5'), 7.76 (t, 1H, pyH4'), 8.28 (m, 3H, pyH4, pyH3', pyH6'), 8.60 (d, 1H, pyH3), 9.05 (s, 1H, pyH6)

^{13}C NMR (63 MHz, $CDCl_3$) δ in ppm 40.91, 42.17, 120.28, 121.39, 124.02, 129.45, 135.64, 136.77, 147.87, 148.97, 154.75, 157.81, 165.93

MS (FAB, pos., Xe) m/z 243 $(M + H)^+$, 226 $(M - NH_2)^+$, 183 $(M - NHC_2H_4NH_2)^+$

Tetradec-2-en-dioic acid 1-benzyl ester 14(2, 5-dioxo-pyrrolidin-1-yl) ester (xi)

1 g (2.9 mmol) of the mono benzyl protected bola amphiphile (iv), 0.58 g (1 eq) of DCC and 0.33 g (1 eq) of N-hydroxy succinimide were dissolved in 10 cm^3 of dioxane and left to stand at 4°C overnight. After filtration of the insoluble by-products and removal of the solvent in vacuo a pale oil was obtained. This was

recrystallised from chloroform/hexane to give (x) in a yield of 0.94 g (73%) as a white powder.

m.p. 83-85°C

^{1}H NMR (250MHz, $CDCl_3$) δ in ppm 1.27 (s, 12H, 6 x CH_2), 1.41 (m, 2H, CH_2), 1.55 (m, 2H CH_2), 3.37 (m, 4H, 2 x CH_2), 2.84 (s, 4H, $OC(CH_2)_2CO$), 5.11 (s, 2H, CH_2Ph), 5.91 (d, 1H, J=11Hz, vinyl α-H), 7.29 (m, 1H, vinyl β-H), 7.43 (s, 5H, Ph)

^{13}C NMR (63 MHz, $CDCl_3$) δ in ppm 24.92, 25.60, 27.55, 29.08, 29.16, 29.25, 39.33, 32.83, 34.30, 66.01, 103.86, 115.31, 126.29, 128.12, 128.51, 156.17, 169.26

MS EI (80eV) m/z 443 $(M)^{\cdot+}$, 336 $(M\text{-}OCH_2Ph)^+$

13-{2-[([2, 2′] Bipyridinyl-5-carbonyl)-amino]-ethylcarbamoyl}-tridec-12-enoic acid benzyl ester (xii)

0.9 g (2 mmol) of the lipid ester (xi) and 0.49 g (1 eq) of the bipyridyl amine (ix) were dissolved in 20 cm^3 of choroform/methanol (1:1) and stirred at room temperature overnight. After removal of the solvent under reduced pressure, the remainder was partitioned between aqueous HCl and chloroform. After 3 extractions, the combined organic phases were dried with magnesium sulphate and subsequently in vacuo. 1 g (86%) was obtained as a white powder.

m.p. 147-150°C

^{1}H NMR (250 MHz, $CDCl_3/CD_3OD$ 3:1) δ in ppm 1.09 (s, 12H, 6 x CH_2), 1.25 (m, 2H, CH_2), 1.53 (m, 2H, CH_2), 2.10 (m, 2H, CH_2-vinyl), 2.33 (t, 2H, CH_2COO), 3.31 (m, 2H, CH_2NHCO-vinyl), 3.48 (m, 2H, $CH_2NHCOBpy$), 5.02 (s, 2H, CH_2Ph), 5.77

(d, 1H, J=11Hz, vinyl α-H), 6.82 (m, 1H, vinyl β-H), 7.32 (s, 5H, Ph), 7.45 (m, 1H, pyH5'), 7.89 (t, 1H, pyH4'), 8.38 (m, 3H, pyH4, pyH3', pyH6'), 8.69 (d, 1H, pyH3), 9.04 (s, 1H, pyH6)

^{13}C NMR (63MHz, $CDCl_3/CD_3OD$ 3:1) δ in ppm 24.61, 27.93, 28.73, 28.85, 29.04, 31.76, 34.02, 38.79, 40.11, 65.88, 120.74, 121.93, 122.84, 124.49, 127.78, 127.87, 128.21, 129.54, 136.16, 137.85, 145.21, 147.96, 148.50, 154.10, 154.39, 156.99, 166.24, 167.90

MS (EI, 80eV) m/z 570 $(M)^{+}$, 479 $(M-C_7H_7)^{+}$

13-{2-[([2, 2'] Bipyridinyl-5-carbonyl)-amino]-ethylcarbamoyl}-tridec-12-enoic acid (xiii)

0.09 g (2.2 mmol) of lithium hydroxide monohydrate was suspended in 25 cm^3 of water/methanol/THF (1:1:3) and added to a solution of 0.6 g (1.1 mmol) of the benzyl ester (xii) in 25 cm^3 of the same solvent system. The resulting mixture was then stirred overnight at room temperature. After removal of the solvent under reduced pressure, the residue was taken up in acidic water and extracted three times with chloroform. The organic phases were dried and evaporated to yield 0.4 g (79%).

m.p. 149-151°C

^{1}H NMR (400 MHz, $CD_3OD/CDCl_3$ 4:1) δ in ppm 1.27 (s, 12H, 6 x CH_2), 1.41 (m, 2H, CH_2), 1.60 (m, 2H, CH_2), 2.19 (m, 2H, CH_2), 2.28 (t, 2H, CH_2), 3.54 (m, 2H, CH_2NHCO-vinyl), 3.60 (m, 2H, CH_2NHCOBpy), 5.94 (d, 1H, J=11Hz, vinyl α-H),

6.81 (m, 1H, vinyl β-H), 8.05 (t, 1H, pyH5'), 8.53 (m, 2H, pyH4, pyH3'), 8.63 (t, 1H, pyH4'), 8.76 (d, 1H, pyH6'), 8.89 (d, 1H, pyH3), 9.28 (s, 1H, pyH6)

^{13}C NMR (100 MHz, $CD_3OD/CDCl_3$ 4:1) δ in ppm 26.56, 29.92, 30.72, 30.88, 31.02, 31.07, 33.67, 35.53, 35.64, 40.37, 118.54, 123.99, 124.91, 125.86, 129.01, 134.29, 139.74, 146.94, 150.34, 170.05, 178.43, 212.07

MS (EI, 80eV) m/z 480 $(M)^{+}$

6.2.2 Synthesis of Model Ruthenium Complexes

Synthesis of $[Ru(bpy)_2(vii)](PF_6)_2$

90 mg (0.35 mmol) of 2, 2'-bipyridine-5-carboxylic acid and 125 mg (0.24 mmol) of $Ru(bpy)_2Cl_2.2H_2O$ were heated to reflux for 4 hours in 10 cm^3 of a 1:1 mixture of ethanol and water. The reaction mixture was concentrated to approximately 5 cm^3 under reduced pressure. The PF_6 salt of the complex was crashed out by adding a few drops of a saturated ammonium hexafluorophosphate solution, filtered and washed well with diethyl ether before drying *in vacuo*. The complex was purified by column chromatography on silica, with $MeCN/H_2O$/sat. aq. KNO_3 (80/20/1) as the eluent, to yield 125 mg (54%) of the pure compound.

^1H NMR (400 MHz, CD_3CN) δ in ppm 7.45 (m, 5H, 5xH5), 7.73 (m, 4H, 4xH6), 7.85 (m, 1H, H6'), 7.95 (s, 1H, H6), 8.12 (m, 5H, 4xH4, H4'), 8.56 (m, 1H, H4), 8.87 (m, 4H, 3xH3, H3'), 8.94 (m, 2H, H3, H3 (vii))

^{13}C NMR (100 MHz, CD_3CN) δ 123.91, 123.95, 123.99, 124.11, 125.21, 127.23, 127.28, 127.30, 127.40, 128.10, 128.86, 137.36, 137.58, 137.60, 137.65, 137.74, 151.33, 151.44, 151.46, 151.57, 151.62, 151.65, 155.61, 156.41, 156.46, 156.53, 156.66, 159.82, 162.92

Elemental Analysis for $C_{31}H_{24}N_6O_2RuP_2F_{12}$: Calc.: C 41.23, H 2.68, N 9.31, Found: C 41.53, H 2.89, N 9.50

Synthesis of $[Ru(bpy)_2(ix)](PF_6)_2.2H_2O$

50 mg (0.14 mmol) of 2, 2′-Bipyridyl-5-carboxylic acid (2-amino-ethyl)-carbamic acid *tert*-butyl ester (ix) and 70 mg (0.13 mmol) of $Ru(bpy)_2Cl_2.2H_2O$ were heated to reflux for 4 hours in 10 cm^3 of a 1:1 mixture of ethanol and water. After removal of most of the solvent, a few drops of a saturated ammonium hexafluorophosphate solution were added to crash out the complex as the PF_6 salt. This was filtered, washed well with diethyl ether and dried *in vacuo*. 115 mg (84%) of the complex were obtained. The product obtained was pure by NMR and no further purification was necessary.

^1H NMR (400 MHz, CD_3CN) δ in ppm 1.35 (s, 9H, 3 x CH_3), 3.17 (m, 2H, CH_2NHBOC), 3.33 (m, 2H, CH_2), 5.44 (m, 1H, NHBOC), 7.42 (m, 6H, 5 x H5, NH), 7.76 (m, 5H, 5xH6), 8.08 (m, 6H, 5 x H4, H6 (ix)), 8.28 (m, 1H, H4 (ix)), 8.55 (m, 6H, 6xH3)

^{13}C NMR (100 MHz, CD_3CN) δ 27.21, 38.15, 40.01, 78.20, 117.02, 123.52, 123.94, 124.09, 124.75, 127.19, 127.28, 127.33, 127.75, 132.84, 134.93, 137.54, 137.60, 150.51, 151.29, 151.42, 156.22, 157.95

Elemental Analysis for $C_{38}H_{41}N_8O_{4.5}RuP_2F_{12}$: Calc.: C 42.19, H 3.91, N 10.35, Found: C 42.51, H 3.55, N 10.17

Synthesis of $[Ru(bpy)_2(x)](PF_6)_2.2NaCl.2H_2O$

50 mg (0.048 mmol) of $[Ru(bpy)_2(ix)](PF_6)_2$ were dissolved in 5 cm^3 of a 3N solution of HCl in ethyl acetate. After stirring overnight at room temperature, the solvent was removed in vacuo. The residue was taken up in basic water and extracted three times with dichloromethane, which was dried with magnesium sulphate and evaporated to dryness to yield 35 mg (75%) as a red solid, which was then recrystalised from acetone/water.

^1H NMR (400 MHz, CD_3CN) δ in ppm 2.52 (m, 2H, NH_2), 3.75 (m, 2H, J=5Hz, CH_2NHCO), 3.98 (t, 2H, J=5Hz, CH_2NH_2), 7.60 (m, 5H, 5xH5), 8.09 (m, 5H, 5xH6), 8.23 (m, 5H, 5xH4), 8.34 (s, 1H, H6 (x)), 8.51 (d, 1H, J=5Hz, H4 (x)), 8.85 (m, 6H, 6xH3)

^{13}C NMR (100 MHz, CD_3CN) δ in ppm 48.52, 49.26, 125.38, 125.70, 125.83, 126.94, 129.32, 130.05, 137.76, 139.43, 139.55, 152.39, 153.07, 153.29, 157.11, 158.50, 164.71

Elemental Analysis for $C_{33}H_{34}N_8O_3RuP_2F_{12}Na_2Cl_2$: Calc.: C 36.63, H 3.16, N 10.35, Found: C 36.65, H 2.83, N 9.83

Synthesis of $[Ru(bpy)_2(xii)](PF_6)_2.(CH_3)_2CO$

19 mg (0.033 mmol) of (xii) and 15 mg (0.028 mmol) of $[Ru(bpy)_2Cl_2].2H_2O$ were heated to reflux for 4 hours in 5 cm^3 of a 1:1 mixture of ethanol and water. After removal of most of the solvent, a few drops of a saturated ammonium hexafluorophosphate solution were added to crash out the complex as the PF_6 salt.

This was filtered, washed well with diethyl ether and dried *in vacuo*. Subsequently, the complex was dissolved in acetonitrile and centrifuged to remove unreacted ligand, prior to recrystalisation from acetone/water (2:1). 29 mg (82%) of the complex were obtained. No further purification was necessary.

^{1}H NMR (400 MHz, CD_3CN) δ in ppm 1.27 (m, 12H, 6xCH_2), 1.42 (m, 2H, CH_2), 1.58 (m, 2H, CH_2), 2.16 (m, 2H, CH_2), 2.34 (m, 2H, CH_2), 3.35 (m, 2H, C*H*$_2$NHCO-vinyl), 3.43 (m, 2H, C*H*$_2$NHCO-bpy), 5.09 (s, 2H, C*H*$_2$Ph), 5.85 (d, 1H, J=11Hz, vinyl *α*-H), 6.70 (m, 1H, vinyl β-H), 7.39 (m, 10H, 5xH5, Ph), 7.77 (m, 5H, 5xH6), 8.08 (m, 6H, 5xH4, H6 (xii)), 8.31 (m, 1H, H4 (xii)), 8.55 (m, 6H, 6xH3)

Elemental Analysis for $C_{57}H_{63}N_8O_5RuP_2F_{12}$: Calc.: C 51.43, H 4.77, N 8.42, Found: C 51.96, H 4.78, N 8.79

Synthesis of [Ru(bpy)$_2$(xiii)](PF$_6$)$_2$.4H$_2$O

15 mg (0.012 mmol) of [Ru(bpy)$_2$(xii)](PF$_6$)$_2$ were dissolved in 6ml of water/methanol (2:1) containing ~0.06 mmol NaOH. The solution was heated to reflux for 1 hour and cooled to room temperature. After removal of the volatile solvent under reduced pressure, a few drops of conc. aq. NH_4PF_6 were added. The precipitate was filtered and washed well with water and diethyl ether, before being recrystalised from acetone/water (2:1) to yield 12 mg (86%) as a red solid.

^{1}H NMR (400 MHz, $(CD_3)_2CO$) δ in ppm 1.16 (m, 12H, 6xCH_2), 1.28 (m, 2H, CH_2), 1.44 (m, 2H, CH_2), 2.05 (m, 2H, CH_2), 2.14 (m, 2H, CH_2), 3.26 (m, 2H, C*H*$_2$NHCO-vinyl), 3.34 (m, 2H, C*H*$_2$NHCO-bpy), 5.83 (d, 1H, J=11Hz, vinyl *α*-H), 6.65 (m, 1H,

vinyl β-H), 7.47 (m, 5H, 5xH5), 7.97 (m, 5H, 5xH6), 8.10 (m, 5H, 5xH4), 8.19 (s, 1H, H6 (xiii)), 8.35 (m, 1H, H4 (xiii)), 8.71 (m, 6H, 6xH3)

Elemental Analysis for $C_{47}H_{60}N_8O_8RuP_2F_{12}$: Calc.: C 44.95, H 4.82, N 8.92, Found: C 45.13, H 4.54, N 8.49

6.3 Results and Discussion

6.3.1 Synthesis

The synthesis of this novel lipid membrane, although still incomplete, appears to be quite successful. Yields in general are satisfactory and the compounds obtained from each step of the synthesis require little or no purification. The synthesis of all of the compounds, up to and including tetradec-2-enedioic acid 14-benzyl ester, was developed by Marc Skupin in the Freie Universität in Berlin. All of the synthesis in this chapter was carried out in Berlin with the collaboration of Prof. J. H. Fuhrhop's research group.

The aim of the synthesis of Skupin's bola was to have a long hydrocarbon chain separating two carboxylic acids. The inclusion of a double bond present in the chain was also desired, so that various reactions may be carried out on this double bond while immobilised in a membrane. In order to achieve this, one started from hydroxydodecanoic acid (See *Scheme 6.1.*). Initially, the carboxylic acid was protected by making its benzyl ester (i). Reaction of the acid with benzyl bromide proceeded smoothly and efficiently to yield the ester. The hydroxyl moiety was then oxidised to the corresponding aldehyde (ii) using pyridinium chlorochromate (Corey's reagent)[25]. This is a commonly used reagent for the oxidation of alcohols to aldehydes. The purification of the aldehyde was carried out by filtration through a florisil column. This visibly separated the organic compounds from all inorganic by-

products which remained on the column. It was possible to use these florisil columns twice before they lost their effectiveness. The next step of the synthesis was the introduction of the double bond into the molecule. This was carried out using *tert*-butyl P, P-dimethylphosphono acetate which converts the aldehyde into a vinyl group whilst introducing a new ester moiety into the compound by means of a Horner-Emmons reaction[26]. This is similar to a Wittig reaction, but utilises a phosphonate which is more reactive than triphenyl phosphine. In addition, the phosphorous by-product is water soluble, unlike Ph_3PO, which makes it easy to separate from the olefin. The *tert*-butyl ester (iii) may be hydrolysed in the presence of p-toluene sulphonic acid to give the free acid (iv) [27]. This method is highly selective and does not deprotect the benzyl ester to any significant degree. This free acid may then be reacted with any suitable amine to functionalise what will later become the top of the lipid membrane.

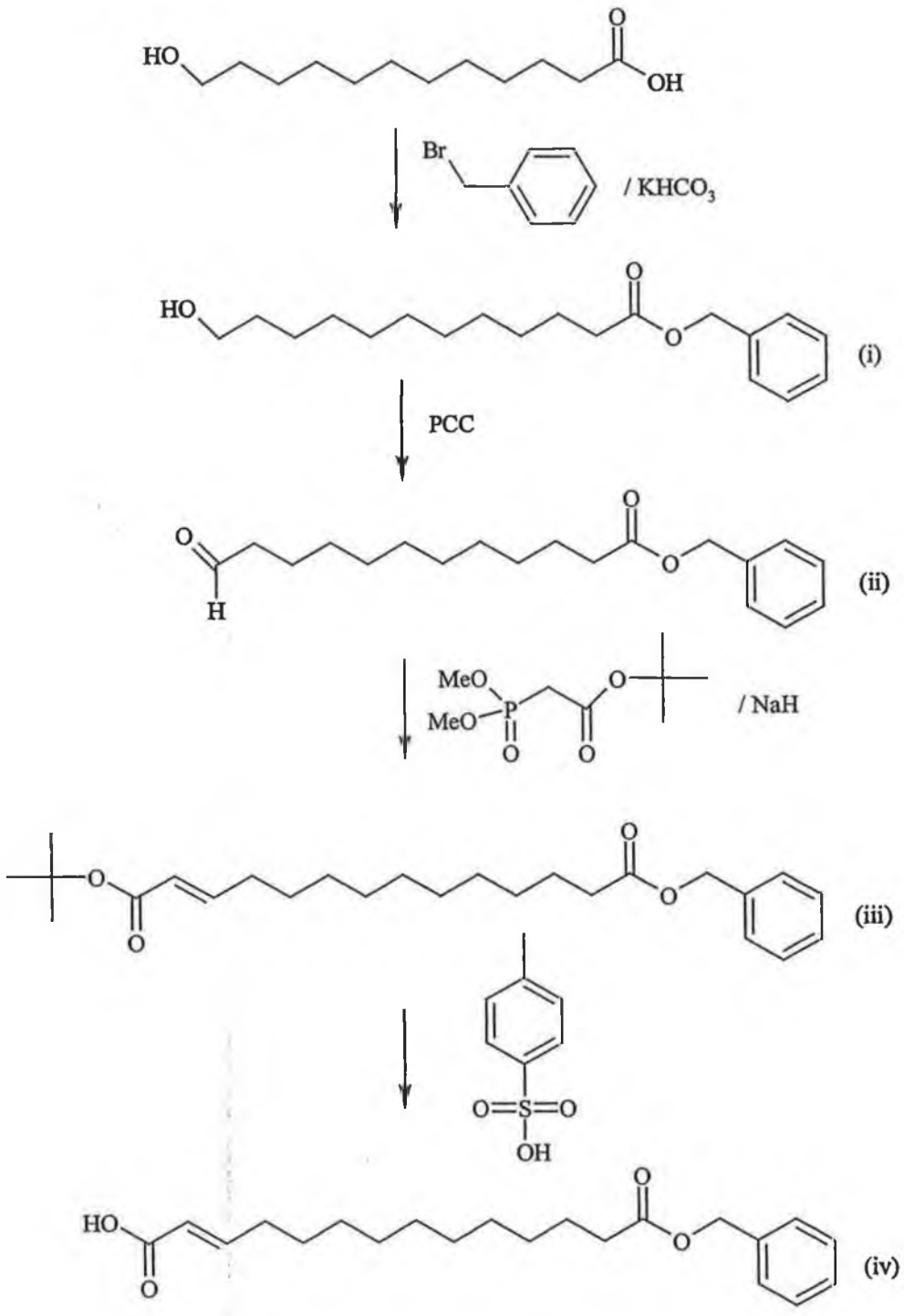

Scheme 6.1. Synthesis of the lipid

5-Substituted 2,2'-bipyridyl compounds are not as common as the corresponding 4,4'-disubstituted derivatives. However, in this case it was desirable to have a 5-

mono-substituted bpy, so as to obtain the correct geometry when placed at the end of the membrane. This asymmetry was not expected to have any adverse effects on the properties of the final metal complex. Upon complexation with a metal, no co-ordination isomers could be formed. This is a major advantage when compared with a pyridyl triazole derivative, which would also have had the correct geometry if it was substituted in the 5 position of the triazole. Coordination isomers may be formed upon complexation with a triazole ligand, as the metal may bind in either the N2 or N4 position. Although the introduction of a bulky substituent into the 5 position of the triazole hinders the formation of the N4 isomer, small amounts (~5-10%) may still be formed. Reproducibility of the experiments on the membranes is already a problem and the additional issue of coordination isomers would further complicate this. With this in mind, 2, 2'-bipyridyl seemed to be the best choice.

When planning the synthesis of the compound it was resolved that the acid derivative of the bpy would firstly be bound to an ethylenediamine spacer to provide extra rigidity and a terminal amine group (*Scheme 6.2.*). The diamine would need to be protected to reduce the formation of the diamide compound. However, once deprotected, this could be reacted with the protected bola, before deprotection and introduction of the terminal thiol (*Scheme 6.3.*). It was decided to proceed in this order due to the expense involved in preparing the protected bola and to aid in the purification of the intermediate compounds.

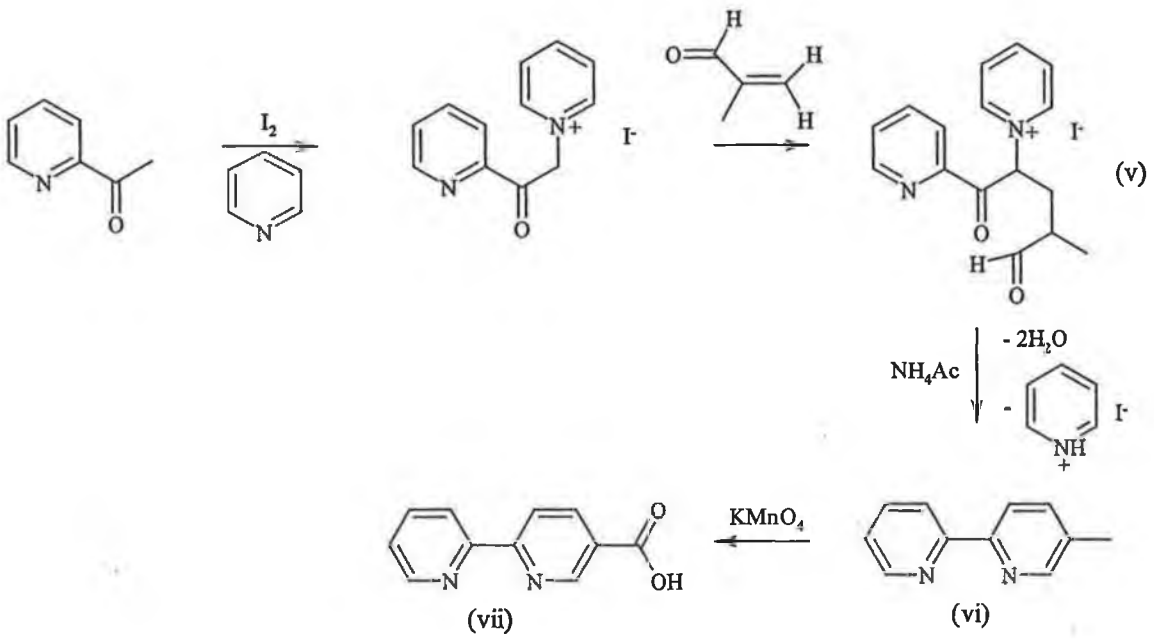

Scheme 6.2. Synthesis of (vii)

Literature methods for the synthesis of 2, 2′-bipyridyl-5-carboxylic acid were based on two methods. One of these methods was the coupling of two pyridine rings, one of which contained an ester in the 5 position, using an organotin coupling reagent. Subsequent hydrolysis of the ester then yielded the acid[28,29]. Other aryl coupling reactions would be possible also, but they have not been investigated to the same extent. However, in an attempt to avoid the use of organotin compounds from a health and safety point of view, it was decided to proceed via the other approach, i.e. direct synthesis of a 5-substituted bpy and its oxidation to the acid. Unfortunately, this is the lesser-used route and the methods described are neither as efficient nor as well defined as would be desired.

There are many methods available to prepare 5-Methyl-2,2'-bipyridyl (vi) [30, 31]. In this case it was prepared according to a method devised by F. Kröhnke et al[19]. This is

an extremely versatile reaction and can be used to make almost any polypyridine derivative desired. The first step in this method is called the King reaction. This involves the removal of an acidic hydrogen from a compound, such as 2-acetyl pyridine, and its replacement by a pyridinium-iodide salt[18]. As a result, one now has a pyridine derivative with an activated methylene group which may later be used as the starting point for the synthesis of the new polypyridyl compound. Treatment of this salt with an unsaturated ketone in the presence of ammonium acetate gives a 1,5-diketone via a Michael addtion. This diketone, which is only rarely isolated, undergoes ring closure on treatment with the ammonium acetate to give the new pyridine ring. The pyridinium moiety introduced in the King reaction is removed as pyridinium iodide in the last step[19,20,21]. Having now made the bpy derivative, the methyl group must be oxidised to the acid (vii). This can be accomplished in a quite straightforward manner, by using potassium permanganate in aqueous solution. This has been shown to function well on methylpyridines[22] but required some optimisation for use on this ligand.

The synthesis of the mono Boc-protected ethylene diamine (viii) proved to be more problematic than expected. This is a commonly used, though quite expensive, commercially available product, but due to financial constraints, it was decided to prepare it rather than purchase it. Of the different methods available to make this compound, only one actually gave good yields of pure monoprotected product. The two reactions which failed to live up to their reported successes were much more complex. One of these involved the synthesis of an interemdiate from Boc anhydride, and the reaction of this *tert*-butyl 4-nitrophenylcarbonate with ethylene

diamine[32]. Although this does produce the desired compound, it does so only in a poor yield requiring subsequent purification. The other method required reacting the HCl salt of ethylene diamine with Boc anhydride in basic propanol followed by repeated recrystalisation[33]. However, the yields reported were not found to be reproducible. However, the method which did work well simply involved the slow addition of Boc anhydride to a large excess of ethylene diamine in ice cold dioxane. By this method, only a small percentage of diprotected amine was prepared and this was easily removed during the work-up of the reaction. Ironically, this was the easiest and most straightforward method.

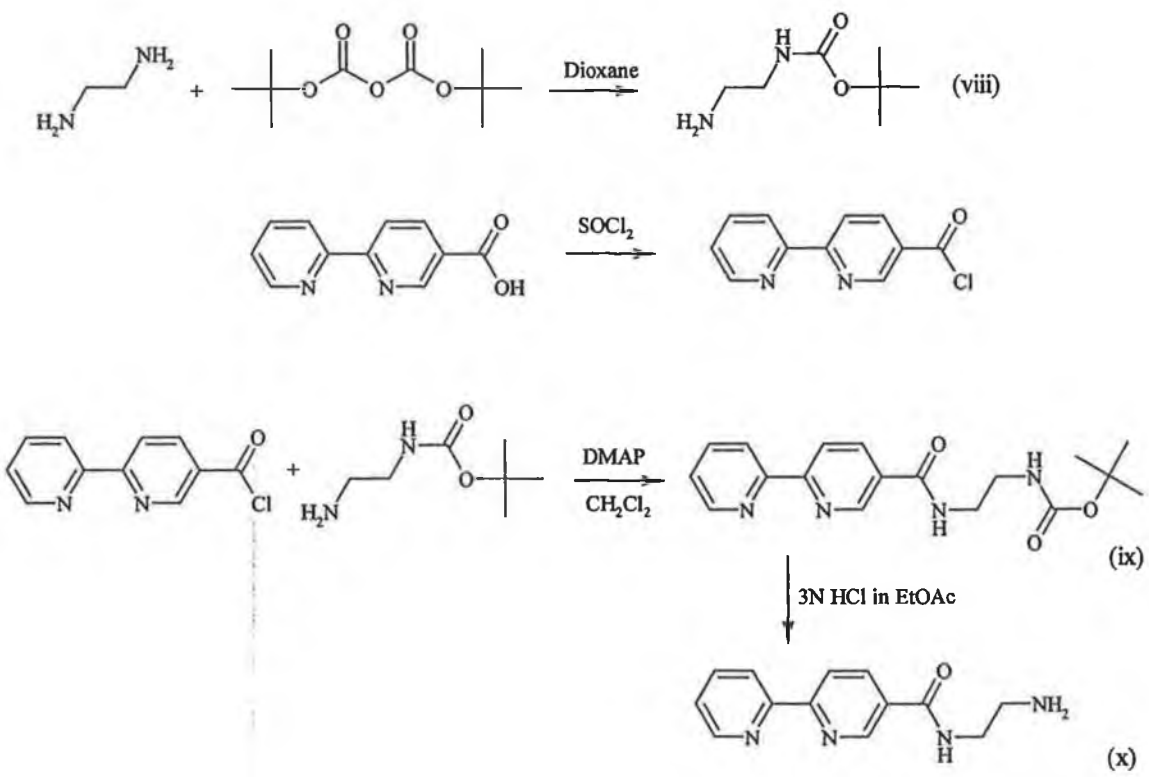

Scheme 6.3. Synthesis of 2, 2′-bipyridyl-5-carboxylic acid (2-amino-ethyl)-amide (x)

The coupling of the bpy acid (vii) with the protected amine was brought about by a standard method (Shown in *Scheme 6.3.*). Heating the acid at reflux in freshly

distilled thionyl chloride gives the acid chloride, which is extremely reactive and must be used immediately. Treatment of this with the amine in a suitable solvent, in the presence of a suitable base would then produce the amide[34,35,36]. The reaction was found to function best in dry dichloromethane with a catalytic amount of 4-N, N-dimethylaminopyridine[37]. The reaction did not proceed well in DMF, nor without the addition of DMAP. Other routes, such as the use of ethyl chloroformate to make the mixed anhydride which is then much more reactive towards amines[38], failed to produce any of the desired compound. BOP has been shown to be moderately successful for the synthesis of amide derivatives of 5-carboxylic acid bpy, but was not used here. The use of DCC (dicyclohexylcarbodiimide) or BBC[39](benzotriazolyloxy-bispyrrolidino-carbonium hexafluorophosphate) as coupling reagents for the direct reaction of the amine and the acid also proved fruitless. DCC and BBC function in a similar manner, by dehydrating the acid to give the anhydride which is then much more reactive towards amines. BBC is however a much better coupling reagent than DCC, with many reaction times being in the order of seconds rather than minutes or hours. It also has the added benefit over other commonly used coupling reagents in that the side product from the reaction is non-toxic, unlike tetramethyl urea which is produced when one uses HBTU (O-benzotriazolyl-N,N,N',N'-tetramethyluronium hexafluorophosphate).

However, once made, the Boc protecting group was easily removed from (ix) at room temperature in a matter of minutes with hydrochloric acid in ethyl acetate to give the free amine (x). It is possible to carry out this deprotection in a number of different ways[40]. The most commonly used method involves treating the amine with

trifluoroacetic acid in dichloromethane. However, other acids such as p-toluene sulphonic acid may also be used. The use of HCl is not solely reserved for ethyl acetate solutions. It has also been shown to work well in both dioxane and methanol, although yields in general appear to be best in EtOAc. Unlike trifluoroacetic acid, which may be removed under reduced pressure, the HCl method produces the salt of the deprotected amine, which must then be neutralised and extracted into a suitable organic solvent.

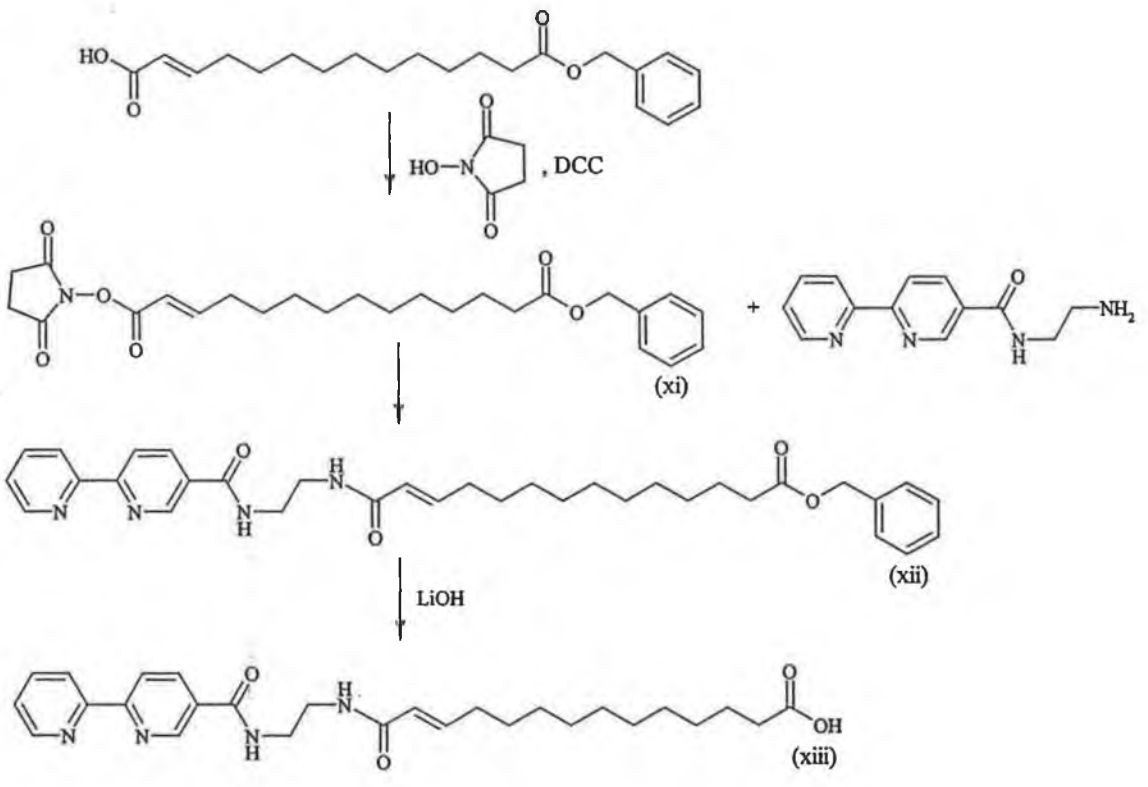

Scheme 6.4. Synthesis of the bipyridyl derivatised bola (xiii)

Again, the coupling of this new amine (x) with the mono-benzylprotected bola (iv) (as seen in *Scheme 6.4.*) caused a few minor problems. The standard method for the introduction of a head group onto this molecule is via the mixed anhydride method mentioned above. This has been shown to be successful for a number of derivatives.

It is a highly versatile method and tends to be easier to purify than when one uses DCC, but it failed to produce significant amounts of the bpy-bola compound. Direct reaction of the two in the presence of DCC was also unsuccessful. Instead of trying to make the acid chloride derivative of the bola, it was decided to activate the acid by means of the synthesis of an active ester. In this case it was N-hydroxy succinimide ester[41] which was made. These are an excellent type of compound. They can be made from the acid in very high yield, usually being separated in a straightforward manner from the acid starting material. In general they are quite robust compounds, being stable at room temperature and neither air, moisture nor light sensitive. They are considerably more reactive towards nucleophiles. From an economic point of view, the cost of the added step in the synthesis is often offset by the increased yield of the two-step reaction when compared to a direct coupling of the acid and the amine. Having prepared the active ester (xi), it reacted readily with the amine to give the amide (xii) in a good yield[42]. Little purification of the amide was required, as the by-product of this method is soluble in water. The benzyl ester was then easily cleaved without any disturbance of any of the peptide bonds by the use of lithium hydroxide in a heterogenous reaction to yield the acid (xiii). This is a mild, yet highly effective method for the base hydrolysis of an ester[43].

At this stage of the synthesis, the new lipid is almost complete. It could be bound directly to a surface such as TiO_2 at this stage, but it would be more desirable to have a thiol tail group. These bind extremely well to gold surfaces. It is essential to have a strong bond between the membrane and the gold, as the bpy must later be complexed with a suitable metal in order to close the pore formed. This step may require some

heating and it is vital that the S-Au bond does not break during this reaction. Should one use a metal such as ruthenium, then heat may be required to form the Ru-bpy bonds. However, using metals such as copper or iron, which have lower activation energies, would not require as much heat to form the complex. Unfortunately, the complexes thus formed would not be as stable as those of ruthenium and reproducible analysis would be even more difficult.

The terminal thiol would normally be introduced by reaction of the free acid with cystamine to give the disulphide intermediate. This disulphide can be easily reduced to the thiol by sodium borohydride or lithium aluminium hydride[44]. These two steps have previously been used in the synthesis of many similar membrane structures. The use of cystamine as the source of the thiol is an important factor. Firstly it introduces a new peptide linkage to the base of the membrane. This gives added stability which helps define the walls of the pore, by means of hydrogen bonding between the lipid molecules. Secondly, the distance from the gold surface to the amide is then also ideal for hydrogen bonding between the carboxylate groups of the porphyrin and the amide. This again produces a well-defined pore and increases its stability and rigidity. This work is currently being undertaken by Prof. Fuhrhop's research group in the FU Berlin.

The synthesis of the ruthenium complexes with the ligands (vii), (ix), (x), (xii) and (xiii) (see *Fig. 6.7.*) was carried out using standard methods. The acid (vii) and the Boc-protected amine (ix) were each complexed directly by their reaction with $[Ru(bpy)_2Cl_2].2H_2O$. The complex $[Ru(bpy)_2(vii)](PF_6)_2$ was purified by column

chromatography on silica. However, due to its highly polar nature it tended to bind to the silica. It proved difficult to remove completely from the column in a pure form and so only a moderate yield for the reaction was obtained. The complex of the ligand (ix) was isolated from the reaction mixture in a pure form and required only recrystalisation. This accounts for the very high yield of the reaction. The ruthenium complex of (x) was prepared by cleaving the Boc group on a small amount of $[Ru(bpy)_2(ix)](PF_6)_2$ by the same method used for the free ligand. The reaction time was longer than before and the yield was slightly lower, but again very little purification was needed. Similarly, whilst $[Ru(bpy)_2(xii)](PF_6)_2$ was prepared by heating the ligand under reflux with the dichloride, $[Ru(bpy)_2(xiii)](PF_6)_2$ was synthesised via hydrolysis of the benzyl ester in boiling basic methanol/water. Neither compounds required chromatographic purification.

It is hoped that the study of the ruthenium complexes prepared will give an insight into their photophysical/electrochemical properties. It is important to be aware of these properties before attempting to study the membrane-bound structures.

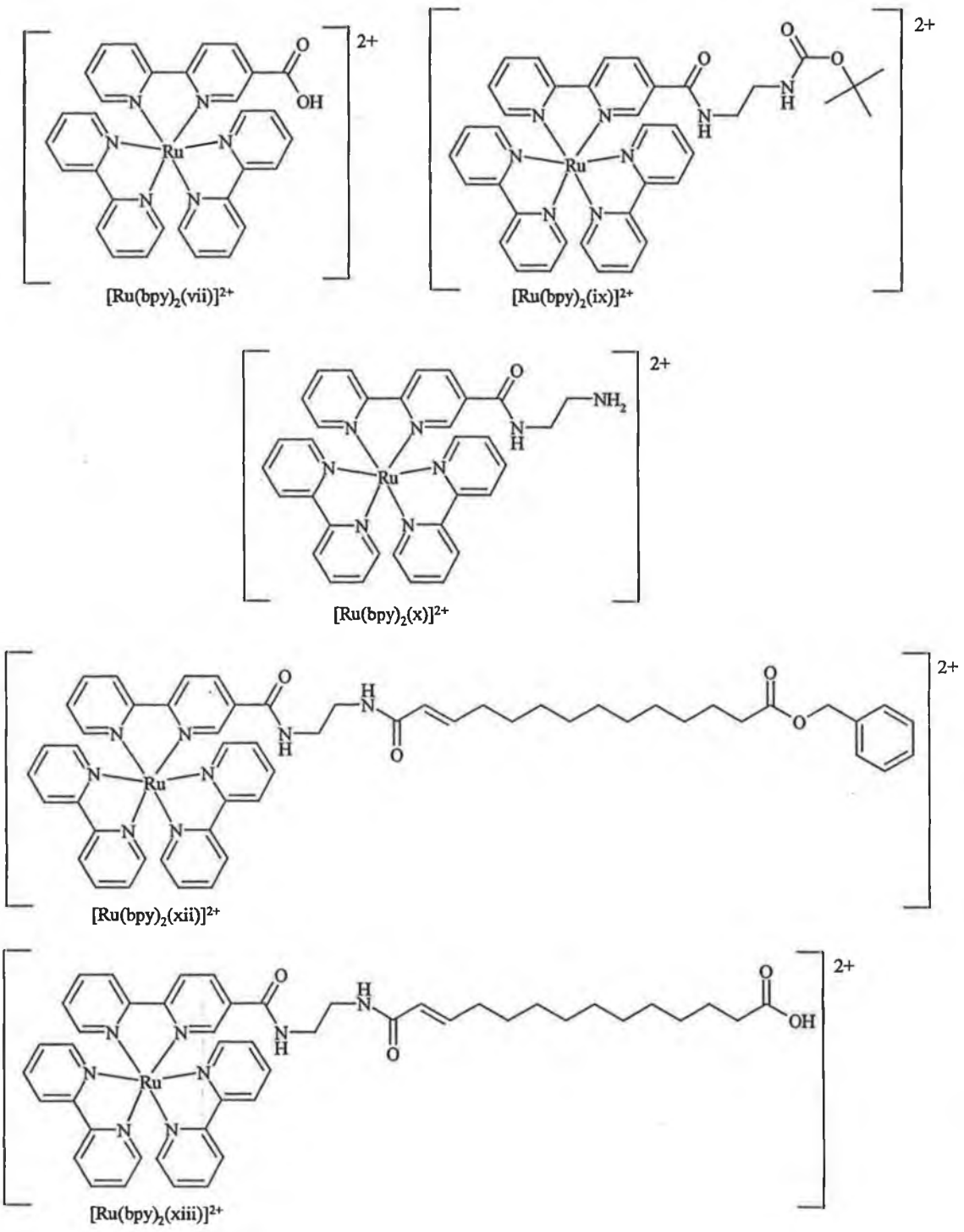

Fig. 6.7. Structures of the ruthenium complexes prepared

6.3.2 Characterisation

Each of the intermediates in the synthesis of the bola were characterised by spectroscopic means and by mass spectrometry. All of the complexes made here have been studied by electrochemical and spectroscopic means. It was intended to investigate their properties in order to compare them with those of $[Ru(bpy)_3]^{2+}$. Shifts in the positions of absorption and emission maxima, as well as altered oxidation and reduction potentials were expected. An investigation of these shifts should help in the determination of the location of the excited state in each of the complexes.

6.3.3 NMR Spectroscopy

The synthesis of the bola (xiii) was followed closely by NMR spectroscopy. The most striking feature in the spectra of the bola was the huge signal at 1.27ppm, obtained for the many protons in the hydrocarbon chain (See *Fig. 6.8.*). Although the protons on the carbons α- to the terminal functionalities were clearly visible at 2.19 and 2.28ppm and showed clear coupling with the adjacent protons, those on the β-carbons were less well defined, being positioned extremely close, at 1.41 and 1.60 ppm, to the large peak for all of the remaining protons in the hydrocarbon chain. It is unsurprising that all of these protons appear in the same position, as even long-range coupling would still mean interaction with more methylene protons. The protons present on the double bond introduced into the compound also display typical

signals. The vinylic α-proton at 5.94ppm shows up as a doublet because it only couples with the other vinylic proton in the β-position at 6.81ppm. A J-value of 11Hz is also typical of a *trans*-configuration. The multiplicity of the β-proton is more complicated as it is further split by its adjacent aliphatic proton, giving a doublet of triplets.

In the case of the bipyridine derivatives, the asymmetry of the ligands became an important factor. The introduction of the methyl group onto one ring of the bpy results in a singlet and two doublets for the aromatic protons of that ring, while the unsubstituted ring still gives the usual splitting pattern of bipyridine[45]. The chemical shifts of the 3 protons on the 5-substituted ring change upon alteration of the substituent. The signal for the proton in the 4 position ranges between 7.55 and 8.48ppm, whilst that of the proton in the 3 position only ranges between 8.35 and 8.69ppm. However, this change is clearest in the position of the signal from the H6 proton of the substituted ring, which is the easiest proton to follow, as it is a singlet and never overlaps with any of the other protons in the spectra. In the case of the methyl bpy it appears at 8.59ppm. The H6 signal in the corresponding amide compound (viii) is shifted downfield to 9.11ppm.

The proton NMR spectrum of the bipyridyl derivatised bola shows all of these properties. The splitting of the bpy protons are clear and the protons are easily assignable. The signals from the various protons in the bola are all also present and clean. Unfortunately, due to the insolubility of this compound, it was not possible to prepare a sample in exactly the same solvent system as was used for measuring the

benzyl ester (xi). As a result, it was not possible to directly compare the spectra of the two compounds. However, as can be seen from the spectrum shown below, the benzyl group was cleaved cleanly to give a very pure sample of the free acid.

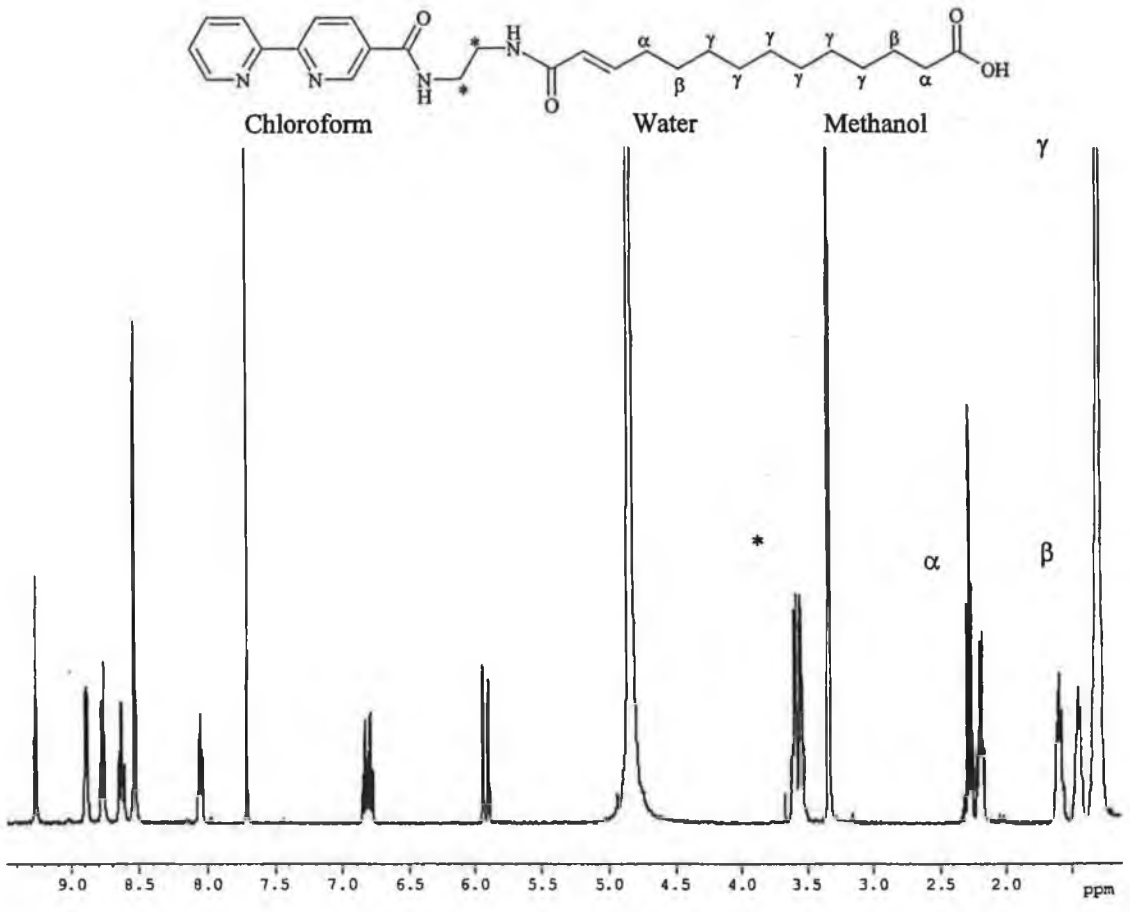

Fig. 6.8. ^{1}H NMR spectrum of bipyridyl derivatised bola in CD_3OD/CD_3Cl (4:1)

The NMR spectra of the ruthenium complexes show many of the standard features observed for such compounds[46]. Upon coordination with the metal centre, a significant change in the spectrum of the ligand is expected. This is mainly due to three reasons. Firstly, upon coordination, the two nitrogens of the bipyridine, which are trans to each other in the free ligand, must rotate to face in the same direction. This results in steric strain being placed on the two protons in the 3 and 3' positions. They are thought to bend slightly out of the plane of the ligand to reduce this strain.

A second reason is due to the electronic interaction that the ligand experiences from the metal centre. In general, downfield shifts observed on chelation may be attributed to a decrease in electron density caused by ligand interaction with the ruthenium(II) cation. The third reason is due to the spatial arrangement of the compound. Protons in the 6 and 6' positions may feel an effect from the ring current of another bipyridine due to their position directly above the ring. In the case of the complexes presented here, the spectra are further complicated by the asymmetry of the ligands.

Normally in the case of a compound of the form $[Ru(bpy)_3bpy']^{2+}$, where bpy' is a symmetrically disubstituted bipyridyl, the signals obtained for each of the two other bpy molecules should be the same. The two rings of the bpy (A and B in *Fig. 6.9.*) are in unique environments, one being trans to a substituted ring and the other trans to an unsubstituted ring. In this way it is possible to distinguish between the two rings of a bpy, but not between the two bpy ligands.

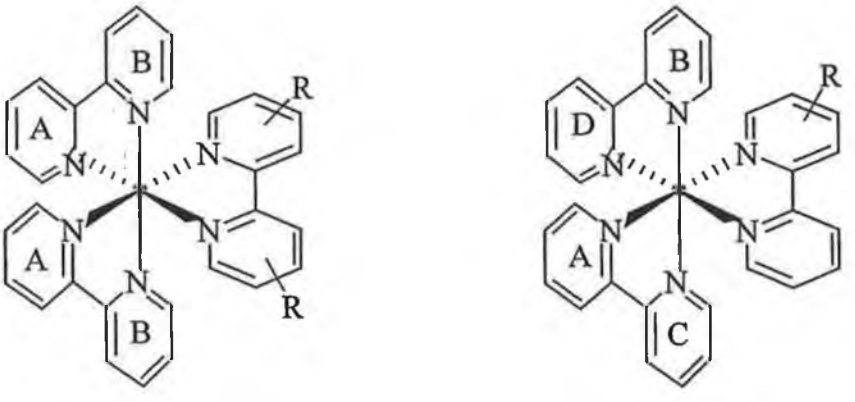

Disubstituted bpy' Monosubstituted bpy'

Fig. 6.9. Comparison of the symmetry of $[Ru(bpy)_2bpy']^{2+}$ complexes

In the case of the complexes prepared here, the asymmetry of the substituted bpy' means that the other two bpy ligands are no longer equivalent. One has both rings (B and D in *Fig. 6.9.*) trans to other unsubstituted rings. However, B and D interact differently through space with the substituted ring of bpy'. The other bpy ring has one ring, (A in *Fig. 6.9.*), trans to the substituted ring of bpy' and the other ring (C) is trans to an unsubstituted ring. As a result, definite assigment of the protons in complexes such as these becomes a much more difficult task, requiring both 2D NMR experiments and comparison with similar compounds[47].

However, as the spectra in *Fig. 6.10.* show, the shifting of the ligand peaks may be followed by obtaining the NMR spectra of both the free ligand and the complex in the same solvent. The most significant shift is seen for H6 which is shifted downfield from 9.12 to 7.95 upon complexation. Other peaks, such as H4', show little or no change. This is typical behaviour for such compounds[48].

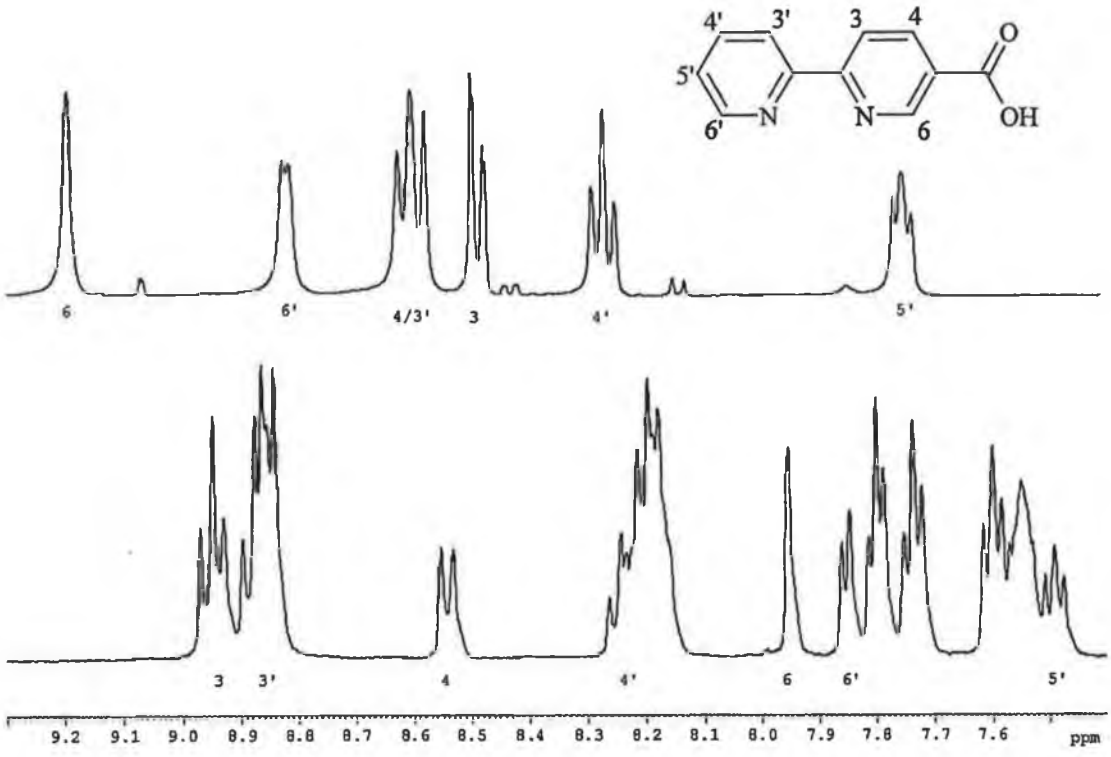

Fig. 6.10. ^1H NMR Spectra of (vii) (top) and [Ru(bpy)$_2$(vii)](PF$_6$)$_2$ (bottom) in d$_6$-DMSO showing the positions of the (vii) protons

6.3.4 UV/Vis Absorption and Emission Spectroscopy

The UV/vis spectra of all compounds show the standard features (see *Fig. 6.11.*). Strong π-π^* bands appear in the region of ~280nm due to the pyridine rings, whilst the characteristic d-π^* MLCT band typically appears in the region of ~450nm. The exact λ_{max} for each of the compounds varies only very slightly as can be seen from *Table 6.1* below. This is the first indicator of any differences in the properties of the ruthenium centres brought about by the introduction of a functional group on one of the bpy ligands. It can also be seen that the extinction coefficients (ε) of the complexes are affected by these substituents.

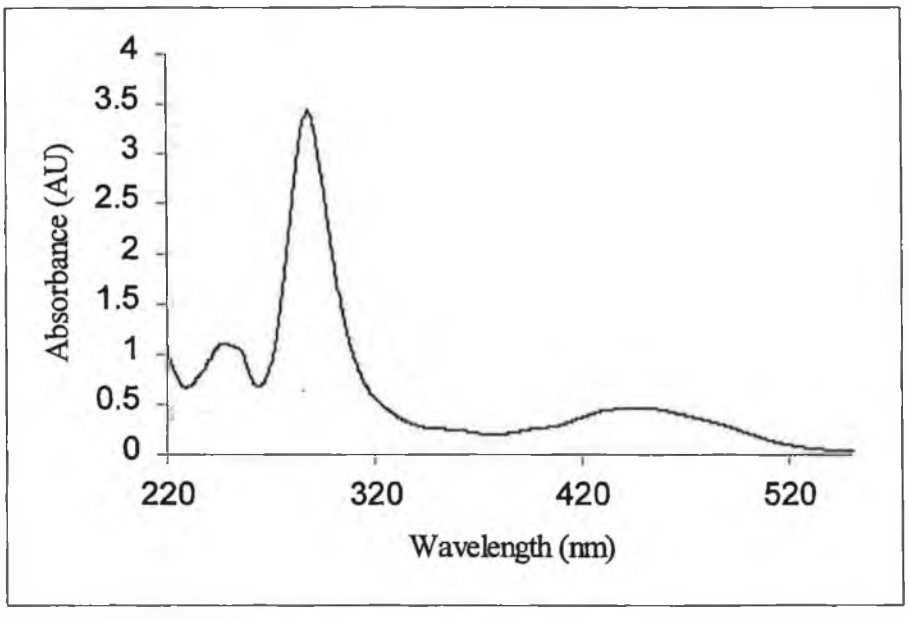

Fig. 6.11. UV/vis absorption spectrum of [Ru(bpy)$_2$(vii)](PF$_6$)$_2$ at 5.3x10^{-5}M in acetonitrile at room temperature

Compound	λ_{max}/nm ($\varepsilon/10^4 M^{-1}cm^{-1}$)	Emission λ_{max}/nm	Lifetime/ns (± 10%)	
			Aerated	Degassed
$[Ru(bpy)_2(vii)](PF_6)_2$	445 (0.88)	673	115	170
$[Ru(bpy)_2(ix)](PF_6)_2$	452 (1.37)	652	180	460
$[Ru(bpy)_2(x)](PF_6)_2$	450 (0.82)	662	190	490
$[Ru(bpy)_2(xii)](PF_6)_2$	452 (1.15)	651	185	480
$[Ru(bpy)_2(xiii)](PF_6)_2$	450 (1.12)	655	188	480
$[Ru(bpy)_3](PF_6)_2$	452 (1.29)	612	180	485

Table 6.1. Spectral data for ruthenium complexes in acetonitrile at room temperature

The fact that the position of the MLCT varies only slightly between the three new compounds is not unusual. Any differences in the bpy derivatives occur on the carbonyl group attached in the 5 position. This means that the electron withdrawing nature of the carbonyl is the most important influence on the electronic properties of the complex. Whether the carbonyl is part of an acid or an amide only heightens or weakens this effect. The major shifts in the MLCT that have been observed for other substituted bpy complexes[49] were not observed here. At this point it is not possible to say what influence the introduction of these substituents has had on the location of the excited state. In order to do this, both the emission and electrochemical properties must first be studied.

It was hoped that the emission properties of these complexes would be of a similar nature to those of $[Ru(bpy)_3]^{2+}$, so as to make their surface chemistry less complicated. As can be seen from *Fig. 6.12.*, the emission spectrum of these compounds takes the standard shape. However, the intensity of the emission of these compounds is less than that of $[Ru(bpy)_3]^{2+}$, and the wavelengths are shifted to lower energies. It has been shown that the introduction of an electron withdrawing substituent into a bpy ring shifts the emission maximum to lower energy[48]. The red shift of the emission here (see *Table 6.1.*) is an indicator that the excited state is located on the substituted bpy ligand. Emission occurs from the lowest energy level to the ground state. Since going from $[Ru(bpy)_3]^{2+}$ to $[Ru(bpy)_2bpy']^{2+}$ results in a red shift in the emission wavelength, one can deduce that bpy' is at a lower energy level than bpy. This would imply that the excited state is most likely located on the substituted bpy.

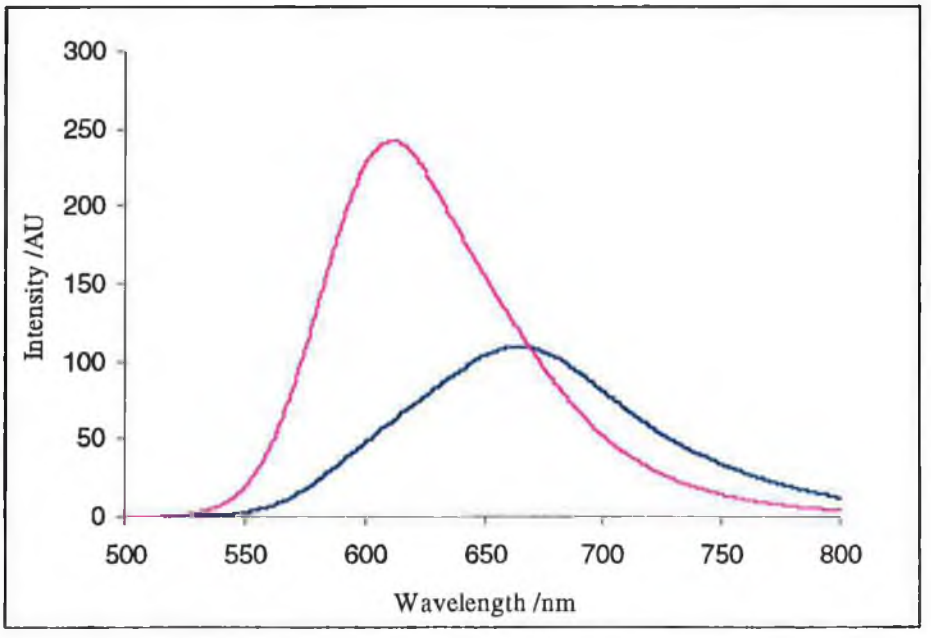

Fig. 6.12. Emission spectrum of $[Ru(bpy)_3](PF_6)_2$ (pink) and $[Ru(bpy)_2(vii)](PF_6)_2$ (blue) in acetonitrile, excited @ 464nm

It is not easy to see a direct correlation between the nature of the substituent on the bpy and the position/intensity of the emission. All substituents are electron withdrawing in nature. However, going from the acid (vii) to the protected amine (ix) and on to the free amine (x) does reduce the electron withdrawing effect of the group, but this is difficult to quantify. Upon elongation of the chain, it becomes more difficult again to quantify this change.

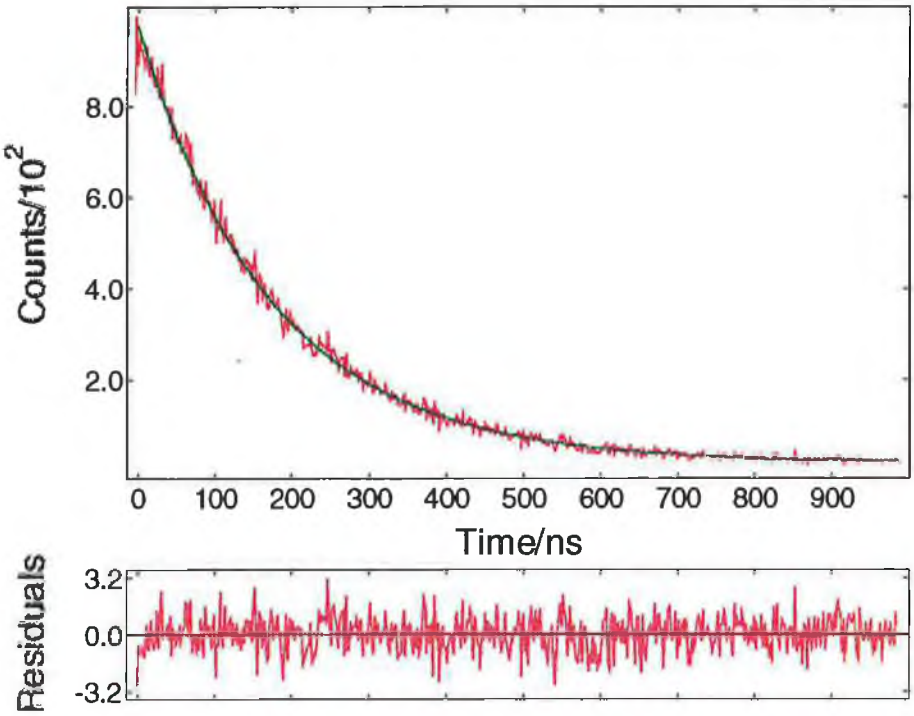

Fig. 6.13. Lifetime measurement (decay, fit and residuals) of [Ru(bpy)$_2$(vii)](PF$_6$)$_2$ in acetonitrile (degassed)

The aerated samples' lifetimes are of the same order of magnitude as that of a sample of $[Ru(bpy)_3]^{2+}$. The four samples mentioned were all measured under identical conditions. Normally, aerated lifetimes are considered inaccurate due to dissolved oxygen in the sample and are therefore not reproducible to a high degree of accuracy.

However, by measuring all the samples under identical conditions, it was hoped that any quenching by oxygen would be constant. Measurement of the degassed lifetimes verified this point, as the lifetimes for two of the complexes increased to the same degree as that for $[Ru(bpy)_3]^{2+}$. The fact that the lifetime of the acid (vii) complex did not increase warrants further investigation. pK_a measurements on the acid complex would also possibly aid in the location of the excited state, as was seen in Section 3.3.6 and 4.3.6, but were not carried out here.

One would normally expect a ruthenium tris-bipyridine derivative to have a lifetime of approximately 1μs when properly degassed. However, to achieve this, one needs to use an efficient freeze/thaw cycle to be certain of removing all dissolved gasses. Unfortunately, this facility was not available for these measurements, so all samples were degassed by bubbling argon through them for 10 minutes prior to use. In order to keep the samples free of oxygen, they were degassed and measured in a cuvette fitted with an airtight septum. While this is not the ideal way to degas a sample, it serves its purpose well and gives a good indication of the behaviour of the complexes.

These compounds have shown that they have suitable photochemical properties to make them useful as photosensitisers. The absorption and emission spectra show differences to those of $[Ru(bpy)_3]^{2+}$, but are not drastically different. One must bear in mind that these are model compounds of the final membrane bound system. One can only speculate as to how the photochemical properties of the complex would be affected after immobilising the membrane on a gold surface.

6.3.5 Electrochemical Properties

The oxidation of the metal centre and the ligand based reductions have been measured for each of the complexes. In order to provide a comparison, the oxidation and reduction potentials of $[Ru(bpy)_3]^{2+}$ have also been included. A comparison of the values obtained for the three complexes prepared earlier with $[Ru(bpy)_3]^{2+}$ (see *Table 6.3*) would help in the prediction of the location of their excited states. Should the derivatised bpy ligand be a stronger π-acceptor, then one would expect a higher oxidation potential and a less negative first reduction potential. This would indicate that the excited state is probably located upon the derivatised bpy. However, care is required. Due to the substituents present on the bipyridines, one might also see a reduction of the extra functional group present.

Compound	Oxidation Potential /V	Reduction Potentials /V
$[Ru(bpy)_2(vii)](PF_6)_2$	1.33	-1.40, -1.59, -1.85 (irr.)
$[Ru(bpy)_2(ix)](PF_6)_2$	1.30	-1.16, -1.51, -1.74
$[Ru(bpy)_2(x)](PF_6)_2$	1.28	-1.38, -1.53, -1.73
$[Ru(bpy)_2(xii)](PF_6)_2$	1.34	-1.29, -1.44, -1.73
$[Ru(bpy)_2(xiii)](PF_6)_2$	1.33	-1.18, -1.50, -1.73
$[Ru(bpy)_3].2PF_6$	1.26	-1.35, -1.55, -1.80

Table 6.3. Oxidation and reduction potentials (vs SCE) of ruthenium complexes measured in 0.1M TEAP in acetonitrile at 200mV/sec

There is no great difference between the Ru^{II}/Ru^{III} oxidation potentials of the series of complexes, although a slight increase is evident for the complexes when compared with $[Ru(bpy)_3]^{2+}$ (See *Table 6.3*). The peak-to-peak separations range from 60 to 120mV, indicating varying degrees or reversibility. No decomposition of the compounds was observed in the region of 0 – 1.8V.

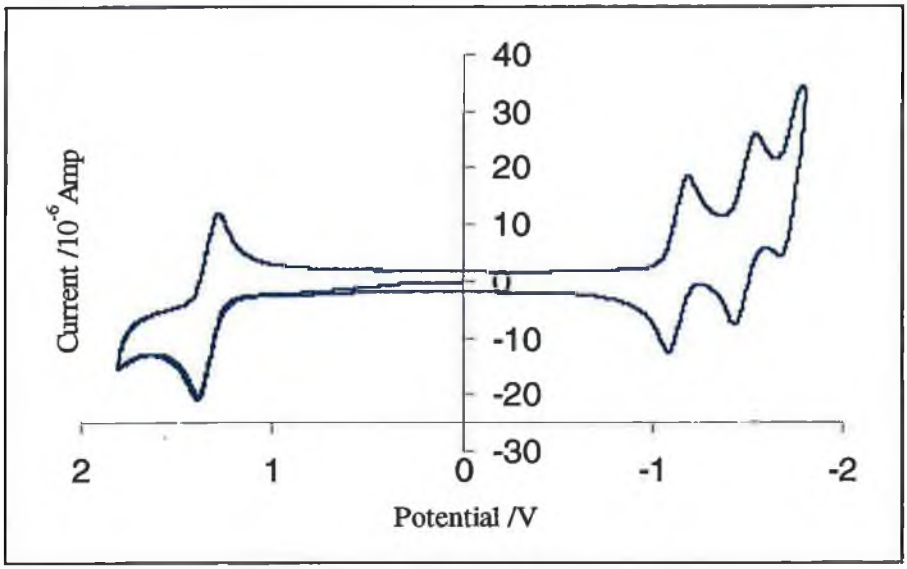

Fig. 6.14. Cyclic voltamagram showing the oxidation and some reductions of $[Ru(bpy)_2(ix)](PF_6)_2$, measured in 0.1M TEAP in acetonitrile at 200mV/sec

The measurement of the reduction potentials was carried out under the same conditions, i.e. in 0.1M TEAP in acetonitrile at room temperature. However, the samples were also degassed prior to measurement. An example of one of the cyclic voltammagrams measured is shown in *Fig. 6.14.* above. The reduction potentials compare well with those obtained for $[Ru(bpy)_3]^{2+}$. All reductions, except the third reduction of $[Ru(bpy)_2(vii)]^{2+}$ with a peak-to-peak value of 150mV, are reversible. However, the first reductions of $[Ru(bpy)_2(ix)]^{2+}$ and $[Ru(bpy)_2(xii)]^{2+}$ are significantly lower. It is possible that this reduction involves some form of reduction

significantly lower. It is possible that this reduction involves some form of reduction of the functional group. In the presence of oxygen at potentials more negative than -1.4V, the reduction peak at –1.16V decays, forming a new peak at –1.36V. Further investigation of this, possibly involving preparative scale electrochemistry, would be necessary to fully explain this process.

The increase of the oxidation potentials due to the substituted bpy's indicates an increase in their π-acceptor nature. The magnitude of this increase is not particularly high. The changes in the first reduction potentials of the complexes, with respect to that of $[Ru(bpy)_3]^{2+}$, are difficult to interpret. Should one assume that those at approx. -1.16V are due to the reduction of the modified bpy's, then these may be disregarded as "real" reductions of the complexes. Then the reductions at –1.36V are comparable with those of $[Ru(bpy)_3]^{2+}$. Had there been a shift in these values to less negative values, then one could have assumed that the excited state lies on the substituted bpy. This would have been in line with the results obtained from the emission spectra.

Further electrochemical analysis or analysis by means of Raman spectroscopy, or spectroscopic measurement of the corresponding $[Ru(d_8\text{-bpy})_2bpy']^{2+}$ complexes would also be necessary to unequivocally determine the excited state location for each of the complexes.

6.5 Conclusion

In conclusion, it can be said that the synthesis of the novel lipid with a terminal bpy group has been a success. At this stage it could be attached to a suitable surface such as TiO_2 and the effects on the spectroscopic and electrochemical properties studied. This will be undertaken by Prof. Fuhrhop's research group. Yields are satisfactory and purification is quite straightforward. All intermediates of the synthesis have been characterised by melting points, NMR spectroscopy and mass spectrometry. The synthesis of model ruthenium complexes, each bearing a different 5-substituted 2,2'-bipyridyl, yielded pure complexes in varying yields.

Characterisation of these complexes by spectroscopic and electrochemical means has shown the differences which the introduction of these substituents can bring about in the properties of $[Ru(bpy)_3]^{2+}$. Absorption spectra were not significantly altered, with λ_{max} shifting by no more than 7nm. Emission maxima are red shifted by up to 60nm, indicating that the excited state is probably located on the derivatised bpy in each of the three cases due to their electron withdrawing nature. The lifetimes of the complexes (with the exception of $[Ru(bpy)_2(vii)]^{2+}$) were shown to be comparable with those of $[Ru(bpy)_3]^{2+}$. Electrochemical analysis has shown a slight increase in the oxidation potential of the ruthenium in each of the complexes. No significant change in the reduction potentials was observed for two of the compounds, whilst for the remaining complexes a significant shift was evident, possibly due to reduction of the substituent on the derivatised bpy ligand.

These complexes are ideal models to characterise the ruthenium centre, prior to its inclusion in the membrane. They have similar properties to $[Ru(bpy)_3]^{2+}$, but with the possibility of locating the excited state on the substituted bpy ligand.

6.5 Bibliography

[1] Fuhrhop, J. H.; Liman, U.; Koesling, V; *J. Am. Chem. Soc.* **1988**, 110, 6840

[2] Fuhrhop, J.H.; David, H. H.; Mathieu, J.; Liman, U.; Winter, H. J.; Boekema, E.; *J. Am. Chem. Soc.* **1986**, 108, 1785

[3] Böhme, P.; Hicke, H. G.; Boettcher, C.; Fuhrhop, J. H.; *J. Am. Chem. Soc.*, **1995**, 117, 5824

[4] Fuhrhop, J. H.; Fritsch, D.; *Acc. Chem. Res.*, **1986**, 19, 130

[5] Laibnis, P. E.; Nuzzo, R. G.; Whitesides, G. M.; *J. Phys. Chem.*, **1992**, 96, 5097

[6] Bain, C. D.; Whitesides, G. M.; *J. Am. Chem. Soc.*, **1988**, 110, 3665

[7] Fuhrhop, J. H.; Liman, U.; *J. Am. Chem. Soc.*, **1984**, 106, 4643

[8] Fuhrhop, J. H.; Mathieu, J.; *Angew. Chem. Int. Ed. Engl.*, **1984**, 23, 100

[9] Fuhrhop, J. H.; Liman, U.; David, H. H.; *Angew. Chem. Int. Ed. Engl.*, **1985**, 24, 339

[10] Colvin, V. L.; Goldstein, A. N.; Alivisatos, A. P.; *J. Am. Chem. Soc.*, **1992**, 114, 5221

[11] Atre, S. V.; Liedberg, B.; Allara, D. L.; *Langmuir*, **1995**, 11, 3882

[12] Bain, C. D.; Whitesides, G. M.; *Angew. Chem. Int. Ed. Engl.*, **1989**, 28, 506

[13] Fuhrhop, J. H.; Bedurke, T.; Gnade, M.; Schneider, J.; Doblhofer, K.; *Langmuir*, **1997**, 13, 455

[14] Bilewicz, R.; Sawaguchi, T.; Chamberlain II, R. V.; Majda, M.; *Langmuir*, **1995**, 11, 2256

[15] Fudikar, W.; Zimmermann, J.; Ruhlmann, L.; Schneider, J.; Röder, B.; Siggel, U.; Fuhrhop, J. H.; *J. Am. Chem. Soc.*, **121**, (1999), 9539

[16] Wagner, P.; Hegner, M.; Güntherodt, H. J.; Semenza, G.; *Langmuir*, **1995**, 11, 3867

[17] Skupin, M.; Li, G.; Fudiakr, W.; Zimmermann, J.; Röder, B.; Fuhrhop, J. H.; *J. Am. Chem. Soc.*, **123**, (2001), 3454

[18] Kröhnke, F.; Gross, K. F.; *Chem. Ber.*, **1959**, 92, 22

[19] Kröhnke, F.; *Angew. Chem.*, **1963**, 75, 181

[20] Kröhnke, F.; Zecher, W.; *Angew. Chem.*, **1962**, 74, 811

[21] Kröhnke, F.; *Synthesis*, **1976**, 1

[22] Black, G.; Depp, E.; Corson, B. B.; *J. Org. Chem.*, **1949**, 14, 14

[23] Krapcho, A. P.; Kuell, C. S.; *Synth. Commun.*, **1990**, 20, 2559

[24] Lochner, M.; Geneste, H.; Hesse, M.; *Helv. Chim. Acta*, **1998**, 81, 2269

[25] Corey, E. J.; Suggs, J. W.; *Tetrahedron Lett.*, **1975**, 2647

[26] Bardili, B.; Marschall-Weyerstahl, H.; Weyerstahl, P.; *Liebigs Ann. Chem.*, **1985**, 275

[27] Anderson, G. W.; Callahan, F. M.; *J. Am. Chem. Soc.*, **1960**, 82, 3359

[28] Ghadiri, M. R.; Soares, C.; Choi, C.; *J. Am. Chem. Soc.*, **1992**, 114, 825

[29] Panetta, C. A.; Kumpaty, H. J.; Heimer, N.; Leavy, M. C.; Hussey, C. L.; *J. Org. Chem.*, **1999**, 64, 1015

[30] Kelly-Basetti, B. M.; Krodkiewska, I.; Sasse, W. H. F.; Savage, G. P.; Simpson, G. W.; *Tetrahedron Lett.*, **1995**, 36, 327

[31] Potts, K. T.; Winslow, P. A.; *J. Org. Chem.*, **1985**, 50, 5405

[32] Hyrup, B.; Egholm, M.; Nielsen, P. E.; Wittung, P.; Norden, B.; Buchardt, O.; *J. Am. Chem. Soc.*, **1994**, 116, 7964

[33] Videnov, G.; Aleksiev, B.; Stoev, M.; Paipanova, T.; Jung, G.; *Liebigs Ann. Chem.*, **1993**, 941

[34] Belser, P.; Dux, R.; Baak, M.; De Cola, L.; Balzani, V.; *Angew. Chem.*, **1995**, 107, 634

[35] Belser, P.; Von Zelewsky, A.; Frank, M.; Seel, C.; Vögtle, F.; De Cola, L.; Barigelletti, F.; Balzani, V.; *J. Am. Chem. Soc.*, **1993**, 115, 4076

[36] Maggini, M.; Dono, A.; Scorrano, G.; Prato, M.; *J. Chem. Soc. Chem. Commun.*, **1995**, 845

[37] Van Esch, J. H.; Hoffmann, M. A. M.; Nolte, R. J. M.; *J. Org. Chem.*, **1995**, 60, 1599

[38] Schneider, J. A.; *Ph.D. Thesis*, **1997**, Freie Universität, Berlin

[39] Chen, S.; Xu, J.; *Tetrahedron Lett.*, **1992**, 33, 647

[40] Cavelier, F.; Enjalbal, C.; *Tetrahedron Lett.*, **1996**, 37, 5131

[41] Anderson, G. W.; Zimmerman, J. E.; Callahan, F. M.; *J. Am. Chem. Soc.*, **1964**, 86, 1839

[42] Cline, G. W.; Hanna, S. B.; *J. Org. Chem.*, **1988**, 53, 3583

[43] Corey, E. J.; Su, W.; *Tetrahedron Lett.*, **1990**, 31, 2089

[44] Arnold, R.C.; Lien, A. P.; Alm, R. M.; *J. Am. Chem. Soc.*, **1950**, 72, 731

[45] Huang, T. L. J.; Brewer, D. G.; *Can. J. Chem.*, **1981**, 59, 1689

[46] Bell-Loncella, E. T., Bessel, C. A.; *Inorg. Chim. Acta*, **2000**, 303, 199

[47] Steullet, V.; Dixon, D. W.; *J. Chem. Soc. Perkin Trans. 2*, **1999**, 1547

[48] O'Connor, C. M.; *Ph.D. Thesis*, **1999**, Dublin City University

[49] Cook, M. J.; Lewis, A. P.; McAuliffe G. S. G.; Skarda, V.; Thomson, A. J.; Glasper, J. L.; Robbins, D. J.; *J. Chem. Soc. Perkin Trans. II*, **1984**, 1293

Chapter 7

Conclusions and Future Work

7.1 Conclusions

Photosynthesis is a remarkably complex process, through which plants may harvest sunlight and use it to convert water and carbon dioxide into sugars and molecular oxygen. While some aspects may be well understood, many of the initial fundamental processes remain enigmatic. It is known that light is harvested by an antenna of porphyrins. This sets off an electron transfer chain reaction resulting in the transfer of an electron from a manganese cluster *via* a tyrosine residue to P_{680}. After four repetitions of this cycle, the manganese is reduced to its original form with the concomitant oxidation of two molecules of water. This water-splitting reaction is the step which makes an investigation of the process all the more enticing. Could one mimic this catalytic reaction efficiently, a potential source of clean, renewable energy would be available. It was the purpose of the work presented in this thesis to design, synthesise and characterise possible materials, which may be used to prepare biomimetic models of the process of catalytic photooxidation of water described above.

The approach taken in the study presented here was to use ruthenium (II) polypyridyl complexes as photosensitisers, as they have been long known to have suitable electronic properties for the oxidation of water. It was hoped to utilise these complexes to build supramolecular systems, capable of displaying electron/energy transfer in a manner similar to the processes observed in photosystem II (PSII). Two different approaches to this end were investigated.

The first approach to this goal involved the synthesis of covalently linked ruthenium-manganese and ruthenium-tyrosine systems. Both manganese complexes and tyrosine are present in PSII, where they serve as electron donors. They have also both been shown to function well as electron donors to photooxidised ruthenium complexes.

Initially, a range of novel pyridyl triazole ligands, bearing various of terminal functional groups, were designed and synthesised. These were hoped to be used later as synthons for the introduction of amine derived potential manganese chelating ligands. The complexes of these ligands were also prepared and characterised by spectroscopic and electrochemical means.

It was found that the properties of the pyridyl triazole complexes are altered when compared with those of $[Ru(bpy)_3]^{2+}$, the traditional ruthenium polypyridyl photosensitiser. These new complexes were found to have interesting pH dependent properties, due to the presence of the triazole. In its deprotonated form, the absorption and emission maxima are red-shifted with respect to $[Ru(bpy)_3]^{2+}$, whilst the protonated complexes displayed absorption and emission maxima at similar wavelengths to $[Ru(bpy)_3]^{2+}$. This is attributed to the change in the σ-donor nature of the triazole. In an attempt to determine the location of the excited state, a number of experiments were undertaken. Luminescent lifetime studies show that, upon deuteration of the bpy ligands, the excited state lifetime increases. This is indicative of the fact that the excited state is located on the bpy ligands and not on the pyridyl triazole ligand. PK_a measurements of the triazole NH in the ground and excited states also hint towards the same conclusion. The increase of the acidity of the

proton in the excited state suggests there is less electron density on the triazole ligand in the excited state. Had the excited state been pyridyl triazole based, the increase in electron density would have resulted in a higher pK_a for the triazole. The electrochemical properties are also found to be pH sensitive, with the oxidation potential of the metal centre increasing by up to 300mV upon protonation. Reduction potentials also indicate that the excited state should be bpy-based.

Consequently, these compounds have well defined electronic properties which make them suitable for use as photosensitisers in supramolecular systems. The fact that the excited state is located on the bpy ligands makes them still more suitable for vectorial electron transfer from a suitable electron donor (tyrosine or manganese) bound to the pyridyl triazole bridging ligand.

A similar series of ligands and complexes based on pyrazyl triazoles was also prepared and characterised. Again, pH dependent properties were found. In this case, however, the situation was more complex than before. Protonation of the triazole results in a blue shift of the absorption maxima and a small red shift in the emission maxima. From electrochemistry, it was seen that the oxidation potential of the metal centre is generally 100mV higher for pyrazyl triazole complexes when compared to pyridyl triazole complexes. Again this was pH dependent, showing an increase of ~200mV upon protonation of the triazole. Luminescent lifetime measurements indicate that the excited state is bpy-based, when the triazole is deprotonated, and usually bpy-based when protonated. Electrochemical studies on the deprotonated complexes also indicate a probable bpy-based excited state. However, pK_a titrations

showed a small increase in the pK_a in the excited state, pointing to the fact that the excited state may be located on the pyrazyl triazole.

In order to unequivocally define the location of the excited state, further studies, such as resonance Raman spectroscopy are necessary. Despite this, one may conclude that pyrazyl triazole complexes, especially in their deprotonated forms, are well suited to use as photosensitisers in supramolecular assemblies. Due to the increase in their oxidation potential, with respect to pyridyl triazole complexes, they offer an insight into the effect of the driving force on electron transfer reactions.

Using these pyridyl and pyrazyl triazole complexes, a number of reactions were attempted. The first of these was to introduce a tyrosyl moiety into a complex, bearing a terminal acid group, by means of an amide coupling. This was carried out in collaboration with Prof. B. Åkkermark and Dr. L. Sun in Stockholm. Two tyrosine derivatives, based on pyridyl triazole and pyrazyl triazole ligands were prepared. The other goal, which was sought was the introduction of new amine-based ligands into the complexes. Attempts to introduce these new chelating sites *via* reductive amination of complexes, bearing terminal aldehyde groups, were unsuccessful. However, an aromatic Mannich reaction proved to be an efficient way to introduce DPA (dipicolylamine) into complexes bearing terminal phenols. The purification of these complexes proved to be extremely demanding and no pure samples were obtainable. However, in preliminary work carried out by Sebastien Blanchard and Prof. J. J. Girerd in Paris, a Ru-Tyr-Mn_2 systems has been prepared. EPR and magnetic susceptibility measurements indicate the presence of bridging acetate and μ-oxo ligands, similar to a model complex $[(bpmp)Mn_2(OAc)_2]^+$.

The second project worked on involved a different approach to the mimicking of PSII and was carried out in Berlin under Prof. J. H. Fuhrhop. Here, the emphasis was on the study of electron/energy transfer between suitable components immobilised in a rigid membrane. In order to carry out this work, a novel lipid had to be prepared. Using a known hydrocarbon chain, functional groups were introduced into the head and tail of this amphiphile. One end contained a carboxylic acid group, suitable to immobilise the membrane on a surface such as TiO_2. The other end was modified by the introduction of a novel 5-substituted bpy derivative. Ruthenium complexes of all the intermediate bpy derivatives have been prepared and characterised by electrochemical and spectroscopic techniques. They were found to posses similar properties to the parent $[Ru(bpy)_3]^{2+}$ complex. Emission spectra and electrochemical measurements indicate that the excited state may be located on the unsubstituted bpy ligands, but this has yet to be confirmed.

7.2 Future Work

This project has been collaborative in nature, under the EU-TMR network "Ru-Mn Artificial Photosynthesis", involving research groups in Sweden, France and Germany. Much of the work presented in this thesis is still undergoing investigation.

In Sweden, the tyrosine containing complexes, $[Ru(bpy)_2pyTyr](PF_6)$ and $[Ru(bpy)_2pzTyr](PF_6)$, shall be investigated for electron transfer from the tyrosine to the photooxidised ruthenium centre. The effect of the change in the driving force for the electron transfer reaction upon going from the pyridine to the pyrazine complex

will be investigated. The effect of the presence of a negatively charged bridging ligand should also be investigated.

The preparation and study of more Ru-Mn complexes from $[Ru(bpy)_2pyTyrDPA](PF_6)$ and $[Ru(bpy)_2pzTyrDPA](PF_6)$ shall be carried out in Paris. It is hoped that these may help to characterise the monomeric manganese impurity that was evident in the EPR spectrum of the Ru-Tyr-Mn_2 system, featured in Section 5.3. For this work, the purity of the ruthenium complexes, containing free coordination sites, is imperative. Silica and alumina have proven themselves to be impractical due to the highly polar and charged nature of the complexes. Size exclusion chromatography has had limited success. Either reverse phase chromatography or charge separation chromatography may provide an answer to the problem. Complexation of the Ru-DPA complexes with metals such as zinc(II) should produce quite stable complexes (in comparison to the Mn equivalents). It may be possible to separate these Ru-Zn and Ru-Zn_2 isomers on Sephadex C-25. Subsequent removal of the zinc in basic media should then provide clean samples of ruthenium complexes bearing one and two DPA arms.

As already mentioned in Chapter 5, the reaction between complexes bearing aldehyde synthons and amine ligands failed to give any of the desired imine-coupled complexes. The use of titanium catalysts for this reaction must yet be investigated. Otherwise, it may be possible to use the acid containing complexes, $[Ru(bpy)_2pyAc](PF_6)$ and $[Ru(bpy)_2pzAc](PF_6)$, to form amide linkages between the ruthenium complex and the free ligand. A subsequent Hoffman rearrangement would yield the same complex as that obtainable from the aldehdye. However, whichever

way these complexes are prepared, similar purification problems to before shall be encountered.

The membrane system, described in Chapter 6, has yet to be studied. Any future work on this system shall be carried out in Berlin. This work shall consist of the immobilisation of the bola on a suitable pre-treated surface. It is hoped that it shall be possible to complex the bpy at the mouth of the pore with $[Ru(bpy)_2Cl_2]$, without disturbing any features of the membrane, especially the bola-surface bond. Subsequently, energy/electron transfer within the rigid ruthenium - porphyrin membrane may be investigated. Similar bolas, containing shorter hydrocarbon chains, may also be prepared in a similar manner, to investigate the importance of the distance between the two moieties.

Appendix A

Crystal Structure Determination

The intensity data for the compounds were collected on a Nonius KappaCCD diffractometer, using graphite-monochromated Mo-K_α radiation. Data were corrected for Lorentz and polarization effects, but not for absorption [1,2].

The structures were solved by direct methods (SHELXS [3]) and refined by full-matrix least squares techniques against Fo^2 (SHELXL-97 [4]). The hydrogen atom of the „amin-group" was located by difference Fourier synthesis and refined isotropically. All other hydrogen atoms were included at calculated positions with fixed thermal parameters. All nonhydrogen atoms were refined anisotropically [4]. XP (SIEMENS Analytical X-ray Instruments, Inc.) was used for structure representations.

Crystal Data for **FO909** : $C_{14}H_{12}N_4$, Mr = 236.28 gmol^{-1}, colourless prism, size 0.32 x 0.30 x 0.20 mm^3, monoclinic, space group C2/c, a = 21.474(2), b = 4.7072(6), c = 23.518(3) Å, β = 96.395(7)°, V = 2362.5(5) Å^3 , T= -90 °C, Z = 8, $\rho_{calcd.}$ = 1.329 gcm^{-3}, μ (Mo-K_α) = .84 cm^{-1}, F(000) = 992, 2955 reflections in h(-23/23), k(-5/0), l(-25/26), measured in the range 3.78° ≤ Θ ≤ 23.23°, completeness Θ_{max} = 96.6 %, 1633 independent reflections, R_{int} = 0.076, 991 reflections with $F_o > 4\sigma(F_o)$, 168 parameters, 0 restraints, $R1_{obs}$ = 0.062, wR^2_{obs} = 0.148, $R1_{all}$ = 0.110, wR^2_{all} = 0.163, GOOF = 0.950, largest difference peak and hole: 0.200 / -0.179 e Å^{-3}.

[1] COLLECT, Data Collection Software; Nonius B.V., Netherlands, **1998**

[2] Z. Otwinowski & W. Minor, „Processing of X-Ray Diffraction Data Collected in Oscillation Mode", in Methods in Enzymology, Vol. 276, Macromolecular Crystallography, Part A, edited by C.W. Carter & R.M. Sweet, pp. 307-326, Academic Press, San Diego,**1997**

[3] G.M. Sheldrick, *Acta Crystallogr. Sect. A* **1990**, *46*, 467-473

[4] G.M. Sheldrick, SHELXL-97, University of Göttingen, Germany, **1993**

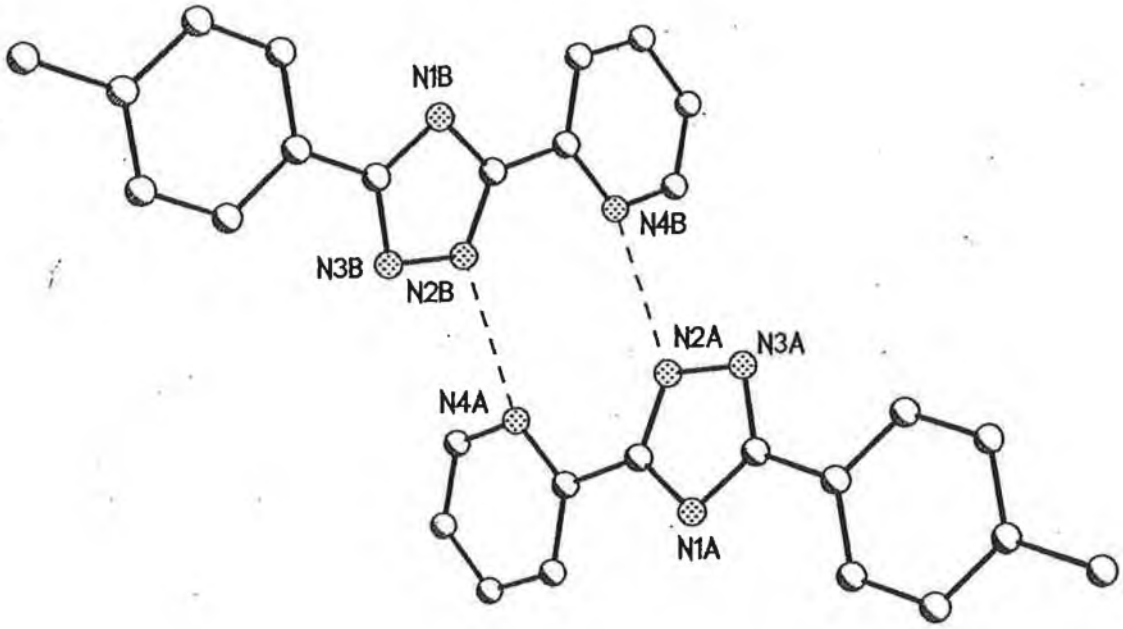
N1B
N4B
N3B
N2B
N2A
N3A
N4A
N1A

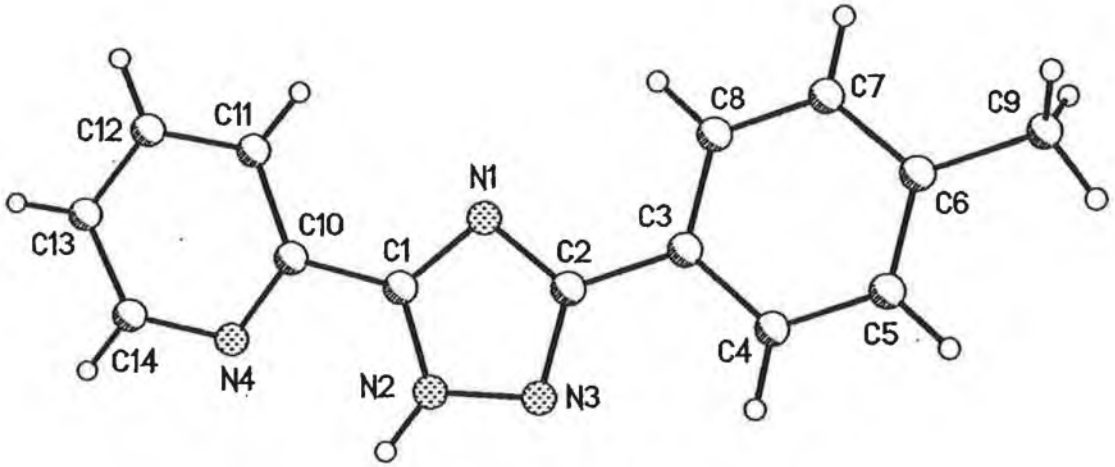
C12
C11
C8
C7
C9
N1
C6
C13
C10
C1
C2
C3
C14
N4
N2
N3
C4
C5

Appendix B

Publications and Presentations

- "Ruthenium Pyridyl Triazole Complexes as Building Blocks for Ruthenium-Manganese Systems", Poster Presentation, EUCHEM "Artificial Photosynthesis", Sigtuna, Sweden, May 1998
- "Ruthenium Pyridyl Triazole Complexes as Building Blocks for Ruthenium-Manganese Systems", Oral Presentation, EU TMR Network "Ru-Mn Artificial Photosynthesis" Meeting, Calabria, Italy, May 1999
- "The Synthesis and Characterisation of a Series of Novel Ruthenium Complexes Containing Triazole Ligands", Poster Presentation, SOLAR '01, Cario, Egypt, April 2001
- "Site-Specific Methylation of Coordinated 1,2,4-Triazoles – A Novel Route to Sterically Hindered Route to $Ru(bpy)_2$ Complexes", Fanni, S.; Murphy, S.; Killeen, J. S.; Vos, J. G.; *Inorg. Chem.*, 39, **2000**, 1320

Notes

Site-Specific Methylation of Coordinated 1,2,4-Triazoles: A Novel Route to Sterically Hindered Ru(bpy)$_2$ Complexes

Stefano Fanni, Suzanne Murphy, J. Scott Killeen, and Johannes G. Vos*

Inorganic Chemistry Research Centre, School of Chemical Sciences, Dublin City University, Dublin 9, Ireland

Received September 15, 1999

Introduction

In the last few years it has been shown that chelating 1,2,4-triazoles such as pyridine− and pyrazine−triazoles are interesting building blocks for supramolecular systems.[1,2] So far most attention has been paid to the study of the photophysical and electrochemical properties of $[Ru(bpy)_2pt]^+$ type complexes (bpy = 2,2′-bipyridyl and pt = a pyridine− or a pyrazine−triazole), containing *negatively* charged (deprotonated) triazole rings. The results obtained have shown that the presence of a negative charge on the ligand gives rise to compounds with unusual photophysical properties.[2,3] To assess the importance of this factor we are now investigating metal complexes containing N-methylated (*neutral*) triazoles.[4] In the traditional route to these complexes, the N-methylated ligand is prepared first and subsequently used to prepare the appropriate metal complex.[5]

In this contribution, we wish to report a novel synthetic route to such complexes. This method is based on the direct methylation of the appropriate precursor metal complex with trimethyl oxonium tetrafluoroborate ($OMe_3^+BF_4^-$). The methylation process was found to be remarkably site-specific, leading to the target complex in a single step under very mild conditions. Surprisingly, the main product of the reaction is always the sterically hindered N1 methylated isomer, which was never obtained using the aforementioned "traditional route". The methylation of heteroaromatic nitrogens has been successfully applied during the synthesis of sophisticated supramolecular assemblies,[6,7] and the methylation of ruthenium complexes has been observed before.[6b] However, this contribution is the first example of the synthesis of sterically hindered ruthenium(II) polypyridyl substrates otherwise not synthetically accessible.

Scheme 1. Reaction Pathway and Complex Structures

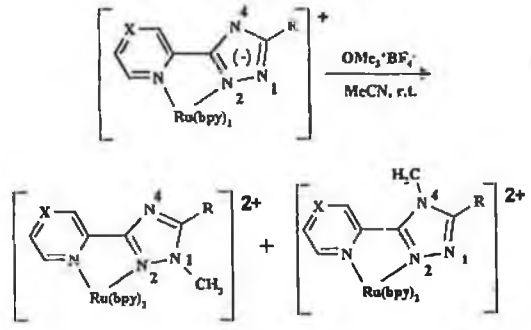

1	X = C, R = H	**5**	X = N, R = H
2	X = C, R = Me	**6**	X = C, R = o-hydroxyphenyl
3	X = C, R = Br	**7**	X = C, R = 9,10-phenothiazine
4	X = C, R = p-toluyl	**8**	X = C, R = p-chloromethoxyphenyl

Experimental Section

Materials. All precursor complexes were available from earlier studies.

Methylation of Complex 1−8. The reaction pathway and ligand structures are shown in Scheme 1. To a stirring suspension of the required metal complex (0.07 mmol) and K_2CO_3 (28 mg, 0.21 mmol) in dry acetonitrile (10 mL) was added $OMe_3^+BF_4^-$ (15 mg, 0.1 mmol) in one portion at room temperature. The resulting mixture was stirred under N_2 for 1 h, after which the solvent was removed under reduced pressure. The residue was dissolved in a mixture of acetone and water from which the product was precipitated as a $[Ru(bpy)_2Mept](PF_6)_2$ salt by the addition of few drops of a NH_4PF_6 saturated water solution. An overall yield (N1 and N4 isomers combined) of 80−88% is obtained for all systems studied. The main isomer (N1 methylated) could be obtained in pure form by double recrystallization from an acetone−water mixture or by semipreparative cation-exchange HPLC.[8]

Results and Discussion

We have applied this direct methylation method to eight different $[Ru(bpy)_2pt]^+$ complexes. As shown in Scheme 1, the triazole moiety in the parent complexes is bound through the N2 atom of the ring, leaving the N1 and N4 positions available for methylation. It is known from previous studies[5,8,9] that for N2-coordinated triazole rings the N4 and N1 methyl groups give rise to ^1H NMR signals around 4.15 and 3.10 ppm, respectively. One can, therefore, conveniently determine the location of the methylation and quantify the N1/N4 product ratio by ^1H NMR

(1) (a) Fanni, S.; Keyes, T. E.; Campagna, S.; Vos, J. G. *Inorg. Chem.* **1998**, *37*, 5933. (b) Coates, C. G.; Keyes, T. E.; Hughes, H. P.; Jayaweere, P. M.; McGarvey, J. J.; Vos J. G.; *J. Phys. Chem. A* **1998**, *102*, 5013.

(2) Wang, R.; Vos J. G.; Schmehl, R. H.; Hage, R. *J. A. Chem. Soc.* **1992**, *114*, 1964.

(3) Similarly negatively charged bridging ligands have been reported by other groups: (a) Beley, M.; Chodorowski-Kimmens, S.; Collin, J.-P.; Louis, R.; Launay, J.-P.; Sauvage, J.-P. *Angew. Chem., Int. Ed. Engl.* **1994**, *33*, 1775. (b) Haga, M.; Bond, M. A. *Inorg. Chem.* **1991**, *30*, 475. (c) Haga, M.; Ali, M. M.; Koseki, S.; Fujimoto, K.; Yoshimura, A.; Nozaki, K.; Takeshi, O.; Nakajima, K.; Stufkens, D. J. *Inorg. Chem.* **1996**, *35*, 3335.

(4) An easy way to access to neutral pt bridging ligands is the protonation of the triazole moiety. However, this method will be limited to a restricted pH range and cannot be applied when other basic/acidic sites are present in the molecule.

(5) Hage, R.; Prins, J. G.; Haasnoot, J. G.; Reedijk, J.; Vos, J. G. *J. Chem. Soc., Dalton Trans* **1987**, 1389.

(6) Serroni, S.; Denti, G. *Inorg. Chem.* **1992**, *31*, 4251. (b) Campagna, S.; Denti, G.; Serroni, S.; Juris, A.; Venturi, M.; Ricevuto, V.; Balzani, V. *Chem.—Eur. J.* **1995**, *1*, 211.

(7) Bassani, D.; Lehn, J.-M.; Fromm, K.; Feuske, D. *Angew. Chem., Int. Ed. Engl.* **1998**, *37*, 2364.

(8) Ryan, E. M.; Wang, R.; Vos, J. G.; Hage, R.; Haasnoot, J. G. *Inorg. Chim. Acta* **1993**, *208*, 49.

(9) Buchanan, B. E.; Wang, R.; Vos, J. G.; Hage, R.; Haasnoot, J. G.; Reedijk, J. *Inorg. Chem.* **1990**, *29*, 3263.

10.1021/ic991103p CCC: $19.00
Published on Web 02/29/2000

Table 1. N1/N4 Selectivites Obtained for the Compounds Investigated

		N−Me δ ^{1}H NMR[a]		
complex	η (%)	N1	N4	N1/N4 selectivity[b]
1	100	3.15	4.21	90/10
2	100	3.08	4.12	90/10
3	100	3.07	4.14	90/10
4	100	3.21	4.16	95/5
5	100	3.17	4.26	70/30
6	70	2.97	4.01	95/5
7	100	3.09	4.13	85/15
8	100	3.16	4.22	85/15

spectroscopy. UV/vis and emission spectra were also recorded, but since these do not differentiate between the different methylation sites, they are not discussed here. All products obtained were NMR and HPLC pure.

Previous studies have shown that when a N1-methylated pt ligand is reacted with a $Ru(bpy)_2$ substrate, coordination took place almost exclusively through the N4 position. Yields for the N2 isomer as identified by HPLC were typically 10% or less.[8] The reason for this behavior was ascribed to the steric hindrance caused on the N2 position by the methyl group in N1. Therefore, one would expect the methylation reaction here described to give exclusively the N4-methylated isomer. However, the data given in Table 1 show that the reaction is remarkably site-specific with a high selectivity for methylation at the N1 position, suggesting that the N1 position is more nucleophilic and that steric hindrance is not an overriding factor for these reactions.

The analysis of the results obtained shows some other interesting features. The selectivity toward the N1 position is hardly affected by the nature of the R substituent. In addition, no sign of products other than the N1- and N4-methyl derivatives was seen for entries **5**, **6**, and **7**, where additional methylation sites are present. The drop on the selectivity observed for entry **5** could be explained in the light of previous studies which suggested a high degree of delocalization of the negative charge on the triazole ring onto the pyrazine grouping.[10]

A 100% conversion was observed for all the complexes under investigation but complex **6**. The lower yield observed for compound **6** is possibly explained by the presence of an hydrogen bond between the hydroxyl group and the N4 nitrogen of the triazole, thereby reducing the negative character of the triazole ring.[11]

A study of the photochemical properties of some of the complexes synthesized yielded interesting results. When the N2-bound/N1-methylated complex **1** is irradiated with white light for 24 h in acetone, it is quantitatively isomerized into the N4-bound/N1-methylated isomer. This isomer is photostable, and neither decomposition nor isomerization is observed after further irradiation. The N2-bound/N4-methylated isomer is also photostable under the same conditions. These results clearly suggest that the N2-bound/N1-methylated isomer is the less stable thermodynamically, an observation that makes the selectivity found even more remarkable. More detailed photochemical and photophysical studies are underway to further investigate this unusual behavior.

In conclusion, the method reported represents a new and simple route for the high yield synthesis of sterically hindered $[Ru(bpy)_2]$ complexes by direct methylation of the appropriate metal complex. The interest of this method resides in the high selectivity achieved and in the fact that the less thermodynamically stable isomer, so far only obtained in very small amounts, is the main product of the reaction. These observations represent a significant example on how "classical" organic reactions could be applied to solve synthetic problems during the synthesis of ruthenium polypyridyl complexes. In the continuing search for larger supramolecular systems, this new approach adds to the synthetic pathways available.

Acknowledgment. The authors wish to thank the EC TMR Program (Contract CT96-0031) for financial support.

IC991103P

(10) Nieuwenhuis, H. A.; Haasnoot, J. G.; Hage, R.; Snoeck T. L.; Stufkens, D. J.; Vos, J. G. *Inorg. Chem.* **1991**, *30*, 48.
(11) Hage, R.; Haasnoot, J. G.; Reedijk, J.; Wang, R.; Ryan, E. M.; Vos, J. G.; Spek, A. L.; Duisenberg, A. J. M. *Inorg. Chim. Acta* **1990**, *174*, 77.